PSFC JA-06-3

Onboard Plasmatron Hydrogen Production for Improved Vehicles

L. Bromberg, D.R. Cohn, A. Rabinovich, N. Alexeev,
A. Samokhin, K. Hadidi, J. Palaia, N. Margarit-Bel

February 6, 2006

MIT Plasma Science and Fusion Center

Work supported by the US Department of Energy, Office of FreedomCar and Vehicle Technologies, Contract number: DE-AC03-99EE50565

Abstract

This paper describes progress in plasmatron fuel reformers and applications to internal combustion vehicles. Several plasmatron configurations and their performance with a variety of fuels are described. Fuels investigated range from methane and propane to gasoline, diesel and biofuels. Applications described include lean spark ignition operation, NOx trap regeneration, diesel particulate filter regeneration and ignition timing control in advanced combustion mode engines.

Table of Contents

1) Introduction and organization of report

This report documents work done on the program entitled "Onboard Plasmatron Hydrogen Production for Improved Vehicles." This program was funded by US Department of Energy, Office of FreedomCar and Vehicle Technologies, from May 27, 1999 through Dec 31, 2005, through grant DE-AC03-99EE50565. The PI of the program was Dr. Daniel Cohn at the Plasma Science and Fusion Center at MIT, with Dr. Leslie Bromberg as Co-PI. The technical point of contact at DoE Office of FreedomCar and Vehicle Technologies was Dr. Sidney Diamond.

Although there were many tasks, the main goals of the program were:

- Develop plasmatron fuel reformers for aftertreatment applications
- Test plasmatron fuel reformers for diesel engine aftertreatment
- Test plasmatron fuel reformer for gasoline engine operation.
- Reform biofuels using plasmatron fuel converters
- Study performance for high flow rates.
- Technology transfer to industry

This report covers the work on the tasks described above. The main highlights of this work are:

- Technology has been transferred to ArvinMeritor, who is applying large resources to develop products for aftertreatment and for lean SI operation.
- Effectiveness of the technology has been demonstrated for NOx trap regeneration and for SI combustion enhancement, as well as advantages of hydrogen rich gas sulfur removal from NOx traps.
- Developed understanding of the operation of the plasmatron through modeling and experiments.
- Demonstrated ability of reform a large variety of fuels, including gasoline, diesel, ethanol, bio-diesel, bio-oils, methane and propane, and other alternative fuels.
- Demonstrated ability to operate over a wide range, and scaled device to operate at large flow rates.

These topics and others are described in the following sections. The report is organized as follows: first the different plasmatron fuel reformers used during the program are described in Section 2, as well as the facility and analytical instrumentation developed for the program. Then applications of the plasmatron are described. Section 3 describes applications to SI engines, including tests carried out in collaboration with ORNL. Section 4 and 5 describe applications for aftertreatment, first to NOx trap regeneration followed by DPF regeneration in Section 5. Section 6 describes application for plasmatron fuel reformers to HCCI (Homogeneous Charge Compression Ignition) engine control. Section 7 describes the modeling effort, including fluid dynamics and well as

chemistry. Section 8 describes the experimental results of reformation using the plasmatron fuel reformer, during steady state operation. Section 9 describes transient operation of the plasmatron fuel reformers for the fuels investigated, with the exception of propane, whose transient operation was integrated with the steady state investigation in section 8. Finally, section 10 provides a brief summary of the work.

Section 11 presents the bibliography as well as the references cited throughout the report.

2) Plasmatron description

There is a need for a compact, efficient hydrogen generator for onboard applications [Ste74, Hou74, Mac76, Jam94, Bro97, Coh97, Bro99a, Kir99, Gre00, Bro00b, Bro01a, Bro01b, Kir02, Bro02, Ath03, Bro03]. Such a device could also find applications, in addition, to the stationary manufacturing of synthetic fuels which starts with the generation of synthesis gas [see, for example, Bro00a]. The development of a homogeneous (without the use of a catalyst) process would be attractive, as the cost of the catalyst and the reactor is a major component of plants used to generate hydrogen rich gas for natural gas upgrading. It may be particularly useful for smaller scale plants.

Homogeneous plasma-based reactors have been studied in the past [Mul86, Ful95, Gau98]. Their performance has been lacking, and thus industrial generators of synthesis gas use catalytic processes.

The plasma assisted fuel converters [Coh98, Bro99e, Bro99f, Cze01a, Cze01b, Sob01, Dem02, Sob02, Cze03a, Cze03b. Cze03c] use continuously generated plasma as means of facilitating the reformation of hydrocarbon fuels. By increasing the reaction rates, plasmatron fuel converters can reduce size requirements for effective reforming, increase speed of response and increase fuel flexibility. A wide range of fuels can be converted to hydrogen rich gas. The boost provided by the plasma can facilitate partial oxidation reactions with negligible soot production and efficient conversion of hydrocarbon fuel into hydrogen-rich gas. Plasmatron fuel converters can alleviate problems associated with catalytic reformation, such as response time limitations, sensitivity to fuel composition, poisoning, soot formation and a narrow operational temperature range.

The process used in plasmatron fuel converters [Coh98, Bro99e, Bro99f] is partial oxidation, where there are as many atoms of oxygen as there are atoms of carbon in the air/fuel mixture. Under ideal circumstances, the oxygen carbon atoms would combine and form carbon monoxide molecules, releasing all the hydrogen atoms as hydrogen molecules. Under ideal stoichiometric partial oxidation conditions, the partial oxidation reaction is

$$C_nH_m + n/2\ O_2 \rightarrow nCO + m/2\ H_2$$

In this case there is just enough oxygen around to convert all the carbon in the fuel into CO. The partial oxidation reaction is exothermic. In the case of liquids fuels (gasoline, diesel), approximately 15% of the heating value of the fuel is released in the partial oxidation reaction.

In practice it is necessary to have more atoms of oxygen than atoms of carbon, and thus the oxygen to carbon atom ratio (O/C ratio), is larger than 1. The process of partial oxidation is exothermic, but with relatively slow kinetics. The use of plasma enhanced partial oxidation process has been proposed and investigated in the past.

There have been many designs of plasmatrons used during this program. However, all the plasmatron designs are based on one of three types: 1) high current, thermal plasmatron (gen 1); 2) low current, non-thermal plasmatron with central electrodes (gen 2); and 3) low current, non-thermal plasmatron with large area electrodes (gen 3). The purpose of this section is to provide a description of the different types of plasmatrons.

a) Thermal plasmatron (gen 1)

All plasmatrons provide ohmic heating of gases to elevated temperatures. At these temperatures the gas is partially ionized. Plasmatrons provide highly controllable electrical heating of this gas. The increased temperatures, ionization levels and mixing provided by plasmatron heating accelerate reformation of hydrocarbon fuels into hydrogen rich gas. The high temperatures can be used for reforming a wide range of hydrocarbon fuels into hydrogen-rich gas without the use of a catalyst. It thus is possible to eliminate problems associated with catalyst use, such as narrow operating temperature, sensitivity to fuel composition, poisoning, and response time limitations.

By increasing the reaction rates, plasma heating could significantly reduce size requirements for effective reforming, increase speed of response and increase fuel flexibility. A wide range of operation is possible, from partial oxidation to steam reforming. The boosting of the reaction rate would occur by creation of a small very high temperature region (5000-10000 K) where radicals are produced and by increasing the average temperature in an extended region.

The additional heating provided by the plasma can ensure a sufficiently high number of chemically reactive species, ionization states, and elevated temperatures for the partial oxidation reaction to occur with negligible soot production and with a high conversion of hydrocarbon fuel into hydrogen-rich gas. The effective conversion of hydrocarbon fuel is aided by both the high peak temperature in the plasma and the high turbulence created by the plasma.

A plasma boosted reformer can be made very small because of the high power density. The rapidly variable plasmatron parameters (energy input, flow rate, product gas composition, etc) make this technology very attractive for application to the dynamic demands for hydrogen-rich gas production in vehicles. It should be possible to practically instantaneously produce hydrogen-rich gas for use during cold startup. Throughout the driving cycle, rapid changes in hydrogen-rich gas flow can be accommodated by variation of plasmatron parameters. [Coh97]

Figure 1 shows a diagram of a multi kilowatt plasmatron. The device operates at atmospheric pressure, with air as the plasma forming gas. The plasmatron operates in DC mode. The plasmatron consist of copper cathode with a hafnium tip, and a copper tubular anode [Rud79]. The electrodes are separated by an electrical insulator. The cathode and anode are water cooled, and this cooling represents a sink of energy. Measurements on the cooling water temperature rise indicate that the plasmatron is about 70–80% efficient.

Hafnium of the cathode tip allows operation on air as the plasma forming gas without excessive oxidation. The hafnium tip has a high electron emissivity and relatively long lifetime at current less than ~100 A.

The plasma arc ignites across the electrode gap. Air is injected tangentially upstream from the electrodes to produce a vortex that elongates the plasma inside the tubular anode. The anode root of the arc is in constant rotation in order to minimize electrode erosion. The hydrocarbon fuel and additional air are injected downstream from the electrodes. The mixture of hot air and vaporized hydrocarbons enter the plasma reactor where the reaction takes place.

Figure 2.1 shows a photograph of the plasmatron without a reaction extension cylinder, operating on air at about 1.5 kW. The plasma jet is pointing upwards. During reforming operation, fuel and additional air are injected downstream from the stainless steel flange shown in Figure 2. 1.

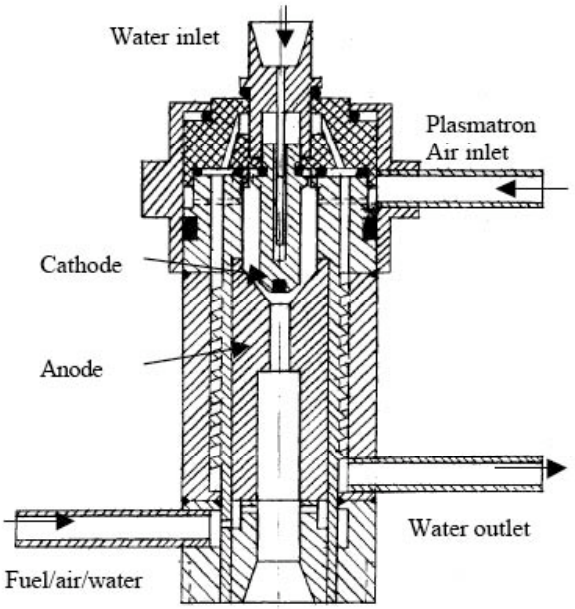

Figure 2.1. Diagram of thermal plasmatron used for the engine experiments.

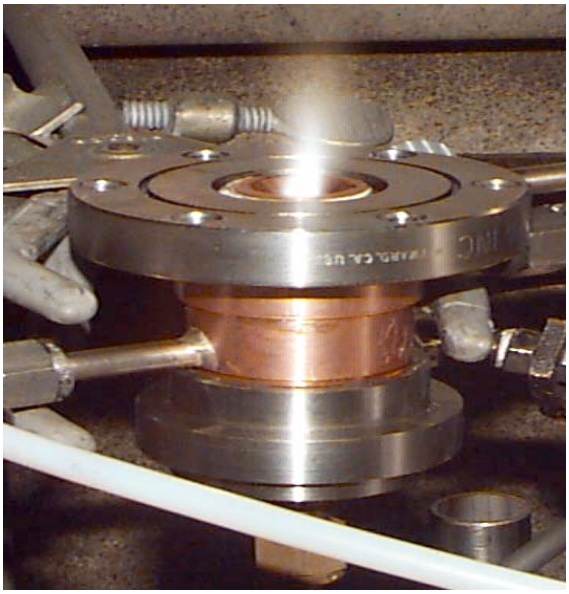

Figure 2.2. DC arc microplasmatron operating in air without fuel.

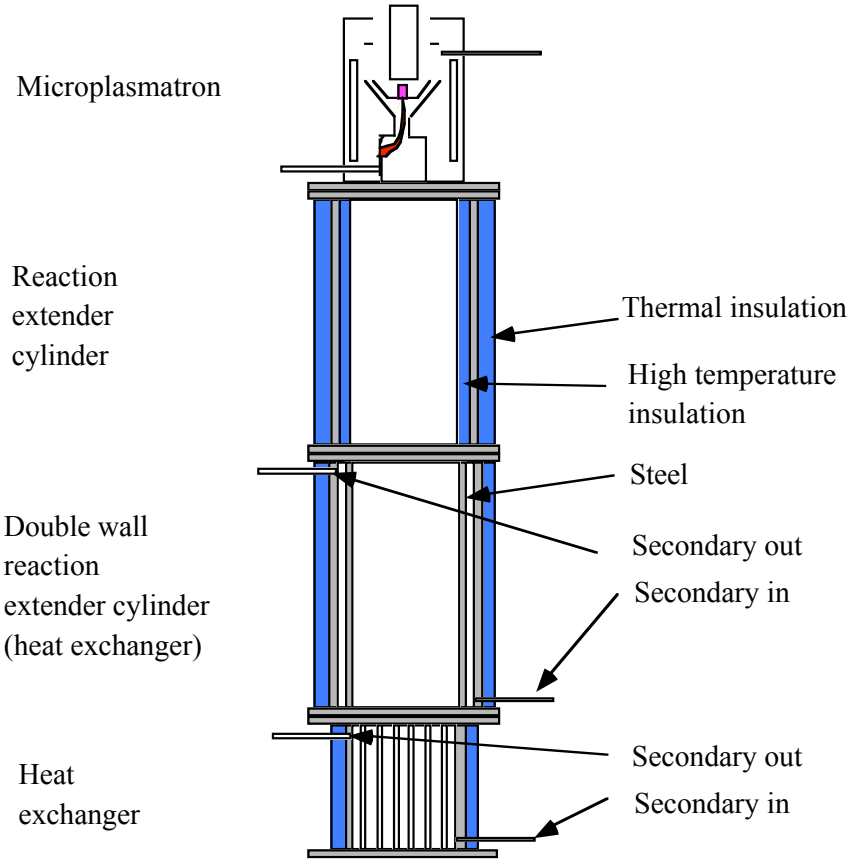

Figure 2.3. Microplasmatron with reaction extender cylinder and two heat exchangers

Figure 2.2 shows a photograph of the plasmatron without a reaction extension cylinder, operating on air at about 1.5 kW. The plasma jet is pointing upwards. During reforming operation, fuel and additional air are injected downstream from the stainless steel flange shown in the Figure 2.2.

Figure 2.3 shows a microplasmatron fuel converter that includes a reaction extender and a heat exchanger. The heat exchanger can be used to simultaneously cool down the hydrogen-rich gas and to preheat the incoming air and fuel. Preheating the air/fuel reduces the electrical energy requirement to the plasmatron and increases the hydrogen yield. Work is continuing in the development of high efficiency, high temperature heat recuperator. Simple calculations show that the use of preheat can half the electrical power requirements to the plasmatron.

A typical microplasmatron fuel converter includes a steel tube 4 cm in diameter and 15 cm long thermally insulated by fiberglass felt and steel screens. The samples of hydrogen rich gas are cooled down and analyzed using gas chromatography (GC). Table 2.1 shows the typical plasmatron range of operating parameters for a DC arc device. Materials that could be used in various components of the plasma boosted reformer are copper, zirconium and molybdenum. Conversion efficiency, electrode life, size, and weight are key feasibility issues and require detailed experimental investigation.

Table 2.1. Parameters of conventional DC Arc plasma boosted reformer.

Power	1.5-10 kW.
Voltage	120-140 V DC
Current	15-75 A DC
Flow rates Air	 0.5-1.5 g/s
Fuel	0.3-0.5 g/s

The setup used in the experiments described below with the engine is shown in Figure 2.3. The plasmatron is followed by a reaction extension cylinder, a simple heat exchanger (not cooled for the present experiments), and a gas-to-water heat exchanger, used to cool the reformate.

Summary of thermal plasmatron features

The thermal plasmatron, because of the high power , can handle very easily transients, with very fast startups, even from room temperature conditions. In addition, the thermal plasmatron can drive slightly endothermic, or slightly exothermic reaction. Thus, it is possible to achieve good reformation at relatively low values of oxygen to carbon ratios.

However, because of the high power, the energy consumption is high, and plasmatron fuel reformers based upon this system have a substantial hit on the system efficiency. In addition, because the system operates at relatively low voltages by high currents, the

electrodes, and in particularly the cathode, have substantial erosion. Typically, a cathode would last for a day or two (20-50 hours).

Finally, the system requires cooling water for aggressively cooling the electrodes. The use of cooling water put a constraint on the potential use of thermal plasmatron fuel converters to mobile sources.

b) Low current plasmatron fuel converters (gen 2)

Plasmatron fuel converters provide low current electrical discharges in flowing gases of hydrocarbon fuels and air (and/or other oxidants). The resulting very local generation of reactive species in the flowing gases along with increased mixing accelerates reformation of hydrocarbon fuels into hydrogen rich gas. Although thermal plasmatron fuel converters may also be utilized for increasing enthalpy, further accelerating the reaction rates, the second generation, low current plasmatron does not increase the enthalpy of the gas substantially. The conditions of the low current, second generation plasmatron, however, still facilitate the reforming of a wide range of hydrocarbon fuels into hydrogen-rich gas without the requirement of using a reformer catalyst. It is possible to eliminate problems associated with reformer catalyst use, such as narrow operating temperature, soot formation, sensitivity to fuel composition, poisoning, and response time limitations.

Figure 2.4 shows a diagram of a low current, second generation plasmatron reformer. Air and fuel are continuously injected in a plasma region provided by a discharge established across an electrode gap. The device operates at atmospheric pressure, with air as the plasma forming gas. Use of a discharge mode with non-equilibrium features allows for operation at relatively small electrical powers, at much reduced current relative to earlier compact arc plasmatron fuel reformers developed at MIT. When operating DC, the cathode can be a spark plug. The ground electrode of the spark plug would have been removed. The anode can be a steel or copper cylinder. Neither electrode is water cooled.

Table 2.2 shows the typical plasmatron parameters for a low current, low power compact plasmatron fuel converter.

The plasma source is followed by a reaction extension cylinder. A simple heat exchanger can be used downstream from the reaction extension cylinder, both to cool the reformate and to preheat the incoming air and/or fuel.

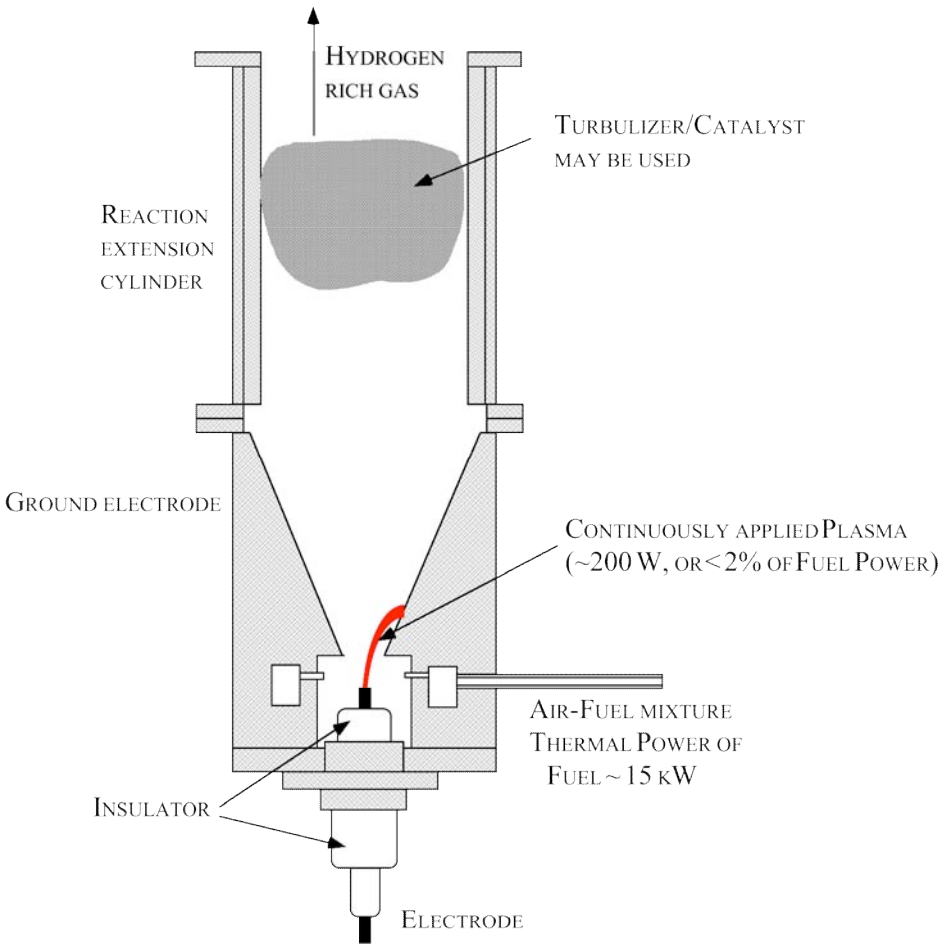

Figure 2.4. Low current, nonthermal plasmatron fuel converter (gen 2).

Table 2.2
Parameters of low current compact plasmatron fuel converter

Power	50–300 W
Current	15–120 mA
H_2 flow rate	30–50 liters/min
Height	25 cm
Volume	2 liter
Weight	3 kg

The required electrical energy input to the compact plasmatron fuel converter is on the order of 2% of the heating value of the input fuel.

The low current device has been used to convert natural gas, gasoline and diesel fuel into hydrogen rich gas. The device showed no evidence of soot, even after extended operation. Typical reforming efficiency in partial oxidation mode of operation was

around 60-70% (ratio of heating value of the hydrogen rich gas to heating value of the fuel). Diesel fuel streams with power levels of 5 to 20 kW have been processed into hydrogen rich gas. It is projected that reforming efficiencies of 80% will be attainable with improved devices. Previously, diesel fuel has been successfully reformed using a compact plasmatron reformer using arc plasmas [Bromberg3]. However, arc plasmatron reforming utilizes substantially higher electrical powers and currents.

Projected parameters for higher throughput versions of low current compact plasmatron fuel converter systems are an H_2 flow rate of 500 liters per minute, and electrical power requirements of 50-1000 W.

Summary of gen 2 plasmatron features

The second generation plasmatron operated adequately although at much lower power than the thermal plasmatron (gen 1). It required operation at slightly value of oxygen to carbon ration, especially during startup. It was able to operate without soot production.

However, the fact that the electrode is on the middle of the system, the place where it would be most convenient to injected liquid fuels, makes the system hard to design, and to avoid conditions where the fuel spray hits the walls. It has been determined that droplet coalescence is one of the largest reasons for soot formation.

In addition, as the axial electrode is much smaller than the other one, it suffers from erosion, although not in the scale of the thermal plasmatron.

c) Wide area electrode, low current plasmatron fuel reformer (gen 3)

Figure 2.5 shows a diagram of the gen 3 plasmatron fuel converter used in the latest phases of this program, both experimental and modeling effort. It consists of an axially symmetric set of concentric electrodes with an axial gap. There is a gaseous input across the gap, and since it has a large swirl flow associated with it, it is referred as the swirl gas. The purpose of this flow is to push the discharge, which originates across the gap, to the volume of the plasmatron. This flow has both a radial component that pushes the discharge towards the axis of the device, as well as a swirl component that rotates it.

The discharge is created by a constant current AC power supply, as is the case with the second generation plasmatron. The power supply can produces very high voltages (on the order of 10-20 kV) under conditions where the plasma is not present, as well as relatively low voltage to maintain the discharge. During the current maintaining phase, the voltage is on the order of 500-2000 V, and it is time varying. As the discharge lifetime increases, its length increases, with an associated increase in the discharge voltage. The electric field away from the sheaths is on the order of 400 V/cm, the gas temperature is on the order of 2400 K and the electron energy is on the order of 1 eV [Anz04]

The setup used in the experiments, as well as the experimental results with methane, have been reported elsewhere, and will only briefly be described here.

The plasmatron shown in Figure 2.5 has three different gaseous flows, introduced through the wall gas, the swirl (plasma) gas, and the axially injected gas. The wall gas is injected in the axial direction at an axial location similar to the axial nozzle, with no swirl. The swirl (plasma) gas is injected downstream from the wall air and the axial gas, with a large amount of vorticity. The swirl gas moves the discharge into the fuel region, and provides the rotation motion that moves the arc roots on the electrodes (to minimize electrode erosion).

There are several other inputs to the plasmatron. There is an axially directed centered input that is commonly used for liquid fuels. The liquid nozzle is surrounded by a fast gas flow, making up an air-assisted injector. The nozzle and axial injection has not been used in the present experiments, as previous experiments with propane indicated that best performance is obtained when the hydrocarbon fuel is mixed with the swirl gas.

There is a third input of gases, an axial gas that is injected at the same axial location of the air assist injector, but at large radii. The wall air is injected mainly in the axial direction. In the cases of the experiments described in this paper, and the modeling to analyze them, the axial gas is composed exclusively of air.

Typical parameters of the gen3 plasmatron are shown in Table 2.3. It is the gen-3 plasmatron that has been used for testing with NOx traps, A device similar to the gen-3 is being developed by ArvinMeritor for combustion enhancement in spark ignited engines.

Table 2.3 Characteristics of a gen-3 plasmatron diesel converter.

Electric power	W	200
O/C		1.2
Diesel flow rate	g/s	0.8
Corresponding chemical power	kW	36
Reformate composition (vol %)		
H2		7.6
O2		1.3
N2		64.0
CH4		2.4
CO		13.0
CO2		4.4
C2H4		2.2
C2H2		0.0
H2O		7.1
Energy efficiency to hydrogen, CO and light HC		65%
H2 flow rate	l/min (STP)	20
Soot (opacity meter)		0.0%

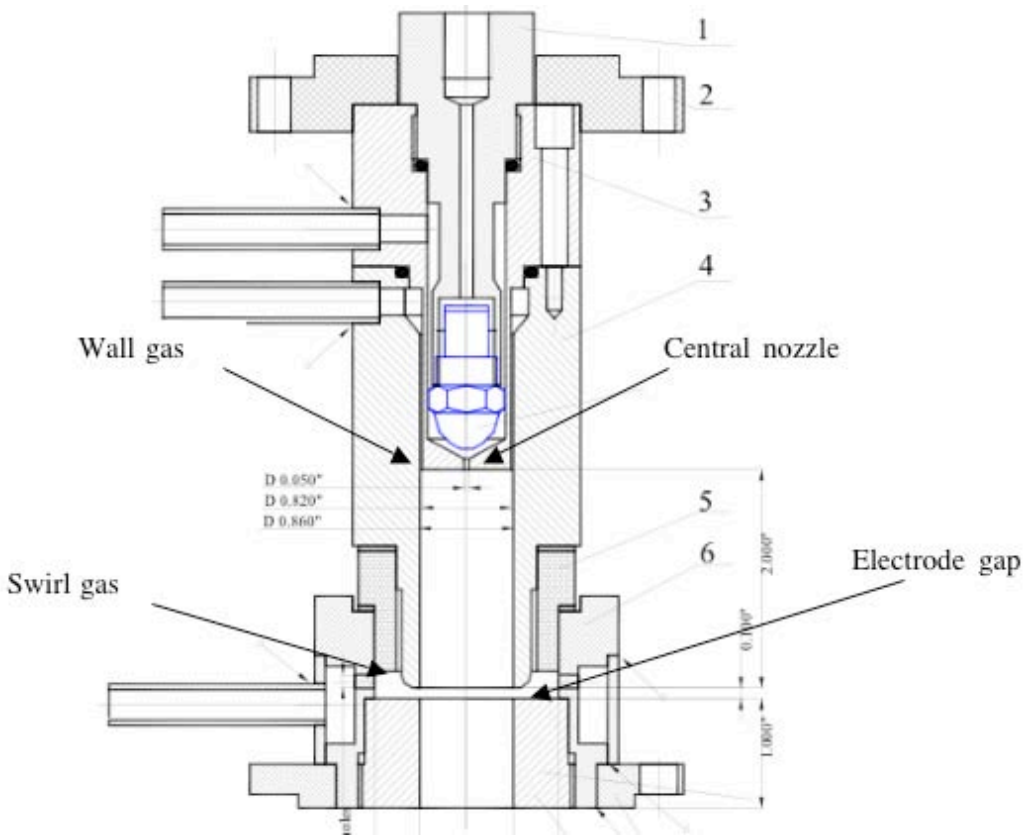

Figure 2.5 Diagram of a gen-3 plasmatron optimized for diesel reforming.

Figure 2.6. Photograph of plasmatron fuel reformer used for experiments with propane, natural gas, gasoline and bio fuels during the last year of the program (gen 3a)

Figure 2.6 shows a photographs of the plasmatron used in the later stages of the program

Summary of the gen 3 plasmatron features

The gen 3 plasmatron is reliable, easy to use, and can operate over very wide range, with no noticeable electrode wear. The flexible introduction of the air and the fuel allows for operation over wide throughputs as well as O/C ratios, with good conversion and no soot production.

However, the system is quite complex, requiring 3 air flows. There has been work to investigate the use of flows produced by a simple set of controllers. For the best performance, the 3 air inputs needed to be controlled independently.

d) Plasmatron development at ArvinMeritor

At the ArvinMeritor Columbus Technical Center, the diesel plasmatron fuel reformer has been further developed for after-treatment applications. With a reformer catalyst, the hydrogen concentration in the reformate was about 22% with low soot production of around 20 mg/m^3. The plasmatron was enclosed in a metallic housing that minimizes electromagnetic interference (EMI) radiation, which could adversely affect operation and control of the plasmatron. For on-board applications, a 250W power supply with full computer control of the power level, requiring minimal cooling, has been developed, for both 12 and 24 volt vehicle electrical systems. A compact high voltage transformer is utilized in this design. This version of the plasmatron was tested extensively on the bench, prior to installation on vehicles.

Figure 2.7. Gen H plasmatron developed at ARM.

Figure 2.7 shows the Gen-H Fuel Reformer which is ArvinMeritor's implementation of the MIT plasmatron .

e) Description of the experimental setup

The plasmatron reformer facility used in the latest sets of experiments is a modification of a plasmatron fuel reformer that had been optimized for diesel fuel operation. The unit was operated mainly at 50-500 W of electrical power. The power supplies were operated as constant current sources operating between 200 kHz and 260 kHz.

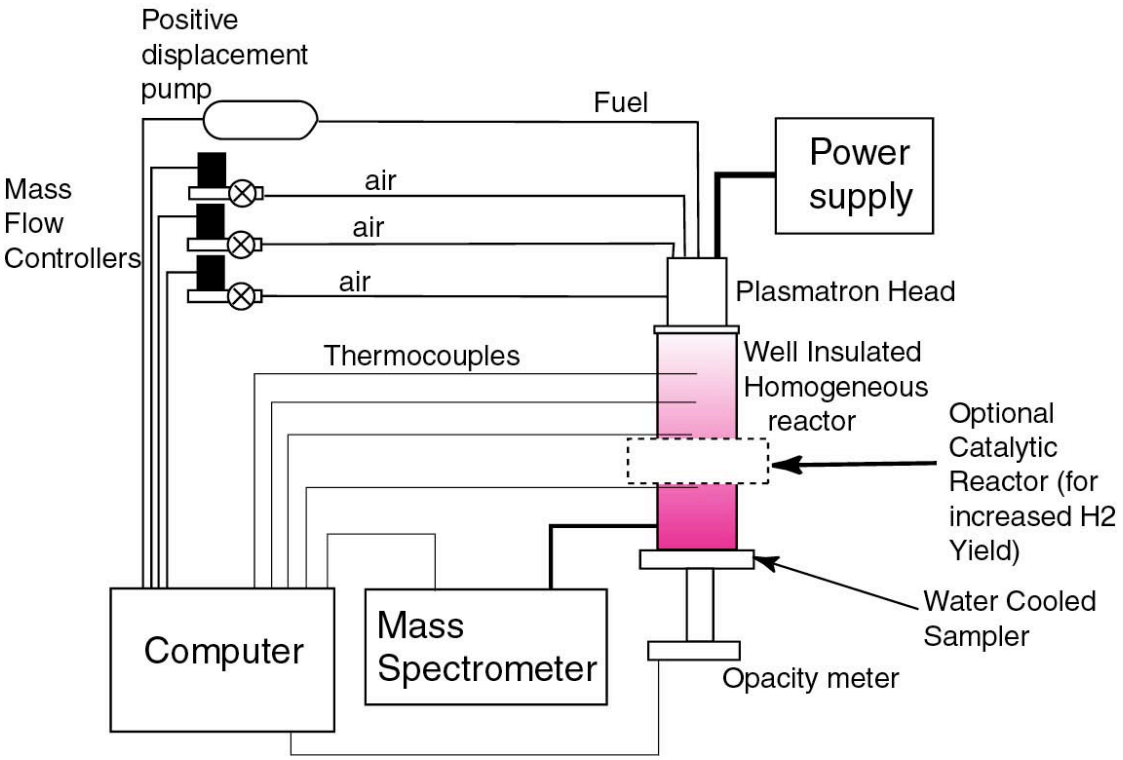

Figure 2.8 Schematic layout of the plasmatron setup

Figure 2.8 depicts the experimental setup used. The plasmatron was mounted on a steel reaction chamber that allows the homogeneous partial oxidation reactions to take place with enough residence time. The dimensions of this chamber are 5 cm diameter by 12.5 cm long. The products of reaction from this chamber go into a 5 cm diameter by 17.5-cm long chamber packed with nickel-based catalyst on an alumina substrate. The chamber is thermally insulated by a half-inch thermal insulation made of porous alumina ceramic.

Two sample ports are used for sampling the reformate gases. The first one is located on the reaction chamber immediately upstream from the catalyst and the second one is located at the exhaust, downstream from the catalyst chamber. Both sampling lines are

water cooled. The temperature inside the reactor is measured by a thermocouple located inside reaction extension cylinder.

Calibrated mass flow controllers are used to control the multiple air inputs into the plasmatron. The atomization air flow rate was monitored by a TSI air flow sensor. The TSI sensor was also used to confirm that the two other mass-flow controllers (for the wall air and for the plasma air) were within certification.

The gaseous fuel (methane, propane) flow is measured using a calibrated rotameter, while the air flows are measured and controlled with mass flow controllers. It was difficult to use a mass flow controller with gaseous fuels because the low flow rates of the fuel made very difficult to maintain proper calibration. Two rotameters in parallel were used to provide the required methane flow, with both operating near the middle of their range. Under these conditions, the methane flow was accurate within 10-20%. The rotameters are compensated for pressure variations that occurs as the swirl air is varied. There is no variation in pressure at the rotameters when the wall air is varied.

For liquid fuels, the approach used in the plasmatron fuel reformer work has been to form a fine spray from the liquid fuel, followed by air assist atomization. We expect to have droplet size on the order of < 20 μm. The liquid fuels in the present tests have been introduced into the plasmatron through a nozzle that forms a fine spray of droplets. The nozzle used in these experiments is a B-37 nozzle. The characteristics of this nozzle are given in Table 2.4.

Table 2.4. Characteristics of B37 nozzle

	40	60	80	100	200
Flow rate (gph)	0.37	0.45	0.52	0.59	0.83
Flow rate (cc/s)	0.38	0.46	0.53	0.61	0.85
Sauter Mean Diameter (μm)	54	39.4	34.5	32.1	26.5

Table 2.4 is shown for water, and thus it is only indicative of the performance for the case of liquid fuels, which may be lighter or more viscous. The stream of droplets is further atomized by the fast flowing atomization air, which has a velocity on the order of 180 m/s at the exit of the air atomization nozzle (at 50 lpm STP flow rate, corresponding to ~ 1 g/s).

The fuel pump used to pressurize and monitor the flow rate was a variable displacement pump attached to a variable speed drive from Fluid Metering. The pump was calibrated by capturing and then weighing the fluid for a given amount of time. The adjusted parameter was the speed of the drive. The pump provides constant flow rate for pressures lower than about 200 psi, and we have stayed below this limit, operating close to 50 psi.

The system is controlled by a LabView software developed in our laboratory. The software continuously acquires and stores several parameters such as temperature, air and fuel flow rates during operation.

The composition of the gas is determined using both a gas chromatograph and a mass spectrometer.

The mass spectrometer is a Pfeiffer OmniScan 200. The device has a 200 micron ID capillary sampling line that is directly introduced into the reactor, at a location close to the exit of the reactor. The volume of the reactor upstream from the sampling point, including the plasmatron head volume, is about 1000 cm^3. The reactor volume is used in the calculations in the accompanying papers. The capillary is heated in order to prevent condensation in the column. The length of the capillary is about 1.5 m, and results in a time delay of about 3 s. This is a pure time delay. The device can take samples at a rate of 3 Hz, and the length of the capillary does result in small but measurable diffusion. Real time concentration of oxygen, methane, water and hydrogen can be obtained. Unfortunately, because of interference between N_2 and CO (with both masses of 28), it is not possible to reliably monitor either. The accompanying paper describing the startup of the plasmatron methane converter further described the MS system. The mass spectrometer is calibrated by placing gas standards through the plasmatron, and then measuring the signal. The signal is compensated by the pressure in the mass spectrometer.

The GC is an Agilent MTI-2000 model with two columns, one for permanent gases and the second one for hydrocarbons. The GC is calibrated using gas standards from BOC gases in the range approximately similar to those that are being measured. The GC sampling point is near the mass spectrometer location.

Special attention was given to measure the composition of the gas as accurate as possible. The results indicated that the GC has a reproducibility of about 8%. The mass flow controllers are calibrated at the manufacturer (Omega), and are supposed to have an accuracy of 1% through the middle of the range. The rotameters used in the experiments have an accuracy of about 5%. It was determined that the key parameter for the reforming, the O/C ratio, could vary by about 15%, and it differed from the measurements of the composition of mixed reagents, and that calculated from the inputs. However, during a given set of runs the deviation remained relatively constant, as some of the parameters were being slightly varied while the other remained constant. Thus, although comparison between experiments carried out in different days have the uncertainty in the O/C ratio of ~15%, results from a given set of results during the same set of experiments have decreased relative uncertainty.

There are one or multiple temperature sensors (thermocouple) located near the axis, at several places along the reaction extension cylinder.

Transient analysis with a mass spectrometer

In order to be able to use the mass spectrometer as quick, real time concentration analysis, it was necessary to develop both software and hardware. This section describes the mass spectrometer setup, which has been used for determining the transient behavior of plasmatron fuel reformers.

Description of the mass spectrometer

Typical conditions of the sample gas near the entrance to the capillary are shown in Table 2.5 for a capillary with an ID of 250 microns. It should be noted that the surface heat transfer coefficient, h, is so high that the gas in the capillary reaches the wall temperature very fast (in distances much smaller than 1 mm). Thus it is a safe assumption that the sample is at the same temperature as the capillary. The temperature of the capillary varies along its length. One section of the capillary is inside reactor, there is a section between the reactor and a heated blanket, and finally is the heating blanket section. At one end of the capillary, the temperature is determined by the gas in the plasmatron, at atmospheric pressure conditions. At the other, the pressure is vacuum, and the temperature is that of the heated capillary. The temperature of the heated capillary is 150 C (423 K).

Table 2.5. Values for a typical case for the capillary

p	Pa	101000
m dot	kg/s	2.5644E-07
T	K	1300
density	kg/m^3	0.27433337
v	m/s	51.2442538
cp	J/kg K	1196.13342
nu	m^2/s	0.00018873
nuf	viscosity	8.804E-05
k	W/mK	0.08331839
Re		88.7052633
Pr		0.74328058
Nu		169.079181
h	W/m^2 K	92437.0406

Next we calculate the velocity of the sample gas and the pressure along the capillary. It is assumed that the pressure drop is given by the Darcy relationship

$$dp/dx = f\ /D\ u^2/2$$

where f is the friction factor (also known as the fanning factor) and u is the local speed of the gas. The friction factor depends on the Reynolds number. For laminar flows, as in the case of flows in the capillary, the friction factor is given by

$$f = 64/Re$$

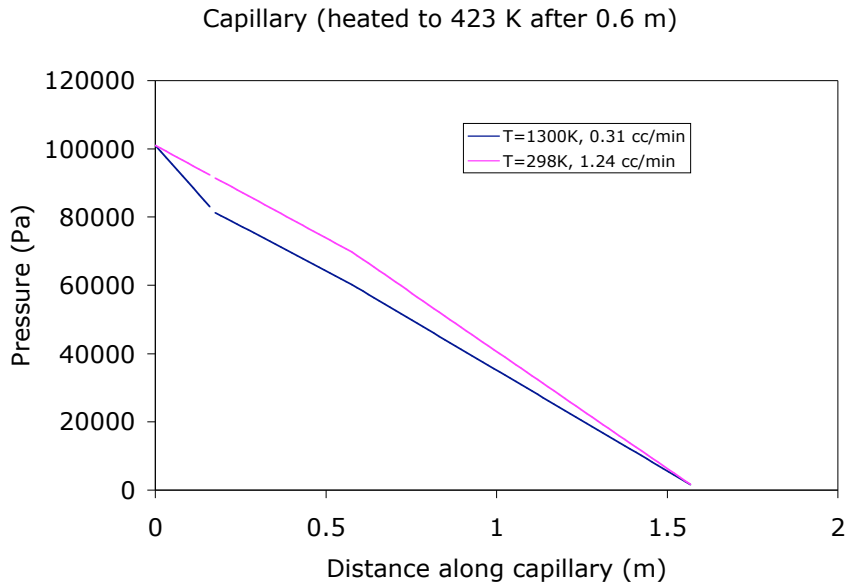

Figure 2.9. Pressure drop as a function of the distance along the capillary

16 cm of the capillary are inside of the plasmatron methane reformer exhaust tube, for direct sampling of the reformate. Two cases are analyzed. During calibration, the temperature of the first 16 cm of capillary is at room temperature (298 K), while during those times when the reformer is operating, the first 16 cm are at approximately1300 K, the temperature of the reformate.. After this region, there are 40 cm of capillary at room temperature, needed to plumb the distance between the reformer and the mass spectrometer. The rest of the capillary, inside a heating blanket and 1 m in length, is heated to 150 C (423 K). It is assumed that a 200 micron capillary is used.

The results are shown in Figures 2.9 and 2.10. Figure 2.9 shows the pressure along the capillary for both cases. The pressure has been calculated by dividing the capillary into small segments and calculating the pressure drop and the fluid properties at each segment. The flow rate is varied until the pressure becomes small and the flow becomes sonic (choke flow) at the capillary end that is in the mass spectrometer. The flow rate for the case of high temperature is 0.31 cc/min, while during calibration the flow rate is 1.24 cc/min (at STP). This result indicates that the pressure at the mass spectrometer should a strong function of the temperature of the gas being sampled. Because of this effect, the operating pressure during the experiments has been in the low 10^{-6} mbar region, somewhat lower than the recommended optimal pressure of the instrument.

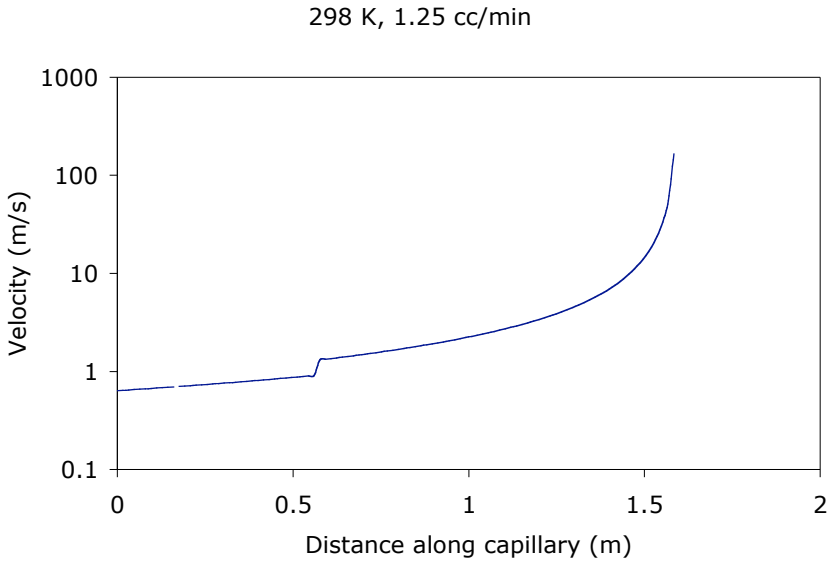

Figure 2.10 Velocity as a function of the capillary distance for the case at 298 K for the first 10 cm, 423K for the other 90 cm, and for a flow rate of 0.6 cc/min, for a 200 micron capillary.

The corresponding velocity of the sample along the capillary is shown in Figure 2.10, for the case with the room temperature inside the reactor. The discontinuity in the velocity and pressure at 0.6 m is due to the sudden change in gas temperature as the sample enters the section of the capillary that is inside the heating blanket. The velocity is increasing very rapidly towards the end of the capillary, and it should be sonic at the end of the capillary, where the model breaks down. The flow for which this happens is called the critical flow. For higher flows, the sonic region occurs inside the capillary, while for lower flows the pressure at the end of the capillary is substantially higher, and not consistent to the fact that the capillary ends in a high vacuum system (a few times 10^{-6} Torr). In these calculations it is assumed that the sonic boundary occurs at the end of the capillary. In principle, this is not necessary, as the flow can become molecular in nature (rather than viscous) through a section of the capillary. But in that case the time delay would be shorter than when the sonic boundary is at the end of the capillary, and thus this calculations provides an upper bound to the time delay.

Figure 2.11 shows the critical flow rate as a function of the capillary size, for the cases of both temperatures. The critical flow rate is proportional to the fourth power of the diameter of the capillary.

The temperature effect on the flow rate is substantial (about a factor of 4), from about 1.2 cc/min for 298 K to 0.3 cc/min for the 1300 K case). As the temperature increases, with viscosity a strong function of temperature, the critical flow through the capillary decreases.

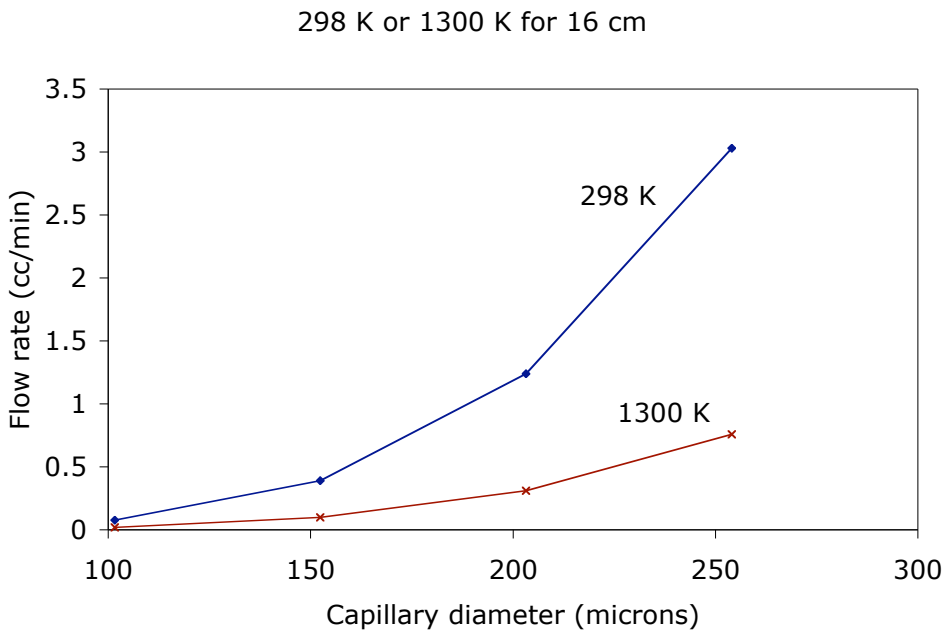

Figure 2.11. Flow rate as a function of the capillary size, for the cases of high and low temperatures in the plasmatron methane reformer exhaust.

Calculations vs experiments

The experimental results indicated that there was a 3 s delay at the high temperature, and a 0.5 s broadened rise time. In the experiments it was not possible to determine whether the broadening is due to the time response of the plasmatron methane reformer, or due to the resolution of the MS system (including the sampling).

The volume of the reactor is estimated to be 0.5 l (2in diameter, 10 in long), with a factor of 2 increase due to the volume in the exhaust tube upstream from the sampling point. Then, with 300 liter/min flow rate, it is estimated that the transit time through the reactor is about 0.2 s at room temperature, and that two transit times (for 2 e-foldings, for the case of mixing) is on the order of 0.4 s. For the warm reformate, the2-transit times are on the order of 0.1 s.

The transport delay time through the capillary is calculated through the integral

$$\tau_{delay} = \text{integral } (dl/v)$$

where dl is the step length along the capillary and v is the sample velocity along the capillary, calculated above.

The calculated time delays as well as the critical flow rates are shown in Table 2.5 as a function of the ID of the capillary, for both the lower temperature operation as well as the high temperature..

Table 2.5 Characteristics of MS capillary using simple model

Capillary ID	microns	102	152	203	254
τdelay (298 K)	s	3.5	1.6	0.9	0.6
Flow rate	cc/min	0.078	0.39	1.24	3.03
τdelay (1300 K)	s	12.35	5.50	3.13	1.99
Flow rate	cc/min	0.02	0.10	0.31	0.76

In order to reduce the response time to less that 5 s, it is necessary to use a 200 micron ID capillary. The flow rates are increased by more than 1 order of magnitude from that using a 100 micron capillary.

The experimentally measured pressure by the internal gauge is on the order of $1.9\ 10^{-6}$ mbar, or about $1.5\ 10^{-6}$ Torr.

In addition to the delay, there is a broadening of the transient, due to diffusion. To estimate the magnitude of the diffusion, assuming that the gas is hydrogen with a diffusion coefficient of about 10 cm^2/s, and assuming a transport time as shown in table 1, the diffusion time that is calculated is small.

It should be noted that there were discrepancies between the observed and measured. For one, when the plasmatron methane reformer was started, and the temperature of the exhaust increased to about 1300 K, there was not a large drop in the pressure of the capillary, as would have been predicted by the results shown in Table 2.5 However, the calculations have been useful in guiding the choice of the capillary, and in understanding the nature of the delay and the loss of resolution due to diffusion.

Using the experimental results it is possible to determined the e-folding of the concentration. The easiest and fastest method to change the concentration in for determining the time response of the mass spectrometer is by turning down the plasma during reforming, and looking at the changes in the ion currents. This is faster in our setup than changing the inputs (due to long piping). Using the results determined in the accompanying paper for propane [Bro05e] the e-folding of the concentration is found to be about 0.5 s, or 1 s for a 90% change. Thus it is not possible with the present setup to determine responses faster than this. As will be seen below and in [Bro05e], this is about the time constant of the changes.

Calibration with CFD code.

The simple model was tested using a commercially available CFD code, FLUENT. The calculations for a 1 m long capillary, 250 micron diameter, at 298 K, indicated a mass flow rate of $3.3\ 10^{-7}$ kg/s (needs double precision to converge). Using the simple model described above, the calculated mass flow rate is $1.15\ 10^{-7}$ kg/s, or about a factor of 3

lower. In order to make the two agree, the Reynolds model for the friction factor f was decreased until the two agreed. They did agree for a multiplier of 0.35.

3) Plasmatron applications to spark-ignition engine

Decreasing emissions from motor vehicles and increasing efficiency is a necessary step toward improving air quality and decreasing greenhouse gases. Internal combustion engines for transportation constitute the single largest consumer of imported oil and are also a major source of ozone-producing gases such as NOx that affect urban areas. A variety of potential improvements are presently being investigated: lean-burn engines; increased compression ratio; improved catalyst formulations; use of close coupled catalysts; new types of exhaust treatment; electric and fuel-cell powered vehicles; and alternative fuels.

A concept that could substantially reduce emissions is onboard hydrogen generation using microplasmatron fuel converters. Plasmatrons are electrical gas heaters that make use of the conductivity of gases at high temperature. Microplasmatron fuel converters are compact, rugged, can be used with a variety of fuels and provide rapid response. Large reductions in emissions from SI engines are possible using the hydrogen-rich gas produced by plasmatron conversion of hydrocarbon fuel. Increased flame speed in the cylinder extends the lean limit of SI engine operation [Hey88]. The combination of increased flame speed and lower flammability limits of hydrogen can thus stabilize combustion during lean operation.

Very lean operation could reduce engine NOx production by a factor of one hundred relative to stoichiometric operation [Bre7, Mac76, Hom83]. Hydrogen addition could also be used to reduce NOx emissions by facilitating use of increased exhaust gas recirculation (EGR) [Kur79]. Onboard production of hydrogen is also attractive for reduction of cold start emissions, as well as for catalyst regeneration and post treatment.

Hydrogen addition can also be found useful to increase the octane of the fuel, as both hydrogen as well as CO have high octane numbers [Top04]. The increase octane provided by the hydrogen rich gas can be used to increase the compression ratio of the engine or allow for turbocharging, further increasing the efficiency of the engine. Finally, the hydrogen rich gas may be useful during cold start, both minimizing the cranking, as well as potentially decreasing the hydrocarbon emissions due to cold start.

Concepts for use of plasmatron generated hydrogen-rich gas in spark ignition engines have been discussed in papers [Rab95, Coh96, Coh98, Bro99a]. Engine experiments have also performed using bottled synthesis gas [Bre73, Mac76, Hom83, Kir99], and with conventional reformers operating on methane [Smi97] or ethanol [Dob98,Hod98]. This program reports the first use of a compact plasma boosted reformer to convert gasoline into hydrogen rich gas which is then combusted in an internal combustion engine resulting in a large decrease in air pollutants [Gre00, Bro99b].

a) SI engine test setup and plasmatron performance

A gen-1 compact plasma boosted reformer was installed and tested on a production in-line four-cylinder SI gasoline-fueled engine (1994 General Motors Quad-4) at Oak Ridge National Laboratory (ORNL)). The Quad4 has a 2.3 L displacement, 9.2 cm bore, 8.5 cm stroke and compression ratio of 9.5. This engine is port-fuel-injected and does not utilize a turbocharger or exhaust gas recirculation. The engine was coupled to a 130 kW (175 hp) eddy-current (Power Dyne, Inc.) dynamometer for engine speed and load control. Engine control management was carried out with a TEC-II control system (Electromotive, Inc.) The TEC-II provided access to all calibration parameters (raw fuel curve, enrichment, spark advance, and exhaust O_2) for proper engine operation. The TEC-II control allows the user to set desired air/fuel ratios (lean, rich, and stoichiometric). It can also adjust the fuel automatically to maintain stoichiometric air/fuel ratio by monitoring the exhaust gas oxygen.

Along with engine operating parameters and in-cylinder pressure, engine out regulated emissions (CO, HC and NO_x) and PM were measured at each operating point. Total mass concentration and rate of PM was measured with a Tapered Element Oscillating Microbalance (TEOM, R and P Co. Model 1105). A scanning mobility particle sizer (SMPS, TSI, Inc.) measured PM size and number. CARB Phase II certification grade gasoline was used for engine and plasmatron operation. The gasoline equivalent air/fuel ratio was measured with a universal exhaust gas oxygen (UEGO) sensor (Horiba MEXA 110) in the exhaust stream. Therefore during reformate addition the reported equivalence ratio is actually slightly higher because of partial combustion in the microplasmatron.

The microplasmatron was operated with a constant gasoline throughput of 0.25 g/s. The reformate was cooled down to room temperature by a low pressure shell-in-tube heat exchanger. The composition of the microplasmatron output was continuously monitored using a conventional tailpipe emissions monitor (Horiba MEXA 554). Table 3.1 shows the measured parameters of the microplasmatron during experiments conducted at ORNL and MIT. The electrical power input to the microplasmatron was about 2% of the heating value of the fuel processed. This microplasmatron incorporated several design improvements which will be discussed in a later publication.

Experiments were conducted at two engine operating conditions: the first one at 2300 rpm and 4.2 bar brake mean effective pressure (BMEP); and the second one at 1500 rpm and 2.6 bar BMEP. Maximum brake torque (MBT) spark timing was defined for both operating conditions at stoichiometric conditions with the engine in closed-loop control mode. Once the MBT spark timing was defined for each condition, spark timing remained fixed as air/fuel ratio was increased with the engine in open-loop control mode. BMEP was also kept constant as air/fuel ratio was increased.

Table 3.1 Operating conditions for the microplasma reformer.

	at MIT (GC)	at ORNL (Horiba)
Power, W		270
Fuel flow rate, g/s		0.25
Composition of reformate		
CO	20%	18-21%
CO2	3.5%	4%
CH4	0.5%	
C2H4+C2H6	0.2%	
H2	16%	
N2	60%	
HC (ppm)		260-410

Reformate was introduced into the engine via the intake manifold downstream of the throttle. The overall hydrogen addition was relatively small, being about 4% of fuel heating value at the 2300 rpm condition and about 9% at the 1500 rpm condition. The maximum reformate flow rate was determined by heat removal limitations of the plasmatron reactor. Bench top tests are being conducted in the laboratory to remove this limitation.

b) Results

Figures 3.1 and 3.2 show the Coefficient of Variation of the gross Indicated Mean Effective Pressure (COV of IMEP) as a function of equivalence ratio for the two operating conditions. Both cases of baseline operation (without reformate addition) and the case with reformate addition are shown in the figures. The equivalence ratio in these figures has been determined from the exhaust gas composition. The presence of hydrogen in the engine substantially reduces the COV of IMEP, even at the 2300 rpm condition, when the reformate addition is a small fraction of the total fuel.

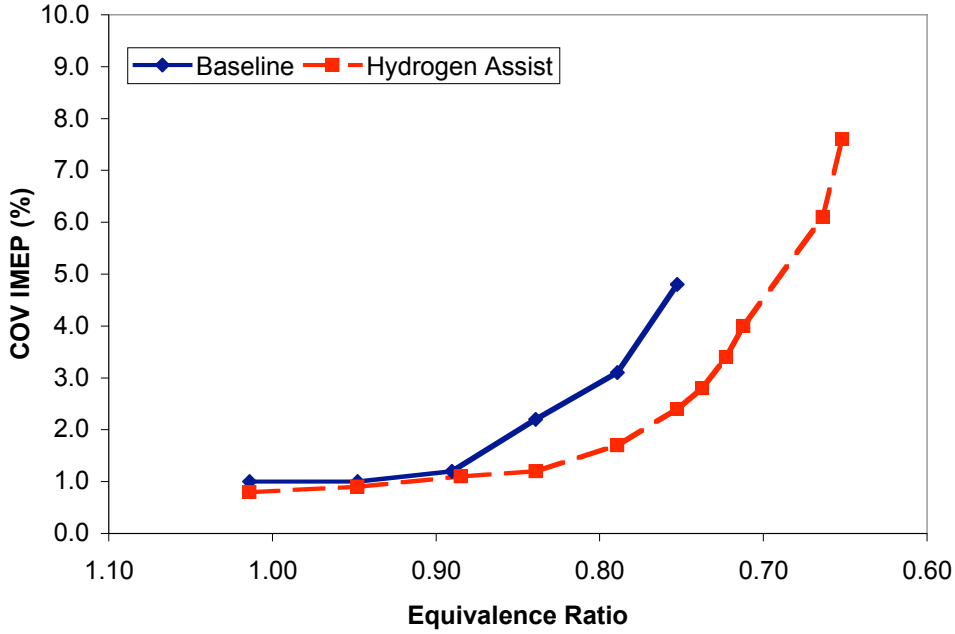

Figure 3.1. COV of IMEP as a function of exhaust equivalence ratio (1500 rpm, 2.6 bar BMEP).

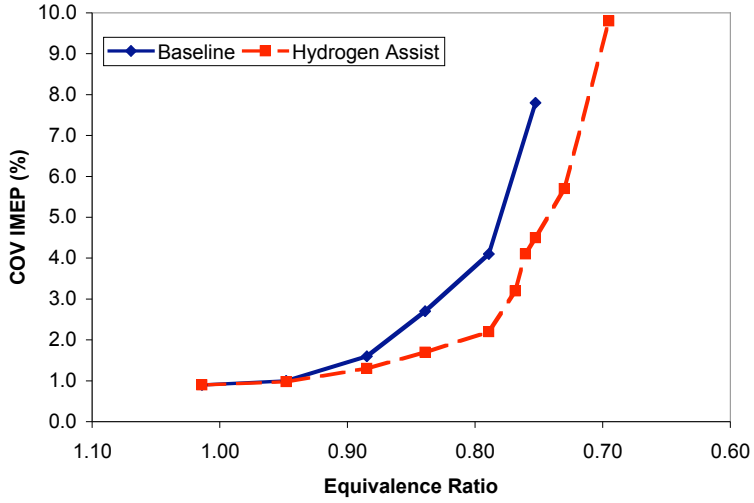

Figure 3.2. COV of IMEP as a function of exhaust equivalence ratio (2300 rpm, 4.2 bar BMEP).

Figures 3.3 and 3.4 show the NO_x emissions as a function of the COV of IMEP. The plots illustrate the reduction of NO_x emissions within acceptable levels of cycle-to-cycle combustion variations (3 to 5% COV of IMEP). The NO_x concentration decreases with the reformate addition for a given COV of IMEP, even with relatively small reformate addition. At a COV of 5%, NO_x is reduced by a factor of about a hundred by the addition of plasma boosted reformer generated hydrogen at 1500 rpm engine operation. Higher

reformate addition may be necessary, especially for the higher load cases. The plasma boosted reformer is presently being modified to provide increased hydrogen generation.

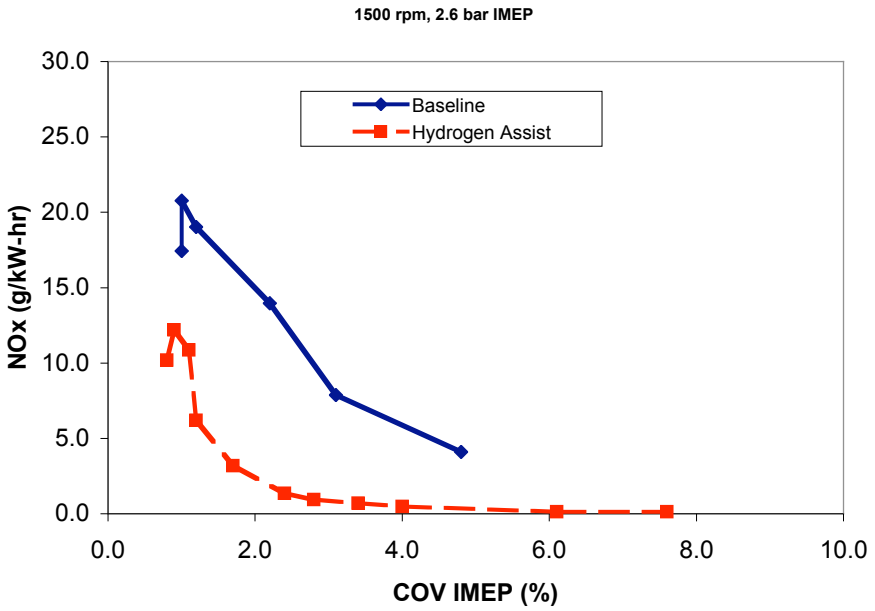

Figure 3.3. NOx emissions as a function of the COV of IMEP (1500 rpm, 2.6 bar BMEP).

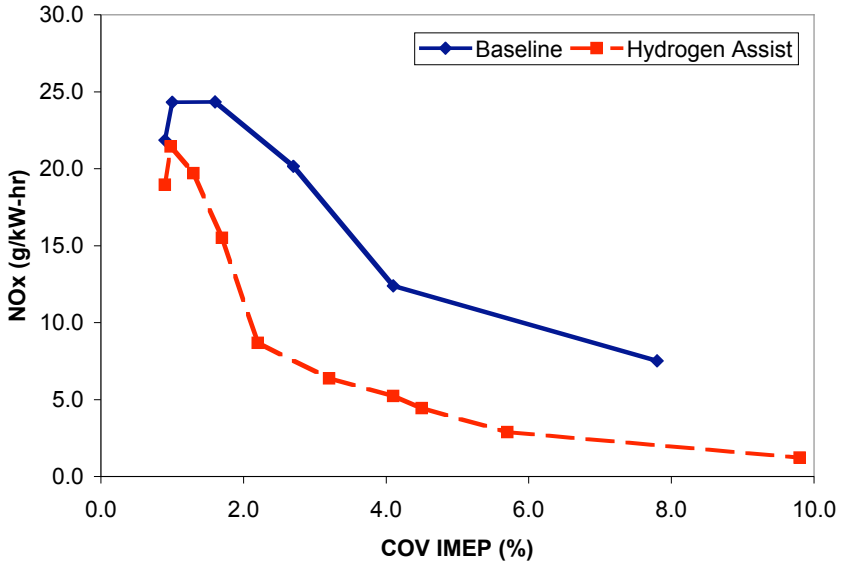

Figure 3.4. NOx emissions as a function of the COV of IMEP (2300 rpm, 4.2 bar BMEP).

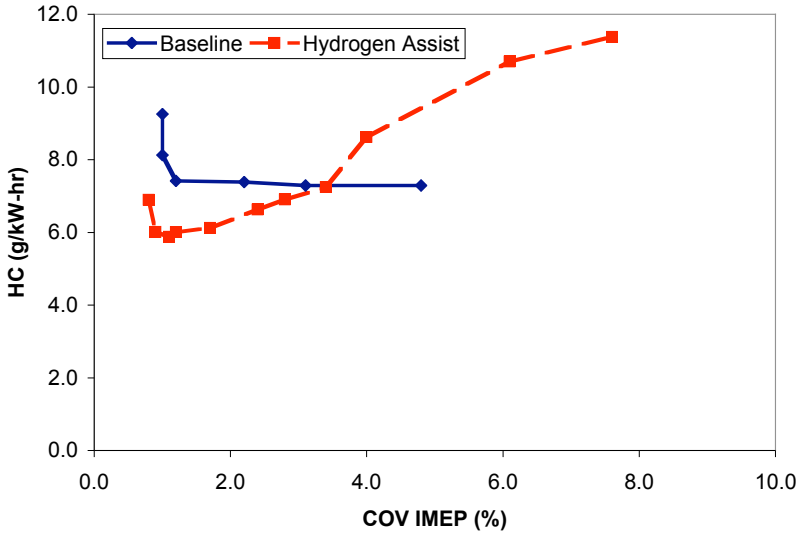

Figure 3.5. Hydrocarbon emissions as a function of the COV of IMEP (1500 rpm, 2.6 bar BMEP).

The corresponding concentration of hydrocarbons is shown in Figures 3.5 and 3.6, for the 1500 and 2300 rpm operating conditions, respectively. Decreases in HC emissions of about 20-30% are possible. Larger effects could be possible with the additional of increased amounts of hydrogen rich gas.

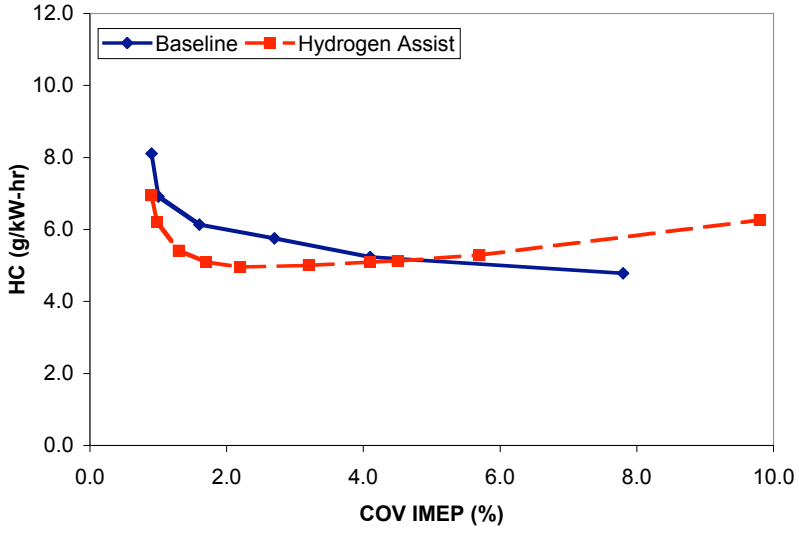

Figure 3.6. Hydrocarbon emissions as a function of the COV of IMEP (2300 rpm, 4.2 bar BMEP).

Particulate mass emissions as measured by the TEOM showed very low values for both the baseline and reformate addition cases. Figure 3.7 shows the relative mass emissions decrease from the baseline stoichiometric case. Although the TEOM was approaching its

lower sensitivity limits, the trend is still clear; decreasing equivalence ratio leads to lower PM mass emissions. In addition to PM mass, PM size distribution was measured. Figure 3.8 shows that there appears to be an *increase* in particle number with decreasing equivalence ratio. Although this seems to contradict the PM mass emissions decrease, the proportion of larger diameter (and heavier) particles decreases with decreasing equivalence ratio.

c) Discussion

The addition of reformate stabilized lean operation resulting in lower NO_x emissions. Similar results should be obtainable with reformate addition at high EGR levels. Actually, the exhaust gas has a larger heat capacity than air (due to the higher concentration of tri-atom molecules in the exhaust gas), and therefore NO_x reduction with EGR should be larger than with air [Hey88]. Tests are being planned to investigate the effects of EGR with reformate addition.

In a similar fashion to other reformer concepts such as those used for reforming ethanol [Dob98,Hod98], the plasma boosted reformer is also ideally suited for cold-start operation, due to the fast turn on time of the plasma. Even in the absence of air/fuel preheat in the plasmatron system, the overall efficiency of the system should be comparable to that in present engines. The time of operation without preheat and with a high fraction of fuel to the plasmatron is limited to the cold start and is thus very small. During cold start a high fraction of the fuel would be converted into hydrogen-rich gas. As soon as the catalyst is warmed up, the fraction of processed fuel would be decreased.

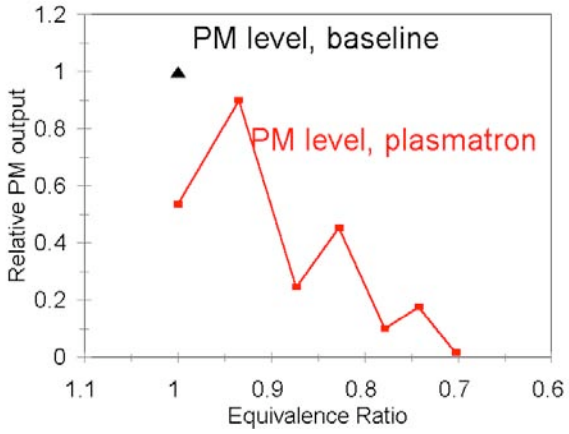

Figure 3.7. Relative PM emissions as a function of equivalence ratio (1500 rpm, 2.6 bar BMEP).

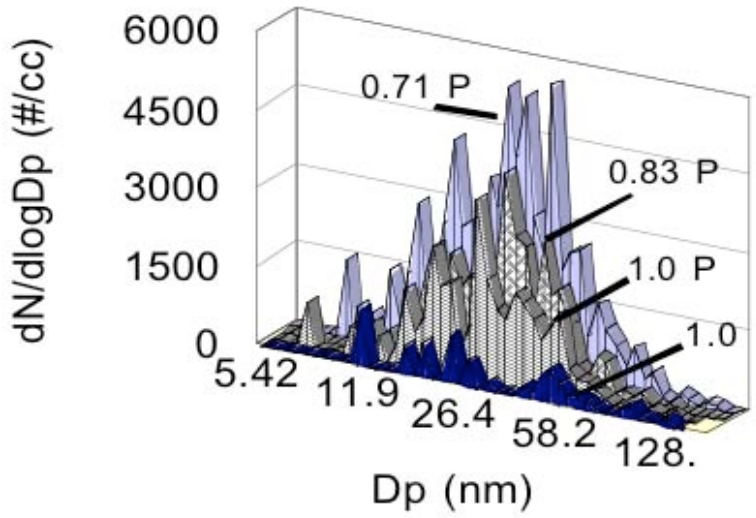

Figure 3.8. Particle size distribution for four different equivalence ratios (designated by labels) at 1500 rpm, 2.6 bar BMEP. P designates microplasmatron assist. Note the overall numbers are very low.

4) Plasmatron application to aftertreatment I: NOx trap

Plasmatron reformer technology has been evaluated for regeneration of NO_x adsorber after-treatment systems. [Bro03] At ArvinMeritor tests were performed on a dual-leg NO_x adsorber system using a Cummins 8.3L diesel engine both in a test cell and on a vehicle. A NO_x adsorber system was tested using the plasmatron reformer as a regenerator and without the reformer (i.e., with straight diesel fuel based regeneration as the baseline case. The plasmatron reformer was shown to improve NO_x regeneration significantly compared to the baseline diesel case. The net result of these initial tests was a significant decrease in fuel penalty, roughly 50% at moderate adsorber temperatures. This fuel penalty improvement is accompanied by a dramatic drop in slipped hydrocarbon emissions, which decreased by 90% or more. Significant advantages are demonstrated across a wide range of engine conditions and temperatures. The study also indicated the potential to regenerate NO_x adsorbers at low temperatures where diesel fuel based regeneration is not effective, such as those typical of idle conditions. Two vehicles, a bus and a light duty truck, have been equipped for plasmatron reformer NO_x adsorber regeneration tests.

a) Introduction

In order to meet stringent US emissions regulations for 2007-2010 diesel vehicle model years, after-treatment technology is being developed. Both particulate and NO_x emissions after-treatment technology will be necessary, as it seems that engine in-cylinder techniques alone will be unable to meet the regulations.

The purpose of the present work is to develop hydrogen based technology for addressing after-treatment issues. In this paper recent developments in both the technology for on-board generation of hydrogen as well as applications to NO_x after-treatment issues will be discussed.

Potential on-board generation of hydrogen from renewable energy biofuels for the transportation sector is also discussed. This application could provide a means to alleviate oil dependency and reduce greenhouse gas emissions.

b) Plasmatron technology for NOx aftertreatment

An absorber catalyst can be used for first trapping the NOx in diesel engine exhaust, and then chemically reducing it during regeneration periods. The process of trapping could be either catalytic absorption or adsorption, or conventional absorption or adsorption [Cam99]. The catalyst for NOx treatment is very sensitive to poisoning by sulfur. In order to solve this problem, a sulfur trap is under development [Par99a, Parks99b], in

conjunction with the development of NOx absorber catalysts that are more sulfur tolerant. In this case, the sulfur and the NOx traps are regenerated simultaneously

Experimental studies of combined SOx and NOx traps have been carried out recently by Goal Line Technologies [Par99a, Par99b]. These studies examined both the use of diesel fuel and hydrogen as reducing agents for trap regeneration. Greater than 90% NOx removal was obtained. Further work is needed to determine effects of sulfur on catalyst lifetime and the differences in the use of diesel fuel and hydrogen rich gas for catalyst regeneration.

Goal Line Environmental Technologies has recently claimed a 98.9% reduction in NOx and Hydrocarbon (HC) emissions from diesel engines at their test facility last spring. Using their proprietary catalyst system, attached to a Cummins 50-kW/86-bhp diesel engine, NOx and HC have been reduced to 0.4 grams per brake horsepower-hour (g/bhph), an emissions reduction that is a full order of magnitude lower than the U.S. EPA's 2002 emission reduction requirement of 4.0 g/bhph for diesel engines.

A similar process may be used for trapping/regenerating particulates. The harmful or noxious emission can be trapped in one system, and then released and treated in a downstream unit (engine or another catalyst).

A recent patent by Daimler Benz [Boe99] describes the regeneration of one of the catalyst while the other is in the adsorbing mode. This patent discusses a motor vehicle exhaust emission control system that has tandem adsorber catalysts connected in parallel for alternate adsorption and desorption. NOx from the engine goes to the operating adsorber catalyst while the other adsorber catalyst is in the desorption mode. An oxidizing converter is located upstream of the adsorber part and near the engine for oxidation of the NO contained in the exhaust to form NO_2, so as to permit an increase in the NOx adsorption rate for the nitrogen adsorber parts. A reducing agent is used to regenerate the catalysts.

c) Advantages of Compact Plasmatron Fuel Converters

The use of compact plasmatron fuel converters in systems for regeneration of these catalysts could provide a number of significant advantages. Hydrogen rich gas is a significantly stronger reducing agent than diesel or gasoline. Use of hydrogen rich gas could potentially provide:

- Higher regeneration effectiveness
- Reduced poisoning of catalyst (since diesel fuel is not used for regeneration)
- Reduced emissions of hydrocarbons, since it is easier to prevent release of hydrogen and CO than hydrocarbons due to faster catalytic removal
- Reduced loss in overall fuel efficiency due to lower requirements on amount of reducing gas and greater ease of reuse of hydrogen rich gas in the engine.
- Shorter regeneration time due to greater reducing capability of hydrogen rich gas and high concentration of reducing gases.

- Reduced adverse effects of sulfur (hydrogen-sulfur interactions could reduce sulfur poisoning effects)

Compact plasmatron reformers are very well suited for the required hydrogen-rich gas generation due to:

- Robustness when operating with diesel fuel
- No soot production
- High efficiency
- Low cost
- Small size and weight
- Rapid reformer response
- Warm up capability provided by hot gas, since the hydrogen rich gas from the compact plasmatron fuel converter is hot; catalyst warm-up time could be decreased, or the catalyst could be further heated up during regeneration.

d) Catalyst regeneration estimation

Figure 4.1 shows a schematic diagram of a compact plasmatron fuel converter feeding hydrogen rich gas to a NOx-absorber/adsorber and/or a particulate trap catalyst. In the case of the NOx absorber catalyst, the injection of hydrogen rich gas reduces the nitrogen in NO and NO_2 to N_2. Hydrogen rich gas produced from partial oxidation (which can consist of approximately 20% H_2, 20% CO with the balance mainly N_2) is a powerful reducing agent.

In catalyst regeneration by direct injection of hydrogen rich gas, the exhaust flow from the engine is diverted from the catalyst to be regenerated. The diverted exhaust flow may be sent to a second catalyst. Hydrogen rich gas is then rapidly injected onto the catalyst. Some of the gas from close-cycle operation of the NOx-absorber catalyst needs to be released, in order to prevent pressure buildup in the closed system. The gas from the catalyst during regeneration can be sent to the engine, a second catalyst and/or the plasmatron fuel converter.

There are several variations in which the compact plasmatron fuel converter can be combined with the catalysts. In one variation, the compact plasmatron fuel converter is integrated with the NOx-absorber catalyst. If there are two NOx-absorber catalyst units, then two compact plasmatron fuel converters are required. An alternative approach consists of a single plasma fuel converter, directing the hydrogen rich gas into the unit that is being regenerated. This method of operation saves on the cost of the plasma fuel converter units, but requires a high temperature valve. A high temperature EGR valve could be used for this purpose. If the gas from the NOx-absorber catalyst being regenerated is to be recycled, either in the engine, in the compact plasmatron fuel converter or in the other NOx-absorber catalyst unit, then it is necessary to have a valve at the exhaust to control the flow of the gases.

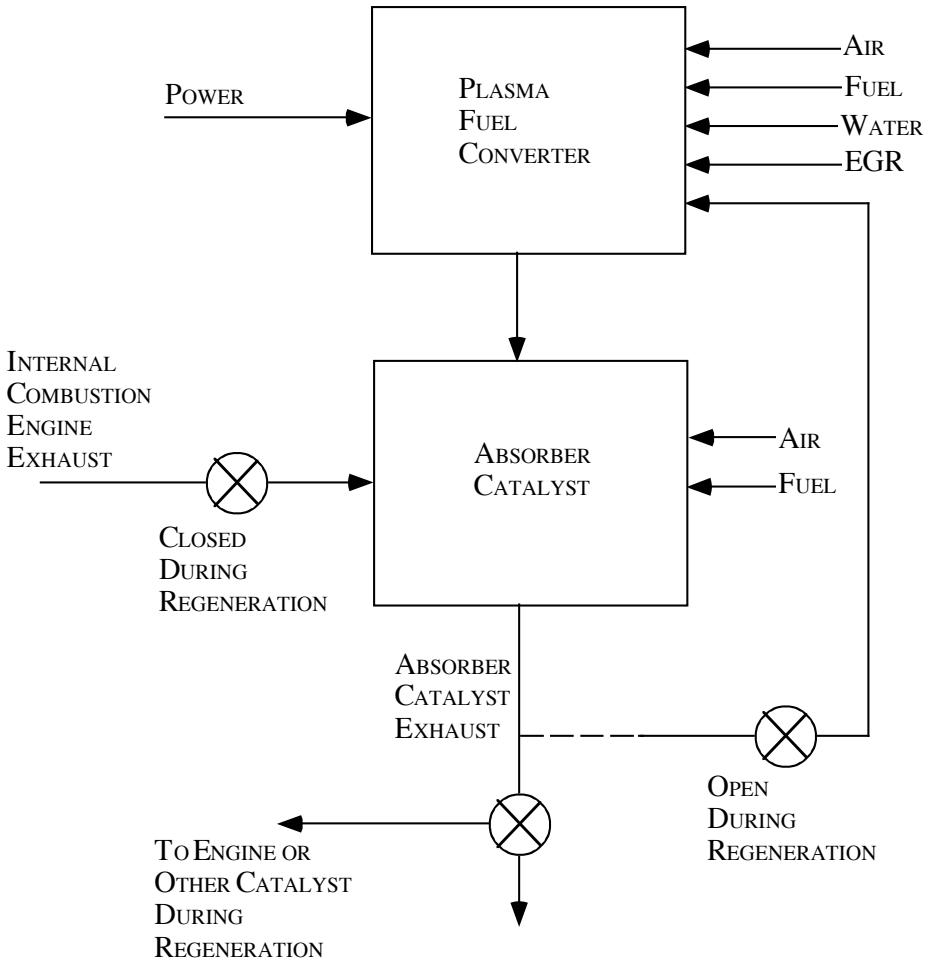

Figure 4.1 Schematic diagram of a compact plasmatron fuel converter/absorber catalyst system for the treatment of engine exhaust emissions.

It is also possible for the plasma fuel converter to operate while the engine is operational. The hydrogen rich gas could be used in the engine and may result in reduced engine-out emissions. During absorber catalyst regeneration, part or all of the hydrogen rich gas from the plasma fuel converter can be redirected into the absorber catalyst unit. The hydrogen rich gas production rate by the compact plasmatron reformer could also be increased.

The devices described above could also be used, with a modification of the absorber catalyst, to treat other emissions. It may be useful to employ a system that uses a particulate trap that is regenerated by the injection of hydrogen rich gas, with or without an oxidant. In this embodiment, the hydrogen rich gas could also be used, along with some free oxygen, for burning the particulates deposited in the particulate trap. Or if the temperature of the trap is high enough, it could be used for gasification of the particulate, without the use of an oxidant. The absorbing and or gasification processes could be either homogeneous of catalytic in nature.

Illustrative parameters for a compact plasmatron-fuel converter system regenerating an absorber catalyst are shown in Table 4.1. It is assumed that the hydrogen throughput requirements are twice stoichiometric, and that the CO that is produced in the compact plasmatron fuel converter does not help reducing the catalyst. Hence, there is a margin of a factor of 4 in the flow rate of reducing agent relative to the best possible conditions. The actual amount needs to be experimentally determined. Based on the illustrative parameters in Table 4.1, if all of the chemical energy in the fuel used for regeneration were lost, the loss in chemical energy would be around 2% of the mechanical energy produced by the engine. Taking engine efficiency into consideration, this loss then translates into less than 1% loss relative to total fuel chemical energy to produce the mechanical power. The required hydrogen-rich gas generation level has been demonstrated in initial tests by the use of low current plasmatron fuel converters for conversion of diesel fuels.

Table 4.1
Compact plasmatron fuel converter/absorber system
Illustrative parameters

Engine NOx production	g/bhp-hr	6		
Engine power	hp (kW)	30 (23)	60 (45)	120 (90)
Engine NOx rate	g/hr	180	360	720
Low power plasmatron				
Average electrical power requirement	W	9	18	35
Plasmatron duty cycle	%	4%	8%	16%
Plasmatron peak power	W	220	220	220
Average chemical power of diesel fuel to plasmatron	kW	0.5	0.9	1.8

Plasma technology can be used to accelerate chemical reactions. Two modes of operation have been explored for promoting fuel reformation into synthesis gas (hydrogen and carbon monoxide). The first uses thermal plasmas, where electrons, ions and neutral particles are generally in thermal equilibrium, and at high average temperature. This technology has the disadvantages of high current operation (associated with high electrode wear), and high energy consumption. The second mode of operation, using special low current plasmas, has the advantage of low power consumption and long electrode life. However, successful operation of the plasma process is more sensitive to design and operation. In this section, operation of a low current plasmatron as a device for converting hard to reform fuels to synthesis gas is described.

Fuel conversion is accomplished using the process of partial oxidation. In this mode, enough oxygen is supplied in order to capture each carbon atom in the fuel as carbon monoxide, with the hydrogen released as hydrogen molecules. The nitrogen from the air (as air is used as the oxidizer), is inert at the temperatures and pressures of operation, and thus goes unaffected in the reactor.

The use of the plasma allows for a robust reaction initiation for air/fuel mixture. The advantages of this technology include

- fast start up and rapid response,
- relaxation or elimination of catalyst requirements
- effective reforming in compact devices, attractive for onboard applications
- efficient conversion from liquid hydrocarbons to synthesis gas

The technology can be used for a broad range of fuels, from light, low viscosity liquids, such as ethanol, to high viscosity liquids, such as diesel and bio-oils.

The small size enables the use of fuel reformers for multiple applications on vehicles. These applications include:

- Diesel engine exhaust after-treatment
- Use of renewable energy bio-oils
- Fuel supply and ignition control in HCCI (homogeneous charge compression ignition) engines
- Spark ignition engines using hydrogen enhanced ultra-lean turbo-charged operation

Figure 4.2. Compact low power plasmatron fuel converter used for these tests

For diesel engine exhaust after-treatment, onboard hydrogen production can be used in the regeneration of either NO_x or particulate traps. The NO_x trap regeneration application will be discussed later in this paper. In the HCCI application, the use of fuel reformation to supply a portion of the fuel allows adjustment of engine charge temperature and fuel ignition characteristics providing a means of ignition control. In the spark ignition engine application, hydrogen rich gas addition allows ultra lean operation and can facilitate the use of high compression ratio and strong boosting. Hydrogen enriched combustion in a turbo-charged high compression ratio engine can provide both increased efficiency and

reduced emissions. System optimization studies indicate that a substantial increase in fuel efficiency (up to a 30% increase in net efficiency) and decrease in NO_x emissions are achievable.

Present plasmatron reformers have volumes on the order of 1-2 liters, with an electrical power consumption of about 250 W. Figure 4.2 shows a photograph of a recently developed plasmatron. The plasmatron is followed by a reaction section which provides time for the development of homogeneous reactions. When high hydrogen yields are desired, a catalyst can be placed downstream from the homogeneous zone.

At present, goals for the diesel plasmatron reformer development includes increased flow rates, operational and configuration optimization and increased simplicity, among other goals.

e) Biofuel reformation

At MIT, plasmatron reforming technology has been used with for a wide range of biofuels. These fuels include corn, canola and soybean oils (both refined and unrefined), and ethanol.

Reformation was achieved with a plasmatron fuel reformer optimized for diesel fuel operation. The device operated at 200 W of electrical power, and at stoichiometry for partial oxidation (O/C ratio ~ 1.1). The available energy from the reformate flow rate was about 20 kW (LHV of the reformate gas, as calculated from the LHV of compounds measured in the gas analysis). Some of the oxygen required for the reformation is provided by the fuel itself; the O/C ratio includes this oxygen,

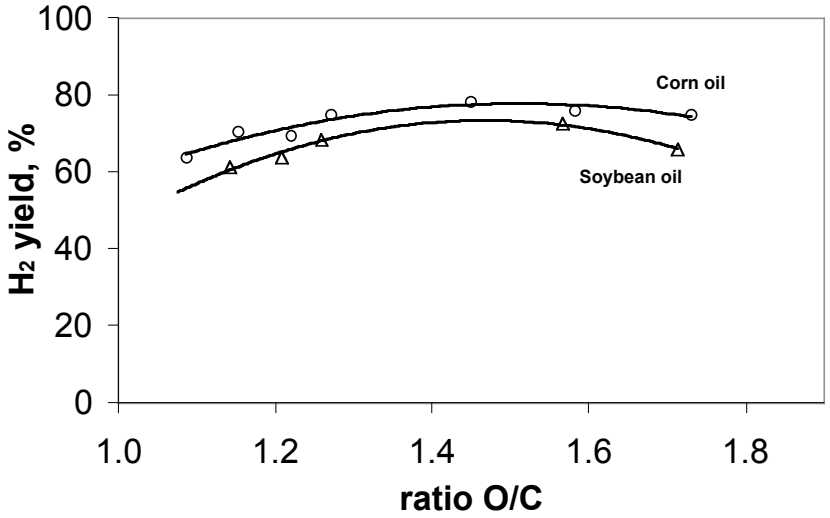

Figure 4.3. Hydrogen yield as a function of the O/C ratio, for corn and soybean oils

Figure 4.3 shows results from the reformation as a function of the O/C ratio, for corn and soybean oils. The hydrogen yield is defined as the ratio of the flow rate of hydrogen in the reformate to the flow rate of hydrogen in the fuel. A hydrogen yield of 1 thus means that all the hydrogen in the fuel has been released as hydrogen in the reformate. High hydrogen yields are possible (greater than 80%), even at relatively high O/C ratios.

The results in Figure 4.3 were carried out with a plasmatron reformer that incorporated a nickel catalyst on a crushed alumina substrate. In the absence of a catalyst (for a homogeneous reaction), the hydrogen yields are about 40%, coupled with high concentration of light hydrocarbons (~4-5% C_2H_4)

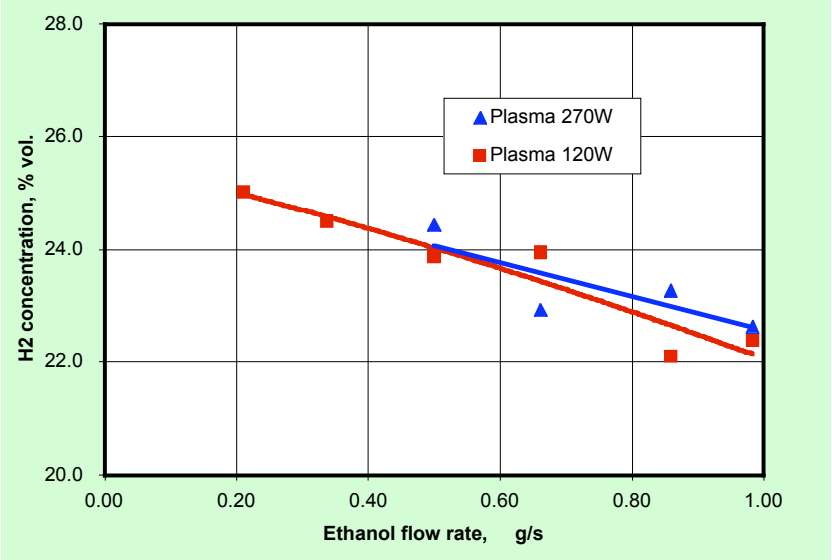

Figure 4.4. Hydrogen concentration in dry gas for ethanol reforming, as a function of flow rates, for O/C ~ 1.2

The presence of soot was determined using an opacity meter. Virtually no soot was observed in these experiments.

Similar experiments for ethanol are shown in Figure 4.4, for different powers and varying flow rates. Ethanol conversion is difficult to perform homogeneously because of the low exothermicity of the partial oxidation reaction. Figure 4.4 shows the hydrogen concentration of the partial oxidation of ethanol, for O/C ~ 1.2.

f) Diesel reformation

The plasmatron fuel converter has been further developed for use with diesel fuel. The goal of reformation of diesel by the plasmatron fuel converter is the conversion of the heavy diesel compounds into hydrogen, carbon monoxide, and light hydrocarbons for use in after-treatment applications. The diesel reformate produced by the plasmatron fuel converter has little residual oxygen and little or no soot. The diesel plasmatron can be cycled on and off quickly(~ 3-5 sec). For diesel after-treatment applications the dynamic performance of the plasmatron fuel reformer is important because of the low duty cycle

of operation. For NO_x catalyst regeneration applications, the plasmatron may be turned on for a few seconds every half minute or so. For diesel particulate filter applications, the plasmatron could well be operated for a few minutes every few hours resulting in much smaller duty cycles.

Results for diesel conversion without a catalyst are shown in Table 4.2. Typical O/C ratios are 1.1, with opacity readings of 0.0% (below the resolution of the device), for flow rates on the order of 1 g/s. The energy conversion efficiency, defined as the lower heating value of the reformate divided by the lower heating value of the fuel, is about 70%. The lower heating value of the reformate is calculated using the measured composition of the reformate.

Table 4.2 Diesel reforming without a catalyst

Electric power	W	250
O/C		1.1
Diesel flow rate	g/s	0.8
Corresponding chemical power	kW	35
Concentration (vol %)		
H2		8.2
O2		1.4
N2		68.7
CH4		2.6
CO		14.3
CO2		4.7
C2H4		2.4
C2H2		0.0
Energy efficiency to hydrogen, CO and light HC		70%
Soot (opacity meter)		0

If higher yields of hydrogen are desired, a catalyst can be placed downstream from the homogeneous zone. The absence of oxygen in the reformate due to the partial oxidation process minimizes the occurrence of hot spots within the catalyst. This alleviates one of the catalyst durability issues.

Hydrogen is a powerful reductant, and its use for the regeneration of NO_x traps has been researched in catalyst reactor labs. The goal of the work presented next is to determine the advantages of H_2 assisted NO_x trap regeneration, using the plasmatron fuel reformer as the source of on-board hydrogen.

g) Hydrogen assisted NO_x Trap Regeneration at ArvinMeritor

The objective of this testing was to determine the advantages of H_2 assisted NO_x trap regeneration [Par02] and to establish the feasibility and effectiveness of H_2 assisted NO_x traps in a bus and light duty vehicle installation. Initially preliminary experiments were carried out in a test cell using simulated reformate bottled gas. Subsequently due to the promising results, tests using an actual plasmatron fuel reformer have been performed, both in a test cell and on board vehicles. Plasmatron diesel fuel reformer systems have

been installed in a Ford F-250 truck to investigate light-duty applications, as well as in a Gillig transit bus, to test heavy-duty applications.

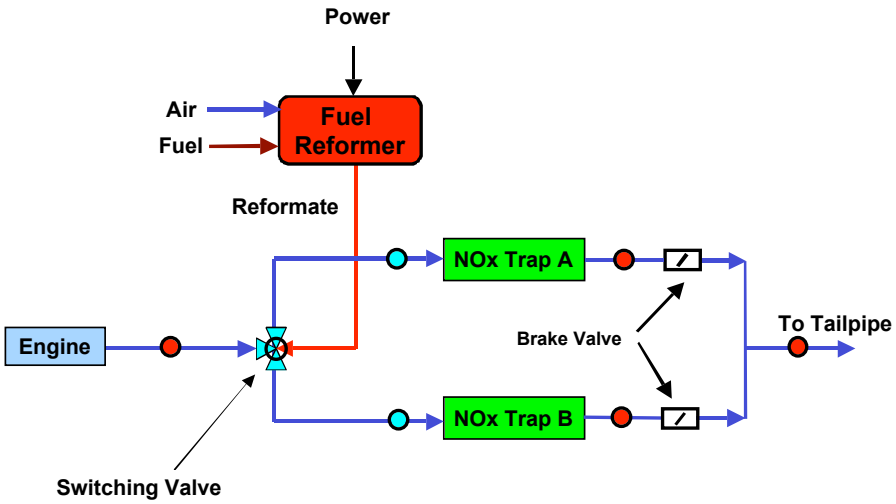

Figure 4.5. Test set-up for hydrogen assisted NOx traps

(a) (b)

Figure 4.6. Test cell installation of hydrogen assisted NOx traps: a) Cummins engine; b) dual leg (14 liter/leg) traps and switching valve

h) Test cell setup and results

A schematic of the test cell NO_x trap system is shown in Figure 4.5. The system is a dual leg arrangement of NO_x traps, with a single valve that simultaneously switches the exhaust and reformate flows, so that while one leg is undergoing regeneration off-line, the other leg is adsorbing NO_x. A single plasmatron is used to feed hydrogen rich reformate to both traps. The regeneration of a NO_x adsorber requires a reducing atmosphere (zero oxygen). Due to the free oxygen in diesel exhaust, any leakage past the

switching valve increases the required reformate flow since this oxygen must be consumed by reaction with the H_2 and CO in the presence of the precious metals on the NO_x adsorber surface in order to reach a reducing environment. Therefore zero exhaust leakage past the switching valve is ideal. Flow bench tests of the switching valve and adsorber system indicated a 3% leakage rate. For the Cummins ISC 8.3L engine used in this testing, the available plasmatron reformate flow rate was marginal at a high engine exhaust flows with 3% leakage. An exhaust brake valve was added to each leg as indicated in the schematic. When the brake valve was closed on the regenerating leg the exhaust flow leakage was reduced to an acceptable 1%.

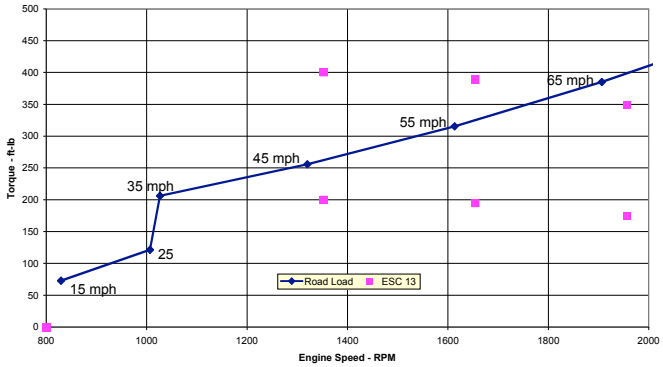

Figure 4.7. Bus Road Load vs ESC 13 mode

A photograph of the actual test cell setup at Analytical Engineering, Inc. (AEI) is shown in Figure 4.6. Extensive instrumentation was utilized including a chemi-luminescent NO_x analyzer, NO_x sensors, multiple thermocouples, and a V&F hydrogen analyzer. The fuel reformer, switching valve, and brake valves were all computer controlled. A MY2000 Cummins 8.3L engine was used in these tests. Zero sulfur diesel fuel was used in this testing to avoid sulfur poisoning of the traps. Also the engine oil used was a special low sulfur formulation for the same reason. Even with these measures some minor adsorption degradation was observed over the course of testing.

Two sets of engine operating points were used in this testing: the European Stationary Cycle (ESC) 13 modes and a calculated Bus Road Load curve. Figure 4.7 compares the operating points. The ESC 13 Mode test is a steady state mode weighted substitute for transient emissions testing. Since the NO_x adsorbers used in these tests were low temperature (barium based) adsorbers [Wan01, Fan02], only the ESC modes below 50% load were tested. The exhaust temperatures at the ESC modes above 50% load were too high (> 450 ˚C) for these traps to adsorb effectively. Due to the potential low temperature application of H_2 assisted NO_x trap regeneration, a series of calculated bus road load points (37K lb. GVW) were also tested. Below bus speeds of 45 mph, the road load points were at lighter loads with lower exhaust temperatures than the ESC points. All of the operating points were tested for NO_x regeneration using both reformate and diesel fuel injected into the exhaust as reductants for performance comparison.

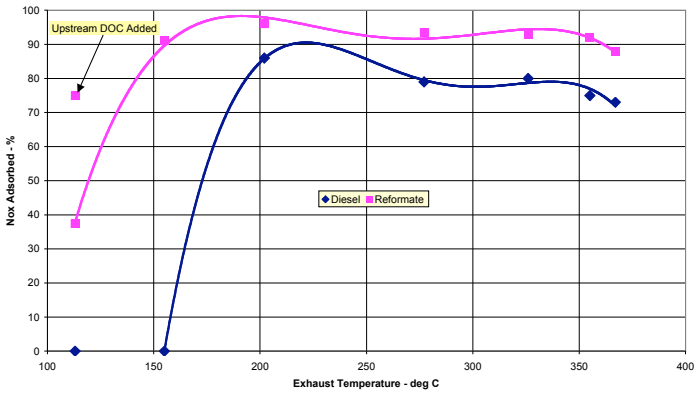

Figure 4.8. NOx adsorption comparison. Bus Road Load, at same fuel penalty (reformate vs diesel)

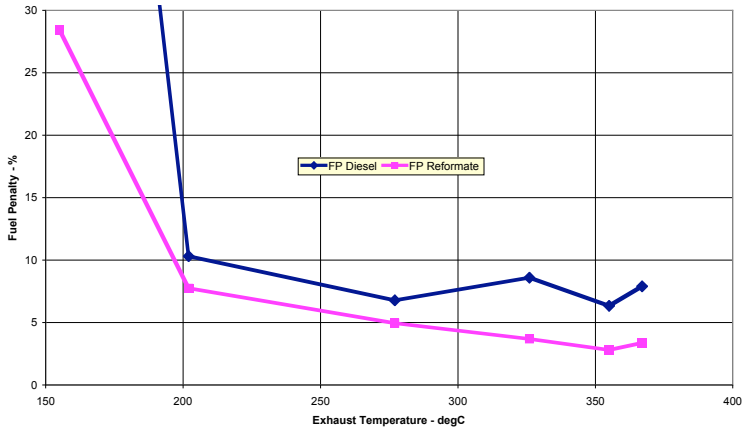

Figure 4.9. Fuel penalty for Bus Road Load, at same NOx adsorption

Two comparisons of performance were tested: (1) %NO_x adsorbed at the same fuel used penalty, and (2) fuel penalty for the same NO_x adsorbed. These two comparisons are made for both the bus road load points and the tested ESC modes. Figures 4.8, 4.9, 4.10, 4.11 show these results. All of the reformate regenerations were for a 5 second duration with the fuel reformer processing 0.8 g/s of fuel. The NO_x trap adsorption time was varied with load to keep the minimum instantaneous NO_x adsorption greater than 70%. For the diesel injection regeneration at constant fuel penalty the total injected fuel quantity was kept at 4 g and the adsorption time was the same as the reformate case. For equivalent NO_x adsorption with diesel injection regeneration the injection rate was constant and the regeneration time varied as well as the adsorption time. Clearly reformate regeneration of

NO_x traps is superior at all the operating points tested both in terms of $\%NO_x$ adsorbed at the same fuel penalty and the fuel penalty for equal NO_x adsorption.

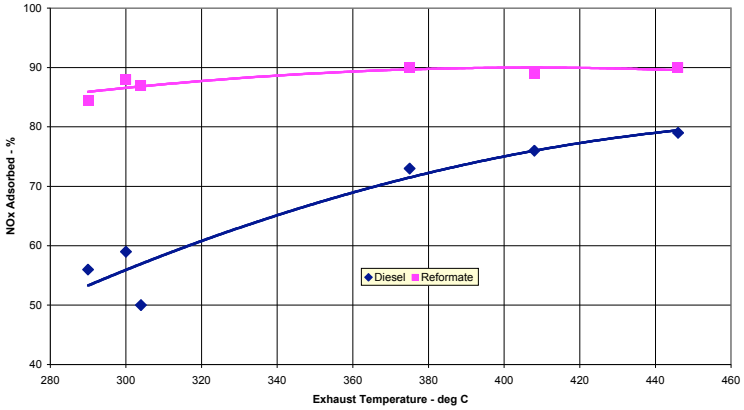

Figure 4.10. NOx adsorption comparison. ESC Modes at same fuel penalty (reformate vs diesel)

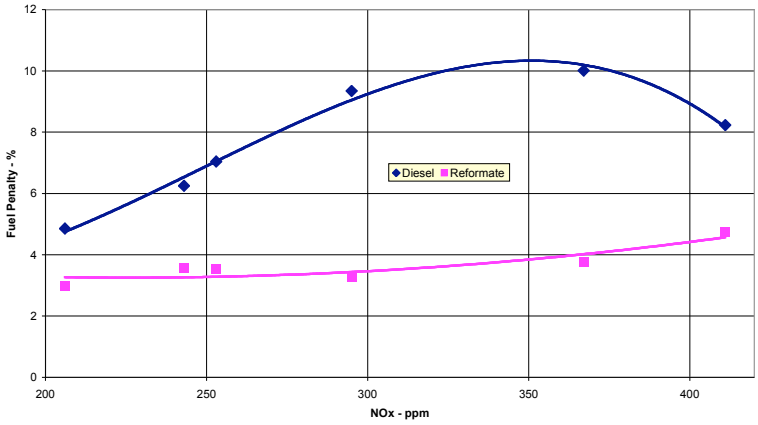

Figure 4.11. Fuel penalty for ECS Modes, at same NOx adsorption

The reformate regeneration advantage at low exhaust temperatures is especially obvious in the bus road load comparisons. Below 180˚C the diesel injection regeneration falls from 70% adsorption to zero at 158˚C. Reformate regeneration still achieves 90% NO_x adsorption at 158˚C. At idle conditions with adsorber inlet temperature at 113˚C reformate regeneration resulted in 38% NO_x adsorption. The addition of an oxidation catalyst upstream of the NO_x trap increased the NO_x adsorption to 75% at 113˚C with reformate regeneration. Note that direct injection of diesel fuel into the exhaust for NO_x trap regeneration at these low temperatures is totally ineffective. In addition other testing with different NO_x trap formulations and simulated reformate has shown regenerations at

exhaust temperatures as low as 80˚C. The ESC modes show a 15 to 50% better NO_x adsorption at the same fuel penalty with reformate versus diesel regeneration. At the same NO_x adsorption the ESC modes show a 40 – 60% fuel penalty advantage of reformate versus diesel regeneration. These fuel penalty comparisons include only the fuel used for regeneration and do not account for required parasitic loads such as electrical and air pumping power. However at most engine operating conditions, these parasitic loads account for a fuel penalty of 0.5%. Only at idle and very light loads are these parasitics significant. Even then the maximum parasitic fuel penalty is about 5%.

In addition to the fuel penalty advantage, reformate regenerations of NO_x traps produce a dramatic reduction in hydrocarbon slip as shown in Figure 4.12. For equivalent NO_x adsorption, reformate regenerations reduce hydrocarbon slip through the adsorbers by 90–95% at exhaust temperatures of 275˚C and above. Below 275˚C exhaust temperatures the reduction in HC slip is still 65% or more.

Additional testing completed after this work indicates that by optimizing the regeneration time and reformate flow rates the reformate NO_x trap regeneration fuel penalties reported here can be lowered another 50% from an average of 4% fuel penalty to 2% fuel penalty.

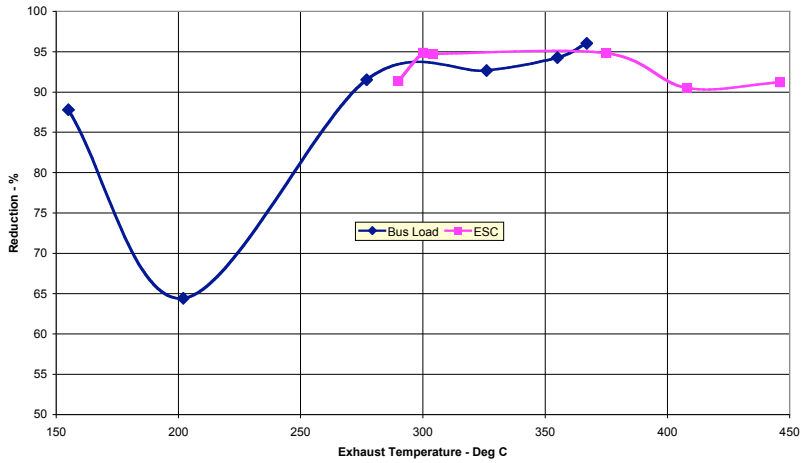

Figure 4.12. Reduction of hydrocarbon slip when using reformate vs diesel for NOx trap regeneration.

i) Vehicle installation and results

The H_2 assisted NO_x trap system installed on a Ford F250 pickup truck, with a 7.3L Powerstroke engine, is illustrated in Figure 4.13. This is a single leg with bypass system using 14 liters of NO_x adsorber with electrically actuated brake valves to switch flow legs. The reformer and brake valves are computer controlled and NO_x concentrations are

measured with Horiba NO_x sensors. With reformate regeneration of the NO_x trap, this system is capable of 70% NO_x adsorption.

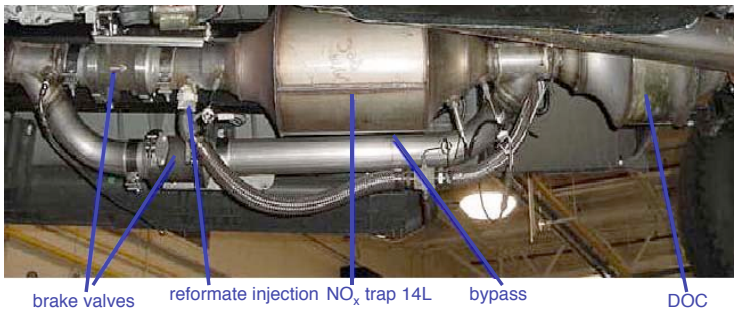

Figure 4.13. F250 hydrogen assisted NOx trap installation

Figure 4.14. Hydrogen assisted NOx trap installation in a bus

The Gillig transit bus installation is shown in Figures 4.14 and 4.15. The bus uses a dual leg system with 21 liter of NO_x adsorber per leg. There are separate pneumatically actuated switching valves for the exhaust flow and reformate flow. A single Gen-H plasmatron fuel reformer is used. A PC, utilizing LabView based software, controls the regeneration including the fuel reformer air-fuel ratio and the switching of the exhaust and reformate flows on a time based cycle. NO_x emissions are measured with NGK NO_x sensors. The engine in this bus is a MY1994 Cummins C8.3L. Due to the high accessory loads, engine out NO_x concentrations as high as 800-900 ppm are observed. This system is capable of NO_x reductions of 80-90% (without optimization).

Figure 4.15 Picture of part of plasmatron diesel reformer system in the back of the bus

j) ArvinMeritor/MIT Results summary

- NO_x trap regeneration fuel penalty reductions of roughly 50% versus diesel injection were achieved
- Idle operation NO_x trap regenerations achieved
- Hydrocarbon slip during regeneration reduced by 90%
- Dual leg NO_x trap system installed and operating on a transit bus: 80-90% NO_x reduction
- Single leg bypass NO_x trap system installed and operating on a Ford F250 truck: 70% NO_x reduction

k) Cummins/MIT NOx trap regeneration tests

The scope of work required testing with one of the truck manufacturers. The generation 2 plasmatron diesel reformer was tested at Cummins during the summer of 2001, described in Section 2.b.

For testing in a vehicle, it was necessary to perform plasmatron diesel reformer characterization when operating in a mode compatible to that of regeneration of a diesel aftertreatment device. Those tests, where the plasmatron was operated by periodically

pulsing (5 s on, 55 s off) are presented in section 9.c. For the tests, the generation 2 plasmatron was used.

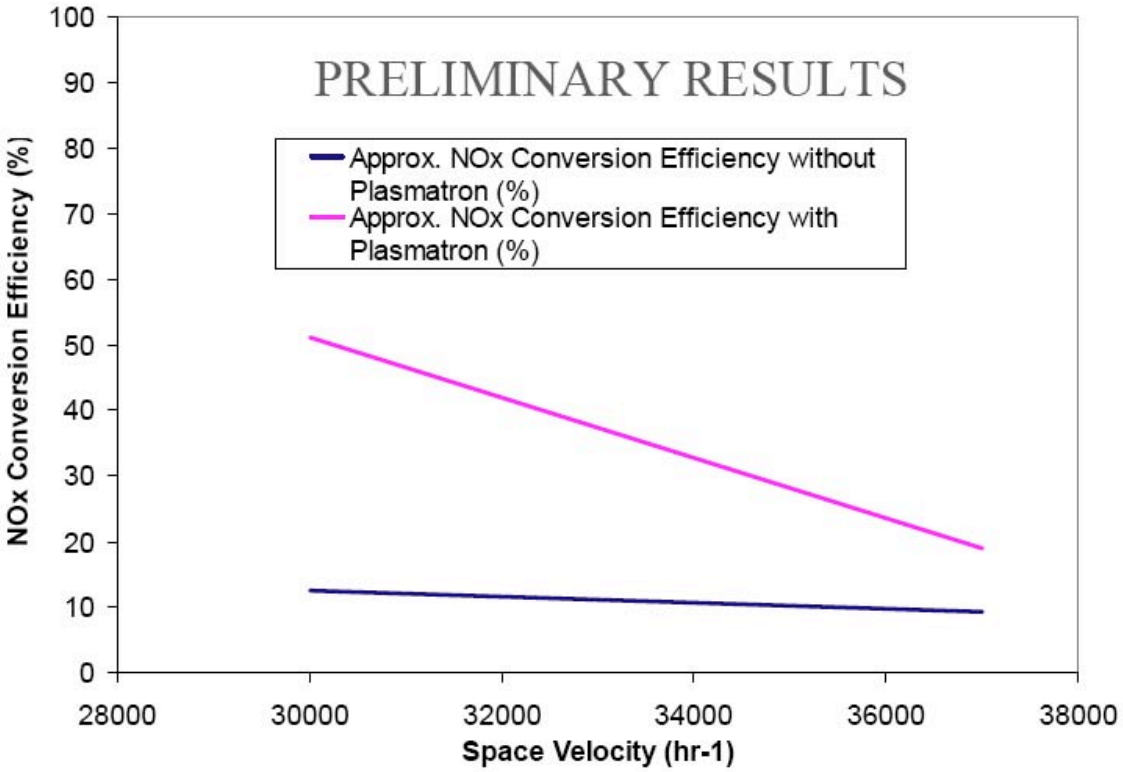

Figure 4.16 Effect of reductant on cycle average NOx conversion efficiency, cycle testing at 150 C.

The results were kept confidential to Cummins, However, they did provide some information on the test results. It is shown in Figure 4.16. The figures shows substantial improvement, at moderate space velocities, over those with the use of diesel fuel as the reductant. Only one temperature, 150C was reported to us from Cummins.

5) **Plasmatron application to aftertreatment II: DPF trap**

Particulate and emissions from diesel vehicles have been determined to be hazardous to health. In addition, particulate emissions may aid to the global warming trends because of the reduced reflectivity of large masses of ice/snow. Diesel emissions have been regulated in the developed countries. Tighter regulations already in the books require substantially decreased emissions in the next 5 years.

A promising technology to accomplish the required reduction is the Diesel Particulate Filter (DPF). The filters are porous ceramics through which the gases flow relatively unimpeded, but the solids in the exhaust are trapped. Eventually there is sufficient buildup of the particulates in the trap that the gas flow is impeded, and regeneration needs to take place.

Two types of traps exist, with or without a catalyst coating. Uncoated DPF are attractive because of reduced cost, and because it is likely that some method of active regeneration will be required even if used rarely. The uncoated DPF need to be regenerated by the combination of temperature and oxygen. Combustor technology has been developed. However, there may be important advantages to regenerate the DPF using hydrogen rich gas, in which the reformate is combusted in the trap itself, hopefully by the soot. The potential advantages are reduced thermal stress, lower temperature of trap regeneration, reduced possibility of uncontrolled regeneration that may result in the destruction of the trap and lower fuel penalty by the use of controlled burn. These advantages may result in enhanced reliability and increased lifetime. For both catalyzed and non-catalyzed traps, there has to be sufficient oxygen in the flow through the DPF in order to combust the soot. For any active regeneration method, the system should be able to operate over a wide range of non-stationary conditions.

In order to "ignite" the particulate matter, it has also determined that a temperature in the range of 600-650 C was required in the presence of oxygen. Measured activation energies varies from ~60 kJ/mol to 170 kJ/mol. The temperature rise of the gas across the DPF (and the temperature of the DPF unit) depends on the oxygen content, the mass loading of the field and the flow rate. The temperature excursion due to the soot combustion can be as low as a few degrees to high temperature excursions that can result in the destruction of the trap.

Two modes of regeneration have been observed in uncatalyzed traps. Visual evidence of the mode modes has been obtained by Haralampous [Har03, Han03]. The first mode results in a uniform regeneration of the trap, with mild temperature excursions and relatively long regeneration times because of the low temperatures. This mode of regeneration built in margins, results in a more uniform regeneration, but increases the fuel consumption due to the fact that the temperatures need to be maintained longer, in the case of non-self-sustaining regeneration. The second regeneration mode results in a self-sustained or near-self sustained burn, with higher temperatures, non-uniform and faster regeneration (in some cases resembling a propagating front). The nature of the

regeneration process is determined mainly by the trap soot loading, the free oxygen content of the exhaust and the exhaust flow rate.

In the second mode of operation the regeneration is performed by increasing the temperature of the exhaust to the point where the soot ignites and starts a self-sustaining burn. Once started, it is uncontrolled. If there is too much soot in the trap or if the free-oxygen concentration is increased (from lower torque operation, for example) the temperatures of the combustion process can exceed the temperature limitations of the filter. A single event may result in unintentional destruction of the filter.

Low temperature regeneration may result in more uniform regeneration. Non-uniform regeneration that results in partial regeneration of the DPF has been modeled and tested by Haralampous et al. [Har03], and others. The flow through the DPF, even if uniformly loaded, changes during regeneration. If some regions are cleaned prior to others, the flow pattern downstream of the clean channel can be substantially modified, with an increasing fraction of the flow occurring through the clean region. Non-uniform channel regeneration affects both the radial and axial flow patterns. Axial flow pattern maldistribution occurs when the upstream region of a channel is cleansed faster, after which the gas flows across the cleansed region instead of the downstream, soot-loaded channel.

The first mode of operation is attractive in that the rate of combustion, and the temperature of the regeneration process, is dominated by the exhaust gas and not by the self-sustained combustion of the soot. From the above discussion, low temperature, slow uniform regeneration has attractive features.

Tests with active regeneration are taking place both in the US [And04] as well as in Europe [Fay04]. Active techniques at present seem to be necessary for those vehicles with substantial idling, where the exhaust temperatures are too low for self-sustained DPF regeneration. These concepts depend on thermal management to increase the temperature of the DPF, as well as active introduction of fuel upstream in the exhaust. The fuel is injected upstream from a diesel oxidation catalyst (DOC) that is located upstream from the trap. The fuel is consumed in the DOC, increasing the temperature of the exhaust. The oxygen content downstream from the DOC is sufficient for soot combustion.

Alternative methods to the catalytic combustor involves a conventional combustor. This technology is being tested by Arvin Meritor.

Fuel reformers are being considered for on-board applications, for hydrogen generation for use with fuel cells, for use in NOx trap regeneration, and for combustion improvement in SI engines. The MIT team is developing plasmatron fuel reformers, both for gasoline and diesel applications. Both catalytic and homogenous reformers are being investigated. Plasma based reformers are robust, fast response and have wide operating capability. It is the purpose of this section to illustrate the options investigated under this

program of using reformate from a plasmatron fuel reformer for the controlled regeneration of DPFs. [Bro05g, Bro05h]

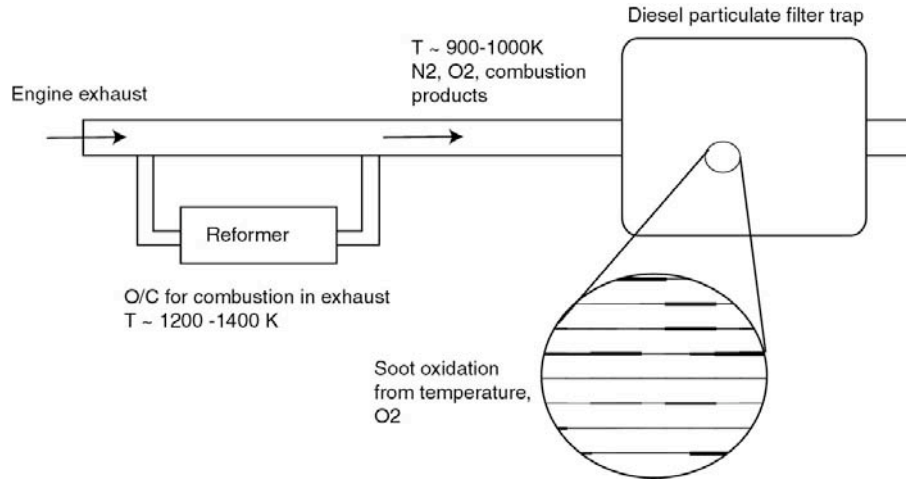

(a)

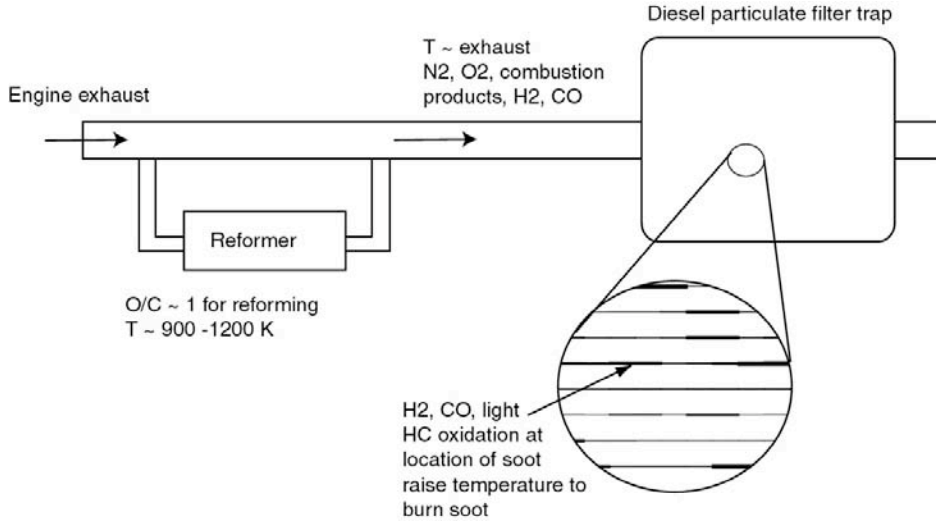

(b)

Figure 5.1. Reformer operating as a (a) combustion for DPF regeneration (b) Generation of hydrogen rich gas

a) Plasmatron Technology for DPF Regeneration

Active techniques for the regeneration of diesel particulate filters use a burner to achieve the temperatures at the catalyst required for filter regeneration. Plasmatron technology can be used as a fuel igniter as well as means to produce hydrogen rich gas. Plasmatron technology can serve as a powerful igniter and thus is attractive because it is possible to combust the diesel fuel using oxygen present in the diesel exhaust, even at conditions when the engine is operating at high load (with reduced oxygen content). Diesel loads

rarely operate above equivalence ratios around 0.7, because of soot production, and thus about 1/3 of the oxygen remains free in the exhaust.

By using the plasmatron unit as a powerful igniter, either very lean mixtures or very rich mixtures can be processed. Very lean conditions can occur when only the thermal process of the fuel is desired. Rich conditions will result in the generation of hydrogen rich gas.

The advantage of combusting the fuel in the exhaust is that it is possible to achieve combustion while minimizing the amount of extra air introduced into the system. The hydrogen rich gas with exhaust gas as oxidizer results in a further net decrease of the amount of free oxygen in the exhaust, decreasing the combustion rate of the soot on the DPF and decreasing the possibility of uncontrolled regeneration. This technology is also attractive because the plasmatron hardware may already exist on-board the vehicle for regeneration of NOx absorber traps.

Figure 5.1 (a) shows a schematic of the use of a reformer as a powerful combustor, operating with exhaust as the oxidizer. There is thermal output from the combustor, but no hydrogen or light hydrocarbons. In figure 5.1(b) the reformer operates under conditions close to partial oxidation (free oxygen to carbon ratio of 1), producing hydrogen, CO, light hydrocarbons and limited thermal output (~ 1/4 of the thermal output of the fuel is combusted in the reformation process). These two are extremes, with the plasmatron operating anywhere in between, generating both easily combustible gases as well as thermal output.

Two options of location of the DPF and NOx trap exist. The DPF can be upstream from the NOx trap, or the other way around. Modeling of the system is required to determine the optimal configuration. Care must be taken that the temperature required for regeneration of the DPF does not damage the NOx trap, as well as the issues having to do with desulfation of the NOx trap.

b) Calculations of Reformer Requirements

For the calculations presented here, the size of the engine is 6 l, operating between 600 and 2400 rpm, with a inlet manifold pressure of 1-3 bars, It is assumed that the entire exhaust flow is treated, as opposed to partial regeneration of a section of the DPF [Bro05g].

The exhaust temperature assumed throughout the engine map is shown in Figure 5.2. For simplicity, it is assumed that the exhaust is insensitive to engine speed and only depends on torque.

It is assumed that the soot burns at temperatures between 600- 700 C. The reformate is mixed with the exhaust to increase the temperature to this range. The flow rates through the plasmatron are calculated, at different O/C ratios.

Because the reformate is combustible, the rates that are calculated will be larger than those actually required. The actual flow rates will thus be lower.

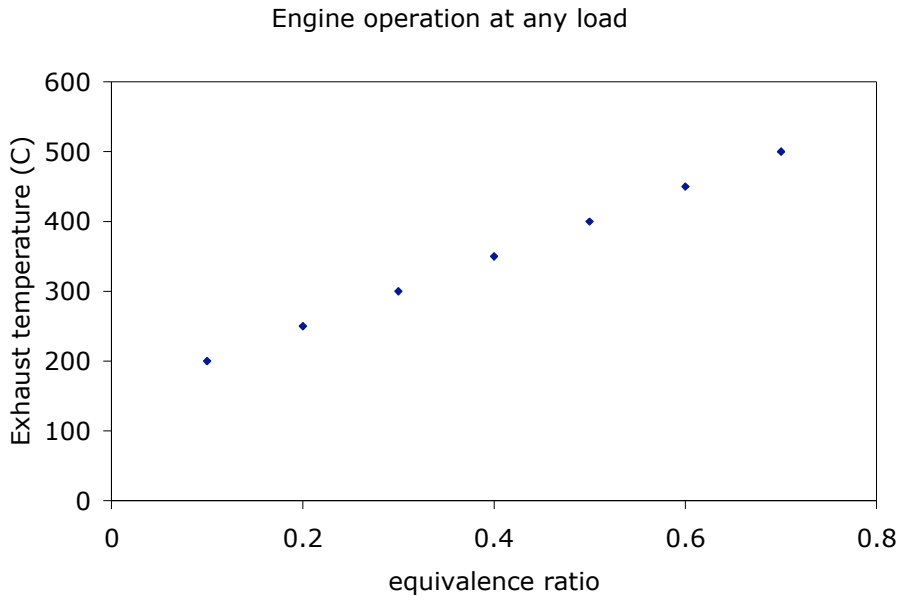

Figure 5.2. Exhaust temperature as a function of the engine equivalence ratio. It is assumed that the exhaust temperature is insensitive to the engine speed.

In addition, it is assumed that turbocharging does not increase the temperature of the exhaust, due to the presence of an intercooler.

Two scenarios for the regeneration with hydrogen rich gas can be envisioned. The first one assumes that it is the thermal content of the hydrogen rich gas that results in the regeneration of the DPF. In this manner it does not really matter where the hydrogen rich gas is combusted. The second scenario assumes that the hydrogen rich gas reacts in the region of the soot (and even is ignited by the soot), resulting in direct deposition of the heat at the soot location. In this scenario, the temperature of the exhaust is low prior to the combustion of the hydrogen rich gas, and thus the velocity of the gas is slower, allowing for increased contact time between the free oxygen and the hydrogen rich gas with the soot. In the second scenario, it is desired that the hydrogen rich gas not be consumed homogeneous prior to the region with the soot. Homogeneous combustion of hot hydrogen rich gas in the exhaust is discussed in the section below.

In both scenarios, the temperature of the gas, assuming combustion of the hydrogen rich gas, is ~ 600 C, thus able to start regeneration of the soot. Because of the light soot loadings assumed, the temperature downstream from the soot is not significantly larger than upstream (*i.e.*, the soot is burning at a low rate).

The reformate power required to bring the temperature of the exhaust to regeneration conditions in the DPF is shown in Figure 5.3. The reformate power refers to the combustion power if the reformate is fully oxidized. The power increases linearly with

speed, at any equivalence ratio. The reformate power also increases with decreasing equivalence ratio, as the exhaust temperature prior to addition of the reformate is cooler in the cases of low equivalence ratio, and thus increased reformation is required to achieve the regeneration temperature.

The range of power is large, from a minimum of ~ 3 kW to about 30 kW, for a dynamic range of ~10. However, this is larger than it need be, since the engine will not work often the region of high rpm and low torque. Thus, the dynamic range requirements are ~5. This dynamic range does not include operation at higher manifold pressure, discussed below. It is the possibility of operating a plasmatron over this wide range of condition that makes it attractive for the DPF regeneration application.

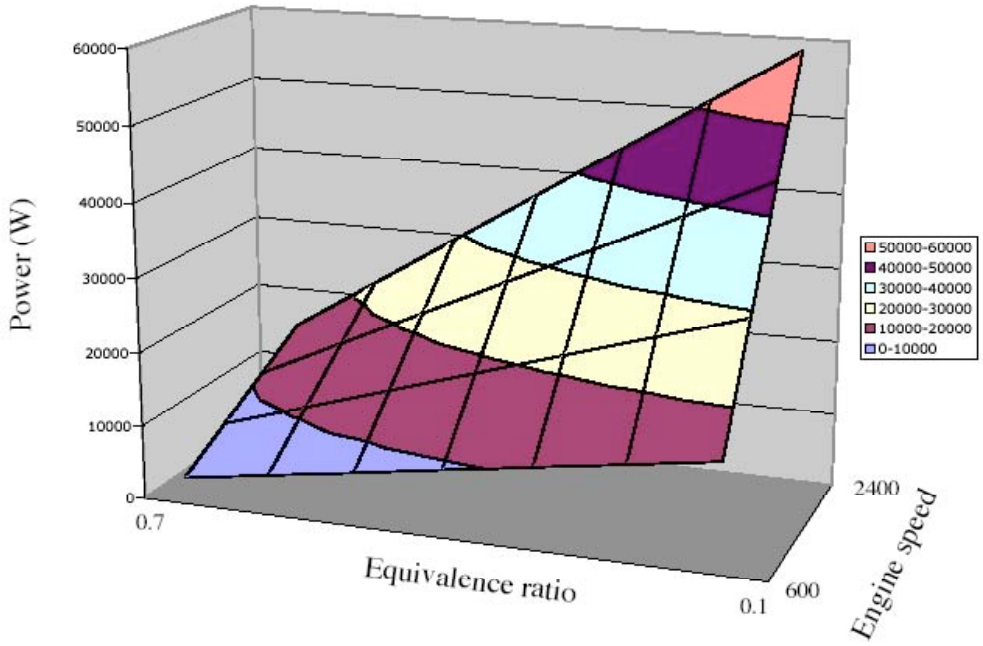

Figure 5.3. Power in reformate (rate of heating value, in Watts), required for reaching regeneration conditions, as a function of the equivalence ratio and the engine speed, for naturally aspirated conditions.

Figure 5.4 shows the fuel flow rates through the plasmatron for achieving regeneration through the engine map for the case of 3-bar operation of the engine (with an intercooler). The behavior is very similar to that shown in Figure 5.3 for naturally aspirated engine, with the largest fuel flow rate requirements at high speed, low torque. The highest fuel flow rate through the fuel processor is 5 g/s, which corresponds to a maximum power of about 160 kW. However, the engine is unlikely to operate under conditions of high speed, low torque and high manifold pressure. Thus, turbocharging does not result in substantial changes in the required dynamic range from the fuel processor.

The time required for regeneration is determined by the PM burn rate, which depends on the temperature and oxygen concentration. The effect of the hydrogen rich gas is unknown and will be determined in the experiments. Calculations of combustion rate of

the soot can be made using the Arrhenius formulation with the activations energies described above, but cannot be used as a predictive tool.

The development of plasmatron fuel reformers demonstrated the capability to operate from about 0.3 g/s to 2 g/s, with activities to achieve 4 g/s fuel flow rate. Most of this work has been carried out with gasoline, but could be extrapolated to diesel. Thus, the capabilities of the present devices match the requirements for DPF regeneration.

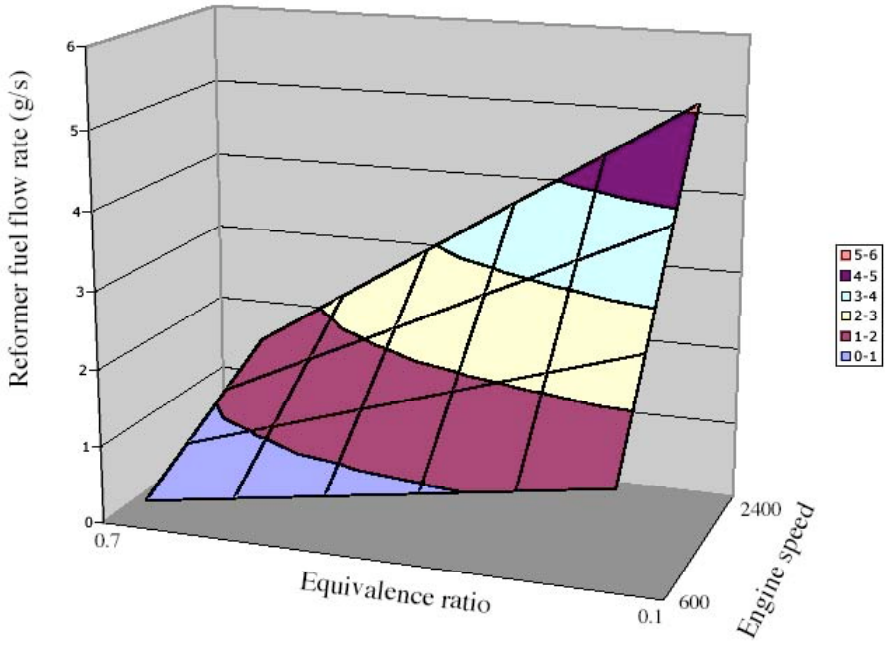

Figure 5.4. Rate of fuel flow rate through the reformer (in g/s) required to achieve regeneration conditions as a function of the equivalence ratio and the engine speed, for 3-bar inlet manifold pressure.

c) Testing Procedure

Testing was designed to be carried out in using an '02 Cummins ISB 300 5.9L inline 6 engine. The engine characteristics are: maximum power ~ 225 kW, maximum torque ~ 895 N•m, compression ratio: ~17, bore diameter: 102.02 mm and piston stroke: 120 mm. The engine setup is described elsewhere.

The cordierite DPFs to be tested were obtained from Corning. They are conventional units 5.66 in diameter, 10 in long traps with a cell density of 100 cpsi.

Full trap and partial traps will be tested. For full trap, the entire trap will be loaded and regenerated, maybe with multiple units. Partial traps will be constructed from 2 in diameter sections of the trap. Experience indicates that if 5 cm (2 in) sections of the PDF

are used, the edge effects are not important [Ogu04]. Using partial trap allows for quicker soot loading, facilitating the tests in a wider range of conditions.

The engine produces a raw exhaust with a PM emission of 0.1 g/kW hr. A 5 cm diameter (2 in) partial unit is about 1/32 of the volume of a DPF that consists of 4 14.4 cm diameter (5.66 in) units. The volume of the partial unit is on the order of 0.3 liter, while the single trap is about 2.5 liters. Typical loadings on traps prior to regeneration are on the order of 10 g/liter. Thus, the time required in order to load the partial unit, at 40 kW (50 hp), is 45 minutes, if all the flow is through the partial unit. Forcing all the flow through a single partial unit may, however, result in large pressure drop.

It should be noted that it has been determined that the loading rate of the trap is important, as the loading of the soot is nonuniform at the higher loading rates [Staerker]. At the high flow rates (320 kg/hr) through the trap, the particle trap experienced loading that peaks off-axis, while at lower exhaust flow rates of 60 kg/hr the soot is deposited uniformly. This is counterintuitive, because at the higher flow rates the Reynolds number is higher and thus increasingly turbulent, which results in a uniform flow profile (but increasingly non-uniform soot profile in the trap).

In order to load the single full unit, at the same engine loading, it would take over 2 hours. Although acceptable, partial units would allow the quick exploration of a large set of parameters.

The present plans call that, after trap loading, a reduction in the flow through the partial unit to the nominal flow. The partial trap will be regenerated from hydrogen rich gas provided from bottled gas.

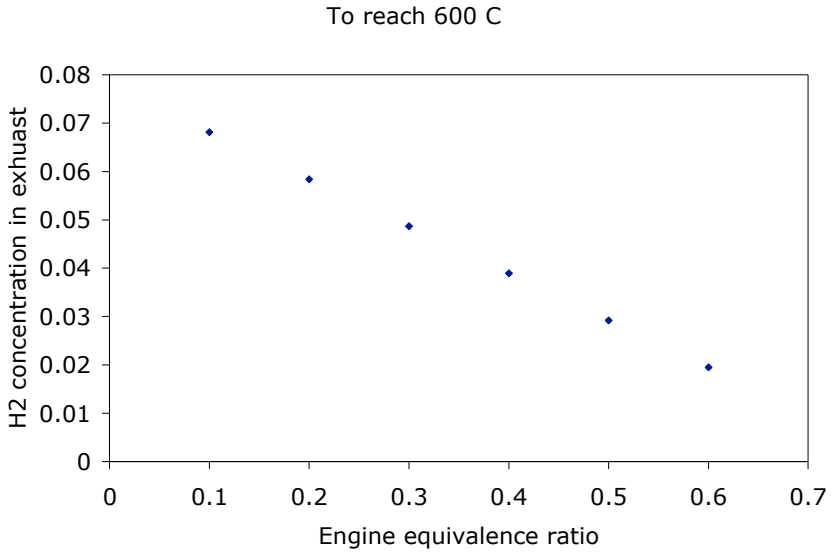

Figure 5.5. Hydrogen concentration in exhaust if reformate reaches equilibrium in the reformer, as a function of the engine equivalence ratio.

To regenerated the DPF at 1200 rpm, half-torque conditions, about 20 kW of reformate are required. Since the flow through the partial unit is 1/32 of this, only about 0.5 kW of reformate is required for the regeneration. This corresponds to a reformate flow rate of 0.2 cfm. With a 300 ft^3 bottle, tests can be carried out for 24 hours of regeneration.

If instead a trap with a single 5.66 in DPF is used, the flow rates would be 8 times larger, and the bottle of gas would be consumed in about 3 hours.

After the testing with the partial unit, with some optimization of the process, tests with a full unit or multiple full units can be carried out. The process would require long periods for time for loading the trap with PM, followed by regeneration.

The hydrogen gas from the plasmatron is by nature hot, on the order of 800 - 1000 C. Because of finite mixing in the exhaust, some of the gas will retain its hot temperature, making it more ignitable by the warm soot particles. To test the effect of temperature, the reformate will be heated using electrical heaters. Again, the reduced flow rate would help in the design of the heaters. In order to preheat the gas to those temperatures, approximately 100 W of electrical heating needs to be provided. This will be done in the absence of oxygen.

Finally, it should be mentioned that in the homogeneous plasmatron fuel reformer, the reformate does not reach equilibrium. Thus the concentration of hydrogen in the case of a homogeneous plasmatron reformer is about 1/3 that of equilibrium, or about 8%. The rest of the hydrogen in the fuel is converted to light hydrocarbon, such as methane and ethylene, that are also relatively easily ignitable (combust with low production of soot). The advantage of this is shown in Figure 5.5 which shows the concentration of hydrogen in the exhaust, from a reformate that reaches equilibrium, if well mixed with the exhaust. If the reforming reaction reaches equilibrium, the concentration of hydrogen reaches explosive limits in the exhaust, especially at the lower engine equivalence ratio, when the oxygen excess is maximum. However, by operating a non-equilibrium reformer and decreasing the concentration of hydrogen in the reformate, the explosive conditions are avoided.

d) Homogeneous Oxidation of Reformate in the Exhaust

In this section, the issue of hydrogen oxidation in the exhaust is considered, to determine whether hot hydrogen-rich gas injected into the exhaust (that contains free oxygen) will spontaneously combust prior to reaching the trap.

Model

For simplicity, it is assumed that the 6 liter engine operates at 600 rpm, and that it is operated at idle (at an equivalence ratio of 10%, without EGR). Thus, the concentration in the engine exhaust is 18.7% O_2, 78.2% N_2, 2% H_2O and 1% CO_2 (assuming methane as the fuel). To this exhaust, which is assumed to be at 423 K (150 C), hydrogen rich gas is

injected. These conditions correspond the worst case, with the highest amount of free oxygen and the largest demand of hydrogen rich gas. In this section it is assumed that the hydrogen rich gas is the result of equilibrium partial oxidation of methane, at different O/C ratios. Methane is used because of the existence of chemical reaction mechanisms that have been benchmarked for operation at the fuel-rich conditions of the reformer.

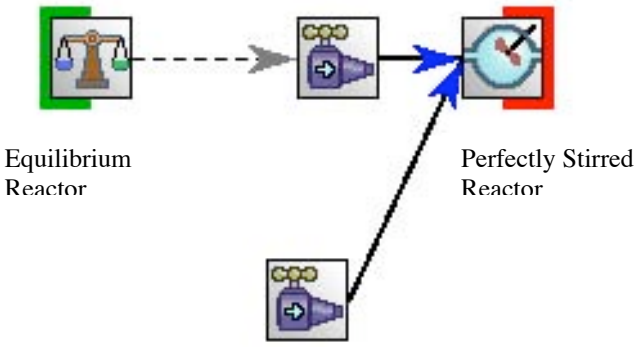

Figure 5.6. Schematic model of the process

The model is schematically shown in Figure 5.6. It is assumed that the equilibrium reactor and the exhaust are introduced into a perfectly stirred reactor (PSR). A model that uses a plug flow reactor is described below, but the constrains of the code made the assumption of the perfectly stirred reactor easier to input. The model shown in Figure 5.6 overestimates the consumption of hydrogen, since as the hydrogen is consumed, the PSR model implies that the temperature upstream from the reactor increases, driving additional hydrogen consumption. The goal is to determine the conditions for which the exhaust will result in substantial amounts of hydrogen oxidation. A more detailed model will be presented in a section below.

The conditions chosen correspond to about 40 g/s exhaust gas, with 10 g/s from the reformate (corresponding to about 1.5 g/s fuel in the plasmatron). This is a large number, but the goal is to determine under the worst of conditions, what is the effect of the hydrogen combustion

Results from the PSR Model

Three cases have been assumed, with oxygen to carbon ratios of 1.333, 1.43 and 1.54. They correspond to methane flow rates of 1.5, 1.39 and 1.29 g/s, for a total flow rate of 10 g/s. The results are shown in Table 5.1. “T equil reactor” represented the temperature from the equilibrium reactor, and it is the equilibrium temperature of the partial oxidation reaction. The temperature of the exhaust is held constant at 423. T PSR represents the temperature of the perfectly stirred reactor (and the outlet from that reactor).

Table 5.1. Results for the PSR case

O/C		1.33	1.43	1.54
Fuel flow rate	g/s	1.49	1.39	1.29
T equil reactor	K	1157	1255	1359
T exhaust	K	423	423	423
T PSR	K	628	654	1489
PSR H2 input	mols/s	0.164	0.147	0.130
PSR H2 out	mols/s	0.164	0.147	0.001

For the first two cases, with relatively low O/C, the hydrogen flow rate out of the PSR reactor is approximately the same as the hydrogen rate into the PSR. That is, there is no oxidation of the hydrogen in the flow rate. The same is the case for the CO that is also produced. The last case, though, with a relatively high O/C, results in almost all consumption of the hydrogen rich gas. The temperature of the system becomes very large, as the hydrogen rich gas has substantial thermal content, increasing the reaction rate of hydrogen. There is oxidation at reformate/exhaust temperatures exceeding 700 K.

This case represents the most pessimistic and unrealistic case, since it requires substantial mass and temperature equilibration in the exhaust pipe. This flow resembles more the plug flow model, which will be described next.

Plug Flow Reactor Simulation

In this section, an alternative reactor is used as a model. This reactor simulates more closely the processes inside the system. The PFR is a more appropriate model for the behavior of the hydrogen rich gas in and environment with free oxygen in the exhaust of a vehicle.

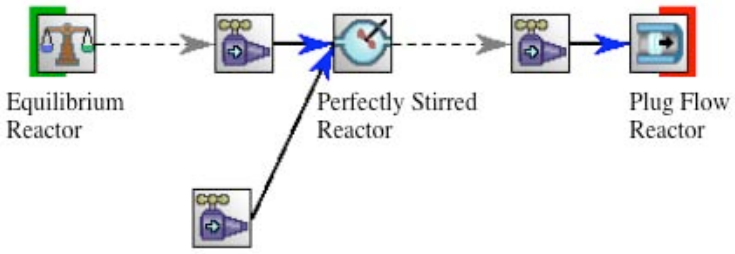

Figure 5.7. Schematic diagram of model for hydrogen oxidation in exhaust pipe.

The model is shown schematically in Figure 5.7. It includes, as in the previous section, an equilibrium reactor that represents the reformer, a second input to the PSR that represents the engine. The PSR is used with very short residence time (0.001 s) as a mixing, nonreacting reactor. The PSR is then followed by a plug flow reactor (PFR). It is assumed that the PFR has a diameter of 5 cm (2 in) and a length of 30 cm (12 in). This distance corresponds to the length between the injection point of the hydrogen rich gas in

the exhaust and the aftertreament unit. In this case, the amount of reformate is decreased to 3 g/s (down from 10 g/s in the previous section), with an O/C ratio of 1.33.

The temperature of the exhaust is varied, until there is homogeneous reaction (i.e., combustion) in the exhaust. A case just above the temperature at which the air/fuel mixture ignites is shown in Figures 5.8 and 5.9. Figure 5.8 shows the temperature of the reformate/exhaust gas as a function of the distance along the plug flow reactor, when the temperature of the engine exhaust is 973 K.

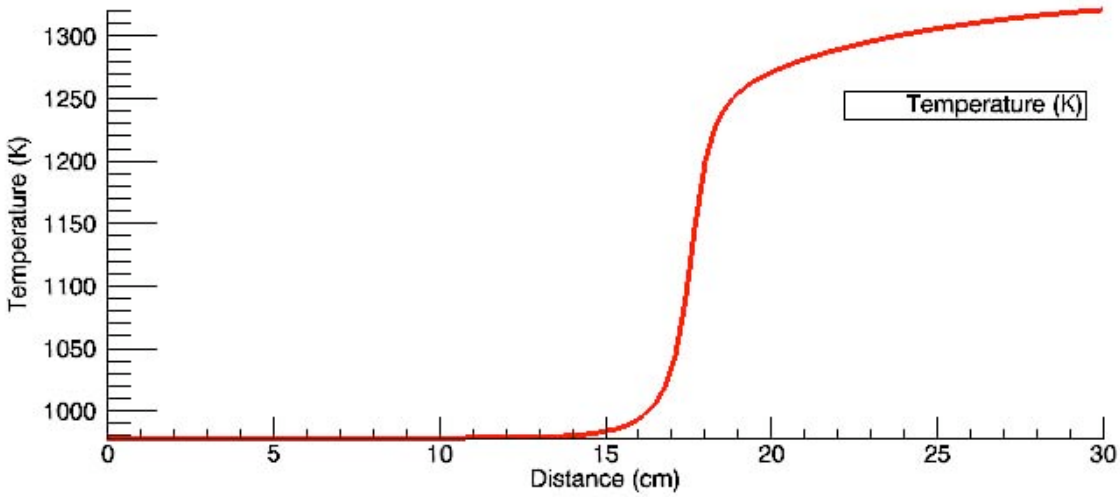

Figure 8. Temperature as a function of distance in the PFR, assuming that the engine exhaust is at 973 K

Half way along the exhaust pipe the fuel (hydrogen rich gas) ignites. The corresponding composition of the reformate/exhaust gas is shown in Figure 5.9. It is interesting to note that hydrogen burns faster than CO.

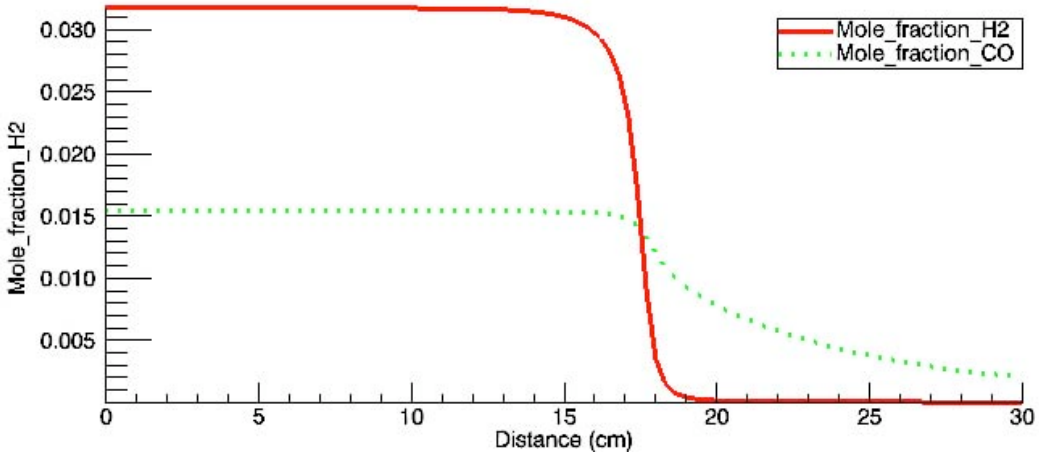

Figure 9. Hydrogen and CO concentration of the gas in the PFR as a function of distance, for the case of engine exhaust temperature of 973 K.

For an exhaust temperature of 923 K (i.e. 50 K lower than the temperature for which the hydrogen rich gas ignites), there is no reaction in the length of the PFR. The hydrogen and CO concentrations remain the same to within 3 significant digits.

The temperatures required for ignition of the hydrogen rich gas are substantially higher than those commonly found in the operation of diesel engines. Thus, it is not thought that hydrogen rich gas from an equilibrium reformer will combust homogeneously in the exhaust.

Non-Equilibrium Reformer

The last case uses the experimentally derived concentrations for a homogeneous plasmatron operating on diesel, utilizing the PFR described in the section above. The model is described in Figure 5.10. It is assumed that the concentration of the reformate is 8% H_2, 10% CO, 3% CH_4, 1% C_2H_6, 4% CO_2, 6% H_2O and 68% N_2. These numbers are typical of operation of the generation 3 plasmatron. In addition, it is assumed that the temperature of the reformate prior to mixing with the exhaust is 1100 K. The flow rates are the same as with the PFR (3 g/s of reformate and 40 g/s of exhaust).

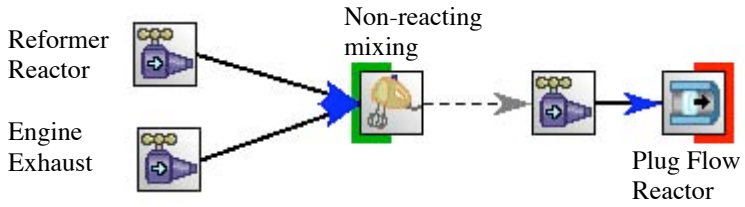

Figure 5.10. System without equilibrium reactor for reformer.

As in the previous section, the temperature of the engine exhaust is varied until there is combustion in the exhaust pipe. It is found that the temperature of engine exhaust has to be increased to 1073 in order to see ignition of the reformate/exhaust flow. Results at this temperature are shown in Figures 5.11 and 5.12.

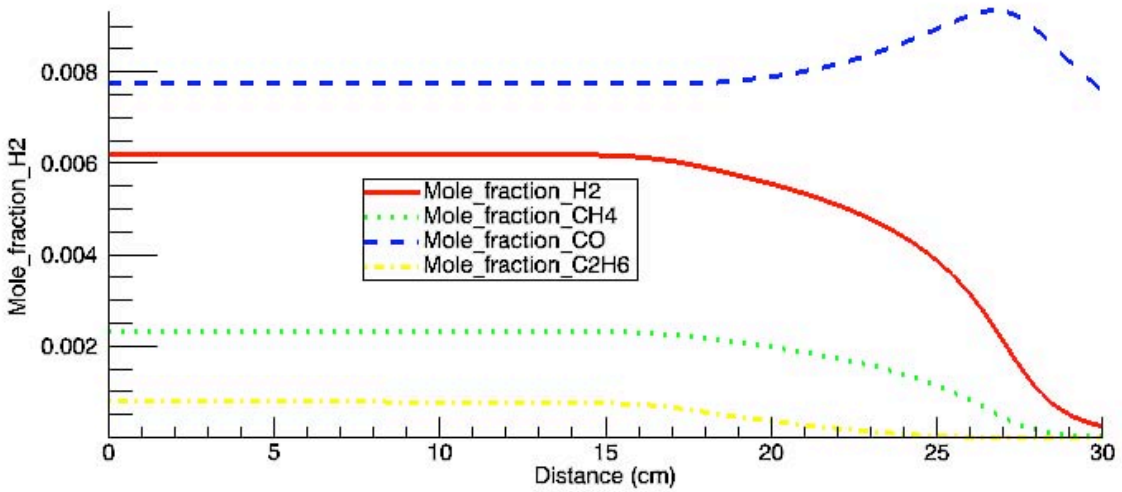

Figure 5.11. Concentration in exhaust as a function of distance for an exhaust temperature of 1073 K, for reformer composition similar to that of present day homogeneous plasmatron reformers.

At an exhaust temperature of 1073, there is combustions. At 50 K lower temperature, there is no reaction at all. The temperature profile is shown in Figure 5.12.

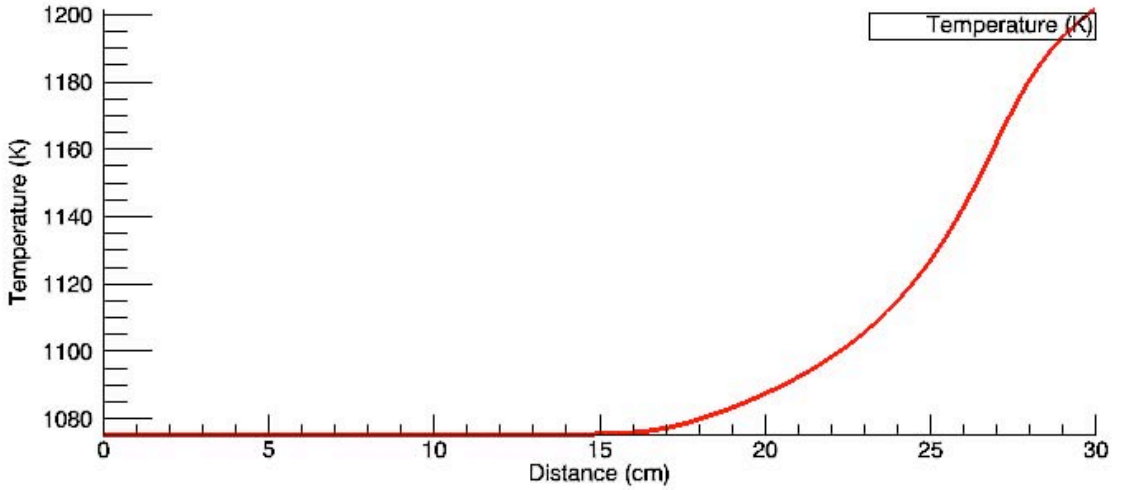

Figure 5.12. Temperature corresponding to the case in Figure 11 as a function of distance

The ignition conditions of the non-equilibrium reformate requires engine exhaust temperatures comparable to the temperature of the reformate. The temperature in this case is even higher than that described above for the equilibrium reformer, and they are not reached in normal operation of a diesel engine.

The results indicated in this memorandum are for homogeneous (gas phase) reactions. The object is that the hot carbon particles can induce combustion of the hydrogen rich gas

locally, substantially increasing the particulate temperature and thus the combustion of the particulates.

6) Plasmatron aided HCCI operation

It has been suggested above that hydrogen rich gas could be an ideal fuel for the cold start phase of an engine that when warm operates in HCCI mode. During the cold start the engine could operate as an spark ignition engine, with the low emissions characteristics of engine operating in lean mode.

In this section, the characteristics of the plasmatron for HCCI applications are discussed. Two of the features of the plasmatron fuel converter features could be useful for control in HCCI combustion are:

1. the exothermicity of the reaction can be used for heating the incoming air with fast response (since the heat is deposited directly in the gas, avoiding heat transfer through metallic or ceramic walls in the heat exchanger, with a resulting time delay.)
2. the octane value of the fuel can be controlled by either use of hydrogen and CO as a fuel additive, or by the production of C2 compounds, mainly ethylene when operating the thermal plasmatron fuel converter at low O/C ratios.

a) Temperature control

As described above in the prior art section, the partial oxidation reforming is exothermic, releasing a small fraction of the heating value of the fuel (around 15%). This heat can be used for controlling the temperature of the gaseous charge that is injected in the engine. The temperature is one of a small number of knobs that can be used for controlling the ignition timing in HCCI.

The temperature excursion of the gas into the cylinder depends on the amount of air that is mixed with the reformate. The composition of the air/reformate fuel ratio can be descried using the equivalence ratio of this mixture. The equivalence ratio of the air/reformate fuel mixture is defined as the ratio between the reformate fuel/air mixture to that for stoichiometric combustion of the reformate fuel/air mixture. Assuming that 15% of the heating value of the fuel is released, for a fuel of composition near C_nH_{2n}, Figure 6.1 shows the temperature excursion of the air/reformate mixture as a function of the equivalence ratio.

During the engine cold start, when the conventional methods of establishing the charge temperature do not work (*i.e.*, EGR or a heat exchanger driven by the exhaust gas), the plasmatron fuel converter can be used to instantaneously increase the charge temperature to the levels required. When the conventional methods are used to increase the temperature of the gas in the cylinder, very low levels of plasmatron fuel reformation could be used to select rather precisely the charge temperature, with a device with fast response..

To increase the charge temperature to the temperatures that are desirable, above 100C, the equivalence ratio of the gaseous mixture should be around 0.1. Since the engine could run at equivalence ratios around 0.5-0.6 to minimize emissions, the maximum required fuel to be processed by the plasmatron fuel converter for startup is on the order of 20% of maximum load. The minimum torque of the engine during startup, when operating the fuel converter for maximum hydrogen yield, is around 20% of maximum torque. At lower loads, the charge temperature would be lower than required for HCCI operation. To operate the engine at lower powers, it would be required to operate the plasmatron in a mode with higher O/C ratios, therefore combusting a fraction of the fuel. Operating the plasmatron in this mode has the advantages of both decreasing the heating value of the reformate fuel (therefore decreasing the engine load) and increasing the enthalpy of the reformate, thus increasing the temperature of the air/reformate fuel mixture.

On the other hand, during the warm phase operation, relatively small values of fuel need to be processed to control the temperature. Assuming that a temperature excursion of 5 K is desirable, then the equivalence ratio of the charge is on the order of .01. If the engine operates at a equivalence ratio of 0.6 (assuming that the engine can be operated at high load in the HCCI mode), then about 2% of the fuel needs to be processed by the plasmatron fuel converter.

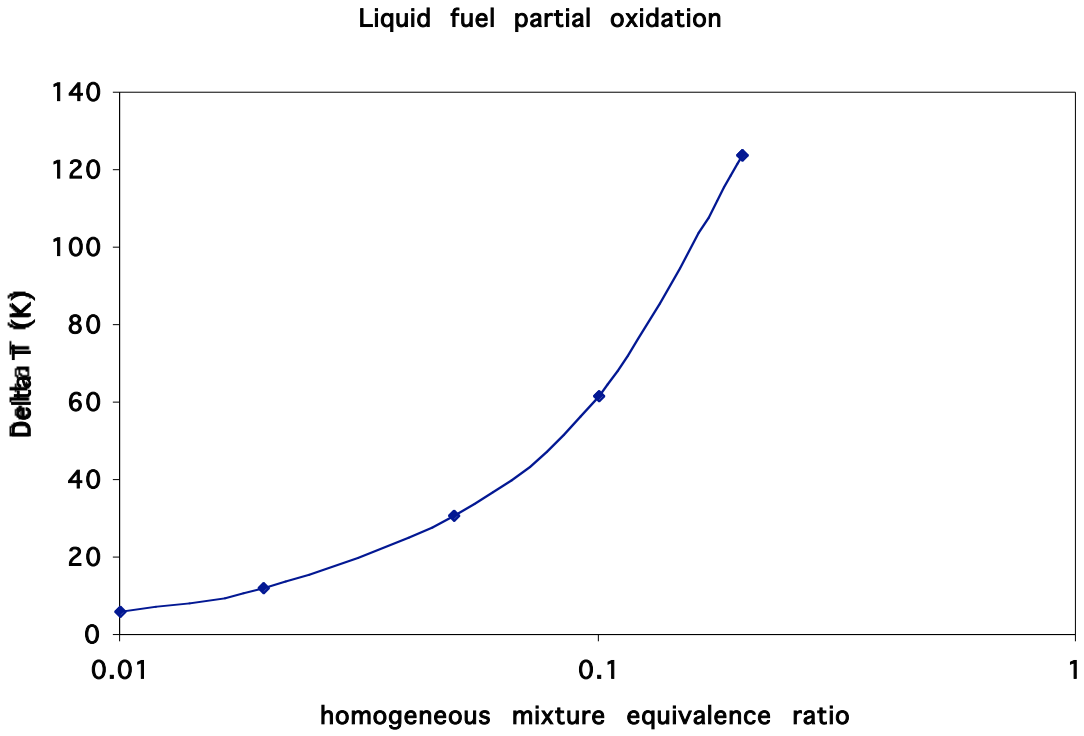

Figure 6.1 Temperature excursion of the gaseous charge to the cylinder as a function of the equivalence ratio of the air/reformate fuel mixture.

b) Octane control

In addition to helping control the temperature in the charge, the plasmatron can be used to generate fuels of different octane value. When operating at O/.C > 1.2, the reformate has a composition similar to synthesis gas, with about 20mol% H_2 and CO, and small concentration of CO_2, C_2's, water, and the balance nitrogen. The synthesis gas can be used to increase the octane value of the fuel (since hydrogen has a very high octane value, while CO is similar to that of methane), but requires its use not as a additive but as a substantial fraction of the fuel.

When the O/C is smaller that 1.2-1.3, it is possible to generate substantial concentration of C_2 compounds, which have very low octane number. In this case, the reformate composition may include a ethylene concentration that can be as high as a few percent. Since the concentration of hydrogen and CO is on the order of 20%, but since the heating value of ethylene is about 4 times that of the reformate, then

Under ideal circumstances, the process can be written as:

$C_nH_{2n} + m/2\ O_2 + 2m\ N_2 \rightarrow mCO + mH_2 + (n\text{-}m)/2\ C_2H_4 + 2m\ N_2$

In practice, the process is somewhat less efficient, but for the process of illustration the above is adequate.

The concentration of hydrogen and CO in the reformate, as a function of the concentration of ethane in the reformate, are shown in Figure 6.2. Since a fraction of the fuel is pyrolyzed into ethylene, the required oxygen, and therefore nitrogen, are reduced. The reduction in the nitrogen concentration is the main reason why the hydrogen and CO concentrations remain relatively constant.

Also shown in Figure 6.2 is the ratio of the heating value of the ethane in the reformate compared to that of hydrogen and CO. Ethane has about 4 times the heating value per mol than does hydrogen or CO.

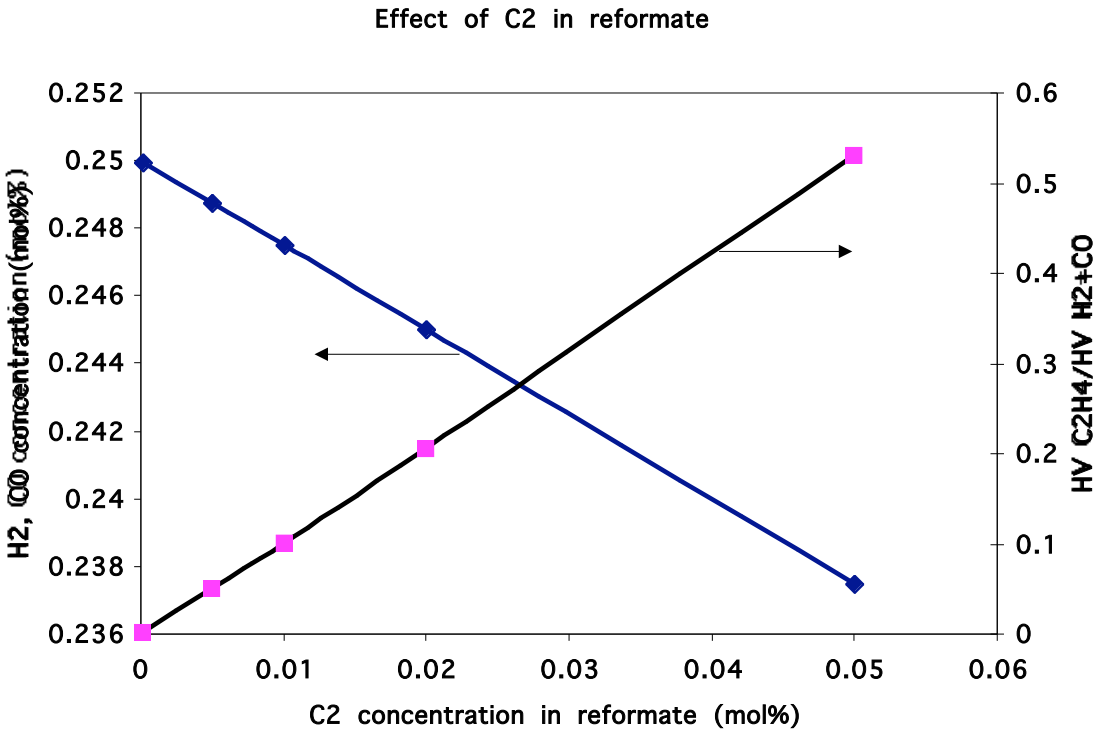

Figure 6.2. Concentration of hydrogen and CO, as a function of the C_2 concentration in the reformate. Also ratio of the heating value of the ethane to that of hydrogen and CO combined.

The reformate can be introduced into the engine to control the ignition timing. Figure 6.3 shows the fraction of that needs to go through the reformer as a function of the reformate equivalence ratio, as defined above (ratio between the air to engine /fuel reformate to the air/fuel reformate for full combustion of the reformate). There is additional fuel injected into the engine, since the reformate is mainly an additive. It is assumed that the overall equivalence ration in the cylinder (fuel+reformate fuel) is 0.7.

In order to process only about 10% of the fuel, the reformate equivalence ratio is about 0.05 (i.e., about 20 times more air than required for full combustion of the air). The ethane concentration in the cylinder is also shown. For 10% of the fuel to the reformate, the ethane concentration is about 0.1%. It is not known the ethane concentration required to control the ignition timing.

The fuel octane rating can therefore be changed via the addition of reformate from a plasmatron fuel converter. The higher the ethylene concentration in the cylinder, the lower the octane number (i.e., the more prone to self ignition).

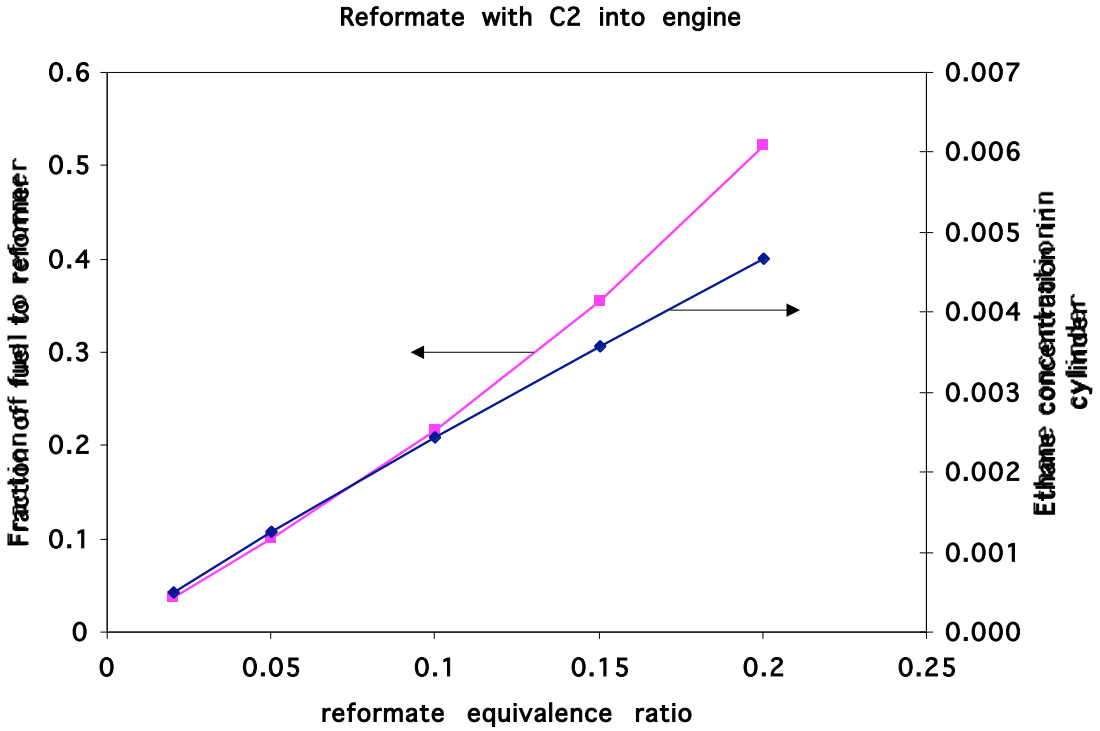

Figure 6.3. Fraction of the fuel that goes through the reformer as a function of the reformate equivalence ratio. Also shown is the ethane concentration in the cylinder.

The rate of heat release in the engine, needed to avoid knock, can be controlled by the establishment of substantial temperature gradients in the air, as suggested by Noda [Nod01]. In that work It was envisioned that EGR would aid in the generation of the temperature gradients. The use of the reformate can aid in the generation of temperature gradients by not-ideal premixing of the air and the plasmatron reformate.

Although hydrogen has a very high temperature for self-ignition, the presence of hydrogen in the combustion chamber may also help ignition, due to the very small energy required for ignition. Under appropriate set of conditions, the local ethylene ignites the local hydrogen that in turn ignites the local fuel, without the need of flame propagation.

Finally, the reformate non-uniformity in the charge to the cylinder can also be used to control ignition.

7) Modeling

In this section, modeling of the plasmatron is described.

There are two aspects of the modeling that have been performed, somewhat independently, to attempt to understand the experimental results. The first model involved fluid dynamics, without chemistry. The reason why chemistry is not included in this model is that the Reynolds average numerical simulation (RANS) is used. The composition of the plasmatron is very inhomogeneous, both in time and spatially. The RANS describe only average quantities, including concentration, but chemistry will not take place until they are mixed at the molecular level (i.e., a pocket of fuel passing through a volume element will not interact with a pocket element of fuel passing through the same element at a different time, even though the code says that in average there are both air and fuel at this locations). Thus the steady state CFD model will not model the plasmatron appropriately.

The second model described the chemistry, using CHEMKIN. Mixing effects are investigated using PSR as well as the PaSR model. Both models will be described in this section.

a) Fluid dynamics modeling

The fluid model is used to understand the mixing upstream from the region where chemistry occurs, to try to determine mixing parameters (such as k, the turbulent kinetic energy, and ε, the turbulent energy dissipation rate.

Methane plasmatron CFD modeling

In the experiments the generation 3 plasmatron is used. The geometry of the plasmatron used in the experiments is shown in Figure 2.5. Details of this model and results are described in [Bro05e].

For the case of methane, only two independent airs are used: the wall air and the swirl air (no axial air is used in the experiments described in Section 8.a). The wall air is injected in the axial direction at the same axial location where the methane nozzle is located. The swirl air is injected downstream from the wall air and the methane, with a large amount of vorticity. The swirl gas moves the discharge into the central region of the plasmatron, and provides the rotation motion that moves the arc roots on the electrodes to minimize electrode erosion.

Two locations for introduction of the methane have been investigated: the methane can be introduced through the axial nozzle, upstream from the plasma, without any air; or the methane can be premixed with the swirl air and injected as the plasma gas.

Downstream from the plasmatron head there is a 5 in long section of the reaction extension cylinder which is also included in the model.

The axisymmetric, steady state solution of the fluid dynamics in the plasmatron methane reformer has been calculated using a commercially available CFD code, FLUENT. The model includes compressibility of the air, using ideal gas. Wall temperatures are at the same temperature as the gas (300K). Inlet conditions in all three ports (swirl air, wall air and methane) are as mass flow rate. The outlet condition is atmospheric pressure.

The effect of changing the grid structure has been investigated to determine the convergence of the problem, by using a grid that has four times the node density, and it has been determined that the mesh is appropriate for the problems investigated in this paper.

The model uses a turbulent model based upon the k-epsilon RNG model, with standard wall functions. The RNG mode is better suited for analysis of flows with substantial swirl, as is the case with the plasmatron methane reformer. The model solved the steady state conditions, using an implicit formulation and segregated solver. The convergence criteria for momentum, swirl, axial and radial velocities, k, epsilon and species concentrations was 10^{-4}. The energy was monitored and controlled, with a convergence criteria of 10^{-8}.

Since no chemistry is included in the model, the model cannot be used to describe the flows downstream from the plasma. The object of these calculations is to determine the conditions at and immediately following the plasma zone. In particular, the presence of recirculating flows that constitute exhaust gas recirculation, are likely to have substantial effect on the performance of the plasmatron methane reformer.

Axial injection of methane

In this section, the results for the case when the methane is injected introduced through the axial nozzle are presented. Although this is not the best configuration for methane, it is the preferred configuration for liquid fuels, which require air-assist atomization. Axial injection minimizes wall wetting.

The swirl air and wall air flows in the model are1.29 and 2.59 g/s respectively, while the input of methane is 0.45 g/s, corresponding to an O/C ratio of about 1.8. The high O/C corresponds to that shown experimentally to produce good conversion of the methane and moderate hydrogen yield in a non-catalytic reactor. The wall air is injected without swirl, but the plasma gas has a swirl ratio of 12/40 (radial to tangential speed).

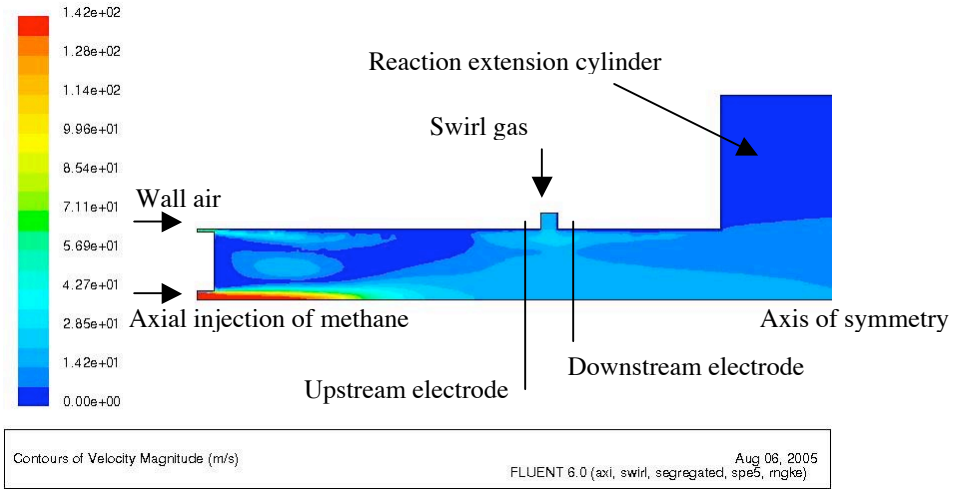

(a)

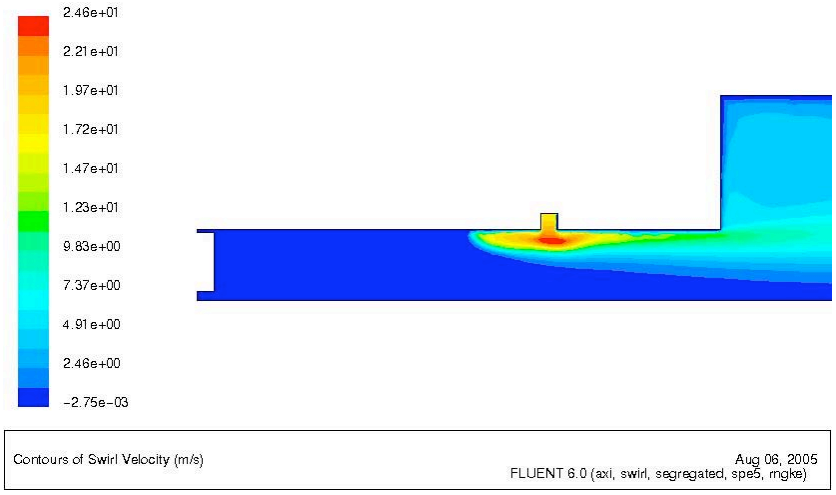

(b)

Figure 7.1. Contours of constant (a) velocity magnitude; (b) swirl velocity

Figure 7.1 shows the velocity profiles in the plasmatron head and the entrance to the reaction extension cylinder. The left region in Figure 7.1 corresponds to the top of the plasmatron in Figure 2.5 (as the plasmatron is axially symmetric only half of the plasmatron in Figure 2.5 is shown, rotated clockwise 90 degrees,). The flows are labeled in Figure 7.1 (a). Only a small section of the reaction extensions cylinder is shown, as the model is not applicable to this region. The methane is injected through the axial nozzle and at the extreme left of the figure.

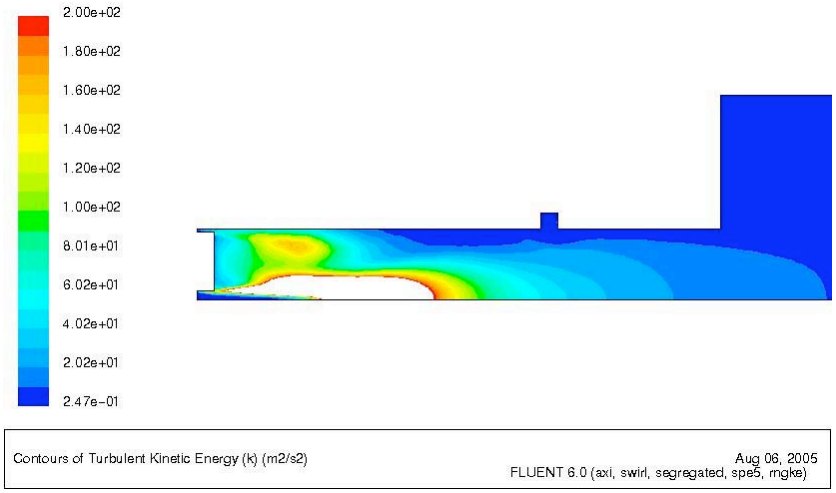

(a)

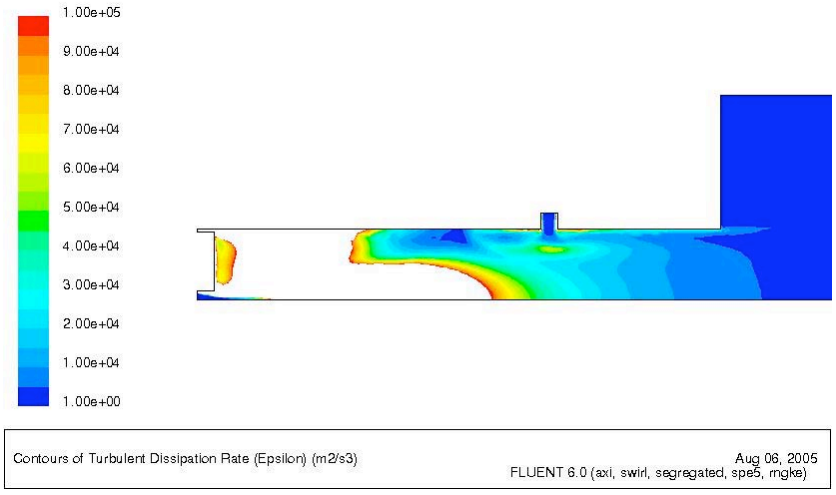

(b)

Figure 7.2. Contours of constant (a) k, turbulent kinetic energy; (b) ε, dissipation rate

The injection velocity of the methane is high (on the order of 120 m/s). The velocity has to be high in order to provide the narrow radial distribution of the methane that results in stratification of the methane, with high concentration on axis. The methane velocity decreases to the bulk velocity downstream, but upstream from the electrode gap region. The swirl gas (in this case, air) has swirl velocities on the order of 20 m/s in the plasmatron, with velocities decreasing to about 10 m/s downstream from the plasma region. It should be noted that the swirl gas flows upstream from the injection point, resulting in longer residence time in the plasmatron. As the swirl flows modify the plasma, it part of the plasma, and the upstream root of the plasma, should move upstream from the electrode gap. This has been observed experimentally.

The turbulence parameters k (turbulent kinetic energy) and ε (turbulent kinetic energy dissipation) are shown in the Figure 7.2. These parameters are important for the chemical modeling because they drive the turbulent mixing. The mixing time, which is the time for

mixing of the flows, is determined by the ratio of k to ε, $\tau_{mixing} \sim k/\varepsilon$. k is in the range from 1-5 m^2/s^2 in the plasma region, while ε varies from $2\ 10^4 - 6\ 10^4\ m^2/s^3$. The mixing time, for these conditions, vary from 0.1 – 0.5 ms

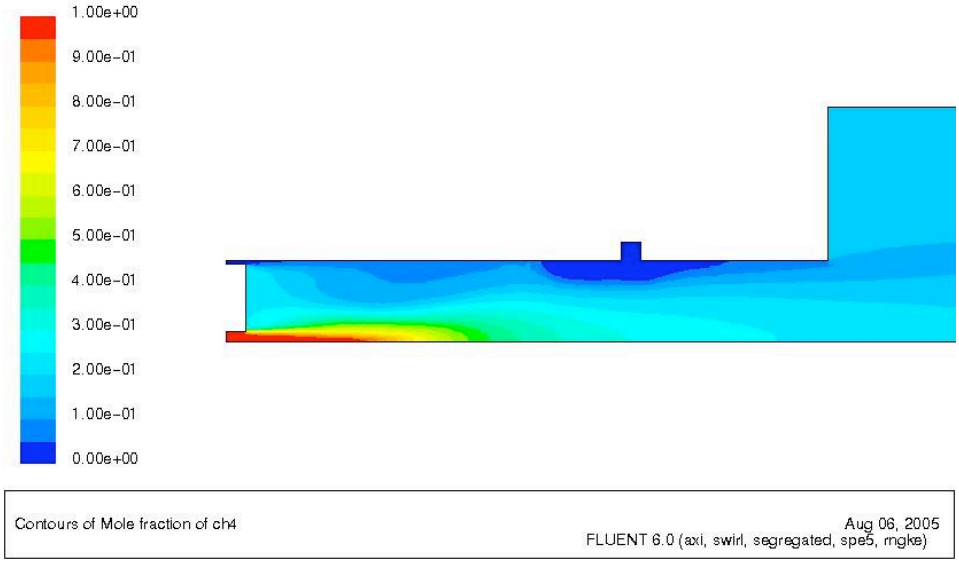

Figure 7.3. Contours of constant methane molar concentration

The molar concentration of methane is shown in Figure 7.3. The methane is stratified in the plasmatron head region, with highest concentration on the axis, decaying radially. It is thought that reforming in plasmatron fuel converters proceeds through a two-stage process, as described in the experimental and chemical model papers [Bor05c, Bro05d]. Reforming is maximized when there are substantial regions with stoichiometric methane/air mixture. The partial mixing is expected to result in ignition of some regions with good flammability characteristics, with mixing controlled reaction proceeding through the low flammability region. Both the Perfectly Stirred Reactor model [Bro05c] and the Partially Stirred reactor PaSR model [Bro05d] are used in the accompanying papers to investigate partial mixing

Only in the region of the reaction extension cylinder the methane and air are well mixed. It should be noted that there is no methane present within the strong swirl next to the plasma electrode. It is thought that the lack of fuel in this plasma region is responsible for poor experimentally determined reforming performance in the case of axial methane injection, and has suggested introduction of at least some of the fuel through the swirl gas. This condition will be discussed in the next section.

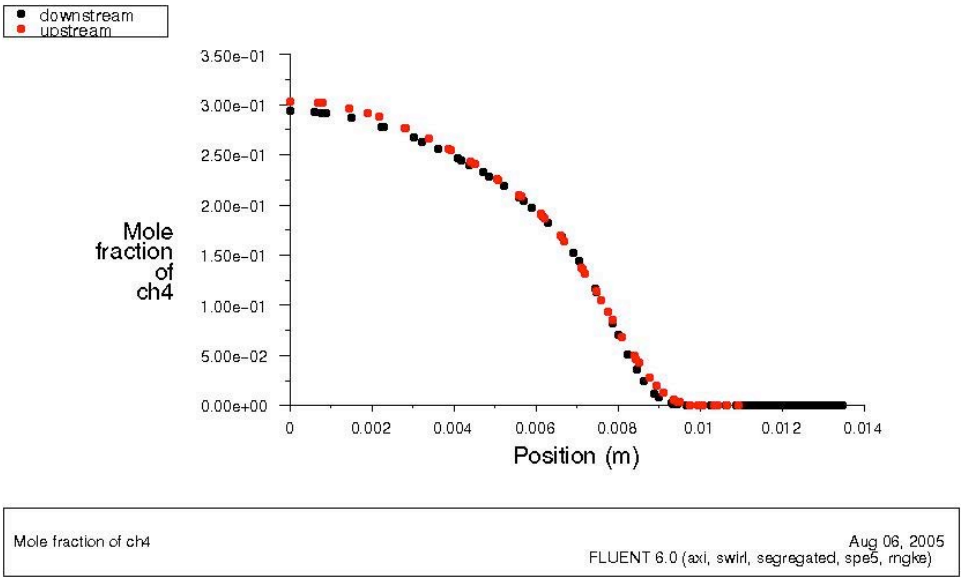

Figure 7.4. Radial molar concentration of methane along a radius at planes coinciding with the upstream and the downstream electrodes, shown in Figure 7.1(a).

The radial concentration of methane, measured along a radius upstream and downstream from the electrode gap (shown in Figure 2(a)), is shown in Figure 7.4. As expected, because the swirl flow does not contain any methane, the upstream and downstream concentrations are very similar.

Stoichiometric combustion of methane occurs for a methane molar concentration of 9% (at an O/C = 4). As the methane concentration gradient is large in the zone where the methane concentration is 9%, the zone with approximately stoichiometric methane/air mixtures is small.

Methane premixed with swirl gas

In this section, results will be shown for the case when the methane is premixed with the swirl air, and injected through the gap between the two electrodes, with strong vorticity. In this case, there is no input through the axial nozzle, and wall air and swirl air flows at the same levels as in the previous section.

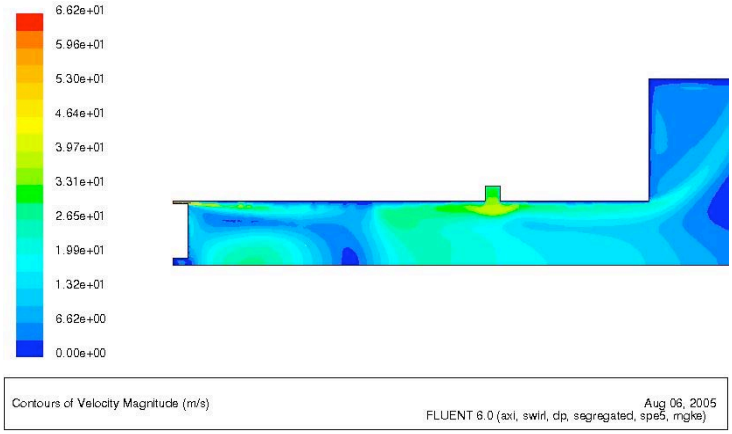

(a)

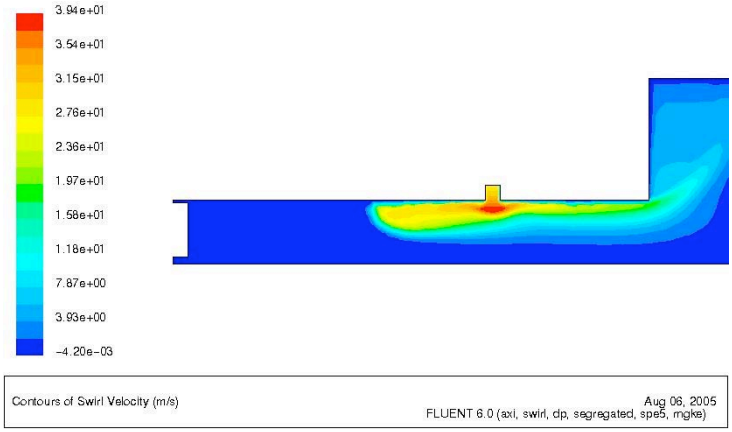

(b)

Figure 7.5. Same as Figure 2 but for case of methane through swirl port.

Figure 7.5 shows contours of constant magnitude of the velocity magnitude and the swirl velocity for the same air flows as Figure 7.1, but for methane through mixed with the swirl air. The swirl velocities are larger, due to the increased flow of swirl gas (which now contains also the methane, about 100 lpm STP in Figure 7.5, vs 60 lpm in Figure 7.1). The swirl motion also moves further upstream in Figure 7.5 than in Figure 7.1.

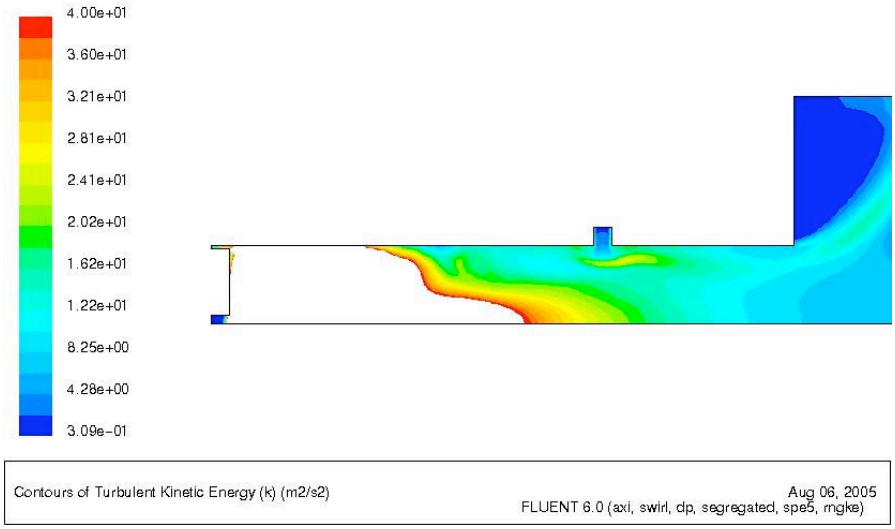

(a)

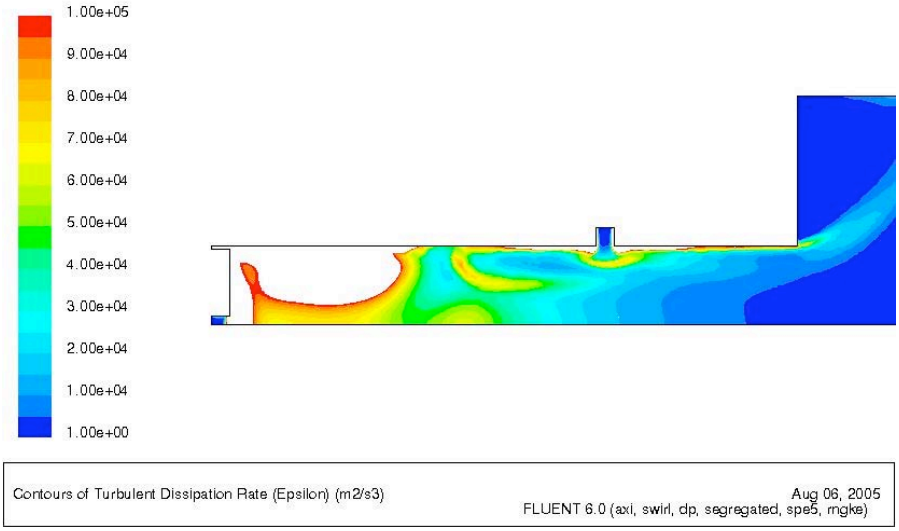

(b)

Figure 7.6. Same as Figure 7.2 but for methane injected through the swirl port.

The turbulence parameters, k and ε, do not change substantially in the region of the plasma when the location of the methane injection is varied, as can be seen by comparing Figure 7.2 and 7.6. Thus, the mixing time is not sensitive of the place of injection of the methane.

However, the methane concentration profile changes substantially in the two cases. Contours of constant methane concentration are shown in Figure 7.7 for methane through the swirl port. The gradients are in the opposite direction from that of figure 7.3, with highest concentration near the wall and smallest near the axis.

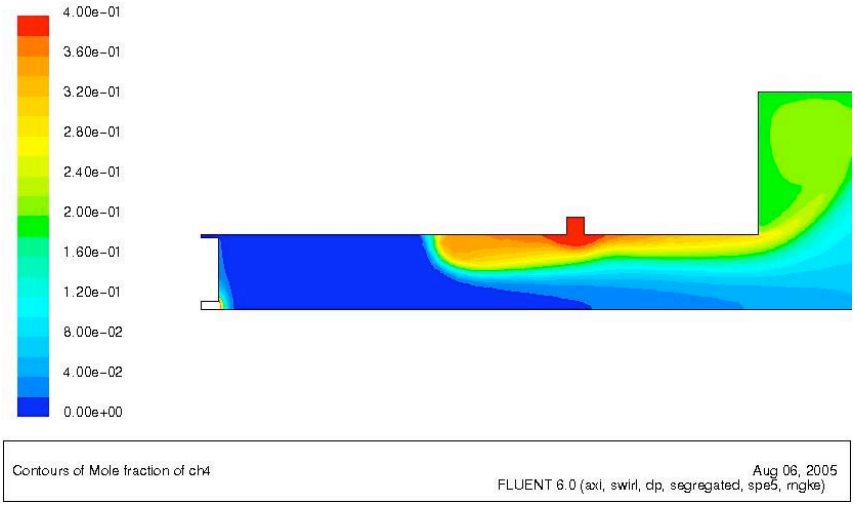

Figure 7.7. Molar concentration of methane for the case of methane premixed with swirl air.

Figure 7.8 shows the molar concentration of methane at the location of the upstream and downstream electrodes. As opposed to the case shown in Figure 7.4, the gradients in the methane concentration are small near the region with stoichiometric methane/air mixture (at around a radius of 0.055 m), which results in a larger fraction of the methane near combustion conditions, and should be better suited to two-stage reforming. The location of the stoichiometric conditions is not that different from the case shown in Figure 7.4, but it is substantially larger because the gradients are smaller.

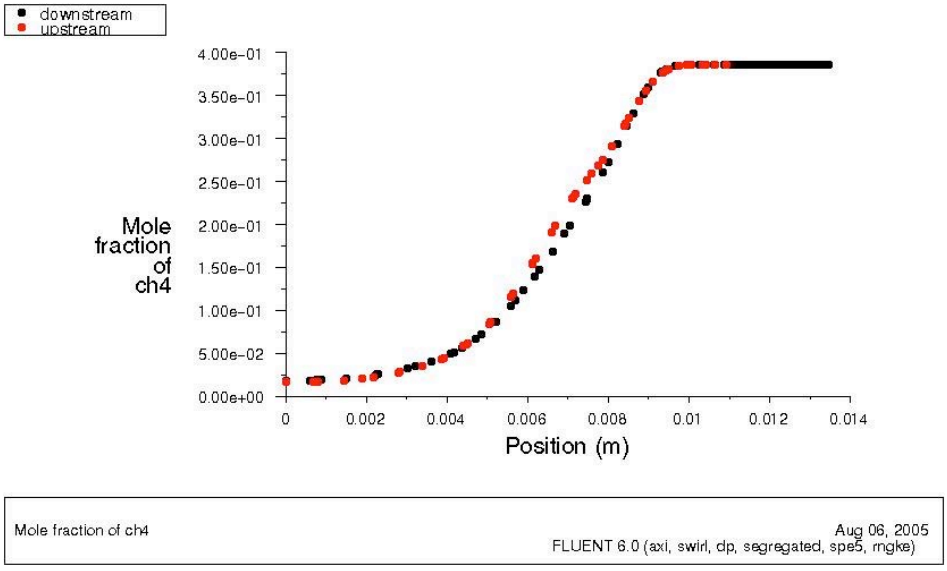

Figure 7.8. Radial concentration of methane at the location of the upstream and downstream electrodes.

In this case, there is a difference between the upstream and downstream planes, as the methane is part of the swirl flow, and some of it moves upstream while the rest moves downstream.

Thus, the conditions generated in the case of methane premixed with the swirl air are more conducive to two-stage reforming than that for axial injection of methane. Results not shown in this paper indicate that premixing the methane with the wall air has similar methane concentration profiles than the case with axial injection, and thus should have comparable reforming characteristics. It has been experimentally shown [Bro05a, Bro05b] that the case of methane through the swirl port results in improved reforming (defined as methane conversion at a given overall O/C and at a given power).

Propane plasmatron CFD modeling

One of the disadvantages of using methane as a surrogate hydrocarbon for heavier fuels is that the methane chemistry is substantially different from that of heavy hydrocarbons. In order to address the issue of the different chemistry, a heavier gaseous hydrocarbon needed to be tested. In this paper, the performance of plasmatron propane reformers is investigated. Propane-air mixture is the simplest hydrocarbon system that exhibits chemical behavior, laminar flame speeds and thicknesses, and extinction limits that are comparable to those of heavier fuels [Tur96]. It is probably the smallest system from which quantitative information directly relevant to the partial oxidation of heavier liquid gasoline and diesel fuels can be extracted, and is therefore an appropriate choice for this study [Haw98]. Unfortunately, unlike the case of methane where chemical modeling of the experiments were performed [Bro05c, Bro05d, Bro05e], propane mechanisms are not as well developed, and we have not performed chemical modeling to compare with these experiments,

The experimental results, and the accompanying calculations, were carried out with propane introduced in 5 different ways: (a) through the axial nozzle, similarly to what is done with liquid fuels (described in section 3); (b) premixed with the wall air; (c) premixed with the swirl (plasma) air; (d) premixed with all the air, so that the air/propane distribution in the plasmatron and the reactor are homogeneous; and finally, (e) stoichiometric conditions in the swirl gas, with the rest of the propane introduced with the wall air.

Downstream from the plasmatron head there is an insulated 12 cm (5 in) long reaction extension cylinder which is also included in the model. The volume of this section is approximately 1000 cm^3.

Air/propane mixtures

The axisymmetric steady state solution of the flows in a plasmatron propane converter is calculated using a commercially available CFD code, FLUENT. Description of the model and results for the case of methane are presented in reference [Bro05e]. The model

was used to determine the effect of initial conditions on the mixing upstream of the region where sufficient thermal energy has been released to modify the result, which occurs downstream from the plasma region.

Because of the multitude of cases, only three cases will be presented: the case of axial injection of propane, propane premixed with the wall air, and propane premixed with the swirl air. The flow rates used in the simulation of the different injection modes are shown in Table 7.1. The flow rates for the different modes correspond to those that experimentally optimize the reforming. The flow rate of propane is held constant in the experiments and in the model (at 0.5 g/s), but the total amount of air and the distribution of the air is varied to optimize the reforming.

Table 7.1. Flow rates (in g/s) for the different modes of injection

Fuel injection	Axial	Premixed wall	Premixed plasma
plasma air	1.29	1.51	1.51
plasma fuel	0	0	0.5
wall air	3.67	2.59	1.51
wall fuel	0	0.5	0
axial fuel	0.5	0	0

The model indicates very different distribution of the air/propane mixture for the different modes of injection. The propane concentrations for the three modes of injection are shown in Figure 7.1. Also shown are the axial velocities of the gas for the three cases. The figure shows a cross-section of the plasmatron. The axis is the horizontals at the bottom of the figure, with the radius in the vertical direction, the axial and wall gas injection are at the left of the figure, the swirl gas is introduced in the upper boundary towards the middle of the narrow section, and wide section at the right is the beginning of the reactor. Only a section of the reactor is shown in the figure, as the model is not appropriate for this region because of the absence of chemistry. The figures therefore show half of the plasmatron section shown in Figure 2.5, rotated counterclockwise by 90 degrees.

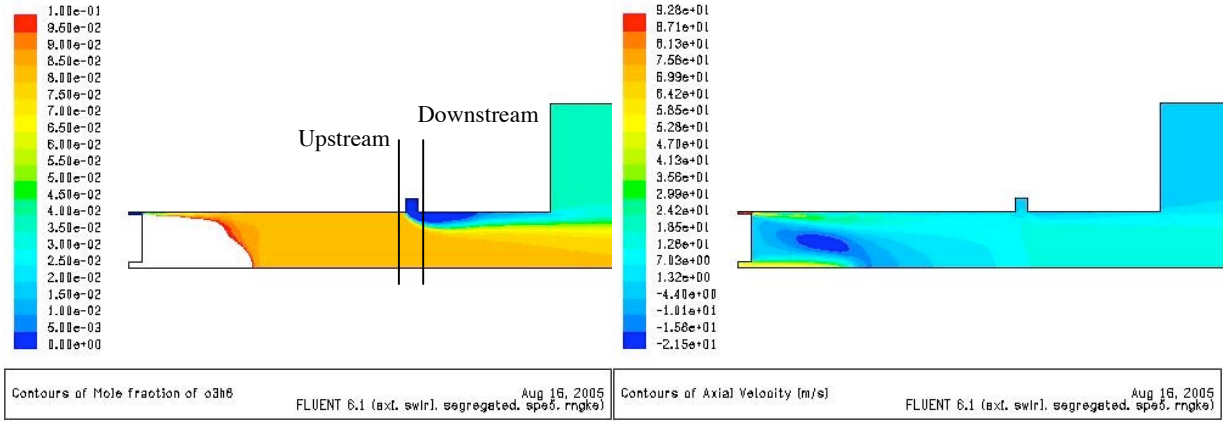

(a) Axial injection of propane: molar concentration (left) and axial velocity (right)

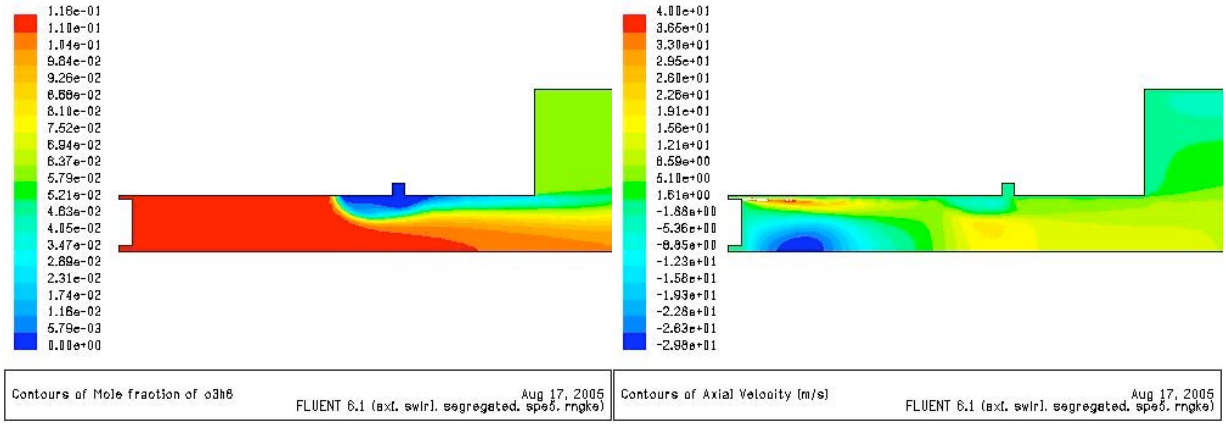

(b) Premixed propane with wall air: molar concentration (left) and axial velocity (right)

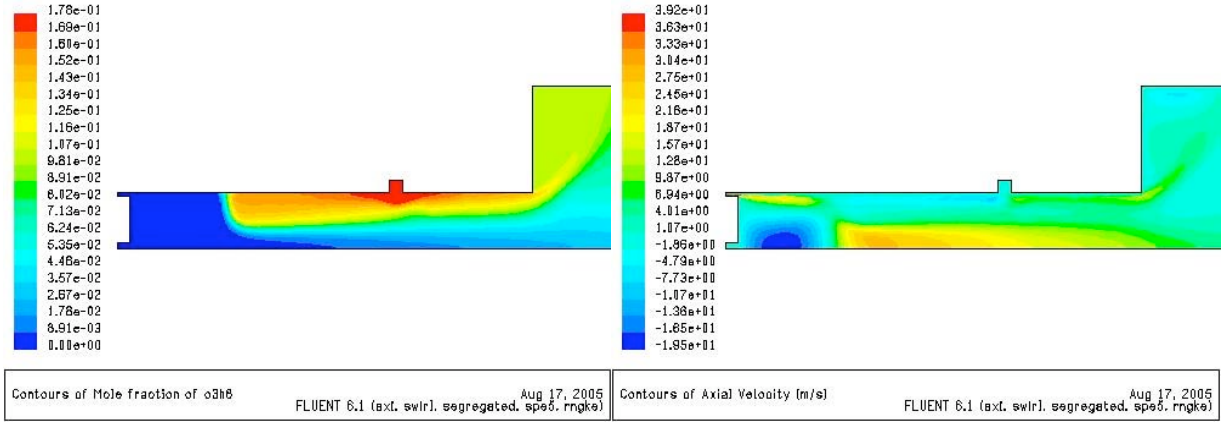

(c) Premixed propane with plasma air: concentration (left) and axial velocity (right)

Figure 7.9. Results from CFD calculations of propane molar concentration (left) and axial velocity (right) for the three modes of injection shown in Table 7.1.

The swirl gas flows upstream from the injection point, because of the strong vorticity. How far upstream is determined by the swirl flow and the axial flows. The case where the propane is premixed with the swirl air results in the largest upstream flow, followed, by the propane premixed with the wall air and finally by the axial fuel injection. The case with the propane premixed with the swirl flow has the lowest wall air flow, followed by the propane premixed with the wall air and by the axial propane injection. This back flow has a large impact on the air/propane distribution at the location of the plasma (around the region of the electrode gas, where the swirl gas is introduced).

In the three cases considered there is a large amount of recirculation upstream the electrodes. In some alternative designs of the plasmatron there is a diaphragm in the region between the axial nozzle and the electrode gap, but it is not needed for the design shown in Figure 2.5, as the recirculation flow happens automatically. This recirculation has a large impact on the air fuel distribution. For the case of axial injection of the propane, the recirculation results in a very high level of mixing between the propane and the wall air, well before the region of injection of the swirl gas. There is nonuniform air/propane distribution only in the small region between the central zone of the wall air plus propane and the periphery where the swirl air is located. Figure 7.10 shows the radial molar concentration of propane for a plane that corresponds to the upper electrode and for a plane corresponding to the lower electrode (downstream). The axial locations of these planes are shown in Figure 7.9 (a, left). The propane concentration is uniform upstream of the electrode gap, and downstream from the electrode gap there are two clearly demarked zones, one with about 8% propane and the second with no propane. For stoichiometric propane air combustion, the concentration of propane is about 4% molar. Thus there is a very small region with easily ignitable fuel.

In contrast, for the case of propane premixed with the swirl air there is a larger zone of stoichiometric air/fuel mixture, with gradients in the opposite direction. The propane molar concentration in Figure 7.9 b shows larger regions of stoichiometric air/propane mixtures, which should be favorable for two stage reforming, as discussed in the accompanying methane papers [Bro05a, Bro05b, Bro05c, Bro05d, Bro05e]. Figure 7.10 shows that indeed there are larger regions of stoichiometric air/propane zone in this case.

The case of propane premixed with the wall air falls between the case with propane axial injection and propane premixed with the swirl air. It will be shown in the experimental section of this paper that indeed, best reforming occurs with propane premixed with the swirl air, followed by premixed with wall air and finally, axially injected propane. The case where propane and air are fully premixed (equal composition of the wall gas and the swirl gas is also discussed in the experimental section. This last case of course has no nonuniform distribution, and the reforming results are comparable to that of the axial propane injection.

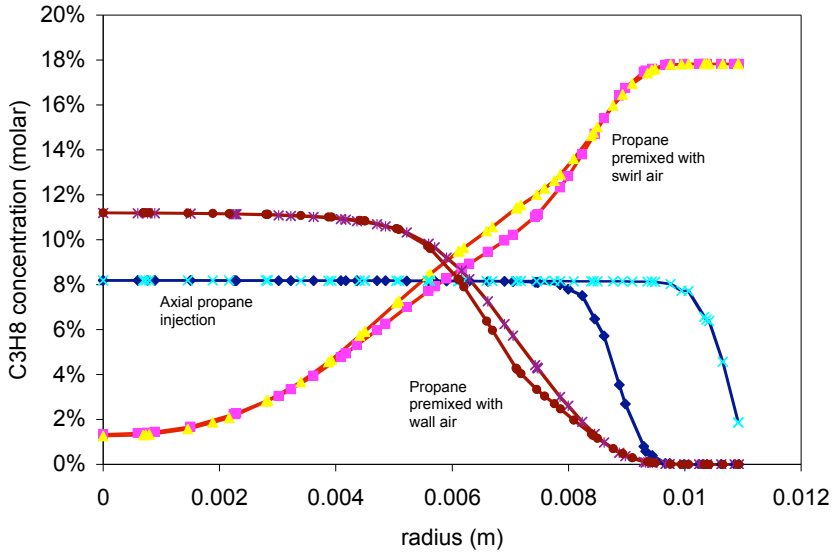

Figure 7.10. Propane concentration as a function of radius for locations upstream and downstream from the electrode gas, for the three difference modes of injection of propane.

Gasoline plasmatron CFD modeling

The performance of liquid fuels and gaseous fuels is very different due to the latent heat of vaporization of the liquid fuel. There are three main differences between liquid and gaseous fuels. First, there is a finite rate of vaporization of the fuel, and thus either combustion occurs as a diffusion flame (as is the case in a diesel engine). The second has to do with the heat of vaporization of the fuel, which cools the air/fuel mixture. Finally, because of the need to prevent wall coating, the liquid fuel is exclusively injected through the axial port, while the gaseous fuels could be injected through any set of ports, and indeed had best performance when injected through the swirl gas.

Section a describes a simple CFD model that is useful to understand the air/fuel mixing, as well as the vaporization of the gasoline droplets. Section b discusses the setup and the characteristics of the plasmatron gasoline reformers, in particular the effect of the fuel atomization and the cooling of the air/fuel mixture due to the latent heat of vaporization of the gasoline.

The calculations were performed using FLUENT 6.0 CFD package. The solution is for a steady state solution, axisymmetric, with air as the fluid. A Reynolds-Average Navier-Stokes model has been chose, with a k-ε formulation for the turbulence. The model includes swirl and compressibility of the air. The energy equation is solved. The solution is shown on half of the cross section of the plasmatron. A small section (1 in) long of the reaction extension cylinder is also included in the model.

No chemistry is assumed. Wall temperatures are at the same temperature as the gas (300K). The outlet condition is atmospheric pressure. Inlet conditions in all three ports (plasma air, wall air, atomization air) are as mass flow rate. Under-relaxation has been used for the pressure (0.3) and momentum (0.7). The scheme for solution is 2nd order upwind.

Table 7.2 shows the parameters used in the calculations. The gasoline flow rate assumed was 1 g/s, twice that of the experiments. The fuel was injected using "surface" injection at the port for the atomization air (uniformly distributed). Fuel droplets were injected exclusively in the axial direction, with no radial or tangential component, that is, with a zero spray angle. It was assumed that the injection velocity of the droplets was 50 m/s. The droplets composition was n-octane and uniform in diameter, with the droplet size in the first set of calculations is assumed to be 50 μm. This is a relatively large drop size. Evaporation of the droplets was included, and the concentrations of the n-octane vapors have been calculated. Smaller drop sizes will be considered later in this paper. Finally, the effects of spray distribution are discussed in the last section.

50 μm diameter droplets

In this section, the upper range of the particulate size is investigated.

Table 7.2

Plasmatron gen 3A

Plasma air	0.0018 g/s	
Velocities: swirl	50./s	
Radial	-12 m/s	
Wall air	0.0028 g/s	
Atomization air	0.0013 g/s	
Atomization air temp	300 K	
Fuel injection		
Droplet size	50 μm	
Initial droplet speed	-50 m/s	
Composition of droplet	n-octane liquid	
Spray angle	0	

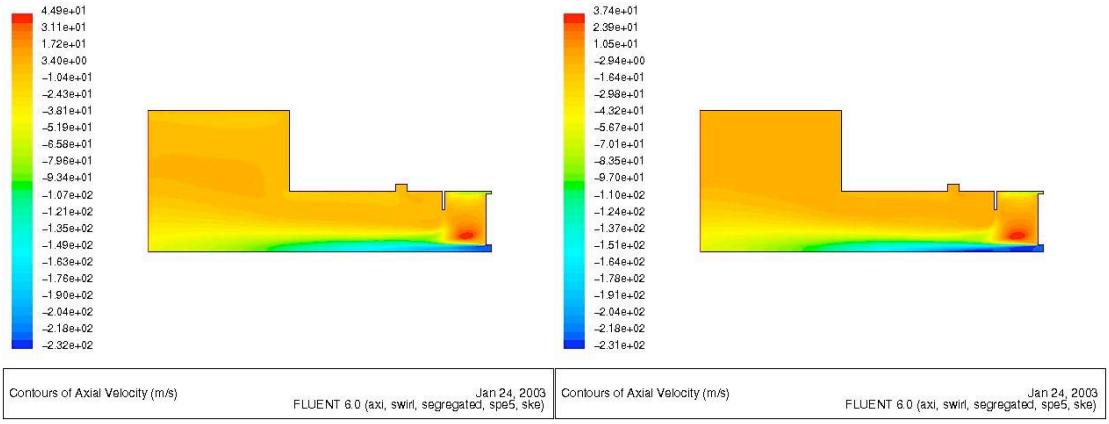

Figure 7.11. Axial velocity of the gas (a) with fuel injection (1 g/s) (b) no fuel injection

Figure 7.11 shows the axial velocity of the gas in the plasmatron for the conditions of Table 7.2 with and without fuel. Note that the axial velocity of the atomization air is lower in the case of the fuel injection than without, reflecting the fact that momentum is being transferred from the gas to the droplets, which are injected with lower speed (50 m/s).

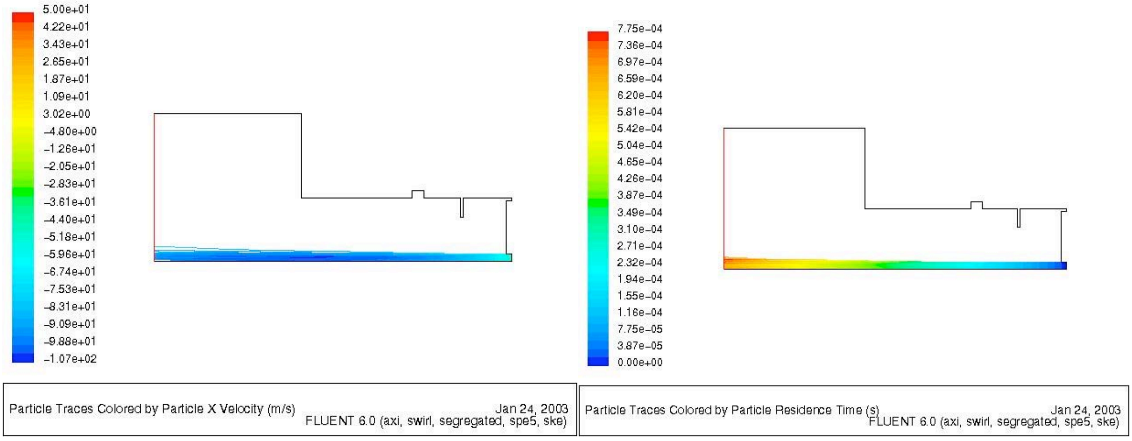

Figure 7.12. Droplet average path (a) droplet axial velocity (b) droplet residence time

Figure 7.12 shows results of calculations of n-octane droplets. The calculations are performed using stochastic air and droplet flow fields, with multiple droplets launched at the surface of the nozzle. Figure 7.12a shows the calculated droplet velocity on the droplet path, while Figure 7.12b shows the residence time. The droplets quickly achieve the velocity of the gas (air), by the time that they reach the interlectrode spacing they are well entrained in the atomization air flow.

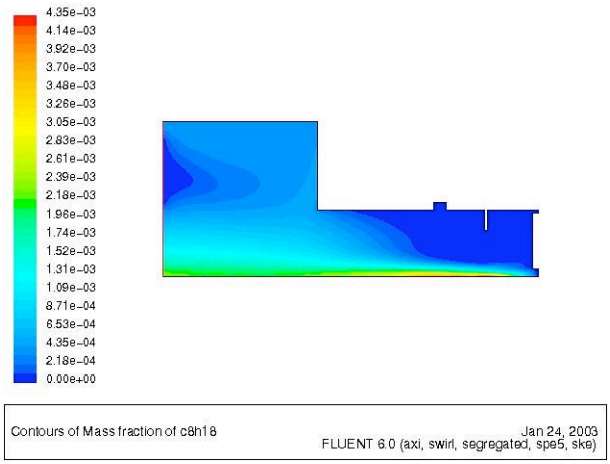

Figure 7.13. Mass fraction of Gaseous C8H18 (relative to nitrogen)

The mass concentration of gaseous n-octane is shown in Figure 7.13 for the case of 50 mm droplets. Only a small fraction of the fuel has vaporized, and the conditions for stoichiometric conditions (about 6% by mass for an air/fuel ratio of 15) are not reached with the fuel vapor.

10 μm diameter droplets

In order to examine the other extreme of the droplet size distribution, the calculations were performed with 10 mm diameter droplets. The smaller droplets size results in increased evaporation of the droplets, due to increased surface area, as well as in reduced particulate inertia, with increased impact on the droplet paths due to the turbulence of the gas.

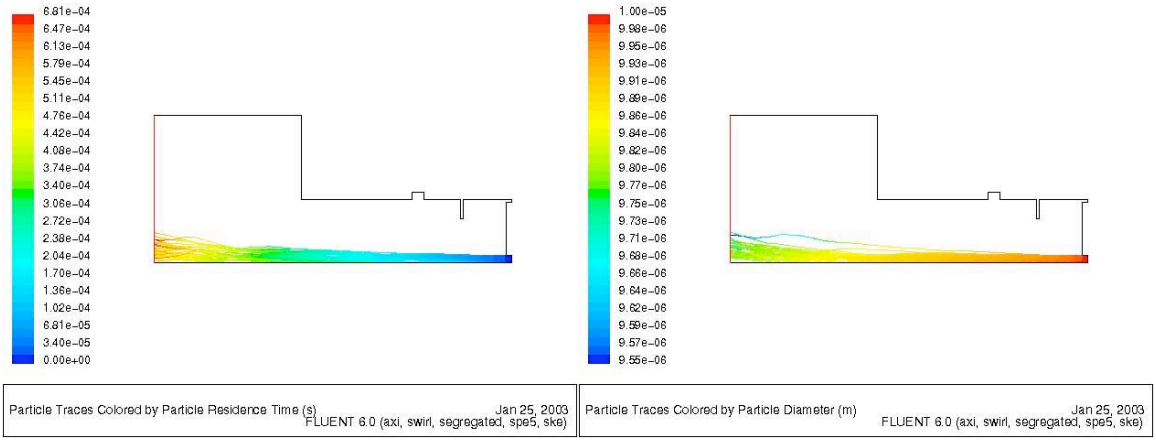

Figure 7.14. Stochastic particle path vs (a) residence time (b) particle diameter

The random paths of some droplets, launched at different locations on the nozzle surface, are shown in Figure 7.14. Different sets of droplets have been used in Figures 7.14 (a) and (b), as noticed by the outermost droplets. Figure 7.14a shows the residence times of the particulates, while Figure 7.14b shows the droplet diameter. Some evaporation of the particle is seen, more than in the case with 50 mm particles. However, even at the inter-electrode location (where the plasma is expected), the droplet diameter has decreased by only about 1%, corresponding to about 3% of the droplet. The corresponding concentration of n-octane is shown in Figure 7.15.

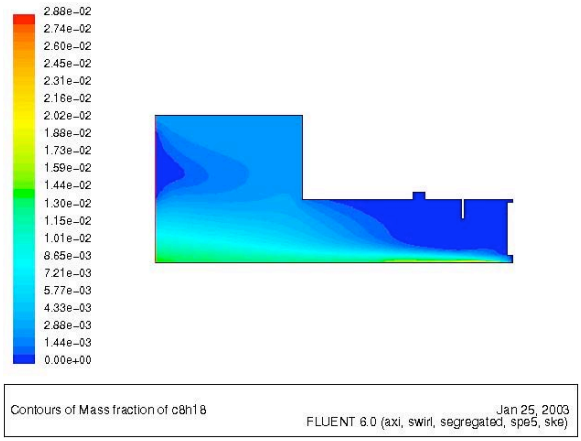

Figure 7.15. Concentration (by mass) of gaseous n-octane

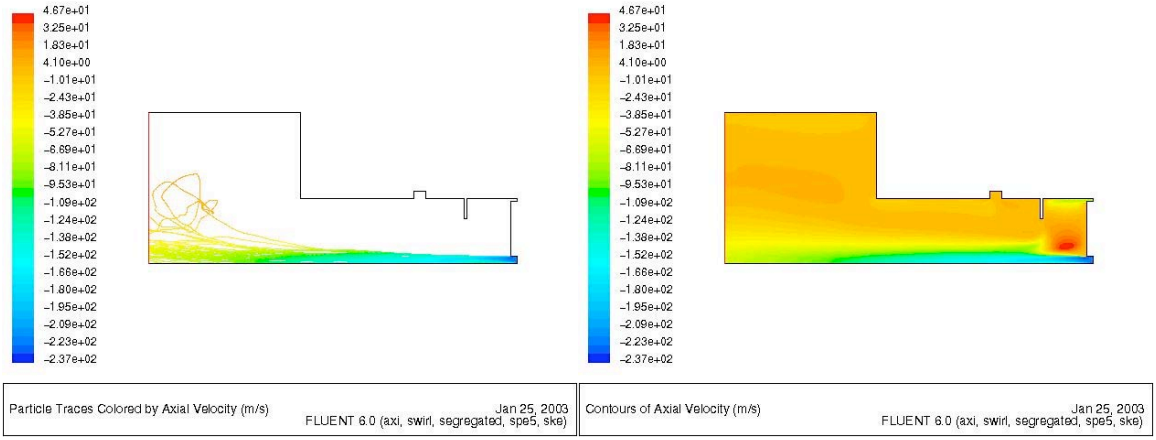

Figure 7.16. Axial velocity (a) of droplets along their path (b) of continuous media

As expected, with the smaller particle size there is stronger interaction between the continuous media and the droplets. Thus, in the case with smaller droplet size the atomization air slows down quicker and the droplets gain speed faster than in the case with larger droplet size. Also, the path of the smaller droplets (stochastically calculated in every plot) is influenced more by the local turbulence of the flow.

Finite spray angle

The surface injection has no capability of spray angle distribution, but it can have a non-zero radial speed (with no spread, therefore resulting in a cone-shape). Since the effect is more pronounced with the smaller droplets, the calculations of the effect of finite spray angle has been performed for 10 μm droplets.

The initial radial speed of the droplets was varied from 0 through 30 m/s. The initial axial speed of the droplets was kept constant at 50 m/s. Therefore, relatively wide spray angles were modeled.

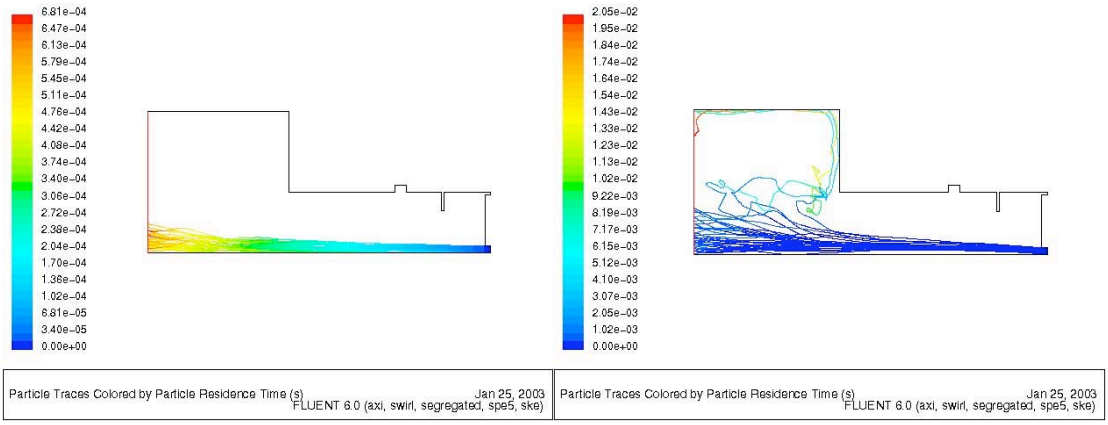

Figure 7.17. Stochastic paths for initial radial velocities of (a) 0 m/s, and (b) 10 m/s

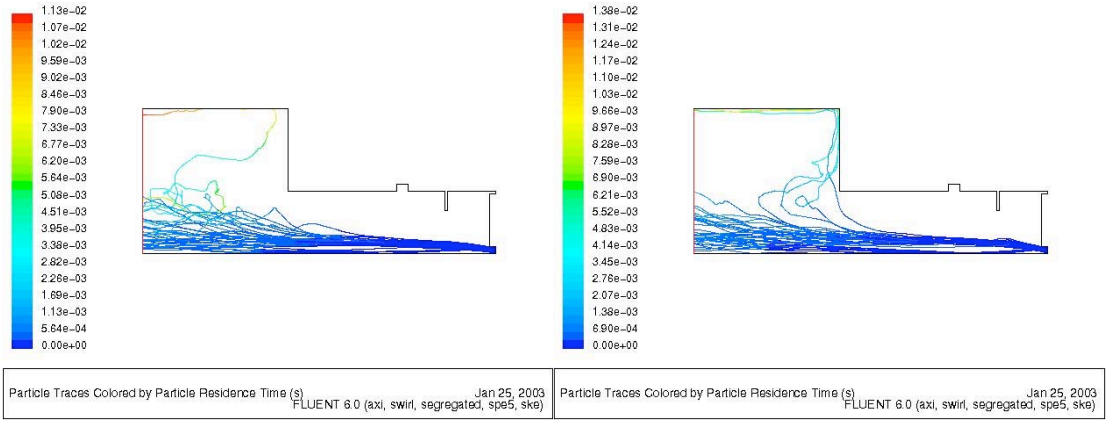

Figure 7.18. Stochastic paths for initial radial velocities of (a) 20 m/s, and (b) 30 m/s

The radius of the droplet "cloud" increases slightly when the initial radial speed of the droplets increases from 0 to 10 m/s. However, the location of the paths in the inter-electrode region do not change substantially when the initial radial velocity of the droplets increases further from 10 through 30 m/s

The complex vaporization process made modeling of the system very difficult, and it has been analyzed in a simplified CFD model. The simple models of the plasmatron, without chemistry, show that indeed very small fraction of the gasoline is vaporized.

Cooling of the gas by evaporating fuel

The gasoline droplets need some heat in order to vaporize. The vaporization rate of the droplets follows the rule

$$dD^2/dt = -K_e$$

Where K_e is the evaporation constant and is a function of temperature. For stoichiometric combustion, the change in the temperature of the air due to the vaporization of the gasoline is about 24 K, assuming constant pressure process. However, for partial oxidation, where the air/fuel mass ratio is about 1/3 that of stoichiometric combustion, the temperature of the air is reduced by as much as 70 K (assuming constant thermodynamic properties of the air). These large drop in temperature means that only a small fraction of the gasoline will be vaporized prior to entering the reaction zone, where exothermic reactions raise the temperature of the gas.

b) Chemical modeling

Hydrogen generation from natural gas has been performed using mainly steam reforming. Although steam reforming has substantial advantages from a system point of view, partial oxidation can have advantages in certain circumstances, particularly where pure hydrogen is not required, and where the hydrogen rich gas will not be compressed downstream from the reformer. [see, for example, Hic92, Hic93, Hic93a, Hic93b, , Deu98, Gor00, Gra94, Ber99]

In the fuel reformation of natural gas the use of catalysts is widespread. The catalyst reduces the required temperatures, increases conversion and maximizes the hydrogen yield. However, the catalyst is expensive and needs to be regularly exchanged, at substantial cost. It has been estimated that the capital cost of the catalytic reformer is on the order of 1/3-1/2 of the cost of the plant.

The conversion of natural gas without the use of a catalyst is attractive. Plasma-driven catalysts have been explored for the conversion of methane and other fuels. Our group at the Plasma Science and Fusion Center at MIT has been investigating the conversion of a wide range of fuel into hydrogen rich gas.

PSR model

The purpose of this section is to describe a simple chemical model of the process with methane, based upon a two stage, Perfectly Stirred Reactor.

Chemkin 4.0 [Kee04] was used to simulate a fuel converter based on a plasmatron. The plasmatron fuel converter and experimental results have been described in accompanying papers, for steady state [Bro05a] and start-up [Bro05b] conditions.

The simple model described in this paper assumes that a fraction of the fuel is consumed in stoichiometric combustion and these combustion products mix perfectly with the rest of the room temperature air/fuel mixture. The model is consistent with observations in the plasmatron fuel converter [Bro05a, Bro05b], in which if the methane and the air are premixed, there is no conversion, and the conversion is a strong function of the methane/air stratification in the plasma region.

The process, as presently understood, is thus a two step process, with pure combustion in the first step which releases enough heat to drive the partial oxidation reactions in the second step.

The simple model uses an equilibrium reactor to combust the stoichiometric methane/air mixture. This mixture is then fed to a perfectly stirred reactor (PSR) that has a secondary input consisting in additional fuel and air (with O/C = 1) at room temperature. The

overall O/C ratio is then substantially higher than for stoichiometric partial oxidation (since the first stage has substantially higher O/C).

The fuel is methane. The GRI 3.0 mechanism was used in the calculations [Smi]. This mechanism has been developed to model methane combustion over a very wide range of conditions. It has 53 species and about 350 equations. The temperature of the combustion products in the first stage is about 2200 K. At this temperature, substantial levels of NO and nitrogen-carbon compounds are made. Nitrogen chemistry is followed.

It is assumed that the reactor is adiabatic and has a volume of 1000 cm^3. Although the volume of the reactor is easy to establish, the region with good mixing is not, and we have performed calculations for various reactor sizes. The residence time varies depending on the temperature of the gases as well as the mass flow rate. It has been assumed that the mass flow in the PSR is ~ 5 g/s (corresponding to a few hundred l/min).

The stoichiometric flow rate to the equilibrium reactor is varied in order to investigate the effect of additional enthalpy. The secondary flow (with O/C = 1) is held constant. In the experiments, the methane flow rate was constant [Bro05a, Bro05b].

The reactor network used in the simulation is schematically shown in Figure 7.19. There is no preheating of any of the reagents. The object of the plasma is to ignite the stoichiometric methane/air fuel mixture, but in terms of energy balance it provides only a small fraction of the exothermic energy of the partial oxidation reaction and is actually not included in the model.

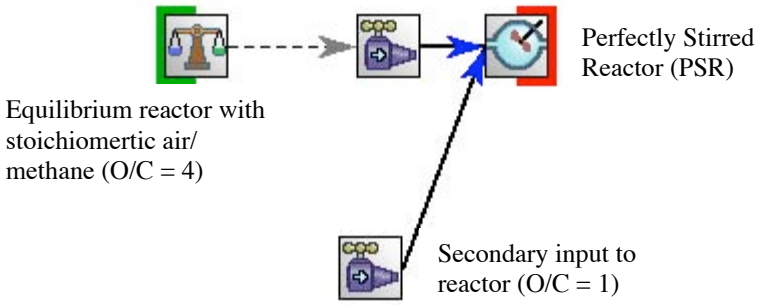

Figure 7.19. Schematic diagram of the process

Two Stage PSR results

The composition of the output from the PSR is shown in Figure 7.20 for the case of a reactor with 1000 cm^3. The secondary input flow rate (with O/C = 1) was 3 g/s, and the stoichiometric flow rate was varied to vary the overall O/C. It is clear that the hydrogen production and methane conversion processes experience a discontinuous jump around an O/C ~ 1.4 (corresponding to 1.5 g/s of stoichiometrtic air/methane mixture). There is very little hydrogen in the output for O/C < 1.4, and relatively constant after the transition. The amount of hydrogen produced in this homogeneous system is about 7-

8%, relatively independent on the overall O/C ratio. It should be noted that with increased stoichiometric mass flow rate (more combustion), the residence time decreases, both because of the increased mass flow rate as well as increased temperature.

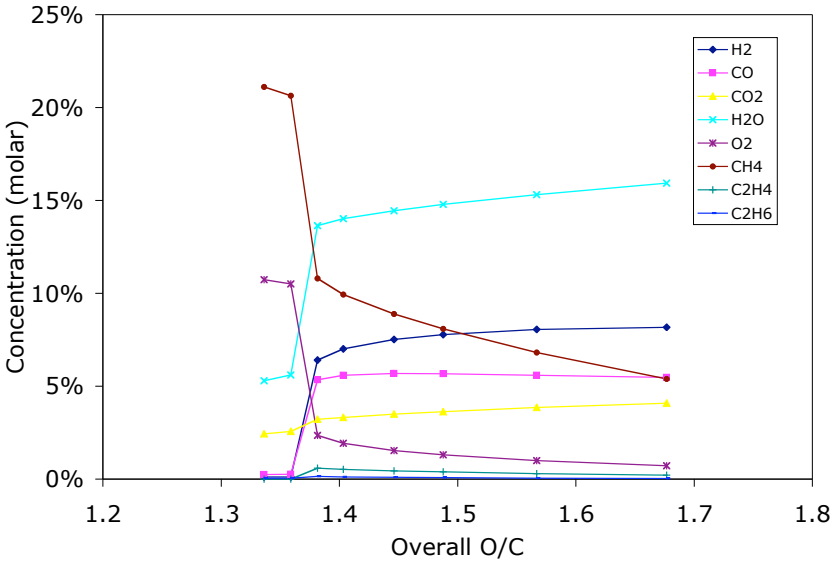

Figure 7.20. Composition of the exhaust as a function of the overall O/C ratio.

The PSR temperature and residence time are shown in Figure 7.21. The temperature increases with increasing stoichiometric flow rate. The temperature of the PSR reaches values where substantial reactions can take place, at which point the fuel rich mixture in the PSR ignites. The steady state temperatures of the PSR are on the order of 1400-1500 K. The residence time varied from about 80 ms at the conditions of the lowest O/C values considered, to about 30 ms to the highest flow rates.

The corresponding stoichiometric flow rate is plotted in Figure 7.22 as a function of the calculated O/C ratio. Substantial precombustion of the methane is required in order to drive the reforming reaction. A stoichiometric flow rate of 1.5 g/s is required for a secondary flow rate of 3 g/s, corresponding to an overall O/C of about 1.4. These conditions result in large enough temperatures to maintain the reaction.

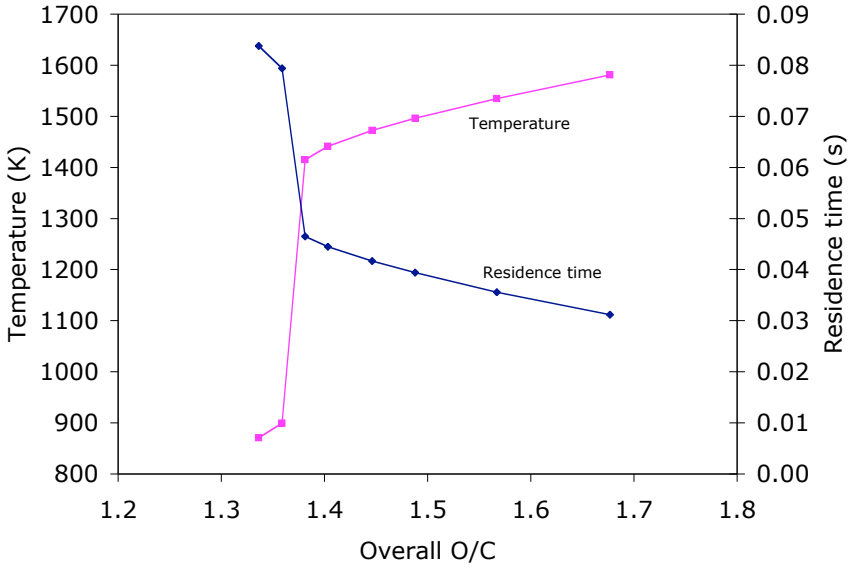

Figure 7.21. Reactor temperature and residence time as a function of the O/C ratio)

It should be noted that once the PSR is ignited, the concentrations are relatively insensitive to further increases in the overall O/C. (see figure 7.20). In addition, it is not expected that the size of the reactor, nor the flow (which affect the residence time), will have a large impact.

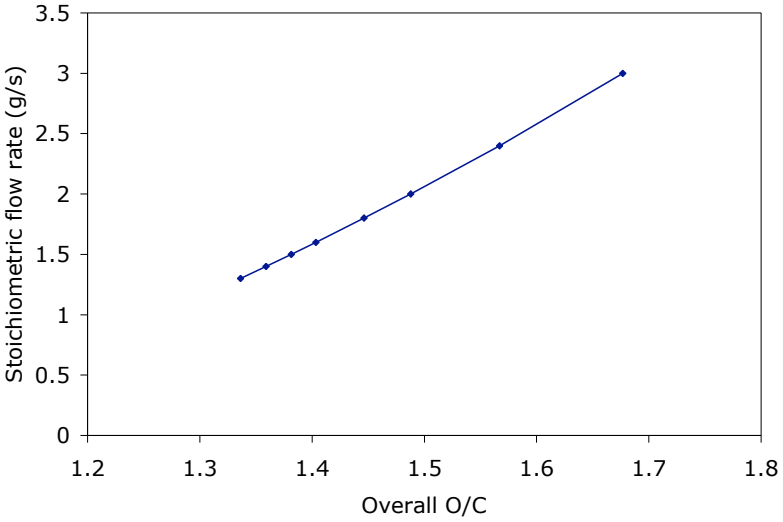

Figure 7.22. Stoichiometric flow rate as a function of overall O/C ratio (overall) (secondary flow rate to the PSR is 3 g/s)

In Figure 7.23, the concentration of fixated nitrogen compounds are shown as a function of the overall O/C ratio. NO (generated in the stoichiometric combustion process) shows a large discontinuity at the point where the PSR ignites, and there s a simultaneous

increase of HCN and NH_3, as would be expected from a system with a reducing environment.

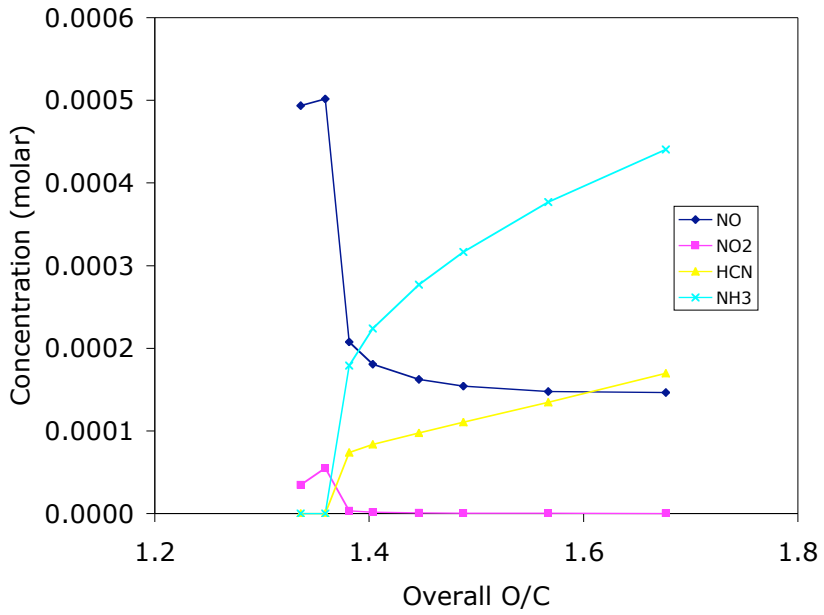

Figure 7.23. Fixated nitrogen as a function overall O/C (secondary flow rate is 3 g/s)

It would be useful to determine whether the fixated is generated in the equilibrium reactor or in the PSR. The equilibrium reactor generates, at a flow rate of 1.5 g/s, an NO flow rate of 10^{-4} moles/s. The output from the PSR has about 0.9 10^{-4} moles/s. Thus, most of the NO from the equilibrium reactor flows to the output of the PSR when there is little reforming in the PSR. Nor surprisingly, as it is in the equilibrium reactor where the nitrogen is fixated.

Effect of residence time in the conversion

In order to determine the effect of residence time, the flow rates were scaled down, with fixed reactor volume. These flow rates do correspond to more realistic flow rates in the experiment.

The total gas flow rate was varied from 2.5 g/s total to 20 g/s. The results are shown in Figure 7.24. Increasing the residence time only slightly increases the hydrogen yield and the methane conversion. The model suggests fast initial chemistry, followed by slow chemistry.

The composition of the fixated nitrogen compounds for different residence times is shown in Figure 7.25. There are changes in the composition of the fixated nitrogen, with NO decreasing and NH_3 increasing. As with the composition of the major components, slow chemistry follows relatively fast chemistry. For residence times larger than about 20 ms, the rates of conversion are very slow and the concentration rate of change is slow. It

is interesting that the total fixated nitrogen does not change much over the range of residence times.

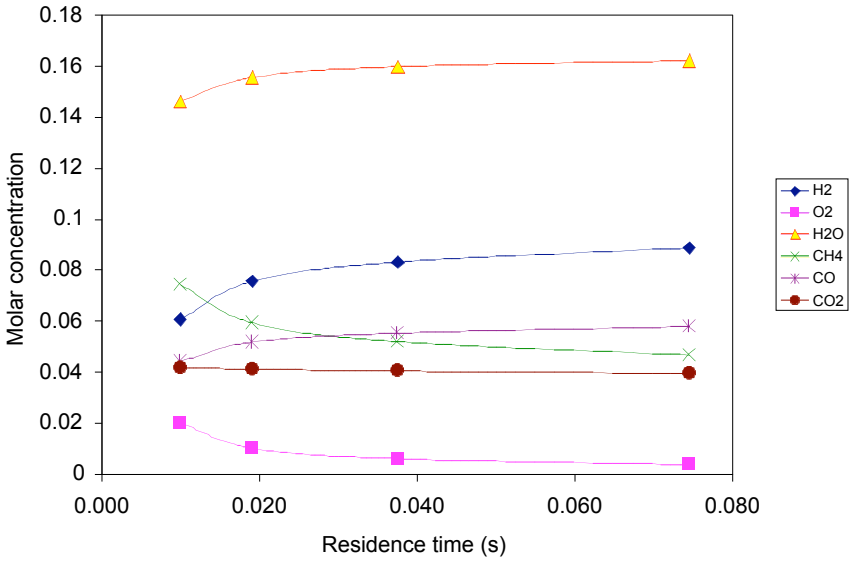

Figure 7.24. Molar concentration of major components as a function of the residence time.

The concentration of fixated nitrogen compounds is about 1400 ppm. The fixated nitrogen was not measured experimentally. However, measurements by Khadya [Kha04] and Stevens [Ste03] are in agreement with these measurements.

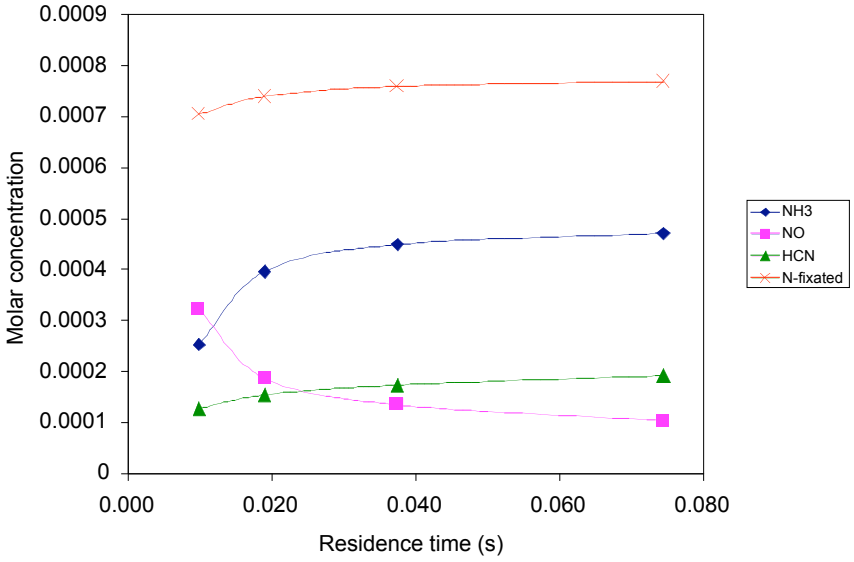

Figure 7.25. Molar concentration of fixated nitrogen.

It is likely that these compounds, when the reformate is used in a combustion process, will turn to nitrogen oxides.

The effect of changing the residence time has little effect upon the conversion, as shown in Figure 7.24. However, it has a substantial effect on the critical flow required for igniting the PSR. Figure 7.26 shows the overall O/C required for ignition corresponding to reactor sizes varying from 150 to 1000 cm^3, for a total mass flow rate of 4.5 g/s. As the reactor size decreases, the required temperature for ignition increases to compensate for the decreased residence time, increasing the required stoichiometric flow rate and thus the overall O/C.

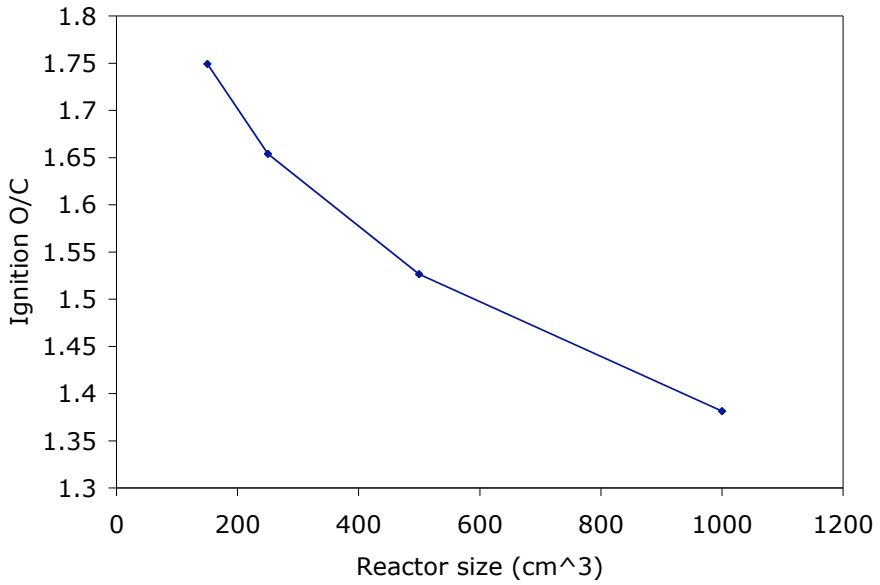

Figure 7.26. Required overall O/C for ignition of a PSR of various sizes, for a constant mass flow rate of 4.5 g/s

Discussion

In this section a comparison between the model and the experimental results is presented.

Results that illustrate the ignition-like behavior of the plasmatron methane reformer are reproduced in Figure 7.27 (from reference [Bro05a]). As explained in reference [Bro05a], there is a problem determining the O/C ratio, which has a ~10% spread. The results in Figure 7.27 show a required overall O/C of about 1.6 for ignition. Above it was determined that the overall O/C for ignition was closer to 1.4 for a reactor size of 1000 cm^3, but as discussed above, the physical reactor size may be substantially larger than the PSR, as the downstream sections of the actual reactor may be closer to plug-flow, rather than perfectly-stirred. Using results from Figure 7.26, a reactor needs to be about 250 cm^3 in order to match the experimentally obtained O/C ~ 1.6. It is not unlikely that the actual size of the PSR be this size, as recirculating flow (that generated the idea of the PSR model instead of Plug-Flow model), occur over substantially smaller sections of the

actual reactor, as shown in the paper on fluid simulation [Bro05e]. Although those simulations [Bro05e] did not include chemistry, the existence and size of the recirculation zone was suggested.

The model has been successful in predicting the experimental result that at relatively high values of O/C (> 1.6) there is a sudden increase the methane conversion. The experimental program was designed to test this hypothesis.

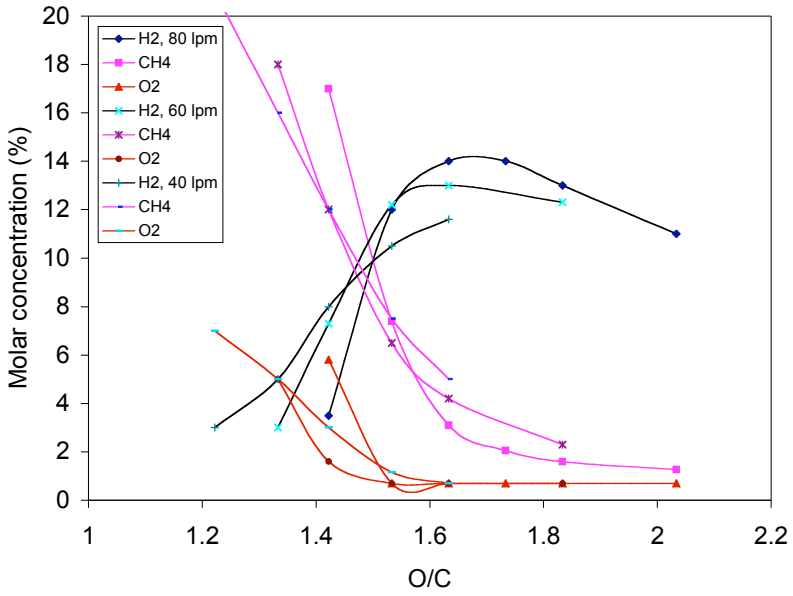

Figure 7.27. Experimental results (from reference [PSR9]),

Table 7.3. Comparison between experimental and model results

		5/2/2005-2	PaSR	PSR	
Power in	W	375	375		
Axial air	g/s	2.59	2.59		
Swirl air	g/s	0.86	0.86		
Swirl methane	g/s	0.45	0.45		
O/C ratio		1.63	1.63		
Composition		Experiment		Composition	Dry gas composition
H2	vol.%	13.5	11.5	8.2	9.6
O2	vol.%	0.5	0.8	0.7	0.8
N2	vol.%	69.8	69.2	58	67.8
CH4	vol.%	1.9	4.3	5.4	6.3
CO	vol.%	9.6	8.4	5.5	6.4
CO2	vol.%	4	4.0	4.1	4.8
C2H4	vol.%	0.8	0.0	0.2	0.2
C2H2	vol.%	0	1.7	1.5	1.8

Table 7.3 shows typical results from the experiment, and compares with the results obtained in this paper. The experimentally obtained dry gas composition of the reformate is under the column labeled 5/2/2005-2. The PSR results have been those calculated of the O/C ~ 1.65. Two columns are indicated, the first one for the actual composition, and

the second one for dry gas composition (to compare with the experiments). Also shown are the modeling results from the PsAR calculation [Bro05d].

The models underestimate the concentration of hydrogen (the PSR by about 40%, while the PaSR by about 20%). The assumption in this paper of very fast combustion in the first stage, followed by very fast mixing in the second stage, are crude approximation for the system. The PaSR model, which includes finite rate mixing, does a better job. A full fledged model using CFD and chemistry is outside the scope of the work.

It is not clear how large is the well mixed reactor, as there are regions in the downstream section of the physical reactor that resemble more a plug flow reactor than a well mixed reactor.

Partially Stirred Reactor Model

In the previous section, the use of two step reforming has been used to model a plasmatron methane reformer [Bro05c]. The model assumes that a fraction of the air/fuel mixture combusts stiochiometricly, and then the combustiong products mix with the balance air/fuel in a Perfectly Stirred Reactor (PSR). The model did provide quantitative agreement with experiments with a plasmatron methane reformer, in particular on the critical O/C ratio needed for homogeneous reaction, but failed to reproduce the observed concentrations. It was speculated in that paper that the reason was the use of instantaneous combustion (equilibrium conditions) in the first step and instantaneous mixing in the second step that is characteristic of the Perfectly Stirred Reactor, although the model did include finite kinetics in the second step. In this section, we investigate the possibility of improved agreement by including finite rate of mixing. [Bro05d]

The experimental results are described in accompanying papers that describe the steady state experiments with the plasmatron methane reformer [Bro05a] and experiments with transients, mainly cold startups [Bro05b]. All these experiments and the modeling in this and in the accompanying papers were carried in a reactor without a catalyst to investigate the gas phase chemistry of the plasmatron methane reformer. In an additional accompanying paper [Bro05e] a model of fluid dynamics of the plasmatron methane reformer has been investigated. The model in that paper does not include chemistry, and thus can be used to investigate the mixing prior to the region of substantial energy release from the chemistry. However, it provides a framework as for the level of mixing and the distribution of air/fuel mixture through the region of the plasma.

A previous paper attempted to simulate reformers, and in particular plasma reformers, using the Partial Stirred Reactor (PaSR) [Bel05]. That work used the PaSR code [Che97] available from CHEMKIN 3.7 [CHE37], which did not provide an adequate model because of inadequate input flexibility.

To simulate the limited mixing rates, the PaSR model [Bel05] from CHEMKIN 4.0.2 [Kee04] has been used. The code used was an updated, beta version of the PaSR routine, provided to us by Chou [Cho05]. The code assumes a large number of elements, each individual element being a perfectly stirred reactor. For the present calculations 1000 elements were used. Several initial conditions have been used. The code allows for control of the mixing time and the residence time. The model allows for flexible input of the elements; however, there is a single number of the mixing time, which is assumed constant throughout the reaction volume.

The GRI 3.0 mechanism was used in the calculations [Smi]. This mechanism has been developed to model methane combustion over a very wide range of conditions. It has 53 species and about 350 equations. The temperature of the combustion products in the first step is about 2200 K, at which temperature substantial levels of NO and nitrogen-carbon compounds are made. Nitrogen chemistry is followed.

Figure 7.28 shows schematically the reactor network. Since it is in steady state, the input flow rates are balanced by output flow rates, not show in Figure 7.28. The parameter of the inputs will be described below. The PaSR reactor is described by identifying the number of elements (1000), the residence and the mixing times, the pressure and the initial conditions. The results are dependent on the initial conditions, but it has also been experimentally determined that certain parameters are more conducive to ignition and good conversion.

The experimental setup had two independent flows, the swirl flow and the axial flow. The experimental results evaluated in this paper have swirl gas that is composed of all the methane and some of the air. The methane flow in the experiment was 0.45 g/s, corresponding to a heat of combustion of about 25 kW. The O/C ratio of the experimental points investigated in this section is varied by changing the axial air.

The model used three independent input flows. The first flow represents the arc discharge, which is modeled using a high temperature gas, with the composition of the swirl gas. The assumed temperature of the plasma gas is 2400 K. There is some indirect evidence that this is the temperature of the arc, through high temperature chemistry (formation of nitrogen oxides in the absence of fuel, formation of acetylene in the absence of air), and power balance from fast frame images of the discharge [Anz04].

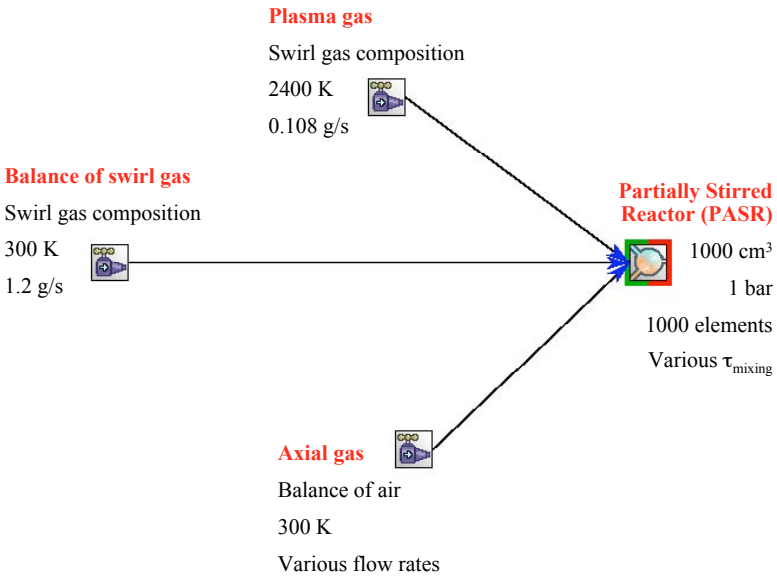

Figure 7.28. Schematic diagram of the PASR model showing the different flow inputs

The total flow rate of the swirl air is 1.2 g/s. The swirl air is premixed with the methane, 0.45 g/s, thus the flow of swirl air of 0.86 g/s, or 40 lpm (STP). The plasma gas is just a fraction of the swirl gas that goes through the plasma region and gets heated to the plasma temperature, 2400 K. The flow rate of this hot gas corresponds to the power delivered by the power supply. In the experiments the plasma power during most of the

steady state experiments is ~ 375 W. For this power, this temperature and gas composition, the flow rate of the high temperature gas is 0.108 g/s. The impact of the turning off the plasma is investigated by changing the temperature of the plasma gas from 2400 K to 300 K. The balance of the swirl flow that is not plasma is at room temperature (300 K).

Table 7.4
Flow rates of axial air for the overall O/C ratios considered

O/C	Axial air (g/s)
1.43	2.16
1.63	2.59
1.83	3.02

The third input flow is the wall air, adding up to the overall air flow rate. The temperature of the third input flow is 300 K. The flow rate of this gas varies, to model the experimental results and to change the O/C ratio. The axial air flow rate varies as shown in Table 7.4.

The residence time in the reactor is variable, as the volume of the reactor is constant (1000 cm^3). The residence time is determined by the volume of the reactor, the average density of the gases in the reactor, and the mass flow rate.

The simulation is a statistical simulation using the MonteCarlo method. Each element of the simulation is modeled as a Perfectly Stirred Reactor. Every MonteCarlo time step random cells are mixed (with both mass and heat transfer), some are removed and new ones are introduced. The overall response of the system is such to reproduce the mixing time, the average residence time in the reactor and the characteristics of the input (mass flow rates, input composition and temperatures of the gases [Che97]).

The MonteCarlo step is an input that has been varied through the calculations, but it is on the order of 150 μs. The time has to be long enough to insure that some elements in the reactor are changed, but small enough to make sure that the number of the introduced elements do not significantly change the instantaneous composition or temperature in the reactor.

Several mixing models have been used. The IEM (Interchange by Exchange with Mean), as well as the CURL methods were used. There was no difference in the results using both methods, and thus only the results from the CURL method will be presented.

Partial Stirred Reactor (PaSR)

It is necessary to provide adequate initial conditions for the system to evolve to a steady state condition with good reforming. The results are dependent on initial conditions (initial composition and temperature). If these initial conditions are not provided, such as

if the reactor is filled with room temperature reagents, the solution reached a low average temperature state, with little chemistry. Mathematically, there are two stable equilibrium states for a given set of inputs, and the one that is reached is dependent on the initial conditions. In this paper we are interested in the high temperature, steady state solution. It has been determined that if the initial temperature is > 1000 K, chemistry takes place and reaches steady state condition with adequate reforming.

The model provided in this paper deals only with steady state conditions, not with the startup conditions, which still need to be understood.

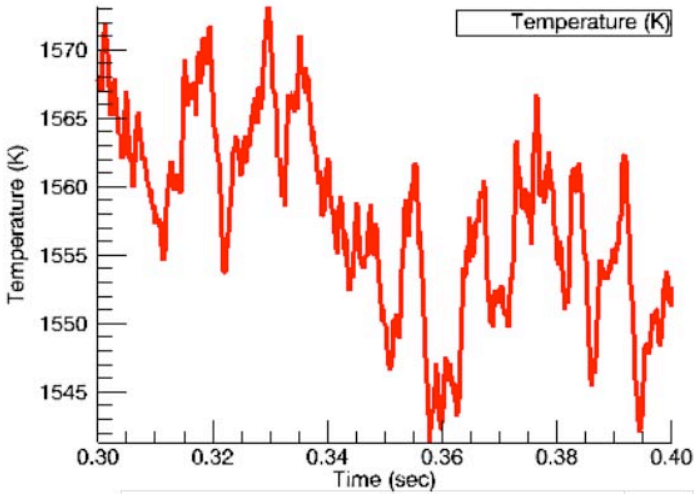

(a)

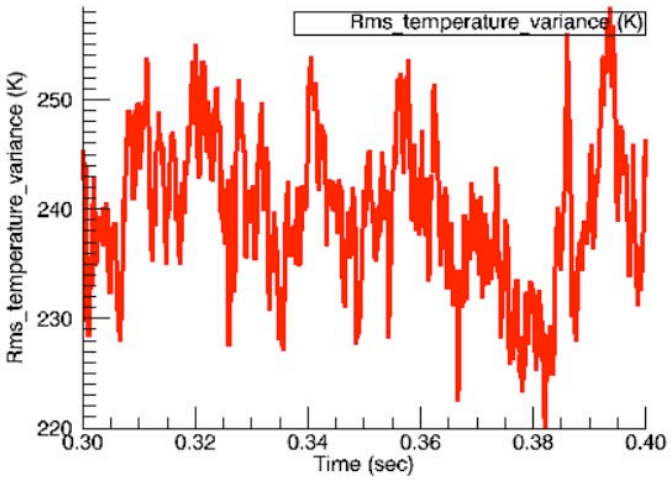

(b)

Figure 7.29. Typical transient (a) average reactor temperature and (b) reactor temperature variance for the case of O/C ~ 1.63 and τ_{mix} = 1 ms.

Once the reactor is started in a mode that results in a good conditions for reforming (high temperature), the inputs are modified and the run restarted to investigate the effect of the new conditions. The run is continued until steady state is obtained.

Figure 7.29 shows the results for the transient to steady state in the case of O/C ~ 1.63 and τ_{mix} = 1 ms. The average temperature is shown in Figure 7.29 (a), while the temperature variance is shown in Figure 7.29 (b). There is a relatively short-lived transient at the start of the simulation (from 0.3 s through about 0.35 s), as the conditions of the simulation have changed. The transients after this short initial period are from fluctuations due to the statistical nature of the MonteCarlo simulation.

Figure 7.29 follows the transient for 0.1 s, starting from conditions obtained in the previous 0.3 s. The mixing time in Figure 7.29 is 1 ms, and thus there are plenty of mixing times for reaching steady state. The residence time, on the other hand is about 0.02 s, and thus there are only about 5 residence times in the transient analyzed.

The mixing time although initially estimated from the fluid dynamic calculations, is not known once chemistry takes place. CFD calculations [Bro05e] indicate that inside the plasmatron head mixing is strong, with mixing times on the order of 100 μs but with short residence times (the plasmatron volume is small), with longer residence times in the reaction extension cylinder (about 20 ms) and longer mixing times (about 1 ms). We have used the mixing time as a parameter, calculating the results for mixing times from 0.5 ms to 10 ms.

The results for O/C ~ 1.43 are shown in Figure 7.30. Figure 7.30a shows the concentrations (molar) of the reformate at the end of the simulation period, for different values of the mixing time, τ_{mix}. The balance is mostly nitrogen, with < 1% of other species.

Figure 7.30 show that the conversion of methane decreases (and so does the hydrogen concentration) as the mixing time is increased. The composition is relatively sensitive with mixing times for short mixing times, but then becomes relatively independent of mixing time. Similarly, the temperature decreases with increasing mixing time, and because of constant reactor volume, the residence time increases. The temperature variance also increases, as a direct result of reduced mixing.

To investigate the effect of statistics, two points were calculated for the residence time of 1 ms. Both points are plotted in Figure 7.30 for the case with plasma. Although not thorough measurement of the statistics, it indicates the amount of spread in the curves, demonstrating that the error bars in Figure 7.30 are small.

Figure 7.30 shows also the case when the plasma is turned off. It is interesting to note that the reaction continues, at reduced temperature (by about 150 K), decreased temperature variance, and slightly reduced methane conversion (methane concentration up by about 30%, with hydrogen concentration decreasing by about 20%).

Figure 7.31 shows the results for the O/C ratio of 1.63. The trends are similar, with slightly higher methane conversion. The hydrogen concentration has remained relatively constant with respect to the previous case of O/C ~ 1.43, but the methane conversion is higher by about 25%. The hydrogen yield is up because although the concentration remained constant, the total flow rate has gone up. The test for spread was also performed in this Figure, but for the case with no plasma and 1 ms mixing time.

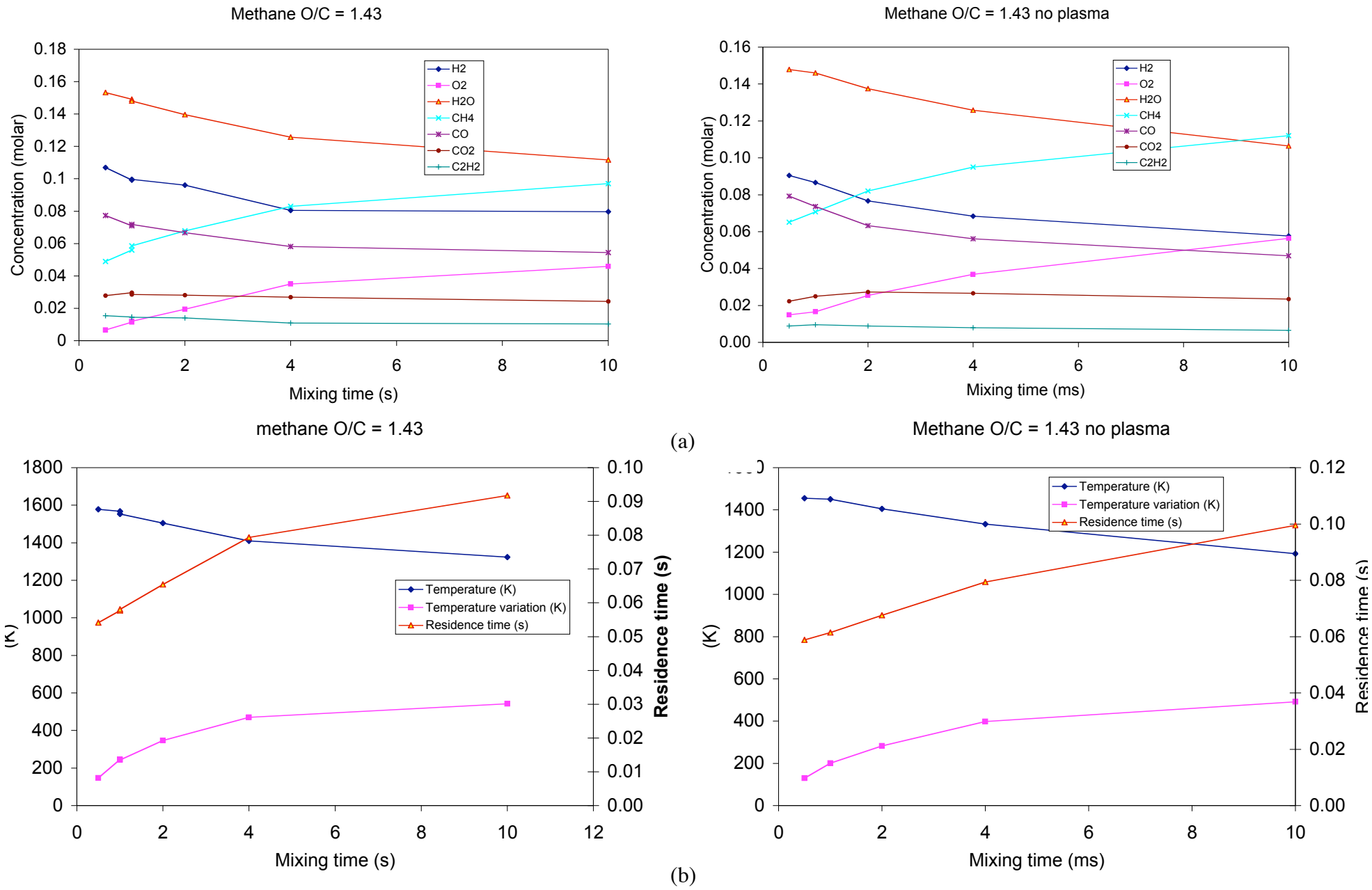

Figure 7.30. (a) Composition and (b) average temperature, temperature variance and residence time as a function of time for a mixing time Figures on left are for plasma on while those on right are for plasma off.

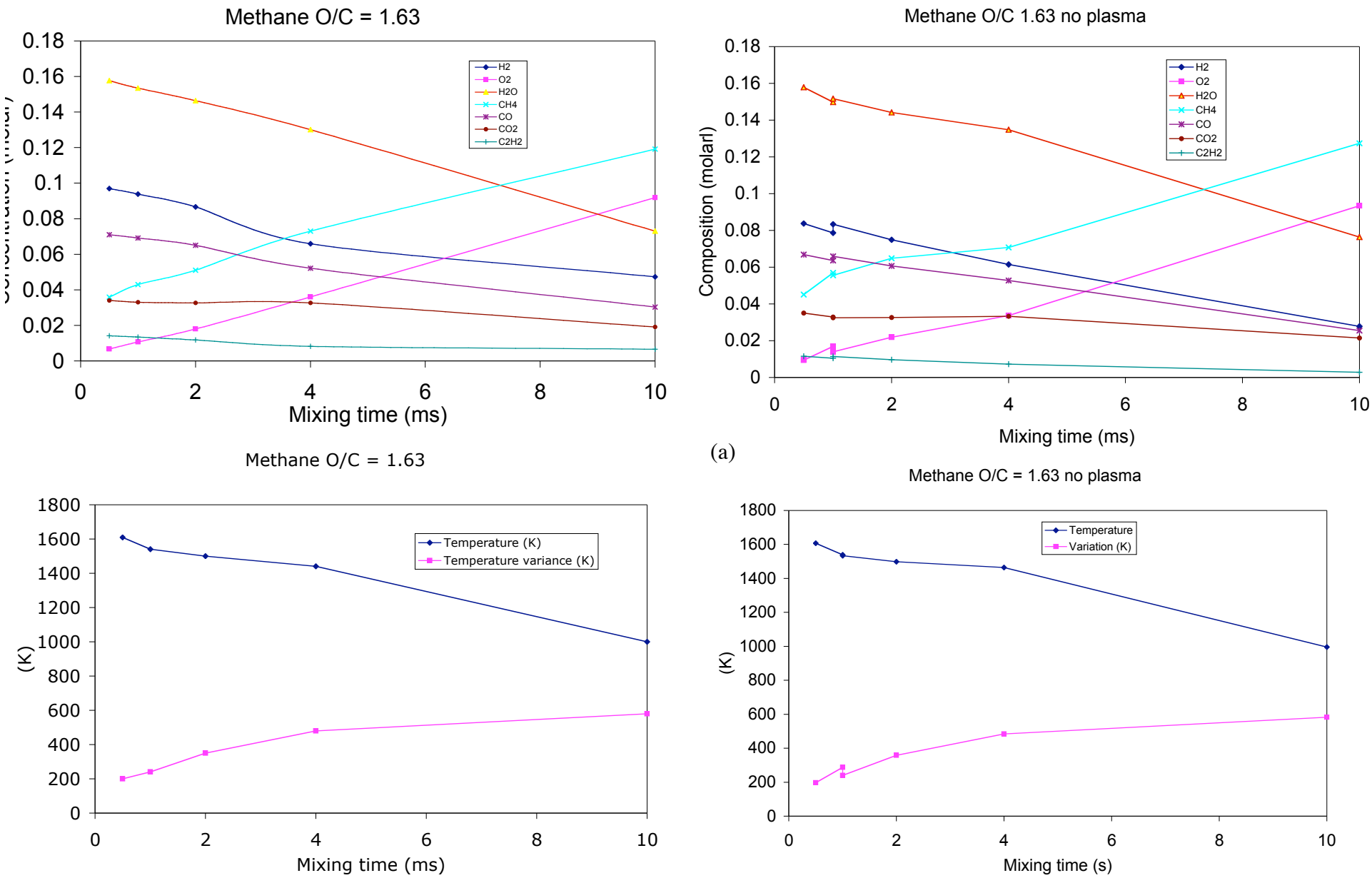

Figure 7.31. Same as Figure 7.30 but for O/C = 1.63.

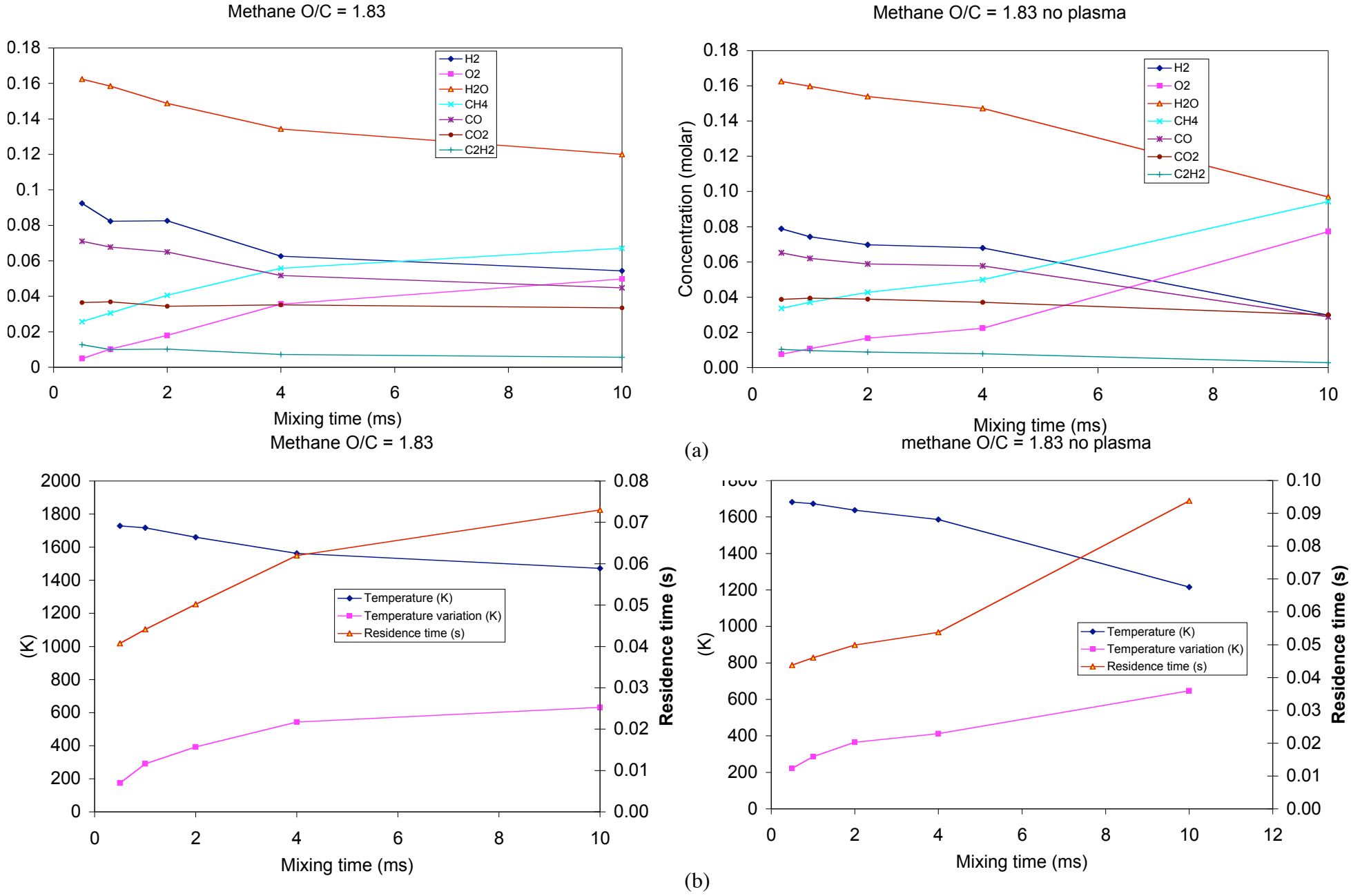

Figure 7.32. Same as Figure 7.31 but for O/C = 1.83.

Again, for increased O/C, the hydrogen concentration decreases, while the methane conversion increases. In the case of O/C ~ 1.83, the conversion increases by about 40% from than of O/C ~ 1.63. However, some of the conversion is to water, and the result of this increased combustion is increased temperature.

Discussion

The comparison between the experimental results and the modeling results are shown in Table 7.5. Because the experimental results do not measure water content, the results are shown for dry gas composition.

Table 7.5
Comparison of experiments and modeling results (τ_{mix} = 0.5 ms)
Experiments with plasma on

		5/2/2005-1	PaSR	5/2/2005-2	PaSR	5/2/2005-3	PaSR
Power in	W	375	375	375	375	375	375
Axial air	g/s	2.16	2.16	2.59	2.59	3.02	3.02
Swirl air	g/s	0.86	0.86	0.86	0.86	0.86	0.86
Swirl methane	g/s	0.45	0.45	0.45	0.45	0.45	0.45
O/C ratio		1.43	1.43	1.63	1.63	1.83	1.83
Composition							
H2	vol.%	12.1	12.7	13.5	11.5	13.9	11.1
O2	vol.%	0.7	0.8	0.5	0.8	0.5	0.6
N2	vol.%	68.9	66.5	69.8	69.2	71.4	70.9
CH4	vol.%	4.2	5.8	1.9	4.3	1.7	3.1
CO	vol.%	9.1	9.1	9.6	8.4	10	8.5
CO2	vol.%	3.8	3.3	4	4.0	4.1	4.4
C2H4	vol.%	0.9	0.0	0.8	0.0	0.7	0.0
C2H2	vol.%	0.2	1.8	0	1.7	0	1.5
ΣC in	mole/min	1.69	1.69	1.69	1.69	1.69	1.69
ΣC out	mole/min	1.44	1.70	1.42	1.64	1.57	1.75
ΔC/C		0.15	-0.01	0.16	0.03	0.07	-0.04

The modeling results agree quantitatively with the experimental ones. One point of small disagreement is in the hydrogen concentration and the methane conversion, which are slightly underestimated in the modeling results for higher O/C ratios. The trend of the calculations also indicates that the hydrogen concentration peaks at low O/C ratios, while the experiments indicate that they peak at the higher O/C ratios, but the peaks, in any case, are rather broad.

It should be noted that the experimental results shown in Table 7.5 correspond to a series of experiments from [Bro05a] where there was good reforming at O/C ~ 1.43. Additional experiments in [Bro05a] show that there is a cliff in the methane conversion at O/C ~ 1.63, and poor conversion at O/C ~ 1.43. As described in the paper, the issue has to do

with reproducibility of the measurement of the O/C ratio, which could be off by as much as 25%.

The code does not reproduce the experimental results with the C_2 compounds. The modeling indicates that the highest conversion is to acetylene, with small yields of C_2H_4 and C_2H_6.(about 0.1% molar each). The experimental results indicate the opposite, with substantial concentration of C_2H_4 and/or C_2H_4 (C_2H_4 and C_2H_6 are not separated by our chromatographic column) and very small concentration of C_2H_2. The impact on the methane conversion and hydrogen yields are, however, small.

Also shown in the table are the carbon balance, for both the modeling and the experiments. The last three rows of Table 7.5 show the sum of the carbon in the input (i.e., the methane), and the carbon sum of the output, and their relative differences. The carbon balance in the experiments are about 10-15%, while in the computation the carbon balance is within 1-4% (due to statistics).

It should be noted that in order for the chemistry to take place, mixing has to be at the molecular level. The effects of turbulence on mixing at this level are still not understood. However, it seems that high Reynolds numbers, higher than laminar-to-turbulent transition, are required (Re > 10,000) to achiever mixing at the molecular level [Dim02]. For reference, the Reynolds number in the plasmatron head region of the device is Re ~ 6000 (prior to chemistry).

The cases analyzed in Figure 7.30-7.32 without plasma show different quantitative results than the experiments. Good performance is only obtained in the experiments by operating at higher values of O/C than the numerical results. It is not clear why this is the case.

Two possible alternative explanations have been conceived to explain the difference observed between the experimental and numerical calculations without the plasma and at low O/C. The first one is that there are power losses not accounted by the code. The code models an adiabatic reactor. At conditions of lower O/C the exothermicity of the reaction is decreased, and reforming would be more sensitive to losses. The absence of the losses would thus explain both the good numerical reforming without the plasma as well as at the lower O/C ratio

The second possible explanation is the implication of the PaSR code itself. The code allows for a single mixing time. There is substantial recirculation in the reactor, but it is not as assumed in the code. When the exothermicity is high, decreased mixing may not affect as much the results. This behavior is shown in Figures 7.30-7.32. On those cases in the presence of the plasma (on the left of the figures), as mixing time increases, reforming degrades but asymptotes to good reforming (that is, the rate of change decreases with increasing mixing time). This is changing for the conditions without the plasma, where as the mixing time increases there no asymptote but instead the rate of change increases. Thus the reforming without the plasma is more sensitive to poor mixing than the case with plasma.

8) Steady state experiments

a) Methane reforming

Tests were carried for a single flow rate of methane, which is injected in the swirl gas. The methane flow rate was 0.45 g/s, about 25 kW heating power. A comprehensive set of tests was carried out, from steady state variations of O/C, catalytic vs uncatalyzed reactors, as well as the effects of shutting the plasma off after steady state conditions are reached. The next section will cover steady state conditions where the plasma was maintained.

Reforming with plasma on

In this section the steady state plasma reforming characteristics are described. We have carried out a series of experiments with a systematic variation of the air in the swirl gas and the axial air. The experiment is carried out at well-determined conditions (flows, electrical power), and the composition is monitored with the mass spectrometer. The temperature is monitored by a thermocouple in the reactor. Gas samples for analysis with the GC are taken when the temperature and composition have stabilized.

Results of these experiments are shown in Figure 8.1. Shown are contours of constant hydrogen, carbon monoxide, carbon dioxide and methane concentrations in the dry gas, as a function of the air flow rates in the axial gas and the swirl gas. The value of the contour is shown in the bar to right of each graph.

The experimental protocol held the swirl air at a given flow rate, while changing the wall air. This process was repeated for 3 different swirl airs. In this manner, the required adjustment of the methane rotameters was minimized. We have followed this method as it is experimentally easier, and more reproducible, to vary one air or the other, instead of varying both in order to keep constant the overall O/C ratio.

The results indicate that the hydrogen concentration has a broad, saddle-like peak, with the maximum along the diagonal. The variation of the hydrogen concentration does not vary much, from about 10 to 14%. The variations of the concentration of CO show the same characteristics as hydrogen, following the maximum for hydrogen, across the diagonal. In contrast, the concentration of CO_2 and the methane conversion increase monotonically towards conditions of higher O/C ratios.

Figure 8.2 shows some of the overall parameters of the conditions analyzed in Figure 8.1. The O-to-C ratio is shown. The constant O/C lines are aligned along the diagonal, just as the H_2 and CO concentrations in Figure 8.1. This indicates the importance of the

parameter O/C for hydrogen generation. The CO_2 concentration and the methane conversion are also functions of the O/C ratio.

Figure 8.2 also shows the temperature in the reactor, which increases, in the general direction of increased O/C (as more of the fuel in fully combusted, as indicated by the increased CO_2 concentration).

The efficiency shown in Figure 8.2 refers to the heating value of the reformate divided by the heating value of the fuel. A substantial fraction of the fuel, about 1/3- 1/2 is spent in driving the gas phase partial oxidation. Thus, it seems that without heat recuperation, the process is rather inefficient.

Finally, the hydrogen yield shows the same saddle-type behavior than the hydrogen concentration, with a maximum along the diagonal (with an O/C of about 1.7).

The results indicate that the performance of the plasmatron fuel reformer is dependent on the overall O/C ratio, and rather independent of the distribution of the air (in either swirl air or wall air). The swirl air needs to be sufficiently high to result in the generation of a plasma in the volume of the plasmatron. For swirl air flow rates less than about 40 lpm, the plasma remained in the electrode gap, not being pushed out into the volume of the reactor.

The results in Figures 8.1 and 8.2 have been used in the Perfectly Stirred reactor (PSR) [Bro05c] as well as the Partially Stirred Reactor (PaSR) [Bro05d] analysis discussed in above in Section 7.b.

The experiments were repeated for lower O/C ratios, in order to determine the dependence of the process parameters in this regime, even though it results in non-optimal reforming. As in the experiments described above, the methane flow is 0.45 g/s. and the axial air flow was changed. However, the swirl air flow was held constant. The methane was premixed with the swirl air, as in the previous experiments. The results are shown in Figure 8.3, as a function of the O/C ratio.

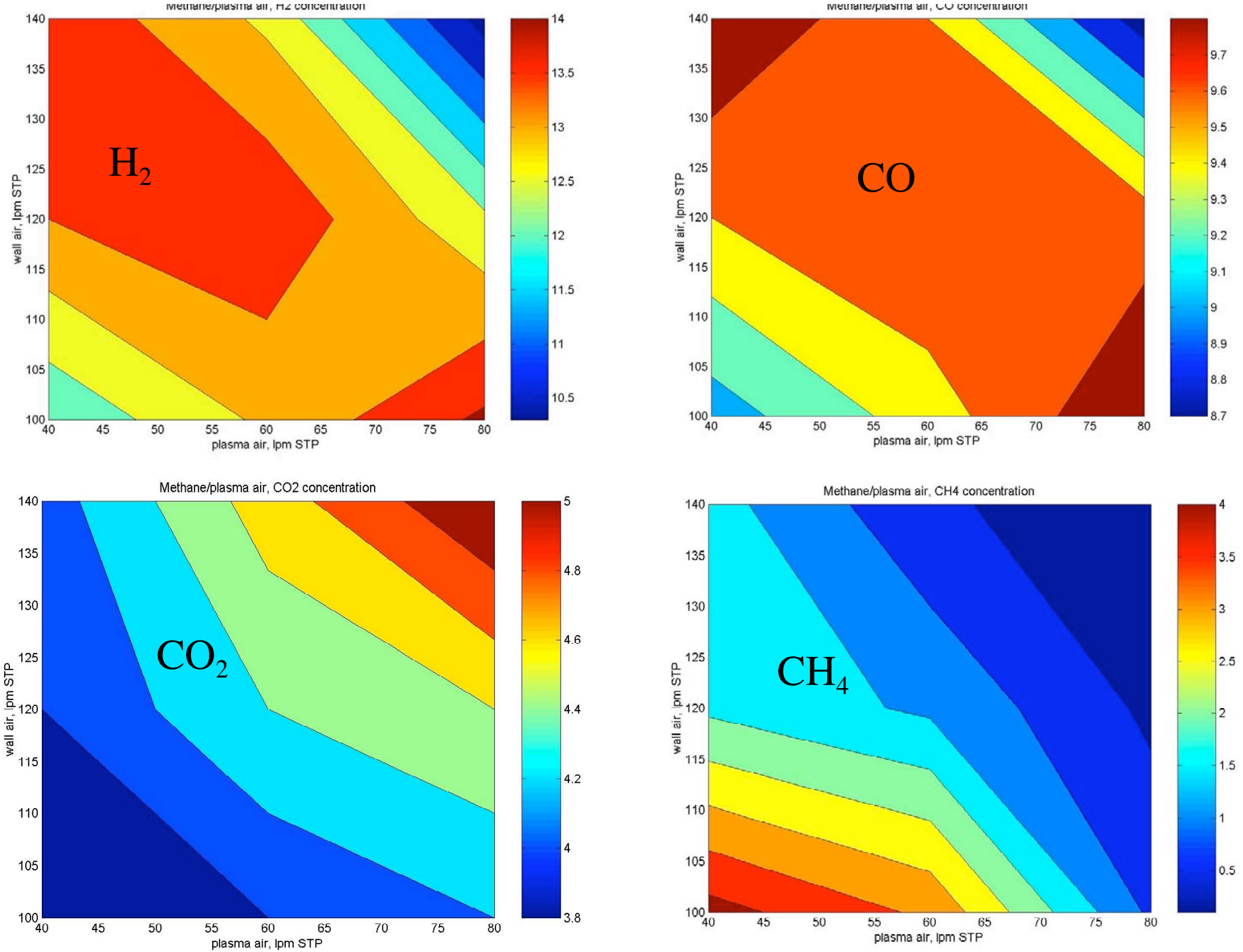

Figure 8.1. Contours of constant H2, CO, CO2 and CH4 as a function of swirl air (plasma air) and axial air (wall air)

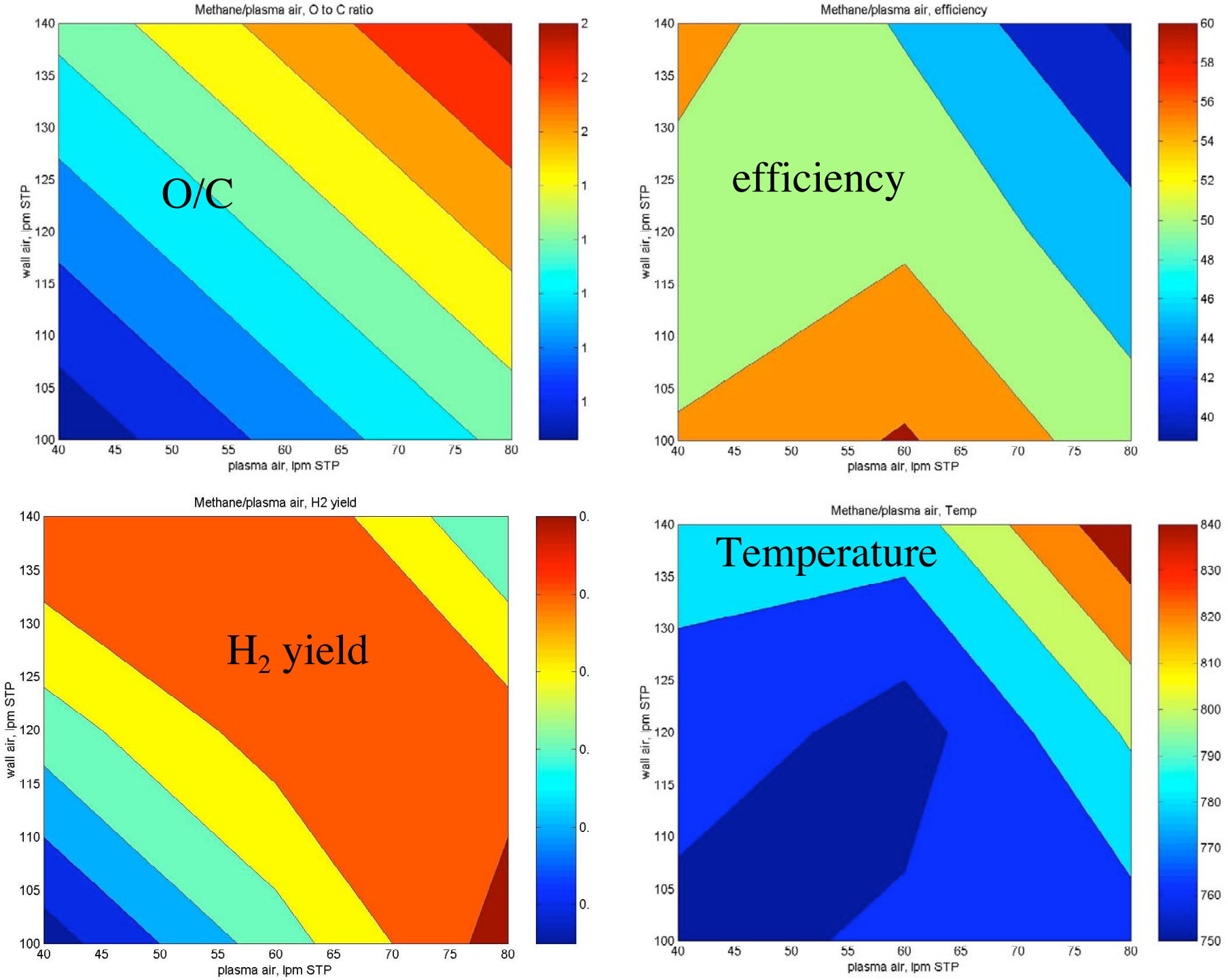

Figure 8.2. System parameters for the same conditions as Figure 8.1; (a) O/C (b) efficiency (c) H2 yield and (d) Reactor temperature

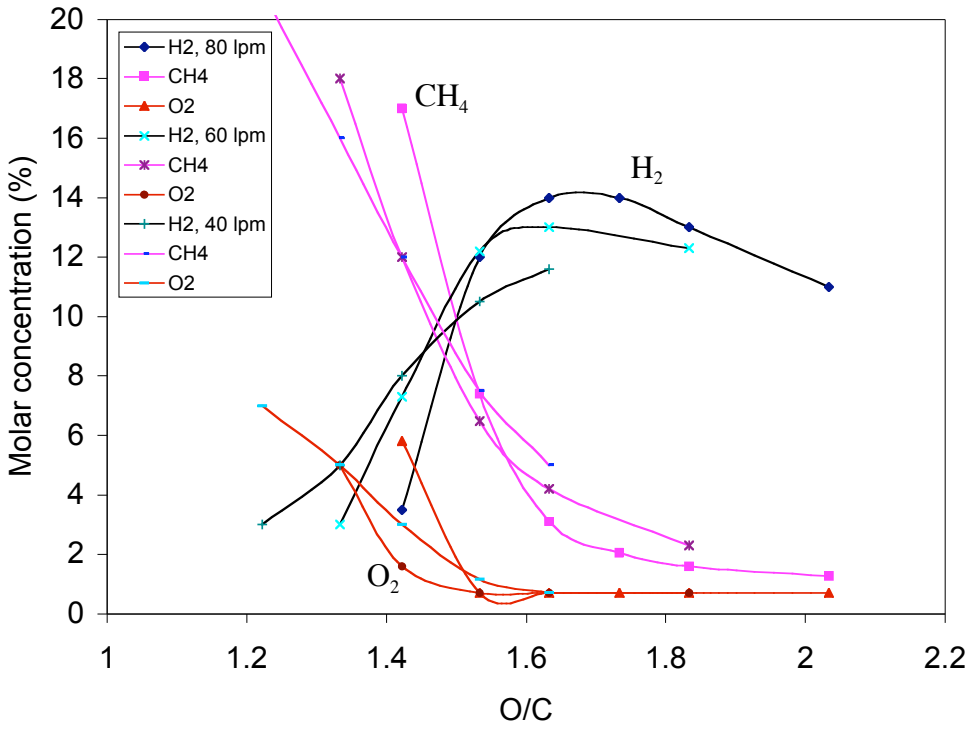

Figure 8.3. Molar concentration of hydrogen, methane and oxygen as a function of O/C for air flows in the swirl gas of 40, 60 and 80 lpm.

Figure 8.3 shows a larger dependence on the hydrogen concentration on the O/C ratios, for ratios lower than those from Figures 8.1 and 8.2. The threshold for good reforming is O/C ~ 1.6, which agrees with the results in an accompanying paper [Bro05c]. The methane conversion also increases relatively fast (and the methane conversion drops) at O/C ratios lower that 1.6. The oxygen concentration follows the methane concentration.

It can be seen that the results of Figure 8.3 do not quite agree with those shown in Figures 8.1 and 8.2. The reforming "cliff" that is clearly seen in Figure 8.3 is not noticed in Figures 8.1 and 8.2, although there is only one point in Figures 8.1 and 8.2 that operate at O/C less than 1.6, and even then it operates at O/C ~ 1.43 for the swirl flow rate where the hydrogen concentration is the least sensitive to O/C in Figure 8.3. This inconsistency is thought to be due to the uncertainty in the measurement of the O/C, as mentioned in the previous section.

Reforming without plasma

In order to determine the effects due to the plasma, we have investigated the reforming in the absence of plasma. Once the reactor achieves steady state with the plasma on, it is shut off and then allowed to reach a new equilibrium.

It has been found that the reforming in the absence of the plasma is very sensitive to the flow rates. The results from the effect of the plasma were obtained in a different run than those in the previous section, where the effect of the plasma was explicitly investigated as a function of the flow rates of swirl air and wall air, for constant methane flow. Because the pressure varied during the experiments, it was necessary to adjust the rotameters. Even then it is hard to control the methane flow to better than about 10-20%. Some of the reproducibility issues in this paper may be due to this issue. By contrast, we think that the air mass flow controllers are relatively accurate.

We have tried to eliminate the problem by using the GC and MS gas analysis to determine the gas composition prior to start up of the reformer, to determine the ratio of O/C, and comparing it with the calculated O/C ratio from the known input flow rates. Using this method shows a disagreement with the O/C calculated from the flow rates of the reagents of about 25%.

Results of reforming without the plasma are shown in Figures 8.4 and 8.5. The hydrogen and CO concentrations are slightly lower than in the case with the plasma on, by about 30%. But the flow rate is about 20% higher, and thus the hydrogen yields are comparable in both cases, about 35-40%. Methane concentration is lower in the case of no plasma by about a factor of 2, while the CO_2 concentration is slightly higher. Thus, more of the methane is being converted but it is going into combustion products rather than hydrogen or CO.

The efficiency is not shown in Figure 8.5, as it is misleading, with best efficiency when there is no conversion.

The effect of plasma vs no plasma is dramatically shown in Figure 8.6. After achieving steady state conditions without plasma, the plasma was turned on. The transients are measured with the mass spectrometer, and steady state concentrations of hydrogen, water, oxygen and methane following the plasma turn-on were measured. It should be noted that the temperature, as indicated by the thermocouple in the middle of the reactor, did not reached steady state conditions.

Figure 8.6 shows the concentration of hydrogen with and without plasma, as a function of O/C, for several values of the swirl air flow. This figure shows that at the high O/C (> 2) the plasma plays a minor role. However, it plays a major role for lower O/C. The critical O/C ratio for the case of no plasma is around 2, as compared in Figure 4 in the case of plasma, of about 1.6.

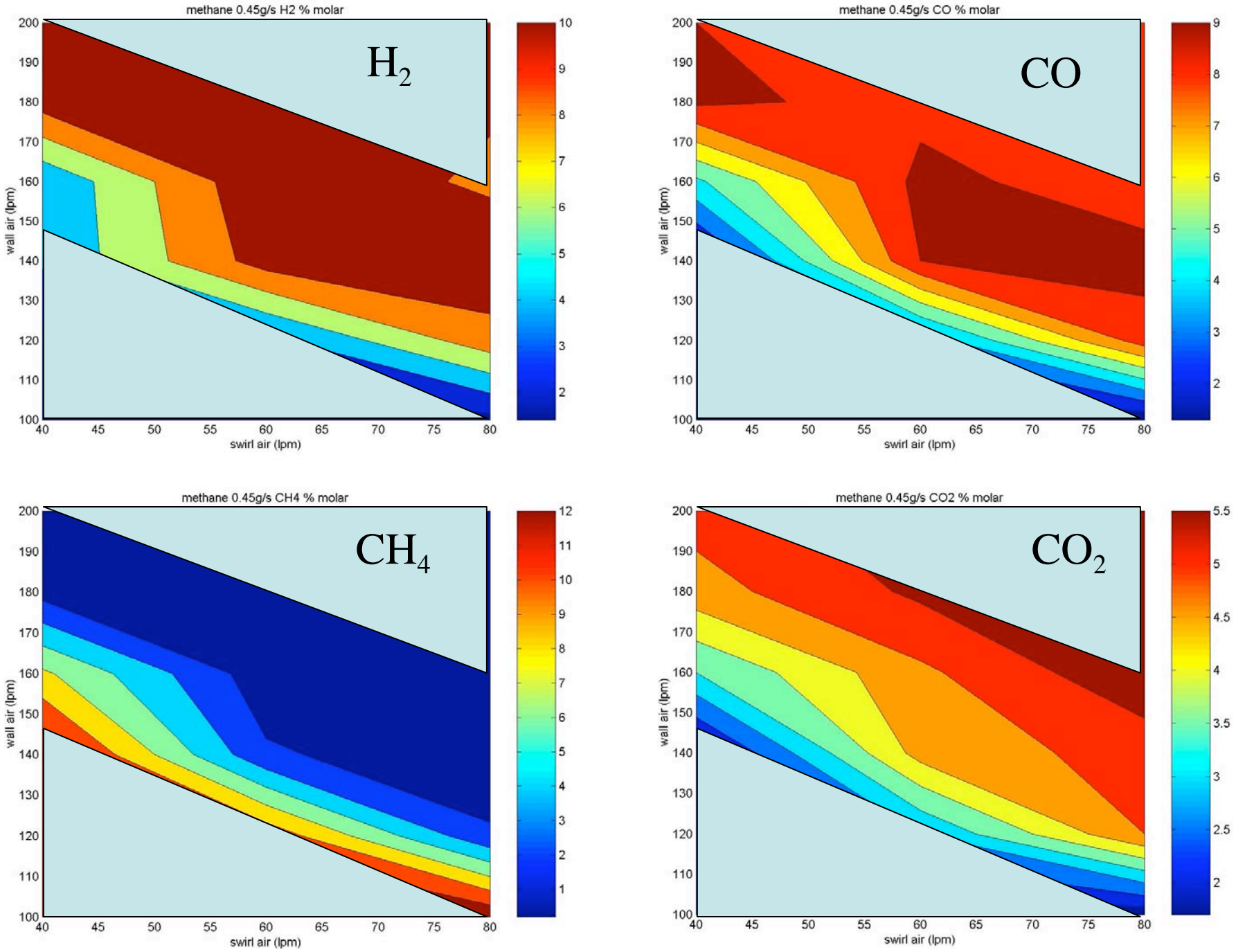

Figure 8.4. Same as Figure 8.1 but in the absence of plasma.

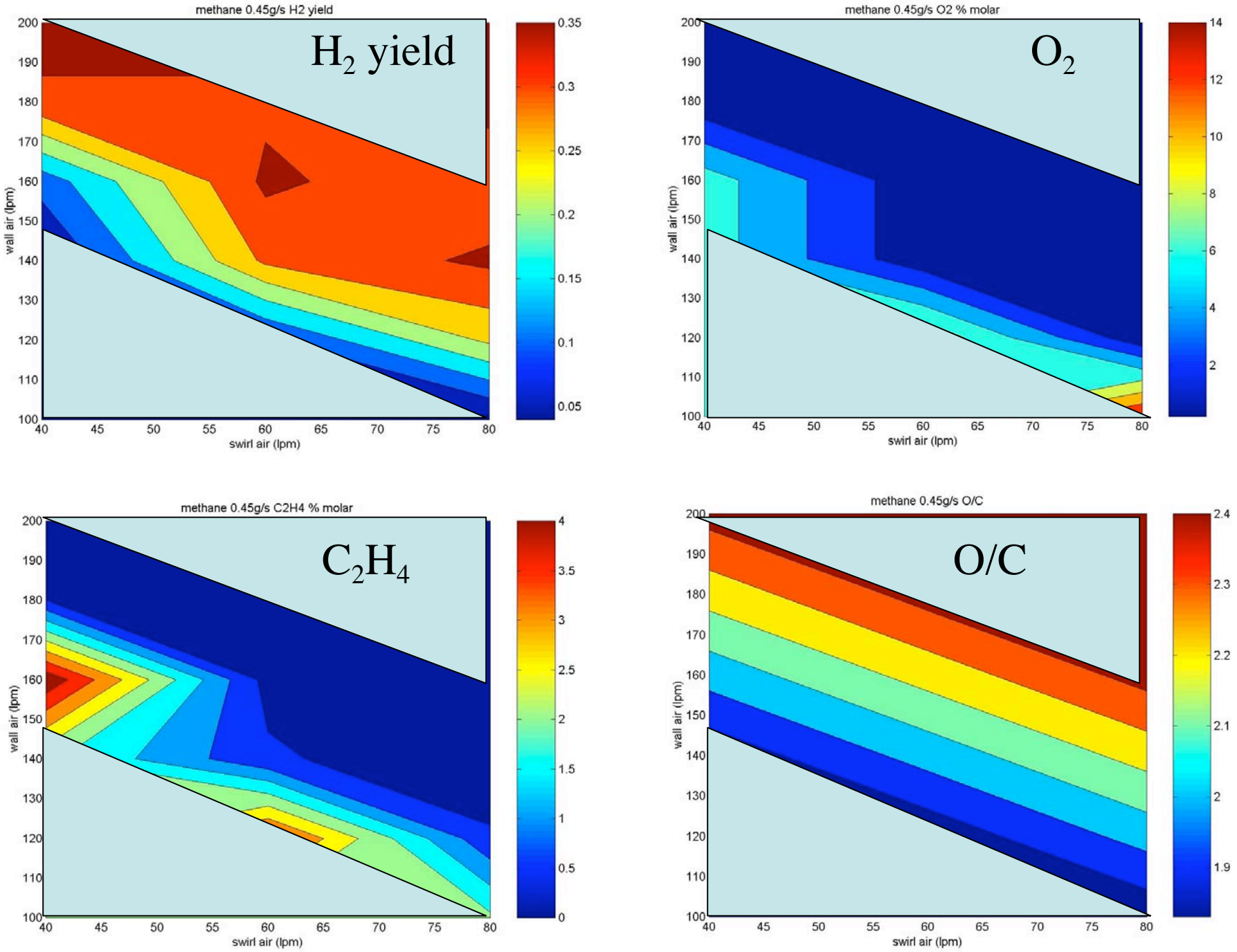

Figure 8.5. Hydrogen yield, oxygen and C2's concentration in reformate, as well as O/C for the cases also shown in Figure 5

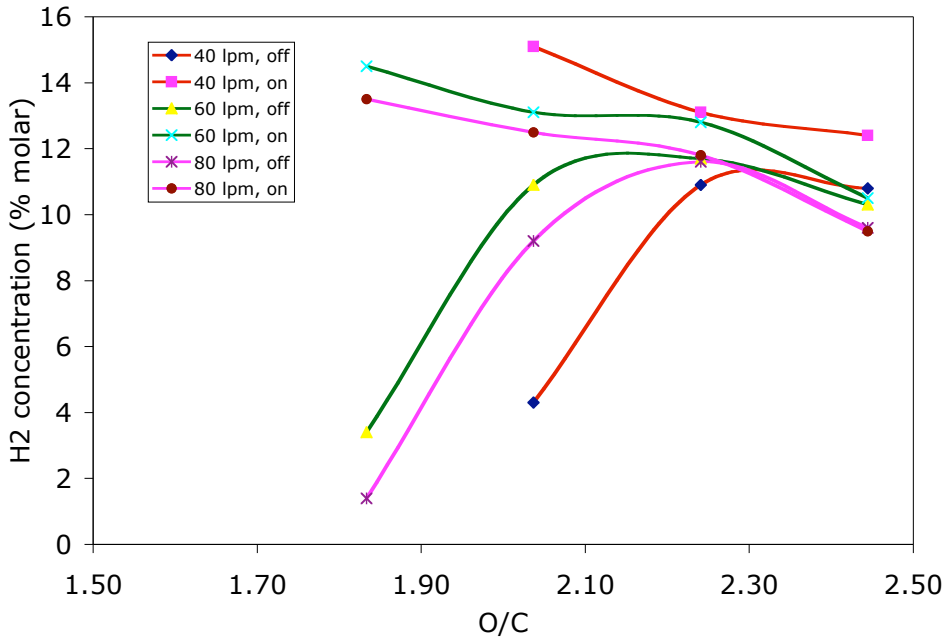

Figure 8.6. Hydrogen concentration as a function of the O/C ratio for several values of the swirl air flow rate, with and without the plasma.

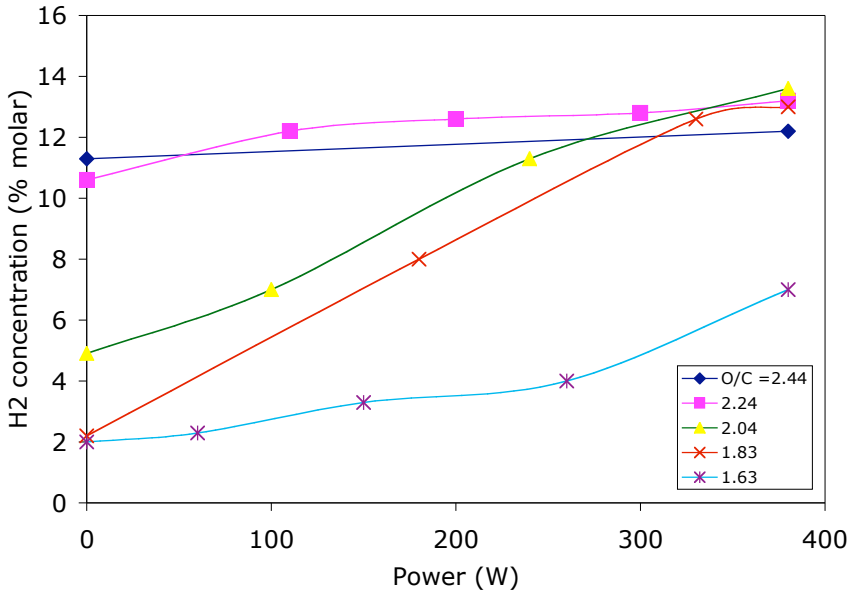

Figure 8.7. Dependence of H_2 concentration as a function of power for various values of O/C, for a swirl air of 60 lpm and 0.45 g/s methane flow.

Power effect

The effect of the plasma power on the methane reforming was also investigated. The experiments were performed at various O/C ratios, with the reactor already warmed up.

The gas composition with high power (~380 W) and no plasma power were measured using the GC and the MS, while at other power levels they were measured only with the MS. The swirl air is held constant at 60 lpm, and the O/C is varied by changes in the wall air.

Figure 8.7 gives the results of these experiments. At high values of O/C, the effect of the plasma power is relatively small, with a ~20% drop in hydrogen concentration. It should be noted that the maximum hydrogen concentration occurs with plasma, at an O/C ~ 2. However, when the hydrogen concentration was optimized at this O/C ratio, there was substantial sensitivity to the plasma power, with large drop in methane conversion at powers less than about 300 W. The carbon balance is within 5%, but as with the previous sections, there is a difference of 7-15% between the O/C calculated from the flows and that measured from the GC. The O/C measured is higher than that calculated from the flows.

b) Propane reforming

In a series of papers [Bro05a, Bro05b, Bro05c, Bro05d, Bro05e] the performance of a plasmatron methane reformer has been discussed. There is interest on the reforming of methane, primarily driven by methane gas upgrading and conversion to liquid fuels, in order to allow economical utilization of stranded natural gas resources. In addition, that work also provides increased understanding of the behavior of the plasmatron reformer operating with heavier hydrocarbons.

Methane is a gaseous fuel, and its attractiveness in this work has been that we can explore a wide range of parameters without having to be concerned with fuel atomization, wall wetting, and other phenomena that occurs when using liquid fuels. In addition, very complete chemical mechanisms exist that allow adequate modeling of the chemistry. Methane has then been used is the accompanying papers [Bro05a, Bro05b, Bro05c, Bro05d, Bro05e].

One of the disadvantages of using methane as a surrogate hydrocarbon for heavier fuels is that the chemistry is substantially different. In order to address the issue of the different chemistry, a heavier gaseous hydrocarbon needed to be tested. In this section, the performance of plasmatron propane reformers is investigated. [Bro05f] Propane-air mixture is the simplest hydrocarbon system that exhibits chemical behavior, laminar flame speeds and thicknesses, and extinction limits that are comparable to those of heavier fuels [Tur96]. It is probably the smallest system from which quantitative information directly relevant to the partial oxidation of heavier liquid gasoline and diesel fuels can be extracted, and is therefore an appropriate choice for this study [Haw98]. Unfortunately, unlike the case of methane where chemical modeling of the experiments were performed [Bro05c, Bro05d, Bro05e], propane mechanisms are not as well developed, and we have not performed chemical modeling to compare with these experiments,

Propane injection through axial nozzle

In this section the results of experiments with propane injected through the axial nozzle are presented. As described in the previous section, this configuration results in highly homogeneous air/fuel mixtures, with constant propane in the central region and with large concentration gradients in the region where the air/propane mixtures form stoichiometric combustion mixtures.

The results of the reforming experiments are shown in Figures 8.8 and 8.9, as contours of constant quantity as a function of the wall air and swirl (plasma) air, for a propane flow rate of 0.5 g/s. Figure 8.8 shows the H_2, CO, CO_2 concentrations and overall O/C ratio, while Figure 8.9 shows methane concentration, reactor temperature, efficiency and carbon balance. The carbon balance is within 5%. Since water is not measured, it is not possible to close the mass balance for oxygen or hydrogen.

The hydrogen concentration peaks in a band that corresponds to constant O/C ~ 2. Stoichiometric combustion of propane occurs at O/C ~ 3.33, and thus O/C ~ 2 is still far away from combustion. Hydrogen concentration is about 12%, with a power efficiency to H_2, CO, CH_4 and C_2's of about 60%. At the higher values of O/C more and more of the hydrogen gets combusted, while at the lower values of O/C the conversion of propane is reduced, thus resulting in a maximum concentration as a function of O/C.

The concentration of CO_2 increases with increasing O/C ratio, as expected, as more of the fuel is combusted. The temperature measured by the thermocouple, which is only an indication of the actual gas temperature, increases with O/C.

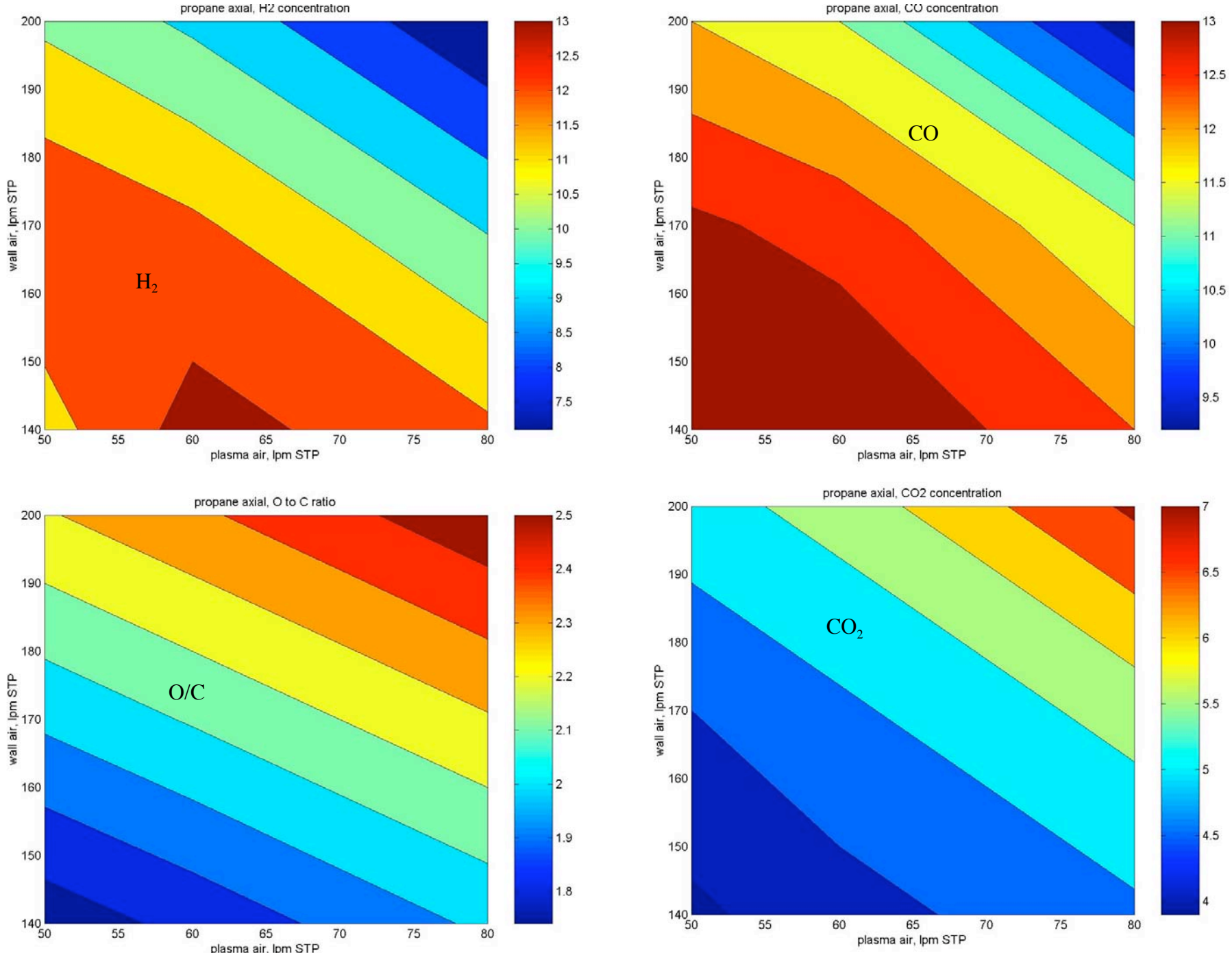

Figure 8.8. Contours of constant (a) H_2 (b) CO (c) O/C ratio (d) CO_2 as a function of wall and swirl air flow rates, for axial propane injection

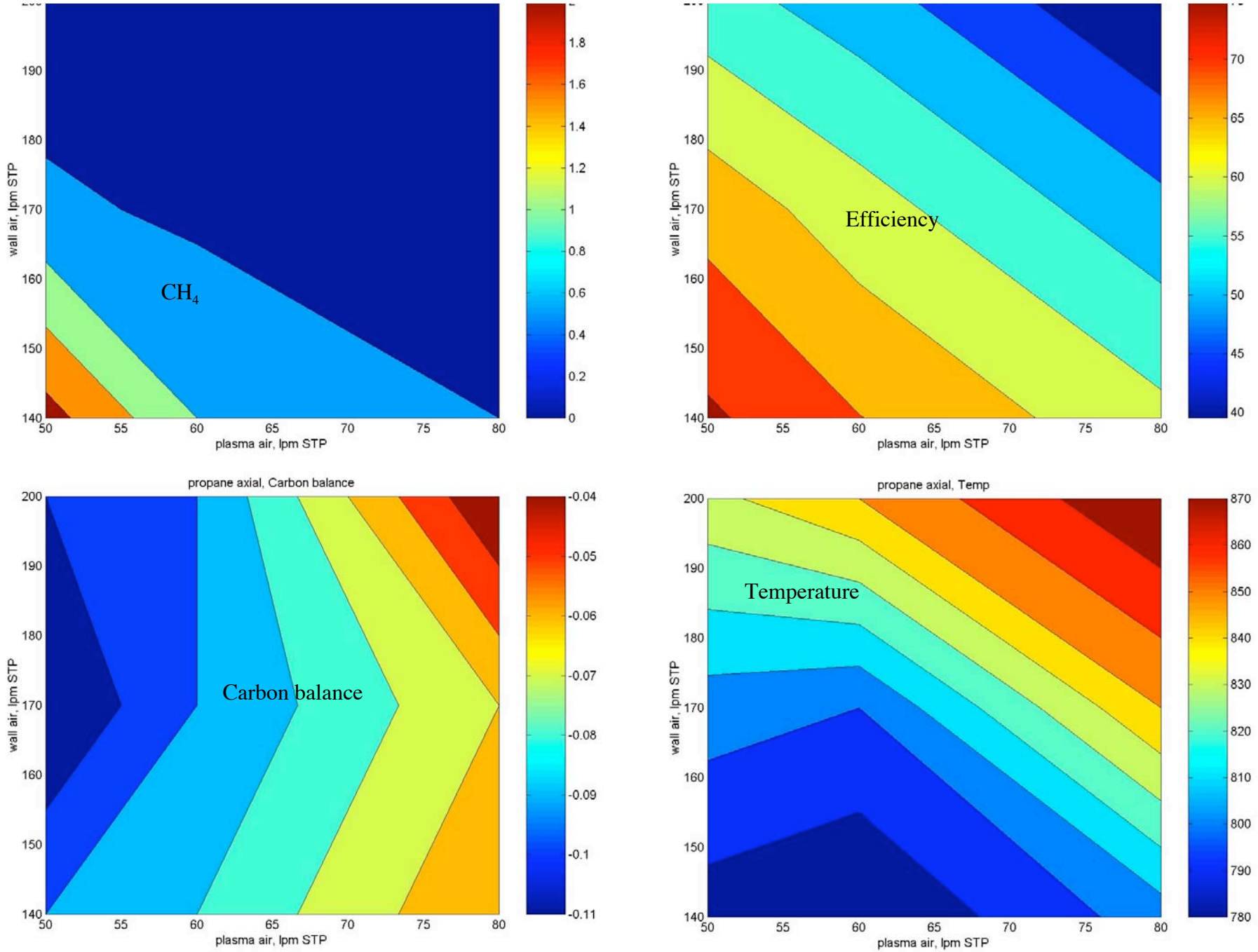

Figure 8.9. Contours of constant (a) CH_4 (b) efficiency (c) carbon balance (d) temperature as a function of wall and swirl air flow rates for the same conditions as Figure 8.8.

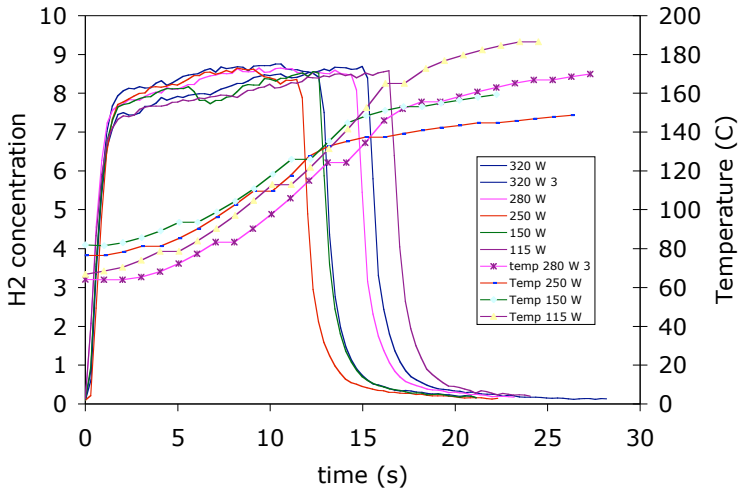

Figure 8.10 Transient in axially-injected propane for several levels of power, for O/C ~ 2.1

The startup transient characteristics with axially injected propane are shown in Figure 8.10, for a wall air of 170 lpm and a swirl (plasma) air of 60 lpm. The air/propane flows are established with the reactor at nearly room temperature, and then the plasma is turned on. Figure 8.10 shows the hydrogen concentration as well as the temperature for different plasma powers. The hydrogen concentration reaches 8% in about 1 s, as was discussed in the transient paper with methane [Bro05b]. At this high value of O/C ~ 2.1, the startup is not sensitive to the power level. This was also found to be the case for methane [Bro05b]

Propane premixed with wall air

Experimental results for propane premixed with the wall air are shown in Figure 8.11 and 8.12. The results have similar trends than those for the case of axially injected propane. Hydrogen concentration peaks at a given O/C ratio, production of CO_2 increases with O/C ratio. The hydrogen concentration is similar to that of section above, but occurring at lower O/C ratios, O/C ~ 1.7,vs O/C ~ 2 for axially injected propane. The efficiency to light hydrocarbons is about 55%. As discussed above, the increased nonuniformity of the air/propane distribution is likely to be reason for this result.

The transients are shown in Figure 8.13, showing 8% H_2 concentration within 1 s, for 120 lpm wall air and 50 lpm swirl (plasma) air, corresponding to an O/C ~ 1.6. The transients are short, about 1 s. In this case the conversion is a stronger function of power than in the case in section 3 that operated at higher O/C ratios. It is also interesting to note that the reformation continued in the absence of plasma. As opposed to the case in Figure 8.10, where the propane was shut down with the plasma on, in Figure 8.13 the plasma was shut down with propane still on. This is a feature that has been investigated in the plasmatron startup methane reformer paper [Bro05b]. For a power of 120 W, the reforming is poor and the rate of temperature rise is low.

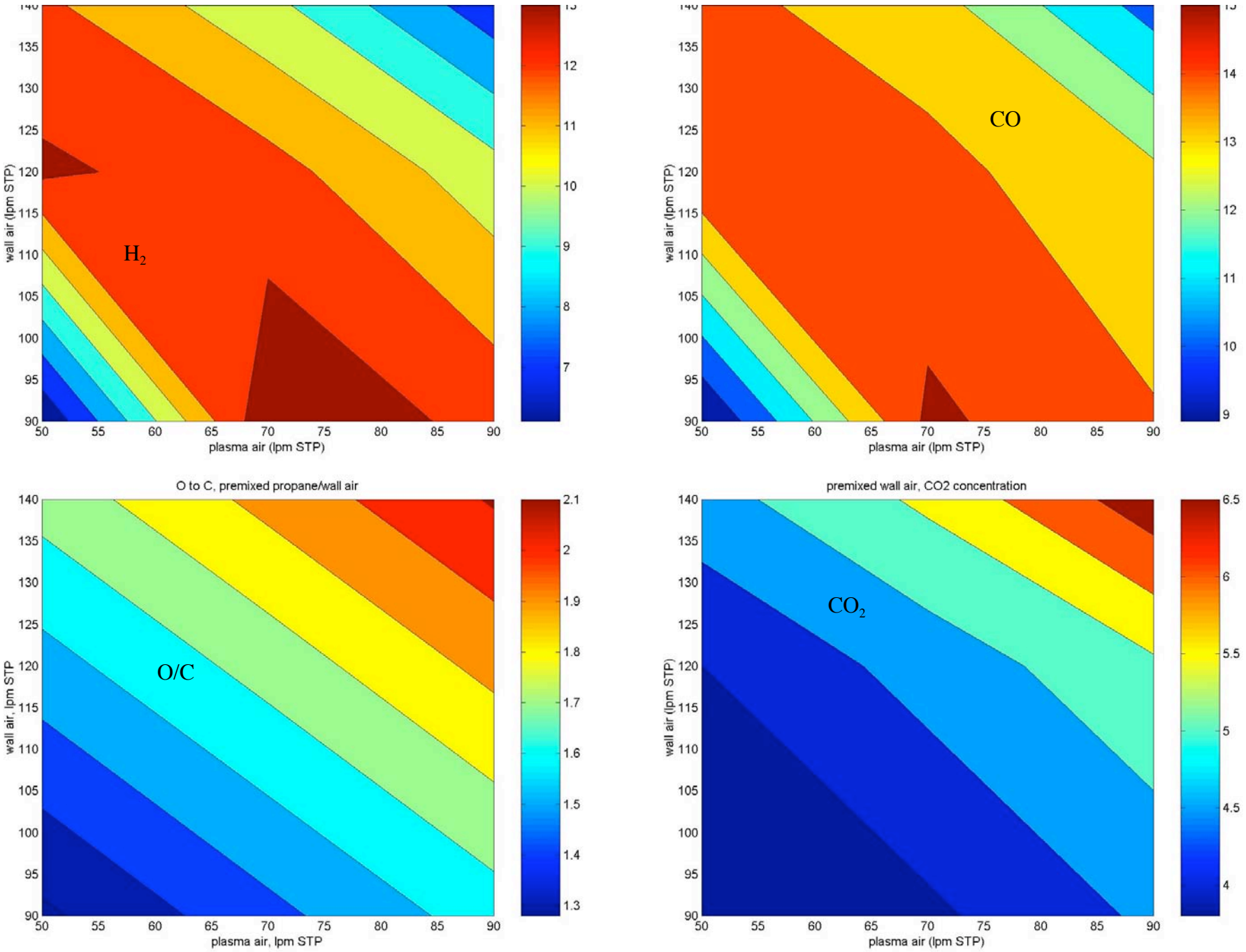

Figure 8.11. Contours of constant (a) H_2 (b) CO (c) O/C ratio (d) CO_2 as a function of wall and swirl air flow rates, for propane premixed with wall air

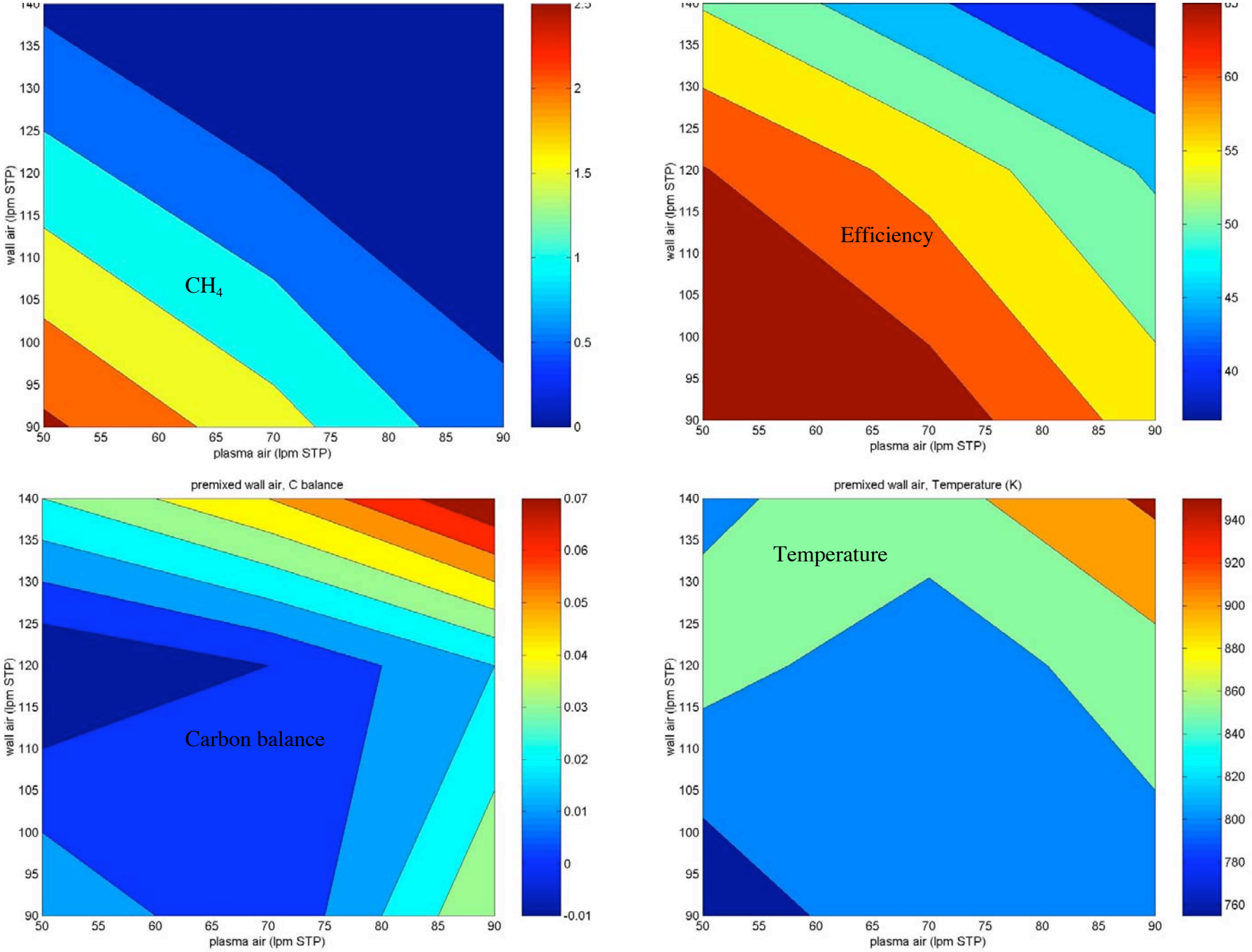

Figure 8.12. Contours of constant (a) CH_4 (b) efficiency (c) carbon balance (d) temperature as a function of wall and swirl air flow rates for the same conditions as Figure 8.9.

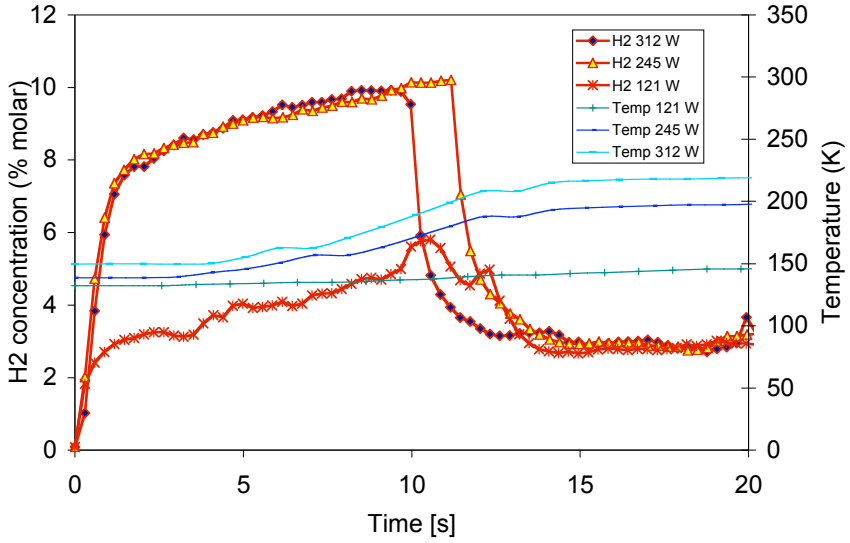

Figure 8.13. Transient response of plasmatron propane converter operating at O/C ~ 1.6, for propane premixed with the wall air, for several power levels.

5. Propane Premixed with plasma air

The fluid dynamic modeling indicated that the air/propane mixtures in the condition when the propane is premixed with the swirl air results in the largest fraction of propane under conditions of stoichiometric combustion. This method of injection was therefore particularly interesting, as the large region with stoichiometric air/propane mixtures should results in faster chemical reaction rates, with the highest release of chemical energy. If the reforming is through the two-stage process, as described in [Bro05c, Bro05d, Bro05e] (with a fraction of the fuel combusting and distributing the energy through mixing with the rest of the air/fuel mixture), then this case should produce the best reforming results.

The experimental results corresponding to this situation are shown in Figures 8.14 and 8.15. The hydrogen concentration in this case is about 14-15%, with 16% CO. The optimal O/C ratio in this case is lower than in the previous 2 cases, O/C ~ 1.3. This mode of operation results in substantially lower concentrations of CO_2, decreased temperatures and increased efficiency (~ 80%), all pointing towards improved reforming. As a matter of fact these conditions are the best conditions obtained in the study, as will be discussed in section 8. The hydrogen concentration is still substantially lower than that of ideal partial oxidation reforming, in part due to the higher O/C ratio (O/C = 1 for ideal partial oxidation). Not only is there additional oxygen, but also the oxygen preferentially oxidizes the hydrogen over the CO. The hydrogen yield is about 45%.

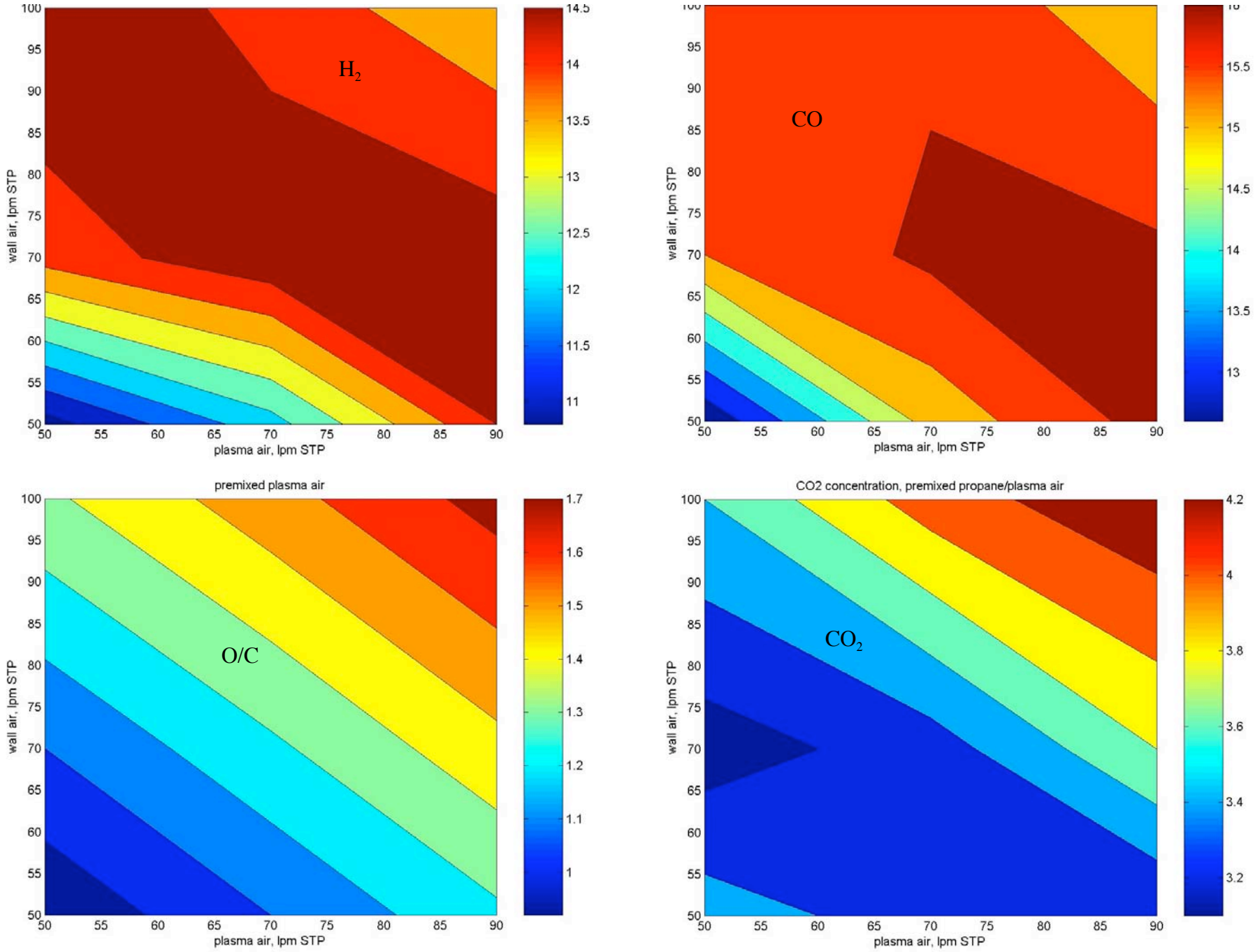

Figure 8.14. Contours of constant (a) H_2 (b) CO (c) O/C ratio (d) CO_2 as a function of wall and swirl air flow rates, for propane premixed with swirl (plasma) air

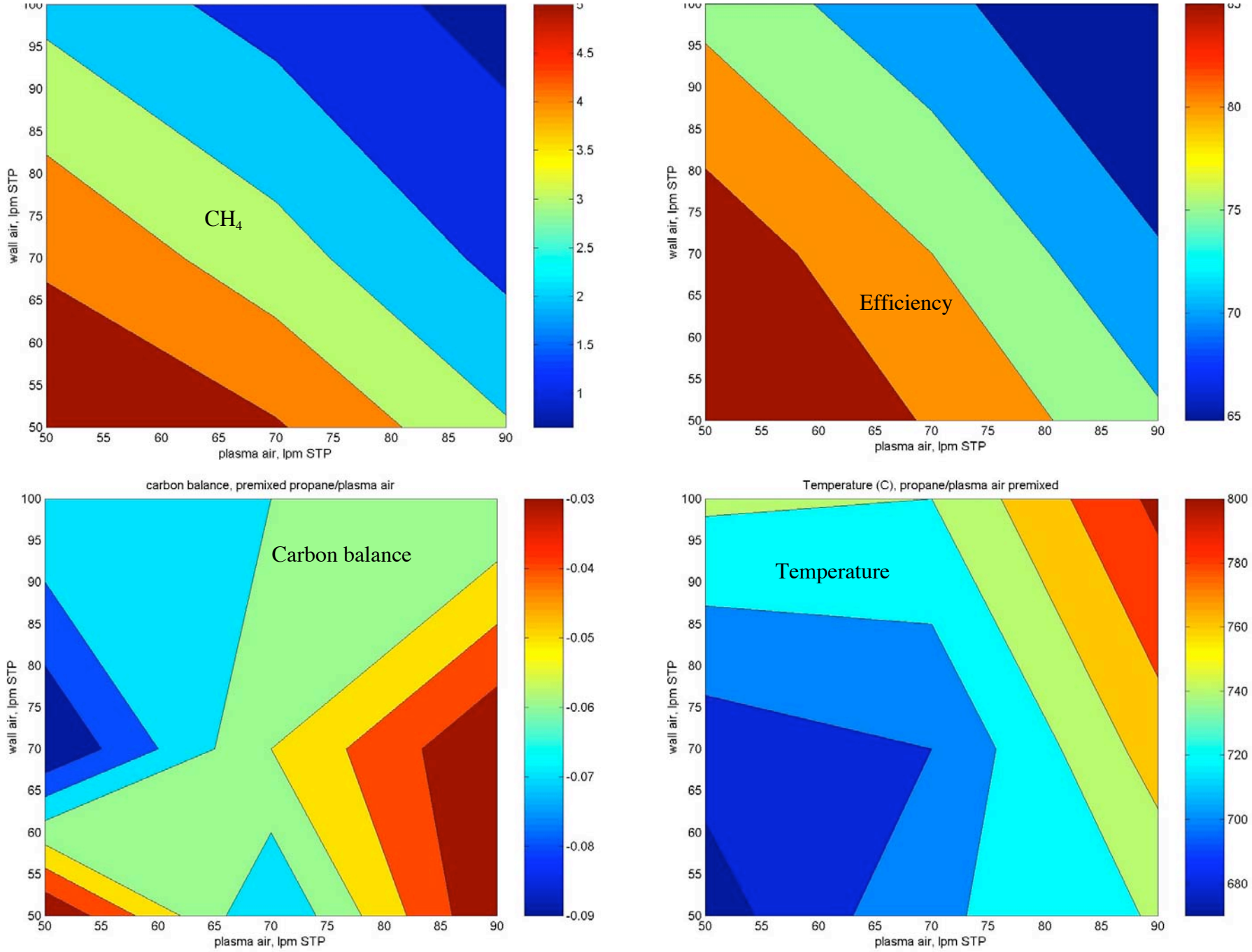

Figure 8.15. Contours of constant (a) CH_4 (b) efficiency (c) carbon balance (d) temperature as a function of wall and swirl air flow rates for the same conditions as Figure 8.12.

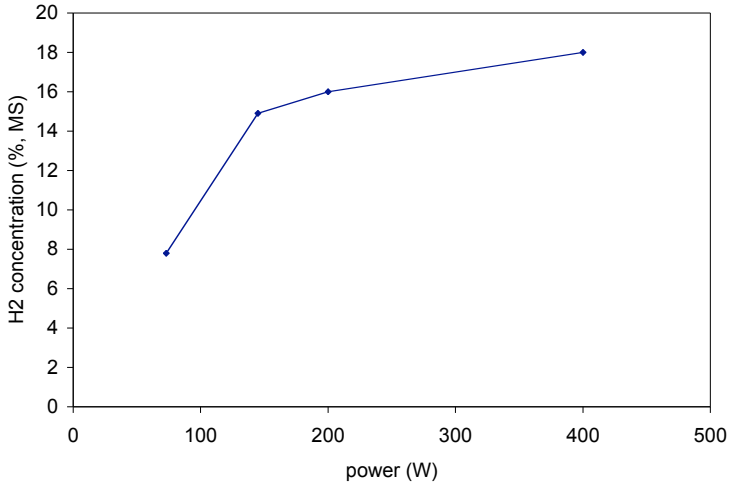

Figure 8.16 Steady state hydrogen concentration as a function of plasma power (O/C ~ 1.3)

The carbon balance, shown in Figure 8.15, is better than 10%. The carbon balance is substantially better than this over most of the experimental regime, with the exception of those regions where the reforming is least optimum, at lower swirl/wall air flow rates and where it is likely that there be substantial unconverted propane.

The steady-state power sensitivity is shown in Figure 8.16, for an O/C of 1.3 (70 lpm for both swirl and wall airs). Higher power does increase the hydrogen concentration.

Transients are shown in Figure 8.17, for several values of power. The transient hydrogen concentration is a sensitive function of the power, as in the case of for premixed propane/wall air. A hydrogen concentration of 10% can be reached in about 1 s at 400 W. At 100 W, the hydrogen concentration is about 3-4%. Not only is the concentration higher at the higher power, but also the slope after the initial transient is higher. This is due to increased rate of increase of the temperature, not shown in Figure 8.17. Note that as in the case for premixed propane/wall air, if the plasma is turned off, there is still reforming, although with hydrogen concentrations ~ 2%. The concentration of hydrogen after the plasma has been turned off is not sensitive to the plasma power. Also shown in Figure 8.17 is one case, one of the traces for 400 W plasma power, where the propane was also shut off.

In Figure 8.17 there are two traces for a given power level with the exception of 100 W. The purpose was to determine reproducibility of the startup, which indeed it is.

The turn off time is comparable to the turn on time, indicating very fast turn-on of the plasmatron. It is likely that the rate limitations in the transients in this paper are instrumental, as discussed in the methane start-up paper [Bro05b]. It is possible to utilize

Figure 8.17 to evaluate the time constant for the turn-off. The e-folding time is about –0.5 s, thus the time for 90% change (2 e-foldings) is about 1 s

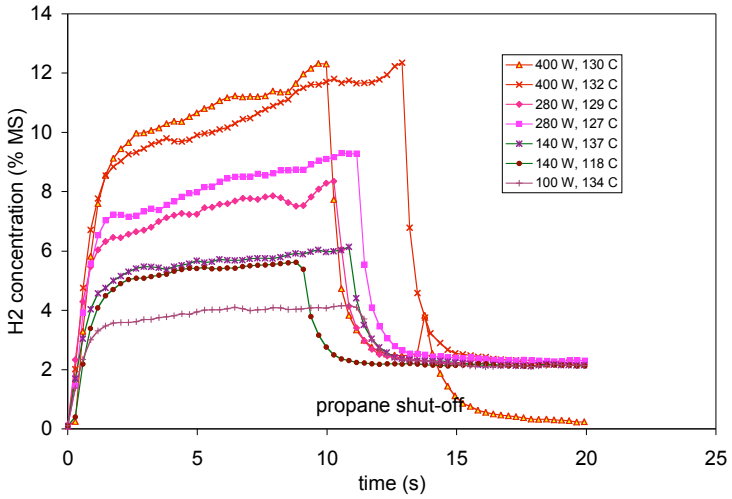

Figure 8.17. Transient characteristics for premixed propane/swirl air for different values of power, for O/C ~ 1.3.

Stoichiometric combustion propane/air mixture for swirl gas

The previous section discussed the case of premixed/swirl air. Because the overall O/C is below stoichiometric combustion, the O/C ratio of the propane/swirl air is very low, much lower than 1. The results of making the propane/swirl air prone to igniting because of operation at stoichiometric combustion, with the rest of the propane premixed with the wall air, is discussed in this section. In order to be able to premix the propane with both the swirl air and the wall air, two independent propane controls are required. Two similar rotameters were used to accomplish this.

Results of the experiments are shown in Figure 8.18. The maximum hydrogen concentration is about 12% at an optimum O/C ~ 1.5. The efficiency at the optimal conditions is on the order of 50%. Carbon balance is particularly bad at the lowest O/C ratios in Figure 8.18, but moderately good (~10%) elsewhere.

The transient hydrogen concentration and temperature are shown in Figure 8.19 for several power levels. Two traces are shown for each power level. The transient looks similar to those other with low values of O/C, with the prompt hydrogen concentration being a function of plasma power. For the lowest value of power, 50 W, startup is not reproducible, and one of the traces shows a failed startup, while the other shows unstable operation with a frequency of about 0.3 Hz. In this case, as the plasma power is shut off, the hydrogen concentration drops to about 6%. Even for 100 W, the hydrogen concentration is not affected by shutting off the plasma.

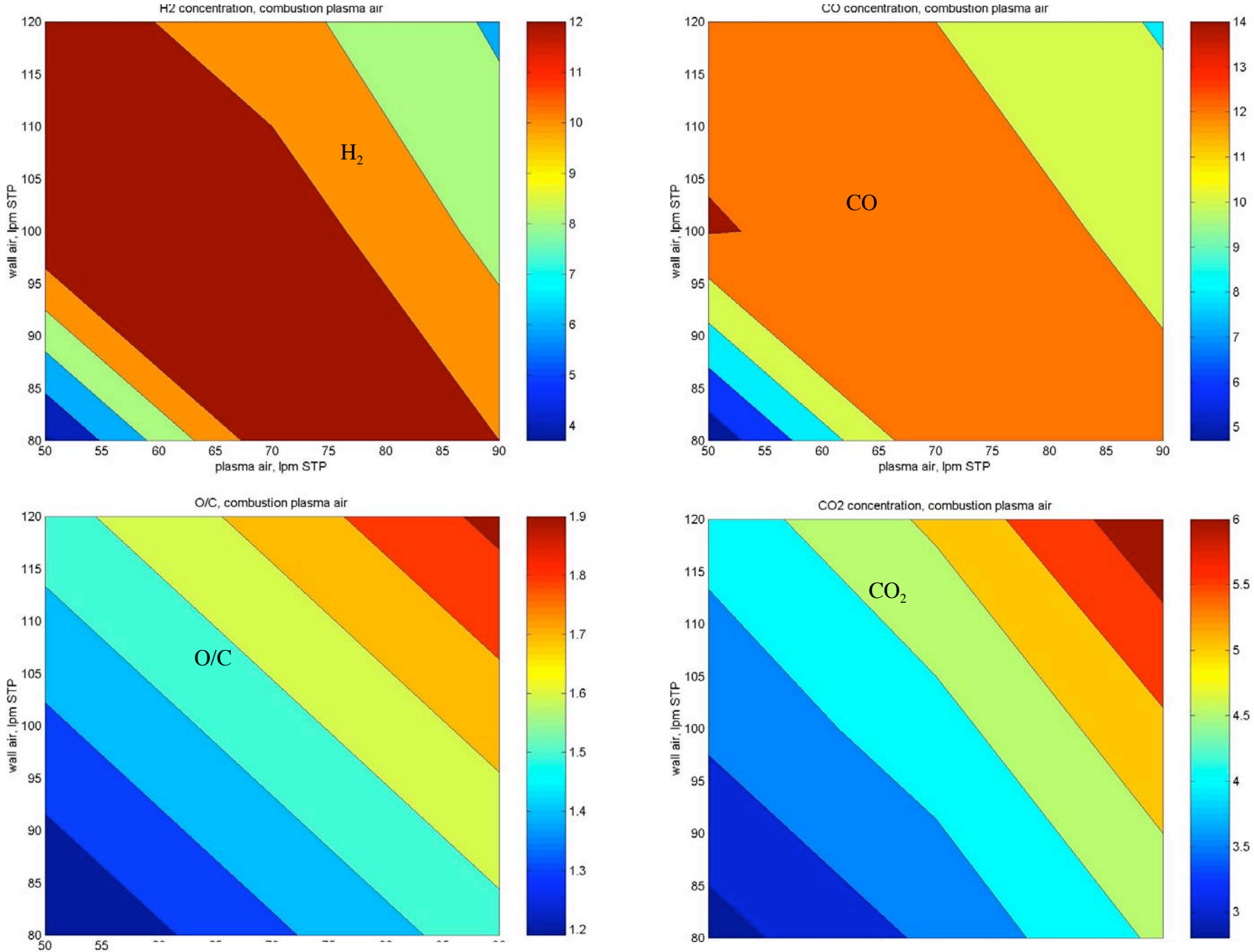

Figure 8.18. Contours of constant (a) H_2 (b) CO (c) O/C ratio (d) CO_2 as a function of wall and swirl air flow rates, for propane/swirl air at stoichiometric combustion composition, with the rest of propane premixed will wall air.

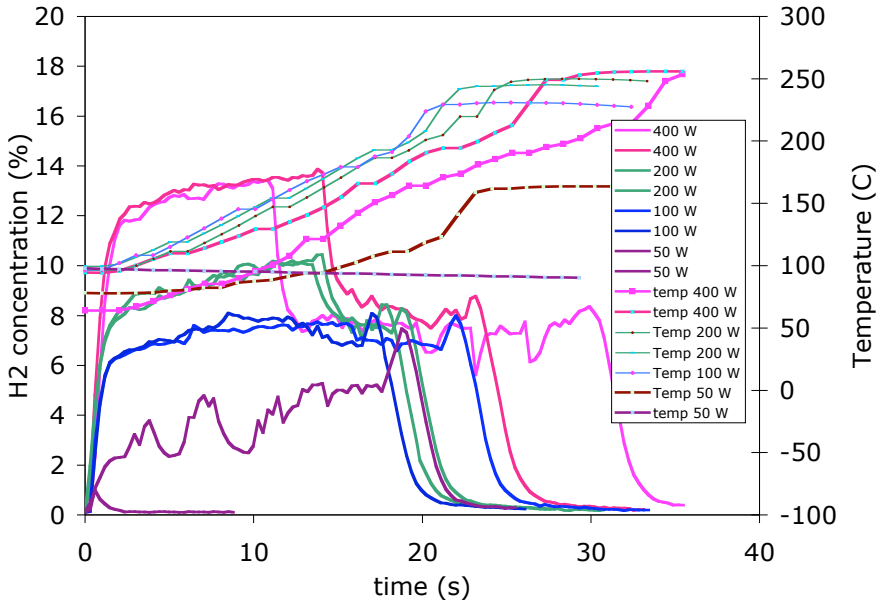

Figure 8.19. Transients for the case of stoichiometric combustion composition of the swirl gas, with the rest of propane premixed with the wall air, for several values of plasma power.

Fully premixed propane and air.

In the last case investigated, the propane and the air are fully premixed. In this case, the plasmatron air/fuel mixture is homogeneous, as all the inputs have the same composition.

Results are presented in Figure 8.20. Hydrogen concentration is about 12%, at an O/C ~ 1.7. The higher value of the O/C ratio results in increased CO_2 concentration (4.5%), higher temperatures (850-880 C) and lower efficiency (55-60%).

Under these conditions the hydrogen concentration was a strong function of power, with the reaction stopping at slightly decreased values of power (300W).

Figure 8.21 shows the transients for two levels of power. At 150 W, the reaction sputters but at 350 W the prompt hydrogen concentration is about 8%, with a relatively high rate of rise of the temperature.

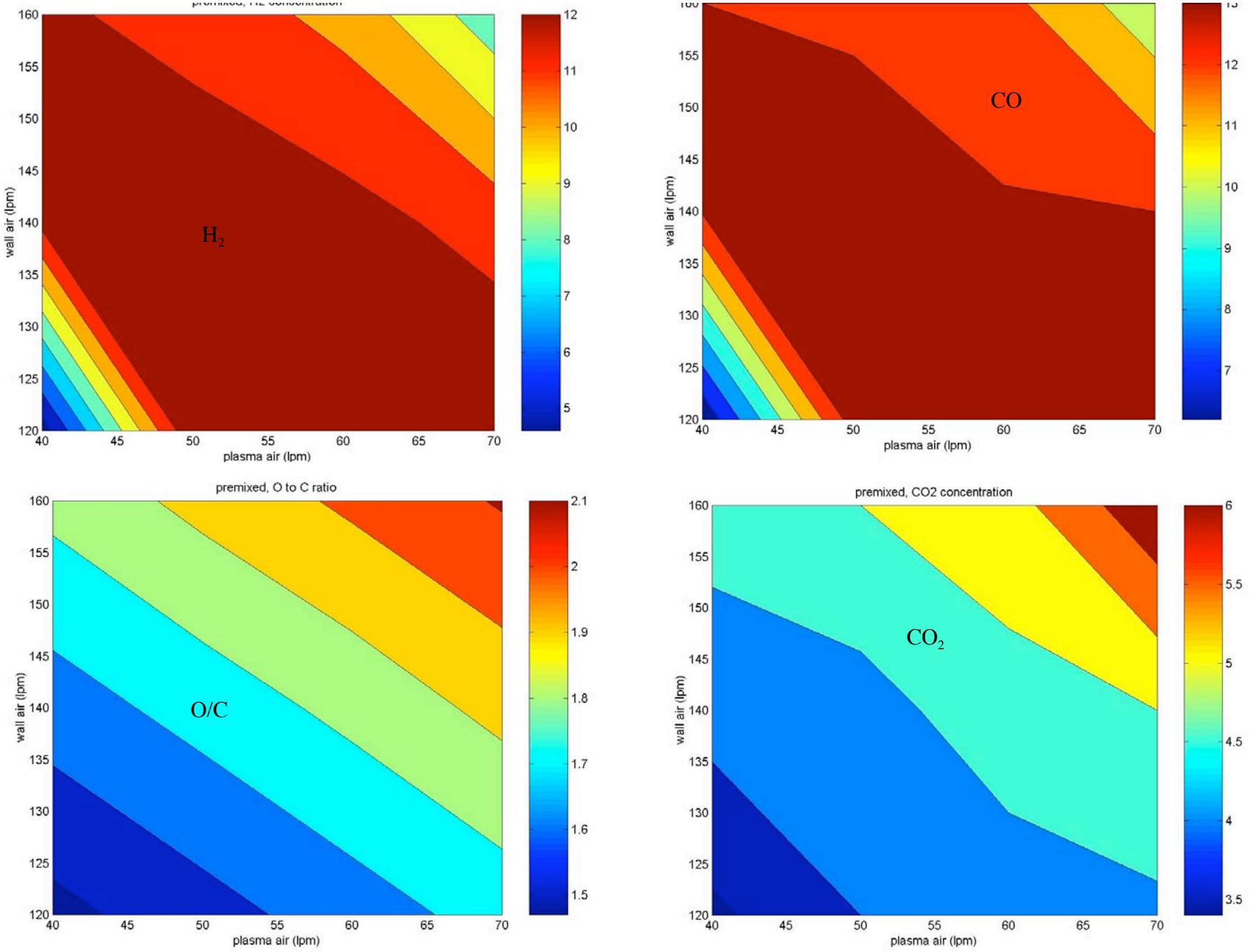

Figure 8.20. Contours of constant (a) H_2 (b) CO (c) O/C ratio (d) CO_2 as a function of wall and swirl air flow rates, for propane premixed with air, thus resulting in a homogeneous air/propane mixture throughout the device

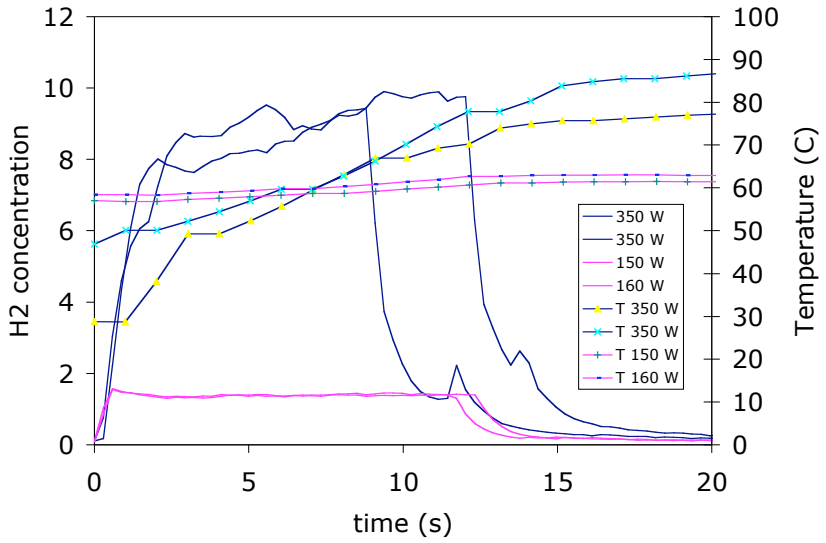

Figure 8.21. Transients for the case of propane/air premixed, resulting in a homogeneous air/fuel mixture.

Discussion

This section has discussed 5 different means of introducing propane into a plasmatron fuel converter. Both the steady state characteristics, as well as some startup properties have been discussed.

Table 8.1 Summary of tests presented in this paper

	O/C ratio	Flow dist	Efficiency	H2 conc	Temp	Dependence on power	Cold start up
Premixed	1.7	140/60	60%	12%	850	> 350 W	8% in 1.5 s
Premixed plasma	1.3	75/70	75%	14.50%	720	> 100W	10% in 2 s Continues ~2% when plasma off
Axial	1.8	160/65	65%	12%	790		8% in 1.5 s
Premixed wall	1.6	110/70	55%	13%	820	Drops 20% when hot, plasma off	8% in 1.5 s Power > 150 W
Combustion plama air	1.45	95/70	60%	12%	800	Drops by 10-20% when plasma off	10% in 1.5 s Power > 100 W

Table 8.1 shows a summary of the work presented in this paper. Conditions of optimal reforming (highest hydrogen concentration) for each case are shown. It is clear that the results are best when the propane is introduced through the swirl port (premixed plasma)

with the highest values of hydrogen concentration with lowest values of CO_2 and temperature (a sign of combustion). Introducing a stoichiometric for combustion mixture in the swirl gas is not better than when all the propane is introduced through the swirl port, but it is better than the other configurations. Some of the results from the fluid dynamic simulation in section 2 suggest that premixing the propane with the swirl air results in the highest fraction of propane in stoichiometric combustion conditions in the plasma region.

It is interesting to note that the worst configuration is that with the fuel injected through the axial port. Unfortunately, this is the configuration that is needed for injection of liquid fuels.

The plasmatron configuration that was chosen for the experiments was designed for conversion of diesel fuel. There is a long path between the axial injection point and the electrode gap, where the plasma is. It is in this region that the axially injected propane premixes with the wall air. For liquid fuels, which require air assist for atomization, the velocity of the fuel droplets is very high, and it is possible to maintain stratification even when axially injecting the fuel.

c) Biofuels

In this section, the reformation of bio-fuels are discussed. The work emphasized fuels of present interest, such as bio-diesel and ethanol, which are being introduced into the market. [Bro05l] In addition, unconventional fuels such as unprocessed and lightly processed bio-oils, were investigated. This work is also described in the section

Biodiesel

Biodiesel is one of a limited number of renewable fuels. It can be obtained from a variety of seeds. Its use in transportation is being investigated. Although there are discussions about the overall energy benefit of the use of renewable biofuels [Pim05, Sha02], it is generally accepted that they produce a net energy benefit.

Table 8.2
Typical Soybean Oil Methyl Esters Profile

Fatty Acid	Wt. %	Mol. Weight	Formula
Palmitic	12.0	270.46	C15H31CO2CH3 ($C_{17}H_{34}O_2$)
Stearic	5.0	298.52	C17H35CO2CH3 ($C_{19}H_{38}O_2$)
Oleic	25.0	296.50	C17H33CO2CH3 ($C_{19}H_{36}O_2$)
Linoleic	52.0	294.48	CH3(CH2)4CH=CHCH2CH=CH(CH2)7CO2CH3 ($C_{19}H_{34}O_2$)
Linolenic	6.0	292.46	CH3(CH2CH=CH)3(CH2)7CO2CH3 ($C_{19}H_{32}O_2$)

The B-100 biodiesel was provided by Renewable Solutions, Oakland Park, Kansas. The average molecular weight of soybean oil methyl esters is 292.2, calculated using the average fatty acid distribution for soybean oil methyl ester shown in Table 8.2 [Bio05]. Shown in Table 8.3 are the molecular weight and chemical formula for each of the component esters [Bio05].

Table 8.3
Carbon Chain Length Distribution and Percent Oxygen
Produced from Typical Soybean Oil.

Compound	CAS#	Bonding	Weight %	% O2
Methyl Palmitate	112-39-0	C-16	10.0	11.8
Methyl Stearate	112-61-8	C –18	4.0	10.7
		% Saturated	14.0	
Methyl Oleate	112-62-9	C-18=1	25.0	10.8
Methyl Linoleate	112-63-0	C-18=2	53.0	10.9
Methyl Linolenate	301-00-8	C-18=3	8.0	10.9
		% Unsaturated	86.0	
Total average O2				11.0

Biodiesel reformation (gen 3)

In this section, experiments of plasmatron biodiesel reformers are described. The flow rate of the biodiesel fuel is about 0.5 g/s, which match those of methane and propane carried out previously [Bro05a, Bro05b, Bro05c, Bro05d, Bro05e, Bro05f] with the same plasmatron setup.

In order to investigate performance with different stoichiometries, the O/C ratio of the plasmatron was changed by adjusting the wall air (see Figure 8.22). The plasma air and the atomization air were kept constant at 50 lpm (1 g/s). The plasma air has a narrow operating region, as too little air does not push the discharge into the volume of the plasmatron (the discharge remains in the inter-electrode region), and too high a flow results in an unstable discharge. Similarly, for atomization air flow rates less than about 50 lpm the fuel atomization decreases substantially, and much higher flow rates can not be obtained because of choke-flow limitations.

The wall air was varied from no flow all the way to 80 lpm.

The steady state composition of the reformate was measured using a calibrated gas chromatograph, described in [Bro05a]. It was assumed that steady state conditions were obtained when the temperature, measured by a thermocouple downstream from the plasmatron [Bro05a], reaches steady state conditions.

The composition of the reformate, as a function of the O/C ratio, is shown in Figure 8.23. The O/C ratio is defined as the ratio of the flows of all the oxygen atoms to the carbon atoms, and thus includes the oxygen atoms in the fuel.

Two sets of experiments were carried out, with the second set going to larger values of O/C, but also overlapping over the first set of experiments. The compositions in Figure 8.23 do not include C_2 compounds. Although the gas chromatograph indicates substantial levels of C_2 compounds, their calibration has been suspect. The carbon balance matches much better when in the analysis the concentrations of C_2H_6, C_2H_4 and C_2H_2 are ignored.

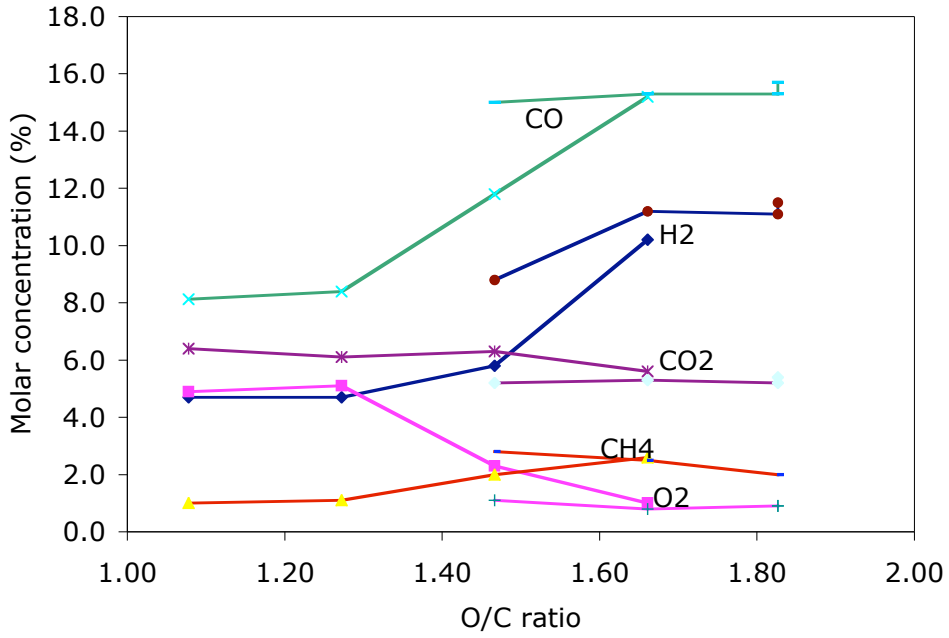

Figure 8.23. Composition of reformate from plasmatron biodiesel reformer as a function of the O/C ratio.

The hydrogen concentration is relatively low at the lower values of O/C, although there is still some present. Increased O/C results in large increase in hydrogen concentration, which approximately doubles when the O/C ratio increases from 1.3 to 1.7. Good conversion of the fuel is also indicated by the disappearance of oxygen, which drops substantially at O/C ~ 1.5 and even further at O/C ~ 1.7. The CO concentration follows the hydrogen concentration. Higher O/C were not investigated because of the limitations of the mass-flow controller, although the curves indicate that hydrogen concentration has peaked at O/C ~ 1.7.

The corresponding temperature measured downstream from the plasmatron and opacity are shown in Figure 8.24.

The energy efficiency of the process (defined as the heating value of the reformate divided by the heating value of the fuel) is poor (~ 20%) at low O/C values. At O/C ~ 1.5,

with good carbon balance, the energy efficiency is about 60%. At O/C ~ 1.7, the energy efficiency is higher, about 66%.

The effect to the plasma power was investigated by turning the power off after steady state operation was achieved. The reaction became unstable without the plasma, as both the temperature decreased, the opacity increased and there was a low frequency (a few tenths of Hz) rumble coming from the plasmatron. The same phenomena was observed throughout the range of O/C ratios investigated with biodiesel. Thus it was concluded that the use of the plasma, for the range of conditions explored, was needed for stable, good reforming.

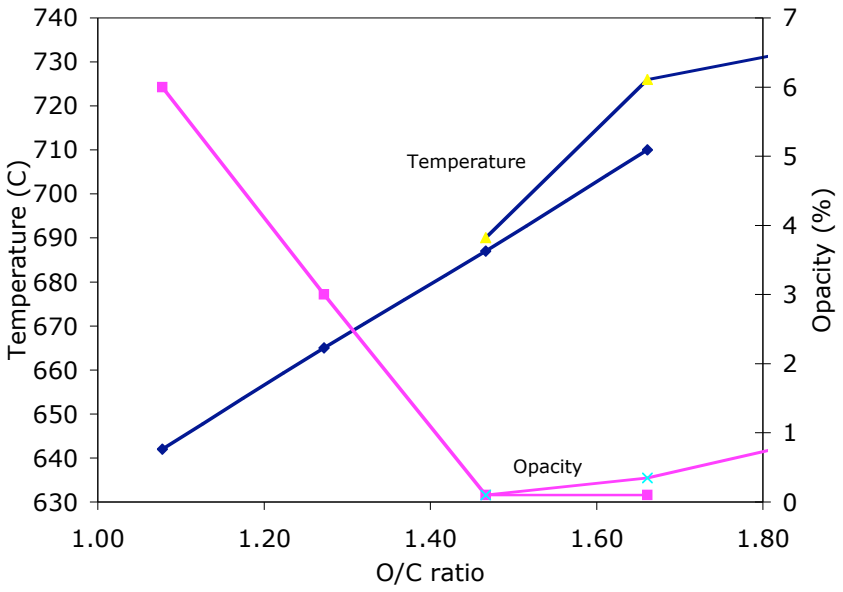

Figure 8.24. Temperature and opacity corresponding to tests in Figure 8.23.

Ethanol

Similarly, ethanol can be obtained from either cellulosic materials, corn, or sugar. Although there are discussions about the overall energy benefit of the use of renewable biofuels [Bio2,Bio3], it is generally accepted that they produce a net energy benefit.

In this section, results for the reforming of neat ethanol are described. The setup was identical to that used for the B-100 experiments. Neat ethanol was introduced instead of the biodiesel through the B37 nozzle. The flow rate of ethanol in these experiments was 0.58 g/s. Only steady state characterization was investigated..

The composition of the reformate for various values of O/C are given in Figure 8.25. As in the previous section, the definition of O/C includes the oxygen in the fuel. Two sets of values are presented, with and without plasma. It is interesting to note, as discussed in the

gaseous fuels as with B-100, that at high values of O/C there is a relatively small impact of the presence of the plasma. For the case of ethanol, at O/C > 2.1, the plasma plays a minor role, and the compositions with and without the plasma are comparable. The plasma has an impact at lower O/C, where the plasmatron is still operating, but with very poor performance.

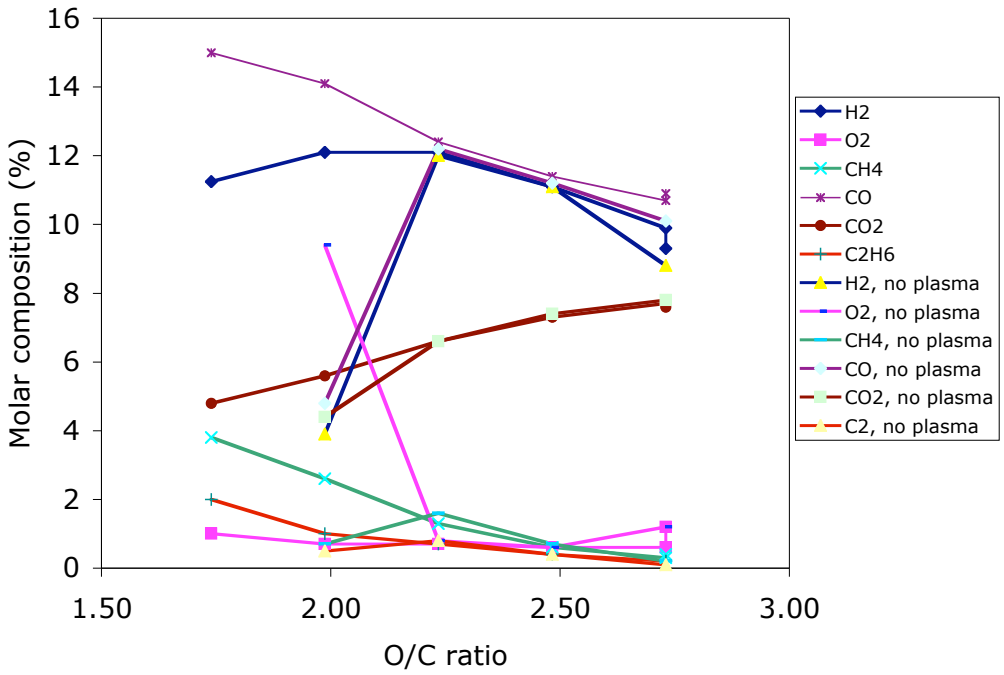

Figure 8.25. Composition of reformate from plasmatron ethanol converter as a function of O/C, with and without plasma on.

Figure 8.26 shows the temperature and the opacity for the same cases in Figure 8.25. The temperature decreases monotonically with O/C, and is similar for both cases with and without plasma. The opacity, however, increases substantially. The opacity is not constant in the case on no plasma, and some averaging had to be made. Opacity in very transient, with a duration less than 1 s (can not be resolved with the present instrumentation).

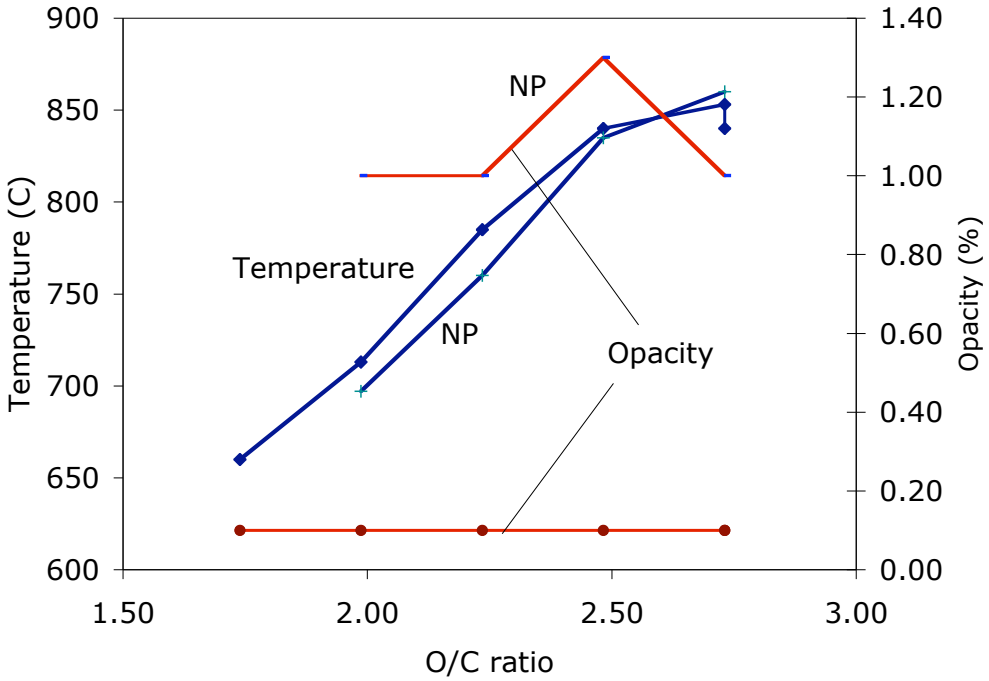

Figure 8.26 Temperature and opacity for the same cases as Figure 8.25. NP stands for No-Plasma.

The carbon balance for the experiments in Figures 8.25 and 8.26 is adequate, better than 10%, with the exception of the case with no plasma and lower O/C, where there is 50% carbon deficit. It is thought that this is due to the poor performance of the reformer, and with raw fuel coming through the device.

The reformer efficiency (ratio of heating value power of the reformate over heating value power of the fuel) in the presence of the plasma increases from about 50% at the highest values of O/C to a very respectable 75-80% at the lowest values considered. In comparison, for the case of no plasma the efficiency maximizes at ~70% at O/C ~ 2.1.

Discussion of biofuel reforming

The O/C ratio, as defined in this paper, includes the oxygen present in the fuel, rather than the free oxygen. The oxygen bound in the fuel does not contribute to the exothermicity of the reaction, as the oxygen is already bound either to carbon or to hydrogen. B-100 has a relatively small fraction of the oxygen (about 10% of the carbon atoms), while for ethanol, the fuel has 1 oxygen atom per 2 carbon atoms, a ratio of 50%. If the oxygen in the fuel is not included, the O_{free}/C ratio for the experiments in Figures 8.25 and 8.26 spans from ~ 1.24 to 2.2. The peak hydrogen concentration is at O_{free}/C ~ 1.5.

Similarly, for B-100 the optimal reforming occurs at about O_{free}/C ~ 1.5. However, ethanol performance remains high at lower values of O_{free}/C than biodiesel.

Hydrogen concentration in the reformate when using ethanol on the order of 12% can be obtained with or without a plasma, and the plasma is needed O/C ratios lower than about 2.1. For B-100, the comparable numbers are 11%, but a plasma is needed throughout the range that was explored. It is interesting to note that the heat of vaporization of ethanol is substantially higher than that of B-100. Under the assumption that the fuel needs to be vaporized prior to reforming, ethanol should be more difficult to reform. However, the experimental evidence points to the contrary, with better performance of ethanol reformers at lower O/C ratios and less sensitivity to the presence of the plasma..

The reformation at lower values of O/C degrades, with decreased conversion and increased opacity. It is possible that the increased opacity is due to raw fuel. However, for the fuel to be raw, the temperature must be lower (fuel would either pyrolyze or evaporate at 700 C). Thus, raw fuel must be accompanied with lower temperatures, from a reformer where the reformation has stopped. It has been determined that in the short residence time in the system, there is not enough surface heat transfer from the walls to the air/fuel mixture to increase the temperature of the air fuel mixture to more than 100 C. Thus, when there is a transient and the reforming stops, the air/fuel mixture remains relatively cold. This behavior may also be behind the "puffing" sounds that come from the exhaust under these conditions, with the reforming turning on and shutting down with a period of a few seconds..

Finally, it is not clear why the carbon balance is poor in the case of B-100. Carbon balance (including C_2H_4 and C_2H_6) is better than 10% for the case of ethanol, but about 30% for the case of B-100.

d) Reformation through plasma catalysis

This section reports further investigations of plasma enhanced partial oxidation reforming of biofuels that include corn, canola and soybean oils, and ethanol. Results were obtained for both homogeneous (non-catalytic) and catalytic reforming.

Other work on methane catalytic reforming has been reported in previous papers [Bro99d. Bro99e, Bro00a]. In addition, biofuel reforming has been reported by Hadidi [Had04, Bro05j].

Bio-fuel reformation

Figure 8.26 shows results for hydrogen yields from the reformation of canola, corn, and soybean oils as a function of O/C ratio for catalytic and homogeneous (non-catalytic) reforming. The hydrogen yield is defined as the ratio of the mass flow rate of hydrogen in the reformat gases to the mass flow rate of hydrogen in the fuel. The bio-oil flow rate was 0.4 g/s, which corresponds to about 17 kW of chemical power.

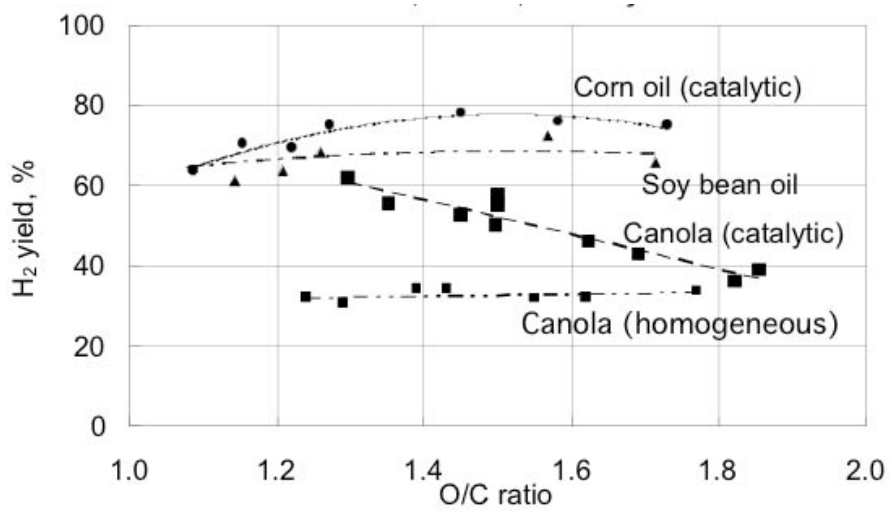

Figure 8.26. Hydrogen concentration for catalytic reformation of corn, canola and soy bean oils

The hydrogen yield for the reformation of corn and soybean oils are very similar in the presence of a catalyst. The difference between the two falls within the error bar due to sampling and GC analysis uncertainties.

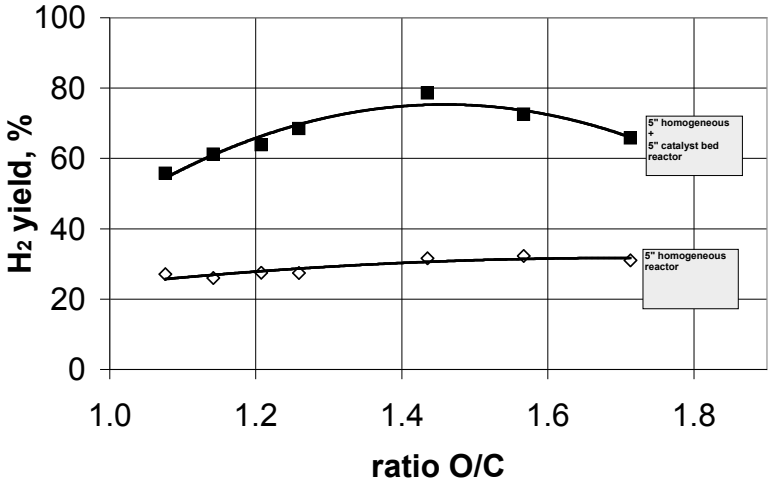

Figure 8.27. Hydrogen yield as a function of O/C ration for partial oxidation reforming of soybean oil

On the other hand, the hydrogen yield for canola oil in the presence of a catalyst appears to be lower than for corn and soybean oils, especially at the higher values of O/C. This may be due to the use of less catalyst in the case of canola, or to issues with the air-fuel injection (for example, misalignments of the injector where the oil spray hit the walls). In the case of corn and soybean oils, the hydrogen yield peaks at an O/C ratio close to 1.5;

this is due to the fact that some of the fuel needs to be combusted in order to provide the heat necessary to drive the partial oxidation reaction.

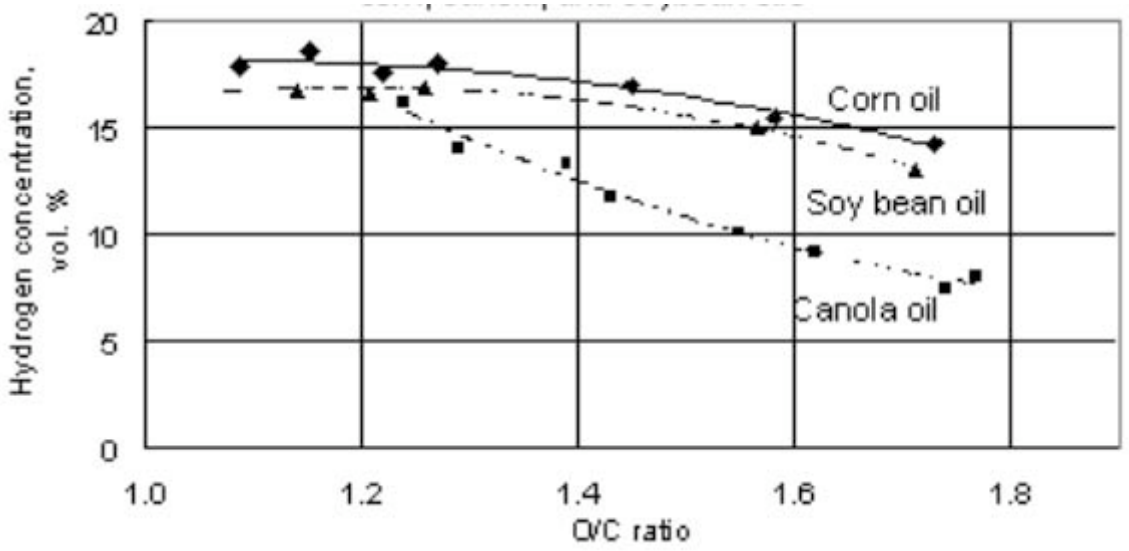

Figure 8.28. Hydrogen concentration for catalytic reformation of corn oil, soybean oil and canola oil.

Comparison between homogeneous (non-catalytic) and catalytic reforming was carried out for the case of corn, canola and soybean oil. Figure 8.27 shows the effect of catalyst on the hydrogen yield, for a fixed soybean oil flow rate of 0.37 g/s. The hydrogen yield is the ratio of hydrogen in the form of H_2 to the hydrogen in the biofuel. For homogeneous reformation of soybean oil, the hydrogen yields are about 30%, while the yield increases to about 80% in the presence of a catalyst. The peak yield occurs at O/C ~ 1.5. The difference between the yield of 80% and the ideal yield of 100% is due primarily to losses of hydrogen resulting from full oxidation into water. For homogeneous reformation, the ratio of the heating value of the hydrogen, CO and light hydrocarbons byproducts to the heating value of the fuel was typically between 60 and 70%.

Hydrogen concentration in the reformate as a function of O/C ratio for the processing of canola, corn, and soybean oils is given by Figure 8.28. Here again, the hydrogen concentration during the reformation of corn and soybean oils are identical and larger than the results with canola oil. It is likely that the difference between the canola and the soybean/corn results are due to the difference in catalyst volume.

The hydrogen concentration for the three oils is higher at lower O/C ratios and decreases when O/C ratio increases. This is because as O/C ratio increases, some of the oxygen reacts with the hydrogen to form water and the reaction tends to move toward combustion. Even though the hydrogen yield increases at the higher O/C ratios, the addition of combustion products decreases the actual hydrogen concentration.

The composition of the gas reformation upstream and downstream the catalyst for soybean oil for an O/C ratio of 1.08 is shown in Table 8.4 bellow. The plasmatron converts homogeneously the high hydrocarbons into hydrogen, carbon monoxide and light hydrocarbons, with minimal soot production and eliminating all free oxygen. The catalyst then takes the oxygen-free plasmatron gas and basically doubles the hydrogen yield performing CO_2 and possibly steam reforming (notice that the CO_2 concentration is decreased downstream the catalyst; water, on the other hand, is not monitored).

It should be stressed that the performance of the system was not optimized, and higher hydrogen yields could be possible by converting the substantial amounts of C_2's present in the gas downstream from the catalyst.

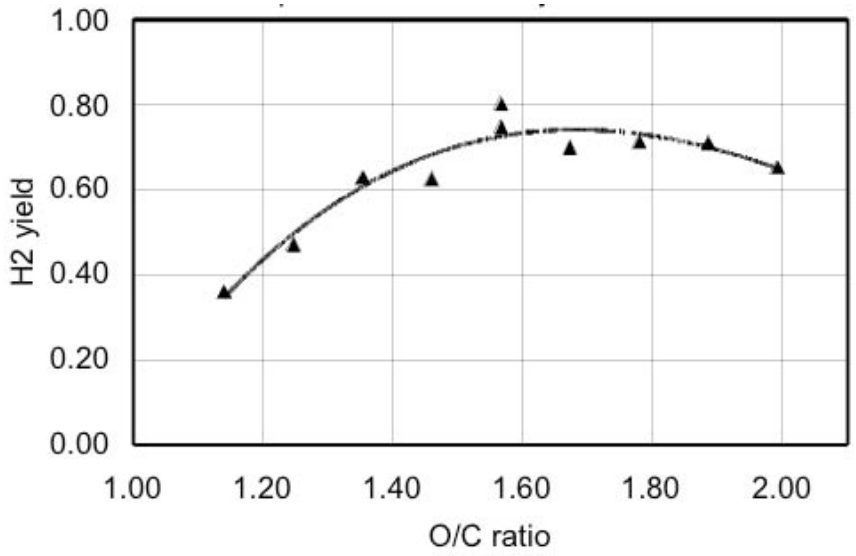

Figure 8.29. Hydrogen yield for catalytic reformation of ethanol as a function of O/C ratio.

For all the experiments performed with veggie oils, the opacity was 0.1, which is the sensitivity limit of the instrument and which indicates that at most very small amounts of soot were produced.

Table 8.4. Composition of the reformate gas

	Homogeneous	Catalytic
	% vol	% vol
H2	9	16
CO	12	17
CO2	7.4	5.2
N2	63	56
CH4	1.4	1
C2H4	5.7	3
C2H2	0.1	0.05
O2	0.7	0.7

Ethanol

The same experiments as for the veggie oils have been carried out for ethanol, but at lower power levels. Figure 8.29 gives the hydrogen yield for catalytic reformation of neat ethanol at 200 W as a function of the oxygen to carbon (O/C) ratio. Homogeneous reformation of ethanol is difficult to achieve because of the presence of oxygen in the molecule, leading to a very mildly exothermic reaction. It appears however that the results of the plasma catalytic reformation of ethanol are comparable to those obtained for veggie oils and at the same O/C ratios.

The hydrogen yield peaks at around O/C ~ 1.5 – 1.7, slightly higher than that for the bio oils. As mentioned previously, the O/C ratio includes the oxygen that is carried out by the fuel, which in the case of ethanol is very substantial.

The opacity measured during ethanol reforming was < 0.1, which indicates that no soot was produced.

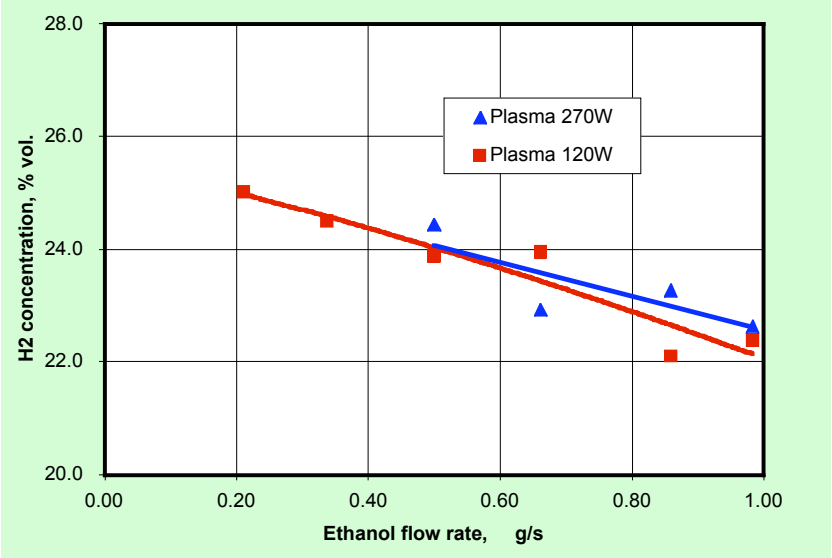

Figure 8.30. Hydrogen concentration in dry gas for ethanol reforming, as a function of flow rates, for O/C ~ 1.2

The results in Figure 8.30 were carried out with a plasmatron reformer that incorporated a nickel catalyst on a crushed alumina substrate. In the absence of a catalyst (for a homogeneous reaction), the hydrogen yields are about 40%, coupled with high concentration of light hydrocarbons (~4-5% C_2H_4).

The presence of soot was determined using an opacity meter. Virtually no soot was observed in these experiments.

Similar experiments for ethanol are shown in Figure 8.30, for different powers and varying flow rates. Ethanol conversion is difficult to perform homogeneously because of the low exothermicity of the partial oxidation reaction. Figure 8.30 shows the hydrogen concentration of the partial oxidation of ethanol, for O/C ~ 1.2.

Energy consumption

In order to make plasma reformation of fuels into syngas attractive, the energy consumption of the process has to be as minimal as possible.

Figure 6 gives the electrical energy consumption for corn, soybean oils, and ethanol versus O/C ratio at a power level of 700 W. For a maximum hydrogen yield at an O/C of 1.5, the electric energy consumption is 10 MJ per kg of hydrogen produced for corn and soybean oils. This is approximately 8 % of the energy in the hydrogen. The flow rate of fuel was limited by the size of the exhaust system being used, and it has not been established that the fuel flow rates at the 700 W level has been maximized. Instead of increasing the flow rate, a few experiments at lower power levels have been performed. As shown on Figure 6, the power consumption for canola and corn oils at respectively an O/C of 1.2 and 1.5 is about 2.5 MJ per kg of hydrogen. This is an important result since it shows that high fuel conversion factors can be achieved with low electrical energy consumption.

Energy consumption for the reformation of ethanol appears to be comparable to the energy consumption with veggie oils.

e) Catalytic vs homogeneous reforming of diesel with gen 2 plasmatron

Table 8.5 shows reforming results for several cases, using the second generation plasmatron fuel converters, at steady state conditions (after about 1 to 2 minutes). Several types of reaction extension cylinders were used with either no catalyst or a catalyst in the reaction extension cylinder. The effect of the presence of water was also studied. The purpose of the water addition is to convert, via a water-shift reaction, a large fraction of the CO generated in the plasmatron fuel converter into additional hydrogen, for those applications were hydrogen is much more preferred than CO. High hydrogen yields higher than 100% (hydrogen in product gas divided by hydrogen in fuel) can be achieved with the use of a catalyst and water shifting. Power conversion efficiencies of close to 90% have also been obtained under certain conditions. However, it is difficult to obtain water onboard vehicles, and this will be a major deterrent to the use of the water shift reaction for onboard applications for internal combustion engines.

Typical second generation low current plasmatron fuel converter parameters are a power level of 300W to 600W, and oxygen/carbon ratio (O/C) of 1.2-1.5, and fuel rate of 0.3-0.5 g/s (corresponding to about 10-20 kW of fuel power).

The composition of the hydrogen rich gas for the cases in Table 8.5 are shown in Table 8.6. High concentrations of hydrogen and CO are obtained. It appears to be possible to operate the low current plasmatron fuel converter in modes with minimal production of soot.

Table 8.5.
Performance of second generation low current plasmatron fuel converter using diesel fuel
Cases for different catalyst, O/C ratio and presence/absence of additional water.

	Electrical Power input kW	O/C ratio	H2O/C	Fuel Flow rate g/s	Fuel Power kW	Hydrogen yield	Energy Consumption MJ/kg	Power Conversio Efficiency %
Empty reactor no water	0.27	1.32	0	0.26	11	0.64	13	56
Ceramic catalyst no water	0.19	1.51	0	0.48	20	0.75	4	64
Honeycomb catalyst no water	0.23	1.21	0	0.34	14	0.91	6	74
Honeycomb catalyst with water	0.15	1.24	1.78	0.31	13	1.22	3	87

Table 8.6.
Gas composition for cases in Table 8.5

	H2 vol.%	CO vol.%	CO2 vol.%	N2 vol.%	CH4 vol.%	C2H4 vol.%
Empty reactor no water	14	16	4.7	64	0.7	0.1
Ceramic catalyst no water	14	17	4.7	64	0.2	0
Honeycomb catalyst no water	19	21	3.3	57	0.3	0
Honeycomb catalyst with water	23	17	6.2	52	1.2	0.4

Previously, diesel fuel has been successfully reformed at O/C ~ 1 using a compact plasmatron reformer that employs a DC arc plasmas [Bro99c, Bro99f]. However, arc plasmatron reforming utilizes substantially higher electrical powers and currents.

Even when operating at stoichiometric partial oxidation (O/C ~ 1), the reaction is exothermic. For the case of liquid fuels, with a composition nearly of $C_nH_{1.9n}$, the reaction releases about 15% of the heating value of the fuel. The temperature of the reformate, assuming near adiabatic conditions, is on the order of 1000K. As in the case of the nonthermal plasmatron, with O/C > 1, the adiabatic temperature is even higher.

f) Thermal plasmatron (gen 1) reformation

Initial in the program, work was carried out reforming multiple fuels with the thermal plasmatron fuel converter (gen 1). Below are summarized the most pointing aspects of the process for several fuels.

Using a DC arc thermal plasmatron fuel converter, conventional fuels were very efficiently converted to hydrogen rich gas, with an electrical power input of ~10% of the heating value of the fuel. However, with heat regeneration and with improved reactor design, it is estimated that the required electrical energy input to the microplasmatron fuel converter will be on the order of 5% of the heating value of the fuel. Furthermore, the reactor showed no evidence of soot, even after extended operation. Innovations to further decrease the energy consumption and to further simplify the microplasma reformer are described at the end of this discussion.

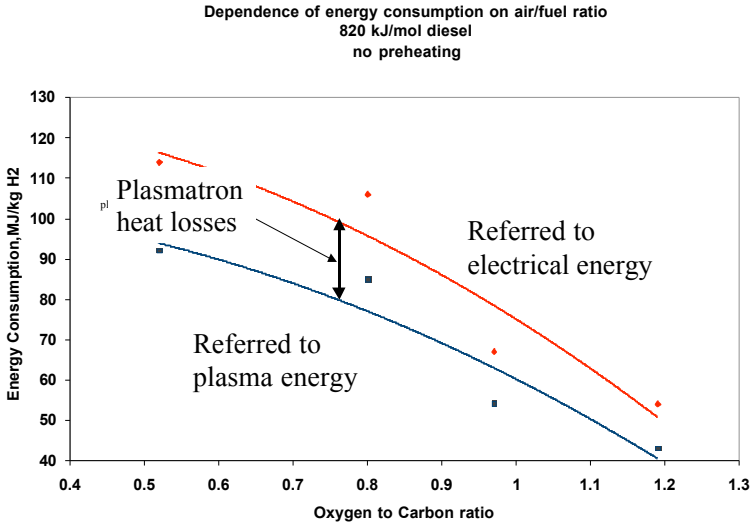

Figure 8.31. Energy consumption for plasma diesel reforming as a function of the oxygen to carbon ratio

Figure 8.31 shows the specific energy consumption of the hydrogen rich gas produced by the DC Arc micrplasmatron fuel converter, in units of MJ/kg H_2 for diesel fuel. The hydrogen and light hydrocarbon yield as a function of oxygen to carbon ratio is shown in Figure 8.32. At the higher oxygen to carbon ratios, the process becomes more exothermic. For a given specific electrical power input, the increase temperature increases the yield (as shown in Figure 8.32) and decreases the specific energy consumption.

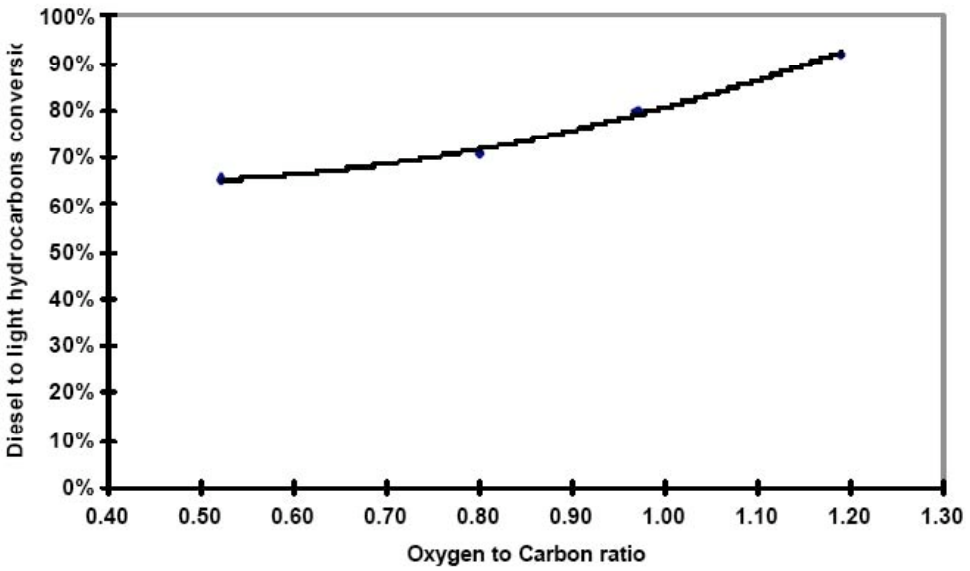

Figure 8.32. Hydrogen and light hydrocarbon yield as a function of the oxygen to carbon ratio

The experiments described above were conducted at constant power. The power requirements and the reformate composition were relatively insensitive to the flow rates as long as the specific power input (power/unit mass) and air/fuel ratios are kept constant. Under these circumstances, although the residence time decreases (because of the higher throughputs) increased efficiency of the system makes up for the decreased residence time. Figure 8.33 shows the composition of the reformate for diesel as the fuel, as a function of the oxygen to carbon ratio. The hydrogen concentration is relatively constant.

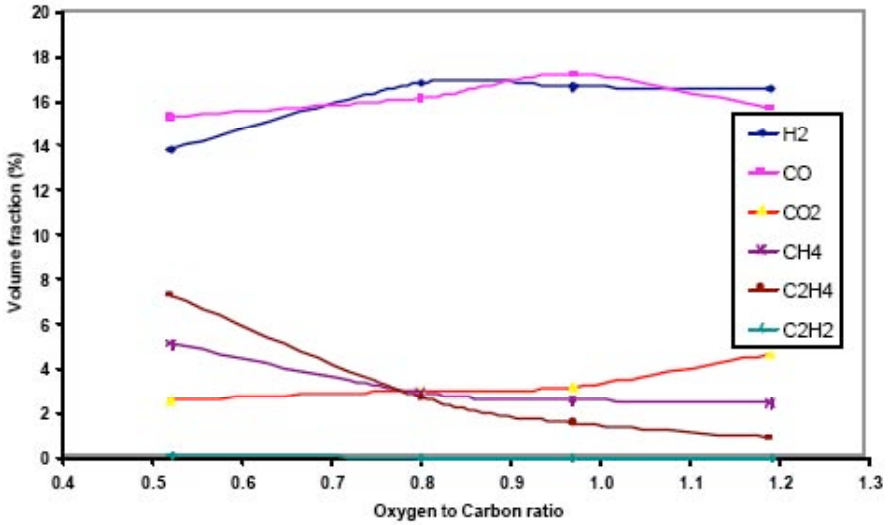

Figure 8.33. Composition of the reformate as a function of oxygen to carbon ratio for diesel fuel.

Microplasmatron fuel converters have substantial dynamic range. The lower power is determined by the maximum voltage capability of the power supply (the voltage increases with decreasing current), while the highest power is determined by erosion of the electrodes. It is expected that a dynamic range of a factor of 10 is possible without substantial modification to the plasmatron device. This is sufficient to provide the required change in throughput for conventional engines. For hybrid vehicles, with engines operating at constant or near constant conditions, the plasmatron fuel converter would operate at near constant conditions, with air/fuel/power management requirements that are much simpler than for conventional drive.

9) Plasmatron transients

In this section, the plasmatron transient performance is described. Limited results are shown for methane and gasoline. More extensive results are presented elsewhere. The results for transients for propane were described in the section of steady state propane in Section 8.b, as they were integral part of the results.

In addition, pulsed performance of diesel plasmatron is described in this section. Operation of plasmatron diesel reformers for NOx aftertreatment applications, as described in Section 4, requires periodic operation of the plasmatron with small duty cycle. Plasmatron performance under these conditions is described in Section 9.c.

a) Methane

In this section, the startup performance of homogeneous plasmatron methane reformers is described. Two start ups have been considered. One where the plasmatron is turned on and kept on, while the other one, pulse ignition, the plasmatron was turned on only for very short period of time.

Start-up experiments – pulse ignition

The experiments were carried out by establishing the flows, and the turning on the plasma. Two sets of experiments were carried out. In this section, experiments with short operation of the plasmatron will be described.

The power supply was turned on and then off, such that the on time was less than 1 s. The process was done manually, and thus the on-time differs from experiment to experiment, but the resulting performance of the plasmatron does not seem to be sensitive to the length of the on-time of the plasmatron.

The value of the instantaneous power in the plasma was varied in these experiments. The process involved adjusting the power without the presence of the methane. Then the power was turned off, the methane turned on, and the plasma pulsed in the manner described above.

The mass spectrometer was calibrated for hydrogen, oxygen and methane. Hydrogen was calibrated using measurements of the reformate with the GC, while oxygen was calibrated using air as the sample gas and methane by measuring the composition of the air/methane mixture and calculating the methane concentration from the known flow rates.

The experiments were carried out at various ratios of O/C. As in [Bro05a], the O/C ratio was varied by changing the wall air, with constant swirl air (60 lpm) and methane (40 lpm). The O/C ratio was varied from 1.63 to 2.24.

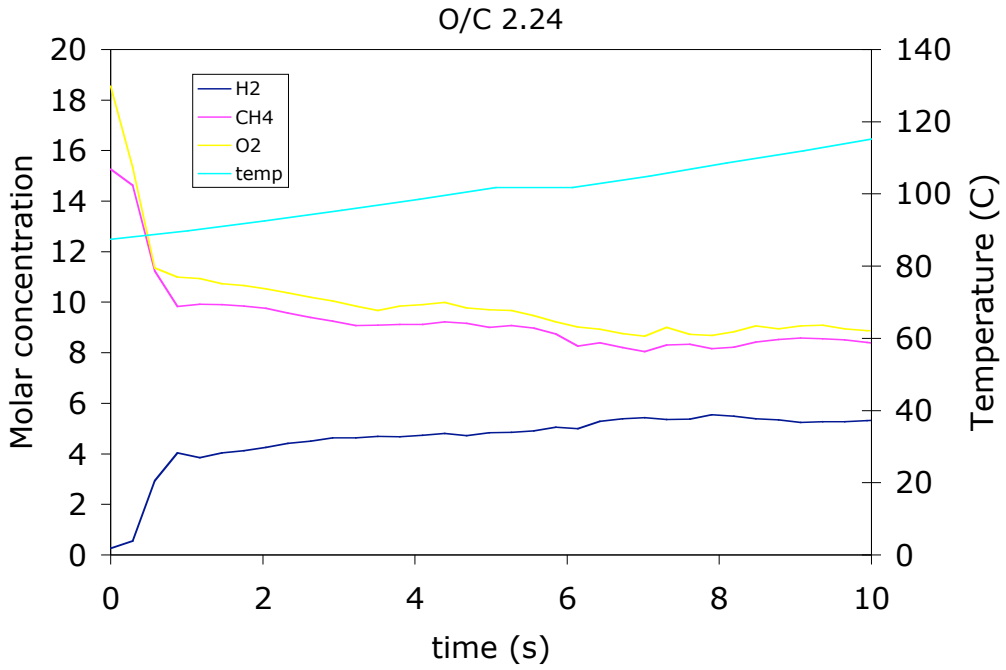

Figure 9.1. Time response of H_2, O_2 and CH_4 for O/C = 2.24 and 160 W.

Results of the hydrogen, oxygen and methane concentrations are show in Figure 9.1 as a function of time for conditions of O/C = 2.24 and 160 W of plasma power. Because of the ~ 3 s time delay, it is not clear where the start up occurs in the mass spectrometer. The second measured point by the MS shows increase of H_2 and decrease of both methane and oxygen. The transient lasts about 0.8 s, where the transient is defined as the time it takes for the 10%-90% change. It is not possible to determine whether the width of the transient is due to instrumental limitations of the MS system or time response implications of the plasmatron methane reformer. However, it can be said that the response of the plasmatron methane reformer cannot be longer than about 0.8 s, and could in fact be smaller.

The hydrogen concentration reaches more than about 4% in less than 1 s, and then slowly increases. The methane conversion is about 30% at times of about 2 s, increasing to about 50% at 10 s. The oxygen concentration follows the methane concentration.

The temperature, as measured by the thermocouple, is also shown in Figure 9.1. The temperature is increasing at a rate of more than 2 K/s. The temperature measured by the thermocouple is not a measurement of the gas temperature and it may be more an indication of the temperature of the walls.

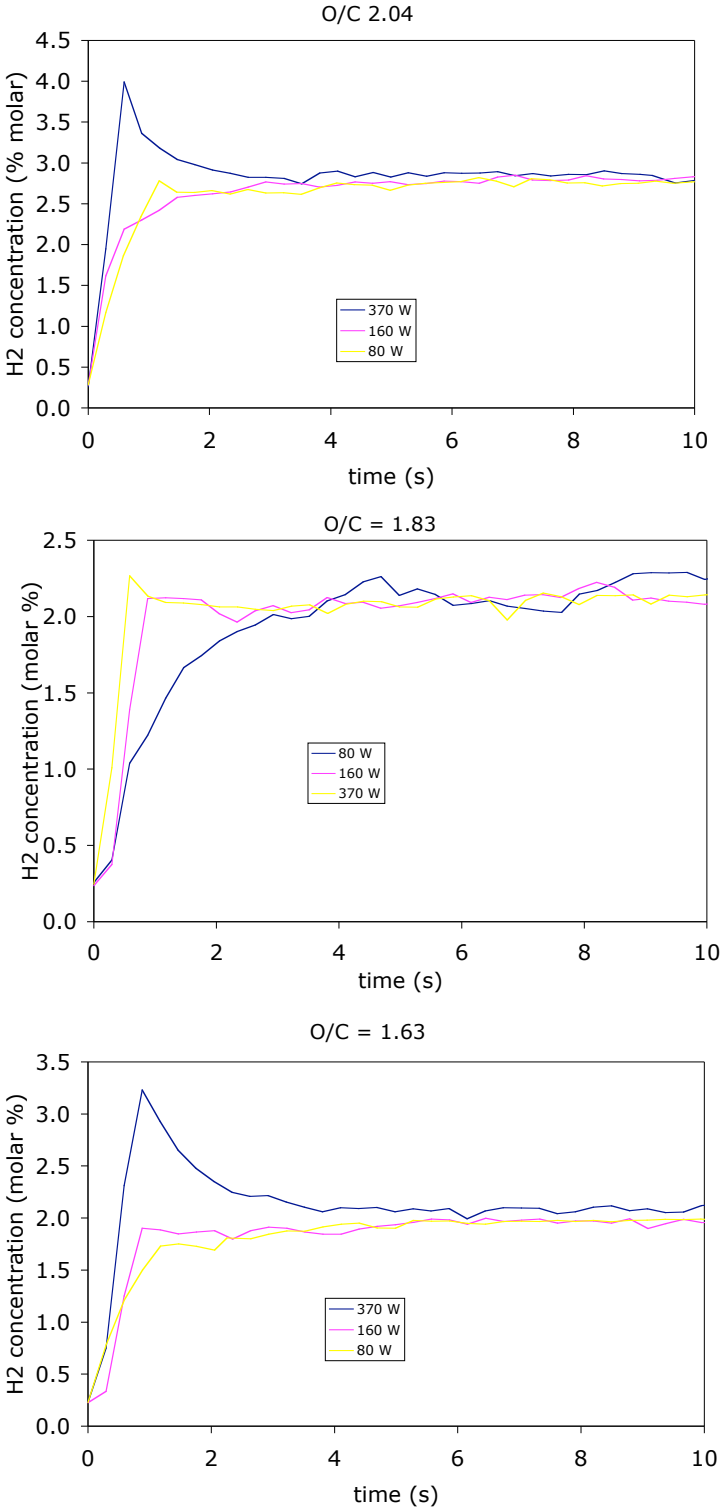

Figure 9.2. H_2 concentration as a function of time for (a) O/C = 2.04, (b) O/C = 1.83 and (c) O/C = 1.63 for several value of electrical plasmatron power

The transients in the hydrogen concentration for O/C = 2.04, 1.83 and 1.63 for several values of plasmatron electrical power are shown in Figure 9.2. It is clear from the figures that increased hydrogen yield occurs for those conditions with higher power right during turn-on and immediately after shut down of the plasma. However, for all these cases, following the turning of the plasma, the hydrogen concentration reaches the same value. The oxygen and methane plots, not shown, follow the same behavior, with concentrations after the transients that are independent of the instantaneous plasma power during the pulsed turn-on.

It is clear from Figure 9.2 that the hydrogen concentration increases with O/C ratio, especially at the higher values of O/C. Figure 9.3 shows the H_2 concentration 10 s after startup, for the cases in Figures 9.1-9.2, as a function of the O/C ratio.

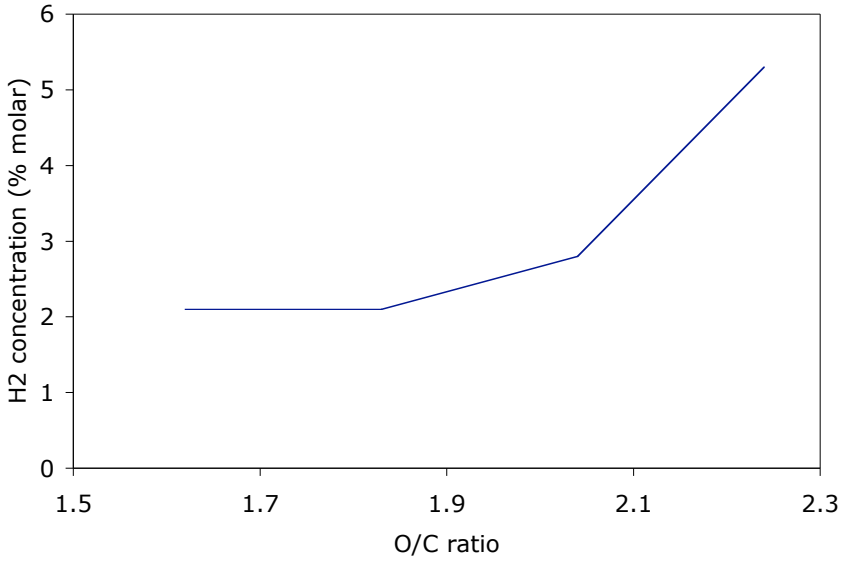

Figure 9.3. H_2 concentration at 10 s for different values of O/C.

H_2 concentrations as high as 5% can be obtained with methane using the plasma device as a short time igniter. It may be possible to obtain even higher concentrations at higher O/C ratios. There should be an optimum value beyond which the hydrogen in the fuel is consumed and turned into water. We have yet to explore these conditions of higher O/C ratio.

It is not clear how the device operates with 2% hydrogen conversion. The modeling that we have performed, and presented in accompanying papers, fails to reproduce the conversion. We also have yet to model the start-up phase.

Start-up – continuous ignition.

In this section, results of varying the power at a constant value of O/C are presented.

The experiments were nominally carried out at 60 lpm swirl air, 120 lpm wall air and 40 lpm methane, premixed with the swirl air. This flow rates would correspond to an O/C of about 1.83. Comparing the results in this section with those of the previous section indicate a discrepancy, and the O/C could be as high as 2.2 (see the discussion on the monitoring of the O/C ratio in Section 8.a and in reference[Bro05a]).

Figure 9.4 shows the results for the conditions described above. The power was varied for several startups, and then the power was shut down, allowing the reaction to continue. After a few seconds, the methane was shut off.

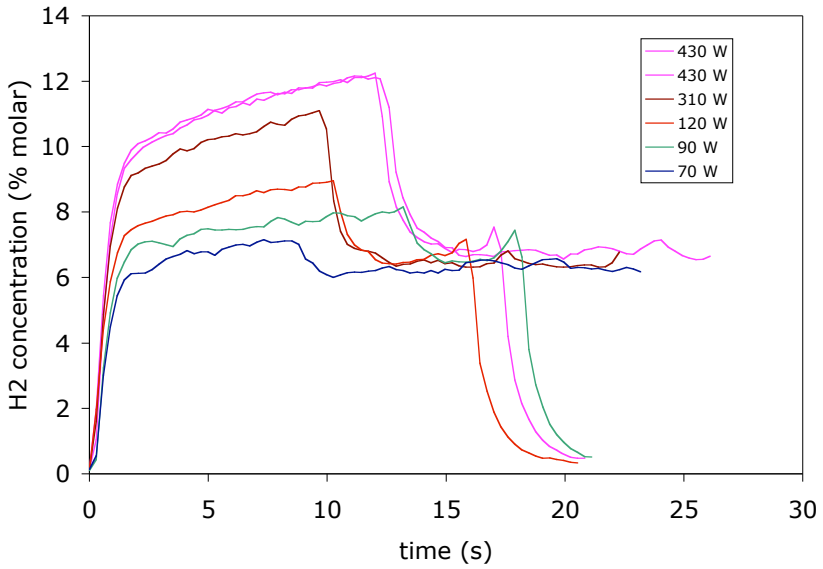

Figure 9.4. H_2 concentration for O/C ~ 2.2 for several values of power.

As in the previous experiments, the hydrogen concentration rises in about 1second after the plasma is started, and similarly decays in about 1 s after the plasma is shut down. The hydrogen concentration is a strong function of power when the plasma is on. Once the plasma is shut down, the reformer continues to operate, as described in the previous section. The transient, again, takes on the order of 1 s. As in the previous section with plasma ignition, the hydrogen concentration after the plasma is shut down is insensitive to the value of the power during the time when the plasma is on. The hydrogen concentration is on the order of 6%, which indicates that the O/C ratio may have been larger than 2.2.

Figure 9.5 shows the hydrogen concentration as a function of power at 2 s after start-up. The concentration at 0 power is that corresponding to the concentration after the plasma has been shut off, and does not correspond to 2 s after start-up. At the highest power, above 400 W, the hydrogen concentration rises to above 10%, indicating the advantages of the plasma at conditions of fixed O/C ratio.

The experiments need to be extended to other values of O/C, and to compare the maximum hydrogen concentration and methane conversion for the cases of pulsed ignition and continuous ignition.

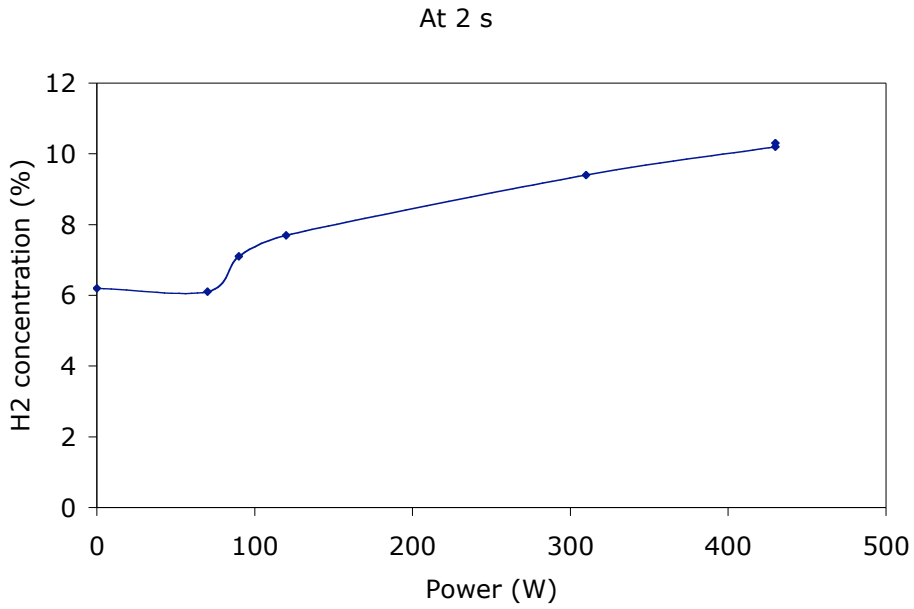

Figure 9.5. H_2 concentration at 2 s as a function of plasma power at fixed O/C.

b) Gasoline transient

The plasmatron setup described in section 2.e was used to determine the startup characteristics of the plasmatron. [Bro05i] Only one set of experiments was carried out, at an O/C ratio of the experiments is 1.06, near ideal partial oxidation, and at a power of 300 W.

The transient gas analysis was determined using an electrostatic quadrupole mass spectrometer, from Pfeiffer. The mass spectrometer setup was described in section 2.e. The soot/raw fuel droplets were measured using a Wagner 2000 opacity meter. Conventional 87 octane gasoline was used in the experiments.

The measured hydrogen concentration is shown in Figure 9.6. The experiments were carried out by turning on the air flow, the plasma, and then the fuel.

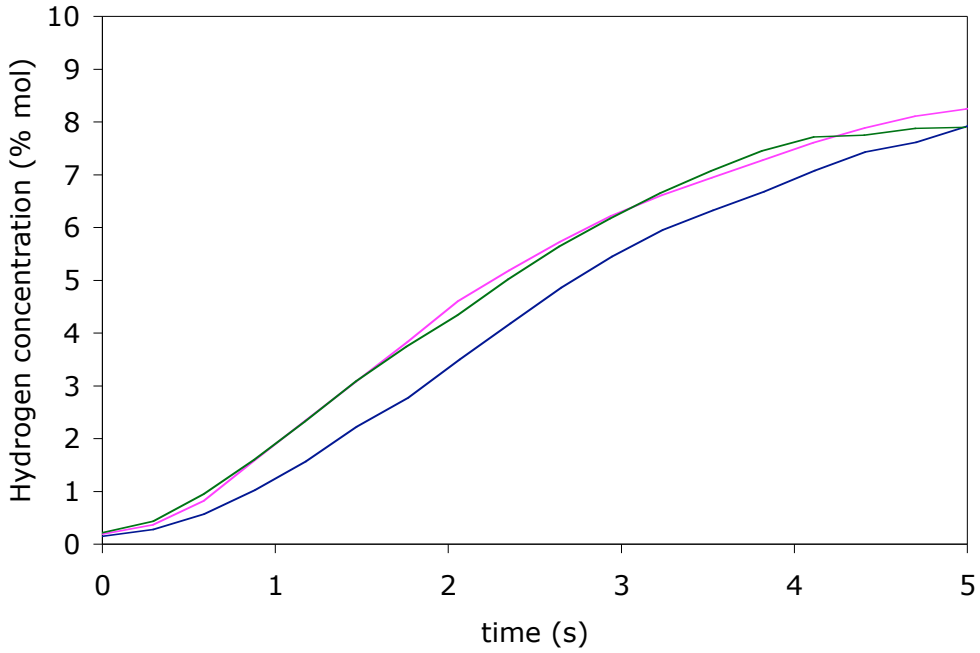

Figure 9.6. Measured concentration of H_2 as a function of time, for 3 startups.

After the early startup, the hydrogen concentration drops to ~ 4 %. It is likely that his process occurs because of changes in the air/fuel mixture characteristics. After a few seconds, the hydrogen concentration starts to increase rapidly.

The soot concentration, as measured with the opacity meter, was below measurable values.

c) Periodically pulsed diesel plasmatron performance

The plasmatron was operated under conditions typical for regeneration cycles. After a brief warm up time, the plasmatron is turned on and off for the periodic regeneration. Results were carefully monitored for a diesel flow rate of 0.35 g/s. The temperature is shown in Figure 9.7. The temperature, after the initial transient, is measured every 30 seconds. The regeneration time is 5 s, and the time between regenerations is 60 s. The corresponding concentration of hydrogen, CO and CO_2 are shown in Figure 9.8.

The O/C ratio was increased to 1.5 at approximately 15 minutes, and decreased to 1.25 at approximately at 23 minutes, in order to determine the sensitivity of the hydrogen production as well as the temperature of the reactor for several values of the O/C ratio.

More than adequate hydrogen yield was obtained for the conditions tested. The device was then taken for Cummins Technology Center in Columbus, IN for testing with an engine.

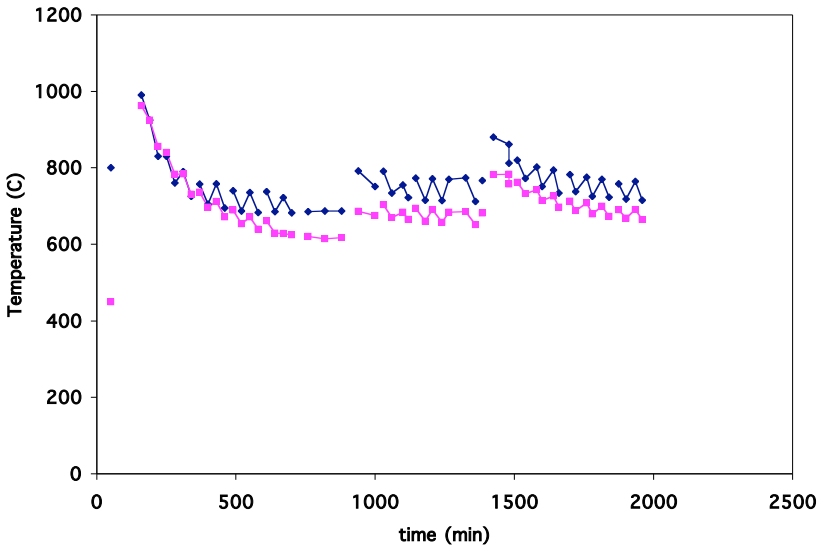

Figure 9.7. Temperature upstream and downstream as a function of time, for pulsed plasmatron operation typical of that required for NOx trap regeneration (5 s on, 55 s off).

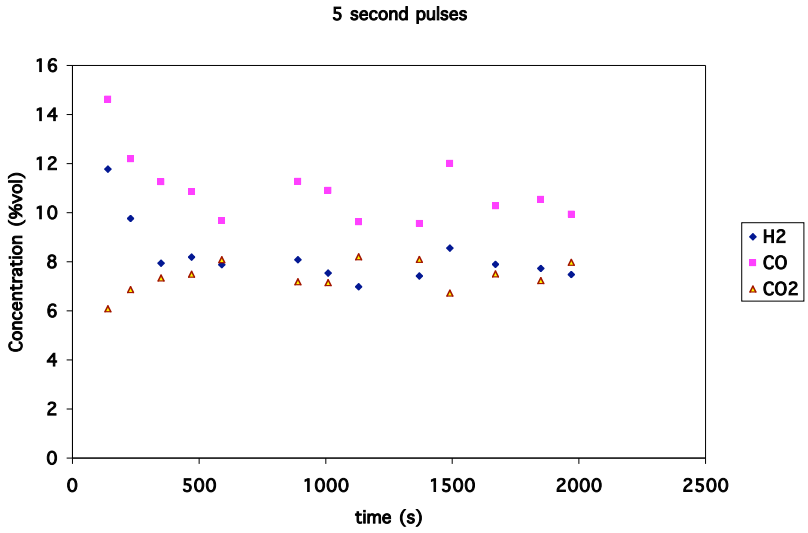

Figure 9.8. Corresponding concentration of H_2, CO and CO_2 for pulsed plasmatron operation typical of that required for NOx trap regeneration.

10) Summary

Engine tests

Onboard generation of hydrogen-rich gas using a plasma boosted microreformer could provide important new opportunities for significantly reduced emissions. A compact plasma boosted reformer was successfully integrated with a gasoline engine on an engine test stand. SI engine experiments were carried out to determine the effect of reformate addition on emission and efficiency. A NOx emissions reduction of approximately two orders of magnitude was obtained under certain conditions. The plasma boosted microreformer operated reliably for the relatively long duration of the experiments (>6 hours per day), operating on gasoline. Additional effort is required to decrease the electromagnetic noise, as well as to better integrate the microplasmatron fuel converter with the engine. The rapid response, as well as the robustness to fuel characteristics and ambient temperature, make the plasma boosted microreformer suitable as a fuel converter for a variety of onboard applications.

NOx trap regeneration

The testing with plasmatron diesel reformer for NOx trap regeneration has indicated that

- Plasmatron fuel converters have been shown to be good sources of hydrogen rich gas for regeneration of NOx traps
- Bio-oils (even unrefined oils) and ethanol can be efficiently and cleanly reformed into hydrogen rich gas.
- Increased hydrogen conversion and hydrogen using plasma catalysis has been demonstrated for diesel, bio-oils and ethanol.
- Plasmatron fuel converters offer advantages for regeneration of DPF.
- Plasmatron fuel converters have also been used to remove sulfur from the NOx trap at substantially lower temperatures than otherwise with an oxidative environment.

DPF regeneration

Reformate requirements for achieving DPF regeneration have been calculated on the basis of simple models. It has been determined that the flow rates requirements for a 6 l turbocharged engine, are within the range of today's plasmatron capabilities. Larger engines can be regenerated using multiple plasmatrons, or by using thermal management/non-uniform regeneration techniques.

It has been determined that the hydrogen rich gas will not spontaneously combust prior to reaching the soot trap under normal operating conditions of the engine. Thus, slow, uniform regeneration of the DPF could be achieved using both the thermal effect from the

reformate as well as reducing capabilities and localized thermal effect of the hydrogen rich gas.

Experimental setup for determining the advantages of the hydrogen rich gas have been determined. Trap soot loading and regeneration tests will be carried out in the near future.

CFD modeling

Computational fluid dynamics tools have been used to investigate the effects of alternative injection points for the fuel, in this case, methane. The purpose was to determine the characteristics of the air/fuel mixture at the location of the plasma, as well as to determine the mixing rates. It was determined that changes in injection point changes significantly the distribution of the methane in the region of the plasma, but does not significantly change the mixing parameters at this location.

This information will be used in accompanying papers to investigate the characteristics of methane reforming in plasmatron fuel converters.

Experiments and modeling of the vaporization with the time response of a plasmatron gasoline reformer were carried out.

We have determined that the response time of the mass spectrometer is on the order of 1 s. Thus, it is likely that the hydrogen concentration reaches about 4% 1 s after turn-on. By comparison, the response time with gaseous fuels was on the order of 2 s, at substantially higher O-to-C ratios.

PSR Modeling of methane

A 2-stage model has been developed for the homogeneous reforming of methane. The model was investigated using a simple Perfectly Stirred Reactor (PSR) with multiple inputs. It was determined that the reforming process ignited the overall O/C ratio is between 1.4 and 1.6. About 10-15% of the methane needs to be stoichiometrically combusted.

The actual composition of the reformate in the calculations underestimate the hydrogen concentration and the methane conversion. The PaSR model does better in predicting the composition of the reformate.

The results show a lack of sensitivity of the conversion to residence time. Increased conversion is difficult through the use of larger reactors. Instead, increased temperature is a more effective way to achieving high conversion of methane. The same results are obtained by increasing the reactor size by a factor of 8 or increasing the O/C ratio from 1.6 to 2. However, there is a minimum PSR size (defined as the section of the actual reactor with good mixing) for good reforming, and increased O/C ratio is needed to compensate for smaller well-mixed reactors.

PASR modeling of methane

A model of a plasmatron methane reformer where limited mixing is included has produced quantitative agreement with experimental results. The process uses only gas phase chemistry, without the use of a catalyst. The model reproduces the hydrogen and other main components of the reformate, as well as the methane conversion.

The model also has been used to determine the effect of the plasma at steady state conditions. It has been shown that the plasma increases the hydrogen concentration by about 20%, but the reaction continues at lower temperatures even in the absence of the plasma. As the cold reagents are introduced into the hot reactor gas, they are heated and release sufficient energy to maintain the reaction, although at decreased temperature.

The composition of the reformate is accurately described by the model. However, there are regimes (low O/C, absence of plasma) where there is only qualitative agreement with the observations. Additional modeling is needed that includes losses or improved description of the fluid dynamics, mainly for the case without plasma.

Methane reforming

The effect of the stratification of the methane/air mixture of the air has been investigated, at fixed methane flow rate. It was determined that the hydrogen concentration and yields depended on the overall O/C ratio, and that the distribution of the air between swirl and wall had only a small effect.

The plasma power required depends on the O/C ratio. At high O/C ratios (O/C ~ 2.2) the dependence on plasma power is small, with a ~20% decrease in hydrogen concentration without the plasma. However, at O/C ~ 2, the plasma is needed, and higher power is better. At even lower O/C ratios (O/C < 1.6), the reforming even in the presence of plasma, is poor.

The start-up of plasmatron methane reformers has been studied. The experiments indicate that when the plasmatron is used as an igniter, the hydrogen concentration is a function of O/C. Furthermore, the tests indicate that it is possible to increase the hydrogen concentration and the methane conversion by increasing the O/C to about 2.2. As the O/C for stoichiometric combustion of methane is O/C ~ 4, the reformer is still operating at very fuel rich conditions.

When the plasmatron is used in continuous ignition mode, the use of the plasma at a given O/C ratio increases the hydrogen concentration and the methane conversion. Increasing the power increases the hydrogen concentration. High hydrogen concentration, as high as 10-12%, can be obtained in ~ 1 s with O/C on the order of 2.2 with 300-400 W.

Propane reforming

In general, the following conclusions can be derived from this work:

- O/C controls the performance of the plasmatron propane reformer, more than where the air is introduced (swirl air, wall air),

- The performance of the plasmatron propane reformer is sensitive to the place of introduction of the propane, with best results premixing the propane with the swirl air and the worst results with the propane injected through the axial nozzle.

- Reforming is sensitive to plasma power at lower values of O/C. At higher values of O/C, the plasma is mainly needed for startup.

- Startup is sensitive to power at lower values of O/C.

Biofuels reforming

Conditions of good non-catalytic bio-oil reforming were investigated, with hydrogen concentration in the dry reformate > 10% and energy efficiency > 70%. Operation at relatively high O-to-C ratio was required. The ratio of free-oxygen to carbon ratio, however, is $O_{free}/C \sim 1.5$ at the conditions of good performance.

The plasma is required for the start up for both ethanol and bio-oils, until conditions near steady state are achieved. However, once steady state is achieved in ethanol, hydrogen concentration in the absence of plasma is maintained for all but the lowest value of O/C ratio, although with higher opacity that in the case with the plasma. For B-100, the plasma is needed throughout the O/C range explored.

Biofuel plasma catalytic reforming

Low-current plasmatron fuel reformer technology has been used to convert both bio-oils and ethanol into a hydrogen-rich gas with high hydrogen yields (70 to 80%) where a catalyst is positioned after the homogeneous reforming zone. For homogeneous reforming alone hydrogen yields are typically about half those obtained with catalytic reforming. However, the conversion rate into H2, CO and light hydrocarbons is still relatively high (close to 70%) for homogeneous reforming. More work is needed to further lower the energy consumption and increase the hydrogen yield by operating the plasmatron fuel reformer closer to an O/C ratio of 1.

11) Acknowledgements

We want to thank the continued support of Dr. Sidney Diamond. His encouragement, depth and width of knowledge, enthusiasm and `*Joye de Vivre'* will serve as standards for us to reach. In addition, encouragement and useful discussions were carried with Dr. Tecle Rufael fromm Chevron Texacon, and with colleagues from Arvin Meritor, in particular Dr Rudi Smalling, Dr. Navin Khadya and Mr. Samuel Crane.

12) Bibliography and references

[Anz04] Anziani, Felipe Rene, *Development and characterization of the magnetic plas*matron, MIT Physics Department S.B. Thesis 2004

[Ath03] Ather A. Quader, John E. Kirwan and M. James Grieve, *Engine Performance and Emissions Near the Dilute Limit with Hydrogen Enrichment Using an On-Board Reforming Strategy,* 2003-01-1356, 2003

[Bel05] N. Margarit Bel1, J.B. Heywood, L. Bromberg, *Simulation of Hydrogen Generation from Methane Partial Oxidation in a Plasma Fuel Reformer,* PSFC-Report RR-05-001

[Ber99] Berger, R.J., Marin, G.B*, Investigation of gas-phase reactions and ignition delay occurring at conditions typical for partial oxidation of methane to synthesis gas*, *Industrial and Engineering Chemistry Research* **38** 7, Jul 1999, p 2582-2592

[Bio05] Data of B-100 fuel used was provided by Bill Ayres, President, Renewable Solutions LLC (2005)

[Boe99] *INTERNAL COMBUSTION ENGINE EXHAUST EMISSION CONTROL SYSTEM WITH ADSORBERS FOR NITROGEN OXIDES THE USE OF TANDEM CATALYSTS,* Boegner; Walter , Haak; Karl-Ernst, Krutzsch; Bernd, Verrelst; Wim, Voigtlaender; Dirk, Wenninger; Guenter, Wirbeleit; Friedrich, US Patent US 5910097, issued 06/08/1999; assignee: Daimler Benz

[Bre73] Breshears, R., Cotrill, H. and Rupe, T., *Partial Hydrogen Injection into Internal Combustion Engines Proc EPA 1st Symp on Low Pollution Power Systems Development*, Ann Arbon, MI Oct (1973)

[Bro97] L. Bromberg, A. Rabinovich and D.R. Cohn, *Plasma Reformer/Fuel Cell Systems for Decentralized Energy Applications, International Journal of Hydrogen Energy* 22 83 (1997)

[Bro99a] L. Bromberg, D.R. Cohn, A. Rabinovich, J.E. Surma and J. Virden, *Compact Plasmatron Boosted Hydrogen Generation Technology for Vehicular Applications, Int. Journal of Hydrogen Energy*, 24, 341-350 (1999)

[Bro99b] L. Bromberg, D.R. Cohn, A. Rabinovich, N. Alexeev, J.B. Green, Jr., N. Domingo, J.M.E. Storey, R.M. Wagner and J. S. Armfield, *Experimental Evaluation of SI Engine Operation Supplemented by Hydrogen Rich Gas from a Compact Plasma Boosted Reformer*, PSFC Report JA-99-32 (November 1999)

[Bro99c] L. Bromberg; A. Rabinovich; N. Alexeev; and D.R. Cohn, *Plasma Reforming of Diesel Fuel*. Plasma Science and Fusion Center Report PSFC/JA-99-4 (presented at the National Meeting of the American Chemical Society, Annaheim, CA March 1999)

[Bro99d] *Plasma Catalytic Reforming of Methane*, L. Bromberg, D.R. Cohn, A. Rabinovich and N. Alexeev, *Int. J. Hydrogen Energy* **24** 1131 (1999)

[Bro99e] Bromberg, L., A. Rabinovitch, N. Alexeev, and D.R. Cohn, 1999, *Plasma Catalytic Reforming of Natural Gas,* Proceedings of the 1999 Hydrogen Program Review, NREL/CP-570-26938, 1999; available at: http://www.psfc.mit.edu/library/99ja/99ja016/99ja016_abs.html

[Bro99f] Bromberg, L., A. Rabinovitch, N. Alexeev, and D.R. Cohn, 1999, *Plasma Reforming of Diesel Fuel,* Proceedings of the 1999 Hydrogen Program Review, NREL/CP-570-26938, 1999; available at http://www.psfc.mit.edu/library/99ja/99ja004/99ja004_abs.html

[Bro00a] L. Bromberg, D.R. Cohn, A. Rabinovich, N. Alexeev, R. Ramprasad and S. Tamhankar, *System Optimization And Cost Analysis Of Plasma Catalytic Reforming Of Hydrocarbons, Int. Journal of Hydrogen Energy* 25 1157 (2000)

[Bro00b] L. Bromberg, D.R. Cohn, A. Rabinovich and J. Heywood, *Emissions Reductions Using Hydrogen from Plasmatron Fuel Converters*, presented at Diesel Engine Emission Reduction (DEER-2000) Workshop (August 20–24, 2000, San Diego, CA)

[Bro01a] L. Bromberg, D.R. Cohn, A. Rabinovich, *Aftertreatment of Diesel Vehicle Emissions Using Compact Plasmatron Fuel Converter-Catalyst Systems, Int. Journal of Vehicle Desig*n 25, n 4, p 275-282 (2001)

[Bro01b] L. Bromberg, D.R. Cohn, A. Rabinovich, J. Heywood, *Emissions reductions using hydrogen from plasmatron fuel converters, Int. Journal of Hydrogen Energy*, v 26, 1115-21 (2001)

[Bro02] L. Bromberg, D.R. Cohn, J. Heywood, A. Rabinovich, N. Alexeev, A. Samokhin, *On-Board Plasmatron generation of Hydrogen Rich Gas for Diesel Aftertreatment and Other Applications*, presented at the 8th DEER Meeting, San Diego CA (August 2002)

[Bro03] L. Bromberg, D.R. Cohn, J. Heywood, A. Rabinovich, N. Alexeev, A. Samokhin, and S. Crane, *Hydrogen Generation from Plasmatron Reformers and Use for Diesel Exhaust Aftertreatment*, presented at the 9th DEER Meeting, Newport RI (August 2003)

[Bro05a] L. Bromberg, K. Hadidi and D.R. Cohn, *Experimental Investigation of Plasma Assisted Reforming of Methane I: Steady State Operation,* Plasma Science and Fusion Center Report JA-05-10

[Bro05b] L. Bromberg, K. Hadidi and D.R. Cohn, *Experimental Investigation of Plasma Assisted Reforming of Methane II: Start-up,* Plasma Science and Fusion Center Report JA-05-11

[Bro05c] L. Bromberg and N. Alexeev Plas*ma assisted reforming of methane: Two stage Perfectly Stirred Reactor (PSR) simulation*, Plasma Science and Fusion Center Report JA-05-12

[Bro05d] L. Bromberg, *Modeling of plasma assisted reforming of methane II: Partially Stirred Reactor (PASR) simulation*, Plasma Science and Fusion Center Report JA-05-13

[Bro05e] L. Bromberg, *CFD modeling of Plasmatron Methane Reformers*, Plasma Science and Fusion Center Report JA-05-14, 2005

[Bro05f] L. Bromberg, K. Hadidi and D.R. Cohn, *Experimental Investigation of Plasma Assisted Reforming of Propane,* Plasma Science and Fusion Center Report JA-05-15

[Bro05g] L. Bromberg, D.R. Cohn, K. Hadidi, J. Heywood, A. Rabinovich and V. Wong, *Optimum Regeneration Of Diesel Particulate Filters And NOx Traps Using Fuel Reformers*, U.S. patent application

[Bro05h] L. Bromberg, D.R. Cohn and V. Wong, *Regeneration Of Diesel Particulate Filters with Hydrogen Rich Gas*, Plasma Science and Fusion Center Report PSFC/RR-05-2 (January 25, 2005)

[Bro05i] L. Bromberg, *Startup Characteristics Of Plasmatron Gasoline Reformers,* Plasma Science and Fusion Center Report PSFC/JA-05-49 (December 15, 2005)

[Bro05j] L. Bromberg, D.R. Cohn, K. Hadidi, J.B. Heywood and A. Rabinovich, *Plasmatron Fuel Reformer Development and Internal Combustion Engine Vehicle Applications*, Plasma Science and Fusion Center Report PSFC/JA-05-22; also presented at the Diesel Engine Exhaust Reduction DEER 2004 (August 2004)

[Bro05k] L. Bromberg, *In-Cylinder Laminar Flame Propagation Speed: Effect of Hydrogen And Hydrogen Rich Gas Addition*, Plasma Science and Fusion Center Report PSFC/JA-05-21

[Bromberg05l] L. Bromberg, K. Hadidi, D.R. Cohn, *Plasmatron Reformation of Renewable Fuels*, Plasma Science and Fusion Center Report PSFC/JA-05-3

[Cam99] *NOX REMOVAL PROCESS*, Campbell, Larry E., Guth, Eugene D., Danziger; Robert, US patent US5650127, issued July 22, 1997; assignee: Goal Line Environmental

Technologies; *REGENERATION OF CATALYST/ABSORBER*, Guth; Eugene D., Campbell; Larry E., Wagner; Gregory J. US patent US5953911, issued Sept. 21, 1999; assignee: Goal Line Environmental Technologies

[Che97] Chen, J. Y., *Stochastic Modeling of Partially Stirred Reactors*, *Combustion Science and Technology* **122** (1-6) 63-94 (1997)

[Che37] CHEMKIN 3.7, released by Reaction Design 2003, http://www.reactiondesign.com/

[Cho05] Chen-Pang Chou, Reaction Design, PASR code, private communication (April 2005)

[Coh96] D.R. Cohn, A. Rabinovich and C. H. Titus, *Onboard Plasmatron Operation Generation of Hydrogen for Extremely Low Emission Vehicles with Internal Combustion Engines, Int. J. Vehicle Design* **17** 550 (1996)

[Coh97] D.R. Cohn, A. Rabinovich, C.H. Titus and L. Bromberg, *Near Term Possibilities for Extremely Low Emission Vehicles using On-Board Plasmatron Generation of Hydrogen*, *International Journal of Hydrogen Energy* .**22**, 715 (1997)

[Coh98] D.R. Cohn, A. Rabinovich, L. Bromberg, J.E. Surma and J. Virden, *Onboard Plasmatron Reforming of Biofuels, Gasoline and Diesel Fuel*, presented at the Future Transportation Technology Conference & Exposition, Costa Mesa, CA (1998); SAE-981920

[And04] Anderson, M., T. Angelo, J. Hou, M. Protas, E. Steinbruck, W. Wagner, P. Way, W. Zhang, *Development of an Active Regeneration Diesel Particulate Filter System*, Diesel Engine Exhaust Reduction DEER 2004 (2004)

[Deu98] O.D. Deutschmann and L.D. Schmidt, *AIChE J.* (1998).

[Dim02] Dimotakis, P.E., *Some Issues on Turbulent Mixing and Turbulence*, Caltech (2002)

[Dob98] K. Dobrot Isherwood, J.R. Linna and P.J. Loftus, *Using Onboard Fuel Reforming by Partial Oxidation to Improve SI Engine Cold-Start Performance and Emissions,* SAE 980939 (SP-1352)

[Hey88] Heywood, John B., *Internal Combustion Engine Fundamentals*, McGraw Hill, 1988.

[Cze01a] A. Czernichowski1, M. Czernichowski, and P. Czernichowski, *International Symp Plasma Chem.* (2001) 55

[Cze01b] A. Czernichowski. *Oil Gas Sci. Technol.*-Rev. IFP 56 (2), 181–198 (2001).

[Cze03a] A. Czernichowski, M. Czernichowski, and K. Wesolowska, *Glidarc-Assisted Production of Synthesis Gas from Biogas,* 1st European Hydrogen Energy Conference, September 2-5, 2003, Grenoble, France, poster and full paper (CP1 63) in CD-Conference Proceedings, 10 pp.

[Cze03b] A. Czernichowski, M. Czernichowski, and P. Czernichowski, Glida*rc-Assisted Reforming of Gasoline and Diesel Oils into Synthesis Gas, idem*, poster and full paper (CP1 64) in CD-Conference Proceedings, 7 pp.

[Cze03c] A. Czernichowski, M. Czernichowski, and P. Czernichowski, *Glidarc-Assisted Production of Synthesis Gas from Natural Gas, idem*, poster and full paper (CP1 65) in CD-Conference Proceedings, 7 pp.

[Dem02] Maxim Deminsky, Victor Jivotov, Boris Potapkin, and Vladimir Rusanov, *Plasma-assisted production of hydrogen from Hydrocarbons*, *Pure Appl. Chem* **74**, 3, pp. 413–418, 2002.

[Jam94] [Jamal, Y.; and Wyszynski, M. L. *On-Board Generation of Hydrogen-Rich Gaseous Fuels: A Review, International Journal of Hydrogen Energy*, Vol. 19, No. 7, pp. 557-572, Elsevier Science, 1994.

[Fan02] Fang, H.L, Huang, S.C., Yu, R.C., Wan, C.Z., Howden, K., *A Fundamental Consideration of Nox Adsorber Technology for DI Diesel Applications*, SAE 2002-01-2889 (2002)

[Fay04] J.C. Fayard, T. Seguelong, *A New Active DPF System for "Stop-&-Go" Duty Cycle Vehicles*, presented at the 2004 Deer Conference

[Ful95] Fulcheri, L., Schwob, Y, *From methane to hydrogen, carbon black and water, International Journal of Hydrogen Energy*, **20**, n 3, Mar, 1995, p 197-202

[Gau98] Gaudernack, Bjorn, Lynum, Steinar, *Hydrogen from natural gas without release of CO2 to the atmosphere, International Journal of Hydrogen Energy*, **23**, n 12, Dec, 1998, p 1087-1093

[Gor00] C.T. Goralski, Jr., R.P. O'Connor and L.D. Schmidt, *Chem. Eng. Sci.* **55** (2000) 1357.

[Gra94] Gray BF, Griffiths JF, Goulds GA, Charlton BG, Walker GS, *The relevance of thermokinetic interactions and numerical modelling to the homogeneous partial oxidation of methane, Industrial and Engineering Chemistry Research*, **33** (1994), 1126-1135.

[Gre00] J.B. Green, L. Bromberg, D. R. Cohn. A., N. Domingo, J.M. Storey, R.M. Wagner, J.S Armfield, *Experimental Evaluation of SI Engine Operation Supplemented by Hydrogen Rich Gas from a Compact Plasma Boosted Reformer*, SAE 2000-01-2206

[Had04] K. Hadidi, L. Bromberg, D.R. Cohn, A. Rabinovich, N. Alexeev, A. Samokhin, *Hydrogen-Rich Gas Production From Plasmatron Reforming Of Biofuels*, presented at the World Renewable Energry Congress VIII and Expo, Denver CO (Aug 2004)

[Han03] K. Hanamura, T. Suzuki, T. Tanaka and Y. Miyairi, *Visualization of Combustion Phenomena in Regeneration of Diesel Particulate Filter,* SAE Paper 2003-01-0836

[Har03] O.C. Haralampous, G.C. Koltsakis, Z.C. Samaran, *Partial Regenerations in Diesel Particulate Filters*, JSAE 20030088 (SAE 2002-01-1881)

[Haw98] D. Haworth, B. Cuenot, T. Poinsot, AND R. Blint*, Numerical simulation of turbulent propane-air combustion with non-homogeneous reactants: initial results*, Stanford Center for Turbulence Research, Proceedings of the Summer Program 1998

[Hic92] Hickman, D., and Schmidt, L. D., *J. Catal.* 138:267 (1992)

[Hic93] D.A. Hickman, E.A. Haupfear and L.D. Schmidt, *Catal. Lett.* **17** (1993) 223.

[Hic93a] D.A. Hickman and L.D. Schmidt, *Science* **259** (1993) 343.

[Hic93b] D.A. Hickman and L.D. Schmidt, *AIChE J.* **39** (1993) 1164.

[Hom83] H.S. Homan *et al.*, *The Effect of Fuel Injection on NOx Emissions and Undesirable Combustion of Hydrogen Fueled Piston Engines, Int J of Hydrogen Ener* 8 1983

[Hod98] J. W. Hodgson, D.K. Irick, and M.V. Whalen, Improving the cold-start performance of alcohol-fueled engines using a rich combustor, SAE Paper 981359, 1998.

[Hou74] Houseman, J., and Cerini, D. J., *On-Board Hydrogen Generator for a Partial Hydrogen Injection Internal Combustion Engine*, SAE paper 740600, 1974.

[Kha04] Khadya, N., ArvinMeritor, private communication (2004)

[Kee04] R. J. Kee, F. M. Rupley, J. A. Miller, M. E. Coltrin, J. F. Grcar, E. Meeks, H. K. Moffat, A. E. Lutz, G. Dixon-Lewis, M. D. Smooke, J. Warnatz, G. H. Evans, R. S. Larson, R. E. Mitchell, L. R. Petzold, W. C.Reynolds, M. Caracotsios, W. E. Stewart, P. Glarborg, C. Wang, O. Adigun, W. G. Houf, C. P. Chou, S. F. Miller, P. Ho, and D. J. Young, *CHEMKIN Release 4.0*, Reaction Design, Inc., San Diego, CA (2004)

[Kir99] John E. Kirwan, Ather A. Quader and M. James Grieve, *Advanced Engine Management Using On-Board Gasoline Partial Oxidation Reforming for Meeting Super-ULEV (SULEV) Emissions Standards,* 1999-01-2927 (SP-1469)

[Kir02] John E. Kirwan, Ather A. Quader and M. James Grieve, *Fast Start-Up On-Board Gasoline Reformer for Near Zero Emissions in Spark-Ignition Engines*, SAE paper 2002-01-1011, 2002

[Kur79] Kuroda, H., Nakajima, Y., Sugihara, K, Takagi, Y. and Muranaka, S. The Fast Burn with Heavy EGR, New Approach for Low NOx and Improved Fuel Economy, Society for Automotive Engineers, 1979, Paper 780006. P1

[Mac76] MacDonald, J.S., *Evaluation of the Hydrogen-Supplemented Fuel Concept with and Experimental Multicylinder Engine*, SAE paper 760101, Detroit, MI (1976)

[Mul86] Muller, R., The Use of Hydrogen Plasma Processes in the Petrochemical and Iron-Smelting Industries, in: *Hydrogen Energy Progress* IV, 3 885(1982); Kaske, G., L. Kerke, and R. Muller, Hydrogen Production in the Huls Plasma-Reforming Process, *Hydrogen Energy Progress* VI, 1 (1986).

[Nod01] Noda, T and D. Foster, *A Numerical Study to Control Combustion Duration of Hydrogen fueld HCCI by using Multi-Zone Chemical Kinetics Simulations*, SAE 2001-01-0250

[Par99a] James E. Parks - Larry E. Campbell - G. J. Wagner - W. E. Epling - M. S. Sanders, *SCONOxTM and SCOSOxTM Sorbate Catalyst System for the Aftertreatment of NO2 Diesel Exhaust,* SAE paper 1999-01-3557; see also http://www.glet.com/update_10-99.htm#CUMMINS

[Par99b] James E. Parks, G. J. Wagner, W. E. Epling, M. S. Sanders and Larry E. Campbell, *Near Zero NOx Control for Diesel Aftertreatment*, SAE paper 1999-01

[Par02] Parks, J.E., Emerachem, private communication (2002)

[Ogu04] Stephen Ogunwumi, Corning Inc, private communication (2004)

[Pim05] Pimentel, D. and T.W. Patzek, *Ethanol Production Using Corn, Switchgrass, and Wood; Biodiesel Production Using Soybean and Sunflower, Natural Resources Research*, **14**, No. 1, March 2005 (2005)

[Rab95] A. Rabinovich, D.R. Cohn and L. Bromberg, *Plasmatron Internal Combustion Engine System for Vehicle Pollution Reduction Int J. Vehicle Design* **15** 234 (1995)

[Rud79] Rudiak, E.M.A, A. Rabinovich and N.A. Tul, USSR patent 700935 (Aug 1979)

[Sob01] M.G. Sobacchi, A.V. Saveliev, A.A. Fridman and Lawrence A. Kennedy, *Hydrocarbon Reforming in Combined Plasma / Catalytic Partial Oxidation System*,, Proc. 15th Int. Symp. on Plasma Chemistry, v VII, 2939-2944, 2001.

[Sob02] M.G. Sobacchi, A.V. Saveliev, A.A. Fridman and Lawrence A. Kennedy, *Experimental Assessment of a Combined Plasma/ Catalytic System for Hydrogen Production via Partial Oxidation of Hydrocarbon Fuels*, *Int. J Hydrogen Energy*, 27/6, 635-642 2002.

[Sha02] Shapouri, H., Duffield, J. A., and Wang, M., *The energy balance of corn ethanol: an update: USDA, Office of Energy Policy and New Uses, Agricultural Economics*. Rept. No. 813 (2002)

[Smi] Gregory P. Smith, David M. Golden, Michael Frenklach, Nigel W. Moriarty, Boris Eiteneer, Mikhail Goldenberg, C. Thomas Bowman, Ronald K. Hanson, Soonho Song, William C. Gardiner, Jr., Vitali V. Lissianski, and Zhiwei Qin, *GRI 3.0 mechanism*, http://www.me.berkeley.edu/gri_mech/

[Smi97] A. Smith and G.J.J. Bartley, Stoichiometric *Operation of a Gas Engine Utilizing Synthesis Gas and EGR for NOx Control,* ASME ICE- 29-3, Engine Combusion Performance and Emission, 1997

[Ste74] R. F. Stebar, F. B. Parks, *Emission control with lean operation using hydrogen-supplemented fuel*, SAE paper 740187 (1974)

[Ste03] Stevens, J., Chevron Texaco, private communication (2003)

[Top04] Topinka, J.A., M.D. Gerty, J.B. Heywood and J.C. Keck, *Knock Behavior of a Lean-Burn, H_2 and CO Enhanced, SI Gasoline Engine Concept*,SAE paper 2004-01-0975

[Tur96] Turns, S. R. *An Introduction to Combustion*. McGraw-Hill, Inc., New York. 1996

[Wan01] Wan, C.Z., Mital, R., Dipshand, J., *Low Temperature Regeneration of Nox Asorber Systems*, Diesel Engine Exhaust Reduction Workshop DEER 2001, 2001

[Yez02] A. Yezerets, N.W. Currier, H. Eadler, S. Popuri and A. Suresh, *Quantitative Flow-Reactor Study of Diesel Soot Oxidation Process,* SAE paper 2002-01-1684

[Zha02] Z Zhang, S.L. Yang and J.H. Johnson, *Modeling and Numerical Simulation of Diesel Particulate Trap Performance During Loading and Regeneration*, SAE Paper 2002-01-1019.